Evaluation of Anti-Ageing Potential of Lemongrass Tea and its Mechanisms of Action

Thesis submitted in fulfilment of the requirements for the degree of Doctor of Food Science and Technology in the Department of Biotechnology and Food Science, Faculty of Applied Sciences, Durban University of Technology, South Africa

By

Mutiu Idowu Kazeem

(Student Number: 22176507)

Supervisor: Prof. Saheed Sabiu

Co-Supervisor: Prof. John J. Mellem

August 2025

DECLARATION

I, Mutiu Idowu Kazeem, student number 22176507, hereby declare that this study titled: Evaluation of the Anti-Ageing Potential of Lemongrass Tea and its Mechanisms of Action, is my original work and has not been submitted in any form to any other academic institution. All references detailed in the thesis have been completed in terms of all personal communications engaged in and published works consulted. The research described in this study was performed in the Department of Biotechnology and Food Science, Faculty of Applied Sciences, Durban University of Technology, South Africa, under the supervision of Prof. Saheed Sabiu and Prof. John Jason Mellem.

08/08/2025

Signature of student **Date**

09.08.2025

Signature of Supervisor **Date**

11 August 2025

Signature of Co-Supervisor **Date**

ACKNOWLEDGEMENTS

All praise, thanks and adoration are due to Allah for giving me life, faith and strength to undertake and complete this degree.

I sincerely acknowledge my Supervisor, Prof. Saheed Sabiu, for providing guidance, expertise, and unwavering support throughout this project. Your qualitative insights, criticism and feedback contributed greatly to the success of this work. I also appreciate my Co-Supervisor, Prof. John Jason Mellem, for allowing me to benefit from his wealth of experience in Food Science. Your advice, mentorship and qualitative tutelage were instrumental in shaping my research endeavour.

I also want to thank the Head of Department, Prof. F. M. Swalaha, for his continuous support throughout the programme. I also acknowledge the duo of Dr. A. K. Puri and Mr. G. M. Makolomakwa for guiding me in using laboratory equipment and providing consumables for experiments. I'm also grateful to Mr. V. Dilrajh for guiding me through determining the nutritional composition of the samples. The support of all other staff members of the Department of Biotechnology & Food Science is greatly appreciated.

I wish to acknowledge the support of the Directorate for Research and Postgraduate Support, Durban University of Technology, for the scholarship award, which enabled me to accomplish this study. I also appreciate all Computational Biology Research Group members' support and criticism during this study. This includes Dr. F. O. Balogun, Mrs. R. A. Abdulsalam, Mr. J. O. Aribisala, Miss A. Akoonjee and Miss A. Rampadarath. I'm very grateful to you all.

I'm extremely grateful to my late parents, Mr. Akanbi Kazeem and Mrs. Saulat Kazeem, for their upbringing, love and sacrifice in preparing me for today. May Allah forgive you, overlook your shortcomings and grant you Paradise. The continuous support and encouragement of my maternal uncle and his wife, Mr. and Mrs. Sabit Babatunde, are greatly appreciated. May you live long, and grow strong and healthy. I equally appreciate the unflinching support of my siblings: Mr. R. Olalekan Kazeem, Mr. R. Oladimeji Kazeem, and Mrs. S. Ajoke Adewale.

This project will not come to fruition without the love, support and understanding of my wife and confidant, Mrs Hafsat Adedoyin Kazeem. May you be elevated and rewarded in this world and the hereafter. To my three adorable children: Zaynab Adeola, Zayd Ademola and Zaneeroh Adesola, thanks for being a source of joy and renewed hope.

PUBLICATION OUTPUTS

1. Kazeem, M. I., Mellem, J. J., Sabiu, S. 2024. Medicinal foods and plants with anti-ageing properties: A review of *in vitro* and *in vivo* studies. *Food Frontiers*, 5: 24-45.

2. Kazeem, M. I., Abdulsalam, R. A., Mellem, J. J., Sabiu, S. 2025. Lemongrass (*Cymbopogon citratus*) infusions exhibit neuroprotective properties: Evidence from *in vitro* and *in silico* studies. *Food Bioscience,* 68: 106355, https://doi.org/10.1016/j.fbio.2025.106355.

3. Kazeem, M. I., Mellem, J. J., Sabiu, S. 2025. Influence of drying on the nutritional composition, phytochemical constituents and *in-vitro* antioxidant properties of *Cymbopogon citratus* (lemongrass) infusions. (Submitted to the journal, *Food and Humanity*).

4. Kazeem, M. I., Mellem, J. J., Sabiu, S. 2025. *Cymbopogon citratus* (DC) Stapf (lemongrass) as a source of nutrients and pharmacological agents for the management of diseases: A review. (Submitted to the journal, *Vegetos*).

5. Kazeem, M. I., Abdulsalam, R. A., Mellem, J. J., Sabiu, S. 2025. Unveiling the inhibitory properties of lemongrass infusion on ageing-related enzymes: Integration of *in vitro* and *in silico* studies. (Submitted to the journal, *Scientific African*).

6. Kazeem, M. I., Mellem, J. J., Sabiu, S. 2025. Caffeic acid-rich lemongrass infusion alleviates metabolic derangement via insulin signalling in D-galactose-induced ageing in *Drosophila melanogaster*. (Submitted to the journal, *Journal of Functional Foods*).

ABSTRACT

Ageing is a complex process that involves the loss of physiological integrity and negatively impacts the well-being of an organism. It is associated with various diseases such as hypertension, cardiovascular and neurodegenerative diseases. However, the proportion of geriatrics is increasing globally, and they are susceptible to these diseases. Regrettably, there is no known medication for managing ageing and its associated complications. One of the plants that is widely consumed as tea is lemongrass (*Cymbopogon citratus*) due to its aroma and refreshing taste. Several studies have reported the pharmacological properties of lemongrass, but there is no information on its effect on ageing. Therefore, this study investigated the anti-ageing properties of *Cymbopogon citratus* (lemongrass) tea using *in vitro*, *in silico* and *in vivo* techniques. Fresh and dry lemongrass infusions were subjected to proximate, mineral, amino acid, and phytochemical analysis using Inductively Coupled Plasma Mass Spectrometry (ICP-MS), high-performance liquid chromatography (HPLC), and Liquid Chromatography – Mass Spectrometer (LC-MS). This was followed by the determination of the antioxidant, anti-ageing and neuroprotective potentials of the lemongrass infusion using *in vitro* methods. Computational techniques, including molecular docking, molecular dynamics simulation and pharmacokinetic profiling, were employed to probe the possible mechanism of anti-ageing effects of the lemongrass teas. The *in vivo* anti-ageing property of the lemongrass teas was evaluated by including different concentrations of the teas in the diet of D-galactose-induced ageing in *Drosophila melanogaster* for 14 days, followed by determination of both biochemical and molecular parameters. The results showed that both fresh and dry lemongrass teas are rich in nutrients and phytochemicals. While both lemongrass infusions have similar neuroprotective effects *in vitro*, the dry lemongrass infusion exhibited better antioxidant activities (with lower EC_{50} values for DPPH, hydroxyl and superoxide radicals), and these are comparable to the reference standard, gallic acid. It also displayed better anti-ageing properties (with lower IC_{50} values for inhibition of collagenase, elastase, hyaluronidase and tyrosinase) similar to the standard, oleanolic acid. In the *in-silico* studies, kaempferitrin had the lowest binding energy for collagenase (-41.57 kcal/mol) and hyaluronidase (-52.09 kcal/mol), while lonicerin and isovitexin-2”-O-arabinoside possessed the lowest binding energies for elastase (-35.55 kcal/mol) and tyrosinase (-53.09 kcal/mol), respectively. Kaempferitrin displayed the highest number of stable interactions with collagenase and hyaluronidase, while limocitrin-7-(6”-acetylglucoside) and isovitexin-2”-O-arabinoside interacted more with elastase and tyrosinase,

respectively. The resulting complexes formed with chamaemeloside (-66.59 kcal/mol), isocarlinoside (-65.79 kcal/mol), neocuscutoside C (-41.09 kcal/mol), and aspulvinone H (-72.28 kcal/mol) against acetylcholinesterase, butyrylcholinesterase, β-secretase and monoamine oxidase, respectively, had the lowest binding free energy values compared to the respective standards. However, benzyl alcohol β-D-rutinoside, kaempferitrin, neocuscutoside C and aspulvinone H possessed the most stable interactions with acetylcholinesterase, butyrylcholinesterase, β-secretase and monoamine oxidase, respectively. The D-galactose-treated flies experienced significant distortion ($p < 0.05$) in their antioxidant status and enzymes (catalase, superoxide dismutase and glutathione peroxidase). However, the inclusion of dry lemongrass infusion in the diet restored all the alterations witnessed in the D-galactose flies. The dry lemongrass infusion also upregulated the SOD1, CAT and dFOXO genes while downregulating the DILP2 gene. It can be concluded that both fresh and dry lemongrass infusions are rich in nutrients and phytochemicals, with the dry infusion displaying better antioxidant and anti-ageing properties *in vitro*. This is confirmed by the *in vivo* studies where the dry lemongrass infusion was more effective in ameliorating ageing-related complications in *Drosophila melanogaster*. Though the phytochemicals present in both teas are similar, they are more abundant in the dry tea, which may account for its more potent activities. These phytochemicals include lonicerin, chamaemeloside, kaempferitrin and neocuscutoside C. Consequent upon the outcome of this study, a ready-to-drink beverage may be developed from the dry lemongrass while its bioactive compounds are isolated for future drug development.

Keywords: Lemongrass, ageing, *Cymbopogon citratus*, antioxidants, neuroprotection, kaempferitrin

TABLE OF CONTENTS

LIST OF TABLES

LIST OF FIGURES

CHAPTER 1

1. GENERAL INTRODUCTION

Ageing is a multifaceted biochemical process in which the physiological integrity of an organism is compromised, leading to impaired bodily functions and an increased tendency to die (Martel *et al.* 2019). It is characterized by a gradual reduction in the efficiency of the cellular machinery and physiological processes, causing a reduction in capabilities which negatively affects the health and well-being of an organism (Cătană, Atanasov and Berindan-Neagoe 2018). This gradual deterioration is responsible for the incidence of many chronic ailments, such as cancer, diabetes, cardiovascular disorders, as well as neurodegenerative diseases (Chen, Wang and Wei 2024). It also affects most of the physiological functions of the organism, including the circulatory, nervous, reproductive and immune systems.

The global prevalence of geriatrics (people aged 60 or above) is on the increase, and it is projected that it will nearly double from 12% in 2015 to 22% by 2050 (Luo *et al.* 2021). Since the number of "senior citizens" has increased drastically in the world, management strategies focusing on healthy ageing and a disease-free phenotype are required to reduce additional healthcare costs (Higo and Khan 2015). While many individuals are glad about the possibility of living longer, these years should be spent in sound health and not with ailments or disability (Grinin, Grinin and Korotayev 2023). This is because it is only when one is healthy that one will enjoy the increased longevity, and this may then call for celebration as part of the gains of civilization. Advancing adult age is therefore the major risk factor for chronic diseases, including diabetes, hypertension, cancer, cardiovascular and neurodegenerative diseases (Fuster 2017). Ageing impairs the entire physiology of the organism, including sensory, motor and cognitive function, and thus lowers quality of life (Luo *et al.* 2021). Ameliorating the duration and the extent of diseases associated with ageing may therefore contribute to the promotion of the well-being of the elderly.

Consequently, it is of paramount importance to improve understanding of the mechanisms involved in ageing process and to provide effective anti-ageing therapeutic interventions, so that the constant rise in the population of geriatrics will offer more benefits rather than detrimental effects to future societies. Previous studies had proposed that reactive oxygen species (ROS) produced as a by-product of cellular respiration in mitochondria may be the cause of ageing (Orr,

Radyuk and Sohal 2013; Azman and Zakaria 2019). In line with this concept, ROS accumulate with age as the function of mitochondria is reduced, and an enormous concentration of ROS may lead to protein damage, organelle dysfunction, DNA damage, and ageing (Cui *et al.* 2004). This process could be responsible for the progressive deterioration of biological systems due to their high reactivity of ROS. This is what led to the free radical theory of ageing, which postulates that the common ageing process is attributable to the initiation of free-radical reactions (Gruber, Schaffer and Halliwell 2008).

Unfortunately, to date, there is no known medication for the management of ageing and its associated diseases. This calls for a continuous search to discover agents that can be used in the management of ageing and its related disorders. From time immemorial, human beings have depended on medicinal plants and foods as the source of their medicine (Gurib-Fakim 2006). Folkloric knowledge of medicinal plants with therapeutic potential has been passed from one generation to the other. Today, about two-thirds of the world's population relies on the use of medicinal plants and foods for the treatment of diseases (Ogunsuyi, Ademiluyi and Oboh 2020). This is mainly due to their availability, perceived efficacy and safety.

The use of plant-based remedies for managing diseases has received increased attention in the 21st century, although humans have been using these plants since the beginning of existence (Babich *et al.* 2022). This time-honoured utilization of medicinal plants has established a valuable database with anecdotal evidence suggesting the safety and efficacy of numerous species (Vyas, Kothari and Kachhwaha 2019). This is coupled with the fact that they are readily available and affordable to obtain by their users. Medicinal plants offer an inexhaustible array of compounds as a result of secondary metabolism, causing high chemical diversity over other natural sources (Iweala *et al.* 2024). Even the currently used drugs are either semi-synthetically or directly derived from plants. These include artemisinin (from *Artemisia annua*), quinine (from *Cinchona officinalis*), galantamine (from *Galanthus nivalis*), atropine (from *Atropa belladonna*), and vinblastine (from *Catharanthus roseus*) (Vyas, Kothari and Kachhwaha 2019).

Despite these advantages, the use of medicinal plants also has some teething challenges. The way plants are used in traditional medicine lacks standardization in terms of preparation and dosages for administration (Bjørklund *et al.* 2018). Plants of the same species can also have a varying chemical composition due to genetic and/or environmental variation, thereby affecting their

efficacy. When administered, medicinal plants could interact with other medications, leading to herb-drug interaction, thereby reducing the efficacy of the medication or causing adverse effects (Chen *et al.* 2024). Though they are acclaimed to be effective, most medicinal plants have not undergone clinical trials to prove their efficacy and safety (Waltenberger *et al.* 2018). The fact that plants are natural makes people believe that they are safe; however, scientific research has revealed that many medicinal plants are toxic, e.g *Datura stramonium*, *Nerium oleander*, and *Ricinus communis* (Kuete 2014).

Consequently, it is expedient that medicinal plants and their products are evaluated for their efficacy and safety in promoting longevity and healthy ageing. One such plant that enjoys acceptance among various categories of inhabitants, be it in Africa, Asia or South America, is *Cymbopogon citratus* (Ekpenyong *et al*. 2015). *Cymbopogon citratus* (DC.) Stapf (Genus: Poaceae), commonly known as lemongrass, is a perennial grass found in the tropical regions of the world, including South America, Asia and Africa (Ekpenyong, Akpan and Nyoh 2015). It is called different names depending on location, such as citronella (USA), citron grass (Sweden), and elephant grass (Nigeria) (Oladeji *et al.* 2019). Lemongrass infusion is commonly consumed for recreational and therapeutic purposes, just like black tea, green tea and rooibos tea (Tazi *et al.* 2024). It is used as an herbal medicine globally for a wide range of applications, including antimicrobial, anti-inflammatory, antimalarial, antidiabetic and cardioprotective properties (Ekpenyong *et al*. 2015). It is also used as an additive in the preparation of foods, cuisines and beverages (Avoseh *et al*. 2015). While many studies have reported its rich nutritional and therapeutic potential (Tibenda *et al.* 2022; Adhikary *et al.* 2024; Kusuma *et al.* 2024), there is a scarcity of information on its therapeutic potential for ageing.

1.1. Aim of the study

This study aims to evaluate the anti-ageing potential of lemongrass (*Cymbopogon citratus*) tea and its mechanisms of action.

1.2. Research questions

i. What are the nutrients and phytochemical compounds present in the fresh and dry lemongrass teas?

ii. What are the mechanisms by which phytochemical constituents of the lemongrass tea interact with enzymes implicated in ageing?

iii. Do fresh and dry lemongrass teas exhibit anti-ageing, antioxidant, and neuroprotective properties in an *in vitro* model?

iv. What is the effect of supplementation of the diet with lemongrass tea on galactose-induced ageing in *Drosophila melanogaster*?

1.3. Objectives of the study

i. To determine the nutritional and phytochemical composition of lemongrass teas using proximate analysis, spectrophotometric and chromatographic techniques.

ii. To establish the structural mechanism of inhibition by the phytochemical constituents of the tea against target enzymes (collagenase, elastase, hyaluronidase and tyrosinase) implicated in the process of ageing using advanced molecular dynamics simulation.

iii. To determine the *in vitro* anti-ageing, antioxidant, and neuroprotective properties of the lemongrass teas using relevant cell-based and enzyme inhibition assays.

iv. To evaluate the effect of supplementation of lemongrass tea-based diet on galactose-induced ageing in *Drosophila melanogaster* and its possible mechanisms of action.

1.3. Organization of the thesis

The thesis is organised into seven chapters. Chapter one is a general introduction to the thesis. Chapter two is a literature review, which is divided into 2 sections: The first section is on the review of medicinal foods and plants with anti-ageing potentials (published in the journal, Food Frontiers). The second section of chapter two is the review of the nutritional, phytochemical and pharmacological properties of *Cymbopogon citratus* (lemongrass). Chapter three presents the influence of drying on the nutritional, phytochemical and antioxidant properties of lemongrass. Chapter four presents *in vitro* and computational studies on the anti-ageing potentials of *Cymbopogon citratus* (lemongrass). Chapter five presents *in vitro* and *in silico* studies on the

neuroprotective properties of *Cymbopogon citratus* (lemongrass) (published in the journal, Food Bioscience). Chapter six presents the effect of dietary inclusion of lemongrass on the longevity of D-galactose-induced ageing in *Drosophila melanogaster*. Chapter seven is the general discussion, conclusion and recommendations.

References

Adhikary, K., Banerjee, P., Barman, S., Bandyopadhyay, B. and Bagchi, D. 2024. Nutritional aspects, chemistry profile, extraction techniques of lemongrass essential oil and it's physiological benefits. *Journal of the American Nutrition Association*, 43 (2): 183-200.

Azman, K. F. and Zakaria, R. 2019. D-Galactose-induced accelerated aging model: An overview. *Biogerontology*, 20 (6): 763-782.

Babich, O., Larina, V., Ivanova, S., Tarasov, A., Povydysh, M., Orlova, A., Strugar, J. and Sukhikh, S. 2022. Phytotherapeutic approaches to the prevention of age-related changes and the extension of active longevity. *Molecules*, 27 (7): 2276.

Bjørklund, G., Dadar, M., Martins, N., Chirumbolo, S., Goh, B. H., Smetanina, K. and Lysiuk, R. 2018. Brief challenges on medicinal plants: An eye-opening look at ageing-related disorders. *Basic & Clinical Pharmacology & Toxicology*, 122 (6): 539-558.

Cătană, C.-S., Atanasov, A. G. and Berindan-Neagoe, I. 2018. Natural products with anti-aging potential: Affected targets and molecular mechanisms. *Biotechnology Advances*, 36 (6): 1649-1656.

Chen, J.-C., Wang, R. and Wei, C.-C. 2024. Anti-aging effects of dietary phytochemicals: From *Caenorhabditis elegans*, *Drosophila melanogaster*, rodents to clinical studies. *Critical Reviews in Food Science and Nutrition*, 64 (17): 5958-5983.

Chen, X., Bahramimehr, F., Shahhamzehei, N., Fu, H., Lin, S., Wang, H., Li, C., Efferth, T. and Hong, C. 2024. Anti-aging effects of medicinal plants and their rapid screening using the nematode *Caenorhabditis elegans*. *Phytomedicine*, 129: 155665.

Cui, X., Wang, L., Zuo, P., Han, Z., Fang, Z., Li, W. and Liu, J. 2004. D-galactose-caused life shortening in *Drosophila melanogaster* and *Musca domestica* is associated with oxidative stress. *Biogerontology*, 5: 317-325.

Ekpenyong, C. E., Akpan, E. and Nyoh, A. 2015. Ethnopharmacology, phytochemistry, and biological activities of *Cymbopogon citratus* (DC.) Stapf extracts. *Chinese Journal of Natural Medicines*, 13 (5): 321-337.

Fuster, V. 2017. Changing Demographics. *Journal of the American College of Cardiology*, 69 (24): 3002-3005.

Grinin, L., Grinin, A. and Korotayev, A. 2023. Global aging: An integral problem of the future. How to turn a problem into a development driver? In: *Reconsidering the limits to growth: A report to the Russian association of the club of Rome*. Springer, 117-135.

Gruber, J., Schaffer, S. and Halliwell, B. 2008. The mitochondrial free radical theory of ageing—where do we stand. *Frontiers in Bioscience*, 13 (17): 6554-6579.

Gurib-Fakim, A. 2006. Medicinal plants: Traditions of yesterday and drugs of tomorrow. *Molecular Aspects of Medicine*, 27 (1): 1-93.

Higo, M. and Khan, H. T. 2015. Global population aging: Unequal distribution of risks in later life between developed and developing countries. *Global Social Policy*, 15 (2): 146-166.

Iweala, E. J., Adurosakin, O. E., Innocent, U., Omonhinmin, C. A., Dania, O. E. and Ugbogu, E. A. 2024. Anti-aging potential of bioactive phytoconstituents found in edible medicinal plants: A review. *Science*, 6 (2): 36.

Kuete, V. 2014. Toxic plants used in African traditional medicine. In: *Toxicological Survey of African Medicinal Plants*. Elsevier, 135-180.

Kusuma, I. Y., Perdana, M. I., Vágvölgyi, C., Csupor, D. and Takó, M. 2024. Exploring the clinical applications of lemongrass essential oil: A scoping review. *Pharmaceuticals*, 17 (2): 159.

Luo, J., Si, H., Jia, Z. and Liu, D. 2021. Dietary anti-aging polyphenols and potential mechanisms. *Antioxidants*, 10 (2): 283.

Martel, J., Ojcius, D. M., Ko, Y. F., Chang, C. J. and Young, J. D. 2019. Antiaging effects of bioactive molecules isolated from plants and fungi. *Medicinal Research Reviews*, 39 (5): 1515-1552.

Ogunsuyi, O. B., Ademiluyi, A. O. and Oboh, G. 2020. Solanum leaves extracts exhibit antioxidant properties and inhibit monoamine oxidase and acetylcholinesterase activities (*in vitro*) in *Drosophila melanogaster*. *Journal of Basic and Clinical Physiology and Pharmacology*, 31 (3): 20190256.

Oladeji, O. S., Adelowo, F. E., Ayodele, D. T. and Odelade, K. A. 2019. Phytochemistry and pharmacological activities of *Cymbopogon citratus*: A review. *Scientific African*, 6: e00137.

Orr, W. C., Radyuk, S. N. and Sohal, R. S. 2013. Involvement of redox state in the aging of *Drosophila melanogaster*. *Antioxidants & Redox Signaling*, 19 (8): 788-803.

Tazi, A., Zinedine, A., Rocha, J. M. and Errachidi, F. 2024. Review on the pharmacological properties of lemongrass (*Cymbopogon citratus*) as a promising source of bioactive compounds. *Pharmacological Research-Natural Products*, Article ID: 100046.

Tibenda, J. J., Yi, Q., Wang, X. and Zhao, Q. 2022. Review of phytomedicine, phytochemistry, ethnopharmacology, toxicology, and pharmacological activities of Cymbopogon genus. *Frontiers in Pharmacology*, 13: 997918.

Vyas, S., Kothari, S. and Kachhwaha, S. 2019. Nootropic medicinal plants: Therapeutic alternatives for Alzheimer's disease. *Journal of Herbal Medicine*, 17: 100291.

Waltenberger, B., Halabalaki, M., Schwaiger, S., Adamopoulos, N., Allouche, N., Fiebich, B. L., Hermans, N., Jansen-Dürr, P., Kesternich, V. and Pieters, L. 2018. Novel natural products for healthy ageing from the Mediterranean diet and food plants of other global sources—The MediHealth Project. *Molecules*, 23 (5): 1097.

CHAPTER 2

2. LITERATURE REVIEW

This chapter is divided into 2 sections: The first section reviews medicinal foods and plants with anti-ageing potentials, published in the journal, *Food Frontiers*. The second section of chapter two is a review of the nutritional, phytochemical and pharmacological properties of *Cymbopogon citratus* (lemongrass).

2.1 Medicinal foods and plants with anti-ageing properties: A review of *in-vitro* and *in-vivo* studies

Mutiu Idowu Kazeem, John Jason Mellem and Saheed Sabiu

Department of Biotechnology and Food Science, Durban University of Technology, P. O. Box 1334, Durban 4000, South Africa

Preface: This article reviewed all studies conducted on the anti-ageing properties of medicinal foods and plants. It also presented the different models used to evaluate the anti-ageing potentials of natural products. This article was published in the journal, *Food Frontiers* 2024; 5: 24-45. The full article is included as an appendix (Appendix 7).

2.1.1 Abstract

Ageing is a natural process by which organisms experience physiological decline, leading to susceptibility to morbidity and mortality. There are no known anti-ageing drugs, but there is a myriad of medicinal foods and plants that have been used in managing the state. Several studies have also been conducted on the anti-ageing properties of medicinal plants and foods, but these pieces of information are scattered. This paper attempts to integrate available information on medicinal foods and plants, as well as isolated chemical compounds with anti-ageing potential. It also provides different models (*in vitro* and *in vivo*) that are used in evaluating the potency of natural products. Current literature on the subject was obtained from different databases such as PubMed, Google Scholar and Web of Science. A total of 119 medicinal plants and 50 isolated compounds were reported in this study. Different models were also used to evaluate the efficacy of these plants, including *in vitro* (enzyme inhibition, use of cell lines) and *in vivo* (*C. elegans*,

yeast, fruit fly, mice and rats) models. It can be concluded that medicinal foods and plants are reservoirs of potential therapeutic agents that can efficiently modulate metabolic processes implicated in ageing and its associated disorders.

Keywords: Ageing, medicinal plants, bioactive compounds, longevity, functional foods

2.1.2 Introduction

One of the goals of procreation is the sustainability of the species, which is a function of how long the individual lives. Conversely, the longer the number of years an individual lives, the higher the tendency for him to experience a decline in physiological and physical functions, which constitutes ageing (Rusu *et al.* 2019; Pandey *et al.* 2020). It is a natural and irreversible biological process marked by structural and functional changes in the cells and tissues, leading to low immunity and increased susceptibility to morbidity and mortality (Klinngam *et al.* 2022). Ageing is a primary risk factor for many chronic diseases like diabetes, hypertension, cancer, and cardiovascular and neurodegenerative disorders (Men *et al.* 2021). Due to the onset of the myriad of diseases at this period, ageing itself can constitute a disease.

According to the World Health Organization (WHO), individuals aged 65 years and above constitute the elderly (WHO 2022). The prevalence of old people is increasing globally due to the increase in life expectancy. For instance, 258 million old people were recorded in 1980, 500 million in 2006 and 771 million in 2022 (UN 2022). Therefore, the number of old people now is about three times the number in 1980. However, this population is projected to increase to 994 million and 1.6 billion in 2030 and 2050, respectively (UN 2022). Old people occupy about 10% of the world population, and this is expected to reach 12% and 16% in 2030 and 2050, respectively (Luo *et al.* 2021). Europe and Northern America have the largest share of aged persons, with about 19% of the population, and this is expected to rise to 27% in 2050 (UN 2022). However, 3% of the people in Sub-Saharan Africa are old, which may increase to 5% in 2050.

Since all organisms desire to live for a long period, ageing is inevitable. However, there is a paucity of information on how to attain old age without necessarily experiencing the pathological conditions associated with it. Consumption of a desirable diet is one of the veritable means of managing ageing and its complications (Rusu *et al.* 2019). Medicinal food plants are plants that provide therapeutic benefits for the consumer in addition to their nutritional benefit (Kazeem *et al.*

2021). The World Health Organization asserted that about two-thirds of the global population (especially in rural areas) depends on medicinal foods and plants for the treatment of their diseases (WHO 2002). This is mainly due to their availability, affordability, efficacy and perceived safety. Studies have also reported the pharmacological potentials of medicinal foods and plants in the treatment and management of several diseases (Nafiu, Salawu and Kazeem 2013; Kazeem and Davies 2016; Sabiu 2022).

Though there are several reviews on the anti-ageing properties of medicinal foods and plants but these are not comprehensive. While many of the studies were conducted on the anti-ageing potentials of specific parts of the plants (Rusu *et al.* 2019; Chen *et al.* 2020), some focused on specific plant products (Bhullar and Wu 2020; Dhanjal *et al.* 2020; Meccariello and D'Angelo 2021; Chen, Wang and Wei 2022) while others presented studies only in specific models (Okoro *et al.* 2021). As such, there is no comprehensive study in the literature that presents an overview of plants and foods that can be used to manage ageing to date. To the best of our knowledge, this is the first paper that synthesizes information on all medicinal plants and foods with anti-ageing properties using different models. It also presents an in-depth review of medicinal foods and plants with anti-ageing properties with a view to guiding future research and development of anti-ageing agents.

2.1.3. Methodology

The available information on anti-ageing properties of medicinal foods and plants was collected via electronic search (using PubMed, SciFinder, Google Scholar, and Web of Science) using the keywords such as 'ageing', 'aging', 'medicinal foods', 'anti-ageing plants', 'anti-aging foods', anti-ageing tea. A library search for articles published in books, including review articles and specific ethnomedical research articles, was also used as a source of information. Reference lists of published research articles were also consulted for relevant data. A total of 268 articles covering between years 2001 and 2022 were obtained from electronic and manual searches. After eliminating duplications and irrelevant ones, 153 articles were used for this study. Our paper excludes all in-silico studies, studies on the anti-ageing potential of polyherbal drugs, clinical trials, as well as all studies on anti-ageing agents of animal or microbial origin.

2.1.4. Experimental models of ageing

Due to the overwhelming nature of ageing and its complications, there are numerous models that have been used in the evaluation of anti-ageing properties of natural products. These are: enzymes' inhibition, yeast, *Caenorhabditis elegans*, *Drosophila melanogaster*, cell lines, and mammalian (mouse and rat) models (Figure 2.1).

2.1.4.1 Enzymatic model

Ageing is a complex biological process that is mediated by many proteins and enzymes (Tlili, Kirkan and Sarikurkcu 2019). Prominent among these enzymes are collagenase, elastase, hyaluronidase and tyrosinase. Collagenase and elastase are involved in the breakdown of collagen (which gives tensile strength) and elastin (which promotes elasticity), respectively, thereby causing wrinkles and severe atrophy on the skin (Jiratchayamaethasakul *et al.* 2020). Hyaluronidase destroys hyaluronic acid (which promotes skin rejuvenation) while tyrosinase plays a crucial role in the rate-limiting step of melanin production (Martel *et al.* 2019). The inhibition of one or more of these enzymes will be an effective approach to prevent or ameliorate the deleterious effects of ageing.

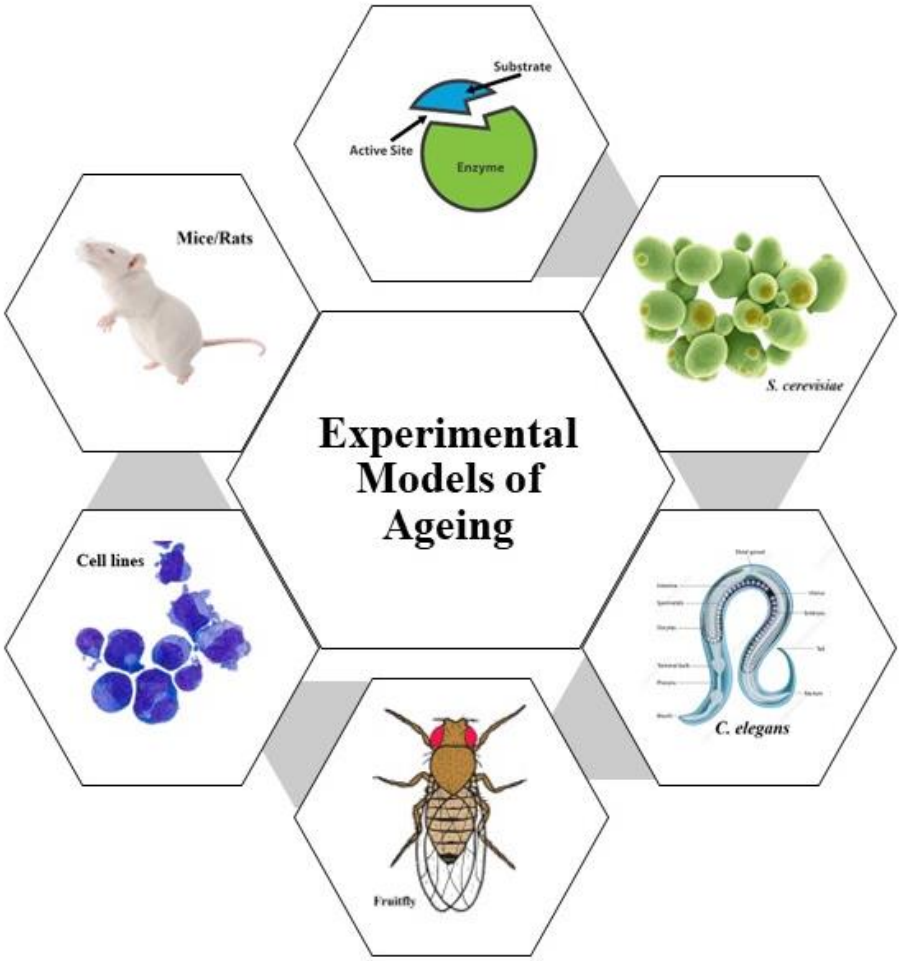

Figure 2.1. Experimental models of ageing.

The inhibitory properties of medicinal foods and plants on the activities of relevant anti-ageing enzymes are presented in Table 2.1. Five of the studies included in this paper tested the inhibitory properties of designated plants on all four enzymes (collagenase, elastase, hyaluronidase and tyrosinase). Of the five studies, two (Ersoy *et al.* 2019; Elgamal *et al.* 2021) presented their results based on the half-maximal inhibitory concentration (IC_{50}). Of the three plants tested in the studies, the essential oil obtained from *Pluchea discoridis* displayed a lower IC_{50} for all the enzymes [collagenase (1.85 µg/mL), elastase (14.63 µg/mL), hyaluronidase (17.18 µg/mL) and tyrosinase (19.52 µg/mL)] (Elgamal *et al.* 2021), which signifies better anti-ageing potential than *Erigeron bonariensis* and *Hypericum* sp (Ersoy *et al.* 2019). Stamen extract of *Nelumbo nucifera* displayed better inhibition of both tyrosinase and collagenase than the whole flower (Tungmunnithum,

Drouet and Hano 2022). *Aquilegia pubiflora* leaf extracts (Jan *et al.* 2021) and *Isodon rugosus* cultures (Abbasi *et al.* 2019) also inhibited the enzymes at varying degrees.

Three studies tested the inhibitory effect of plants on three of the enzymes (collagenase, elastase and hyaluronidase). The aqueous extract of *Cochlospermum vitifolium* leaf displayed potent inhibition of collagenase, elastase and hyaluronidase with IC_{50} values of 708, 5.3 and 0.04 µg/mL, respectively (German-Baez *et al.* 2017). Both the ethanol extract of *Hypericum organifolium* (Boran 2018) and hexane extract of *Ocimum sanctum* (Chaiyana *et al.* 2019) also markedly inhibited the three enzymes. Three studies also presented the effect of plant extracts on the activities of elastase, tyrosinase and hyaluronidase. *Isaria tenuipes* aqueous extract exhibited better inhibition against elastase (IC_{50}: 0.006 µg/mL) and hyaluronidase (IC_{50}: 30.3 µg/mL) (Prommaban *et al.* 2022) compared to *Lagerstroemia speciosa* with IC_{50} values of 6.49 µg/mL and 1880 µg/mL, respectively (Kolakul and Sripanidkulchai 2017). Both plants exhibited a similar effect towards tyrosinase activity, while the results presented for *Thymelaea hirsute* (Amari *et al.* 2021b) were done qualitatively. Also, methanol extract of *Malaxis acuminata* displayed potent anti-ageing activities with IC_{50} values of 35.52, 32.24 and 175.81 µg/mL for collagenase, elastase and tyrosinase, respectively (Bose *et al.* 2017) while the root extract of *Eutrepa japonicum* exhibited better activities than the leaf and flower extracts (Szewczyk *et al.* 2021). In the test for collagenase and elastase only, ethanol extract of *Manilkara zapota* displayed the most potent inhibition of both enzymes with IC_{50} 86.47 and 35.73 µg/mL, respectively (Pientaweeratch, Panapisal and Tansirikongkol 2016).

Table 2.1. Inhibitory properties of medicinal foods and plants on ageing-related enzymes

Scientific name	Common name	Origin	Parts	Extract	Enzymes inhibited	Reference
Alkanna tinctoria L. Tausch	Dyer's bugloss	Palestine	Root	Different solvents	Elastase	(Jaradat *et al.* 2018)
Amygdalus communis	NA	Turkey	Hull	Methanol	Tyrosinase	(Tlili, Kirkan and Sarikurkcu 2019)
Aquilegia pubiflora Wall. Ex Royle	Himalayan columbine	Pakistan	Leaf	Water, ethylacetate, methanol, ethanol	Collagenase, elastase, tyrosinase, hyaluronidase	(Jan *et al.* 2021)
Areca catechu Linn.	NA	Korea	Whole plant	Ethanol	Elastase, hyaluronidase	(Lee *et al.* 2001)
Cassia auriculata Linn.	NA	Sri Lanka	Flower	Hydro-methanol	Tyrosinase	(Napagoda *et al.* 2018)
Cleistocalyx nervosum	Ma Kiang	Thailand	Leaf	Methanol	Tyrosinase	(Manosroi *et al.* 2015)
Cochlospermum vitifolium	Silk-cotton tree	Mexico	Leaf	Water	Collagenase, elastase, hyaluronidase	(German-Baez *et al.* 2017)
Cordyceps militaris (L.) Fr. Link	NA	Thailand	Whole plant	Water	Elastase, tyrosinase, hyaluronidase	(Prommaban *et al.* 2022)
Eutrema japonicum Koidz	Japanese horseradish	Poland	Flower, leaf, root	Methanol-acetone-water	Collagenase, tyrosinase, hyaluronidase	(Szewczyk *et al.* 2021)
Garcinia picrorrhiza Miq.	Sesoot	Indonesia	Fruit	Ethanol	Collagenase, elastase	(Utami *et al.* 2018)
Harungana madagascariens	NA	Cameroon	Stem	Methylene chloride	Elastase, tyrosinase	(Manjia *et al.* 2019a)
Hibiscus sabdarifa	NA	China	Calyx	Water	Collagenase, tyrosinase	(Li *et al.* 2020)
Hypericum organifolium Willd.	NA	Turkey	Aerial part	Ethanol	Collagenase, elastase, hyaluronidase	(Boran 2018)
Hypericum sp.	NA	Turkey	Flower	Methanol	Collagenase, elastase, tyrosinase, hyaluronidase	(Ersoy *et al.* 2019)
Isaria tenuipes Peck	NA	Thailand	Whole plant	Water	Elastase, tyrosinase, hyaluronidase	(Prommaban *et al.* 2022)
Isodon rugosus (Wall. Ex Benth.) Codd.	NA	Pakistan	Seed	Water	Collagenase, elastase, tyrosinase, hyaluronidase	(Abbasi *et al.* 2019)

Lagerstroemia speciosa *Lagerstroemia floribunda*	NA	Thailand	Flower	Ethanol	Elastase, tyrosinase, hyaluronidase	(Kolakul and Sripanidkulchai 2017)
Malaxis acuminata D. Don	Jeevaka	India	Leaf, stem	Methanol	Collagenase, elastase, tyrosinase	(Bose *et al.* 2017)
Manilkara zapota P. Royen	Sapota	Thailand	Fruit	Ethanol	Collagenase, elastase	(Pientaweeratch, Panapisal and Tansirikongkol 2016)
Nelumbo nucifera Gaertn	Sacred lotus	Thailand	Flower	Hydro-ethanol	Collagenase, elastase, tyrosinase, hyaluronidase	(Tungmunnithum, Drouet and Hano 2022)
Ocimum sanctum Linn.	Queen of herb	Thailand	Whole plant	Hexane	Collagenase, elastase, hyaluronidase	(Chaiyana *et al.* 2019)
Phyllantus emblica Linn.	Amla	Thailand	Fruit	Ethanol	Collagenase, elastase	(Pientaweeratch, Panapisal and Tansirikongkol 2016)
Pluchea discoridis (L.) DC *Erigeron bonariensis* Linn.	NA	Egypt	Shoot	Essential oil	Collagenase, elastase, tyrosinase, hyaluronidase	(Elgamal *et al.* 2021)
Psorospermun auranticum	NA	Cameroon	Leaf	Methylene chloride	Elastase, tyrosinase	(Manjia *et al.* 2019a)
Sclerocarya birrea Hochst	Marula	S. Africa	Shoot	Methanol	Collagenase, elastase	(Shoko *et al.* 2018)
Stenoloma chusanum	NA	China	Whole plant	Ethanol	Tyrosinase	(Wu *et al.* 2017)
Thymelaea hirsute (L.) Endl	Methane	Algeria	Leaf, stem, flower	Water	Elastase, tyrosinase, hyaluronidase	(Amari *et al.* 2021a)
Trigonella foenum-graecum	Fenugreek	Thailand	Seed	Ethanol	Collagenase	(Eaknai *et al.* 2022)

NA: Not available, S. Africa: South Africa

Though the inhibitory effect of *Phyllantus emblica* on collagenase is similar to *M. zapota*, it mildly inhibited elastase (IC_{50}: 387.85 µg/mL). However, ethanol extract of *Garcinia picrorrhiza* displayed weak inhibition of collagenase (IC_{50}: 1169.32 µg/mL) and moderate inhibition of the elastase (IC_{50}: 152.93 µg/mL) (Utami *et al.* 2018). Of the three parts of *Sclerocarya birrea* extracts tested, the stem displayed a higher percentage inhibition of both collagenase and elastase (Shoko *et al.* 2018). The extracts of both *Harungana madagascariensis* and *Psorospermun auranticum* had weak inhibition for tyrosinase but strongly inhibited elastase, with *P. auranticum* having an IC_{50} of 15.40 µg/mL (Manjia *et al.* 2019b). Ethanol extract of *Areca catechu* displayed IC_{50} 60.8 and 210 µg/mL for elastase and hyaluronidase, respectively (Lee *et al.* 2001), while *Hibiscus sabdarifa* was not active (Li *et al.* 2020).

Four studies reported only the anti-tyrosinase activity of some medicinal plants and foods. Of all the plants, *Cleistocalyx nervosum* methanol extract (20 µg/mL) displayed the strongest inhibition (Manosroi *et al.* 2015) followed by *Cassia auriculata* hydro-methanol extract (42.49 µg/mL) (Napagoda *et al.* 2018) and *Stenoloma chusanum* petroleum ether fraction (118.6 µg/mL) (Wu *et al.* 2017). Conversely, the methanol extract of *Amygdalus communis* exhibited weak inhibition towards tyrosinase (Tlili, Kirkan and Sarikurkcu 2019). A study on the anti-elastase property of *Alkanna tinctoria* revealed that the acetone extract possessed the best activity with an IC_{50} of 10.02 µg/mL (Jaradat *et al.* 2018) while ethanol extract of *Trigonella foenum-graecum* seed exhibited moderate inhibition of collagenase activity (IC_{50}: 560 µg/mL) (Eaknai *et al.* 2022).

2.1.4.2. Saccharomyces cerevisiae (yeast)

The anti-ageing properties of medicinal foods and plants in yeast are shown in Table 2.2. Treatment of K6001 yeast with ethanol leaf extract of *Humulus japonicus* and methanol extract of *Haberlea rhodopensis* extended the lifespan of the yeast by 22 and 30%, respectively (Georgieva *et al.* 2015; Sung *et al.* 2015). Comparative evaluation of the anti-ageing properties of hesperidin (Fig. 2.2a) and hesperetin (Fig. 2.2b) isolated from citrus fruits revealed that only hesperidin extended the lifespan of the K6001 yeast by about 37% (Sun *et al.* 2012). The study also revealed that hesperidin repressed the UTH1 gene while activated SOD gene and Sir2 signalling pathway (Sun *et al.* 2012). In a related study, sesquiterpene glucosides isolated from *Prunus persica* fruits increased the lifespan of the yeast by a quarter and improved its survival under oxidative stress.

Table 2.2. Anti-ageing properties of medicinal foods and plants in *Saccharomyces cerevisiae*

Scientific name	Common name	Parts	Extract/Compound	Dose	ΔLifespan%	Reference
Citrus species	Citrus	Fruit	Hesperidin	10 μM	36.93	(Sun *et al.* 2012)
Haberlea rhodopensis	NA	Leaf	Methanol	1.0 mg/mL	29.50	(Georgieva *et al.* 2015)
Humulus japonicus	Japanese hop	Leaf	Ethanol	20 μg/mL	22.22	(Sung *et al.* 2015)
Onosma bracteatum Wall	NA	Whole plant	Allomicrophyllone	3.0 μM	30.53	(Farooq *et al.* 2019)
			Ehretiquinone	3.0 μM	28.90	
			Ehretiquinone C	1.0 μM	38.67	
			Ehretiquinone D	1.0 μM	29.17	
Prunus persica	Honey Peach	Fruit	Glucosides	7.5 μM	24.93	(Wang *et al.* 2017)

NA: Not available

Four benzoquinone derivatives namely allomicrophyllone (Fig. 2.2c), ehretiquinone (Fig. 2.2d), ehretiquinone C and ehretiquinone D displayed good anti-ageing properties by extending the lifespan of the yeast but ehretiquinone C exhibited the strongest activity with 38% lifespan extension (Farooq *et al.* 2019).

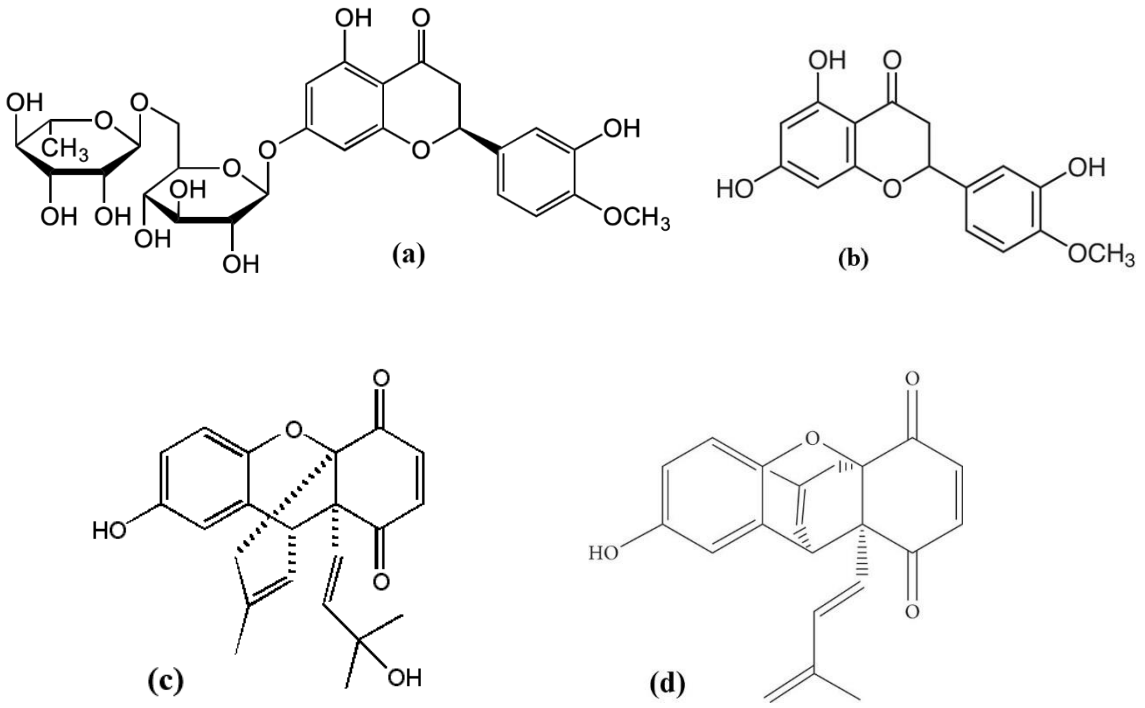

Figure 2.2. Structures of chemical compounds tested for anti-ageing properties in yeast model. (a) Hesperidin (b) Hesperetin (c)Allomicrophyllone and (d) Ehretiquinone (Farooq et al., 2019)

2.1.4.3 Caenorhabditis elegans model

Caenorhabditis elegans is a small (about 1 mm in length and 80 µm in diameter), eukaryotic, and saprophytic nematode that feeds on bacteria such as *E. coli* (Zheng and Greenway 2012). It has a life cycle of about 3 days and can live in the laboratory for about 3 weeks at 20°C (Markaki and Tavernarakis 2020). It is a non-pathogenic animal that exists mostly as hermaphrodites and produces more than 300 offspring within a short period (Markaki and Tavernarakis 2010). This model is suitable for ageing research due to its short life cycle, short generation time, ease, and low maintenance cost in the laboratory (Leung *et al.* 2008). Its transparent body and possession of many organs found in mammals, as well as withstanding indefinite storage in -80°C freezer or liquid nitrogen, encourages researchers to use it to study ageing and related diseases (Giunti *et al.* 2021).

Table 2.3 shows the anti-ageing properties of medicinal foods and plants in *C. elegans*. Treatment of *C. elegans* worms with aqueous extracts of *Acanthopanax sessiliflorus*, *Calycophyllum spruceanum* (Peixoto *et al.* 2018), *Glycyrrhizae radix* (Ruan *et al.* 2016) and *Polygonum multiflorum* (Saier *et al.* 2018) extended the lifespan of the worms by 17.40, 16.00, 11.76, and 18.60%, respectively. Ethanol extracts of *Betula utilis* bark (Pandey *et al.* 2020), *Paeonia suffruticosa* flower (Wang *et al.* 2020b) and *Streblus asper* leaves (Prasansuklab *et al.* 2017) prolonged the lifespan of the worms by 36, 16.5, and 3.5%, respectively. Methanol extracts of *Cuscuta chinensis* seeds (Sayed *et al.* 2021a), *Eucommia ulmoides* bark (Sayed *et al.* 2021a) and *Glochidon zeylanicum* leaf also extended the lifespan of *C. elegans* by 24.35, 9.28, and 10%, respectively. Treatment of the worms with butanol extracts of *Damnacathus officinarum* root (Yang *et al.* 2012) and *Platycladus orientalis* (Liu *et al.* 2013) seed increased their lifespan by 17.24 and 24.54%, respectively. However, ethyl acetate extracts of both *Portulaca oleracea* (Zhang *et al.* 2020) and *Ribes fasciculatum* (Jeon and Cha 2016) produced a 16% increase in the lifespan of the worms. Essential oil from *Juniperus communis* (Pandey *et al.* 2018), *Olea europea* (Cañuelo *et al.* 2012) and *Trachyspermum ammi* (Rathor *et al.* 2017) prolonged the lifespan of the worms by 19, 21, and 12%, respectively. Polysaccharides from *Bletilla striata* (Zhang *et al.* 2015), *Cordyceps militaris* (Liu *et al.* 2016), *Panax notoginseng* (Feng *et al.* 2019) and *Sophora moocroftiana* (Zhang *et al.* 2018) makes the worms live longer by 16.67, 16.58, 21.70, and 67%, respectively.

Table 2.3. Anti-ageing properties of medicinal foods and plants in *Caenorhabditis elegans*

Scientific name	Common name	Parts	Extract/Compound	Dose	ΔLongevity (%)	Reference
Acanthopanax sessiliflorus	Acanthopanax	Stem	Aqueous	500 µg/mL	17.40	(Park *et al.* 2014)
Arctium lappa	Burdock	Seed	Lignans	100 µM	25.00	(Su and Wink 2015)
Mongholicus bunge	Huangqi	Leaf	Calycosin	200 µM	21.42	(Lu *et al.* 2017)
Betula utilis	Silver birch	Bark	Ethanol	50 µg/mL	35.99	(Pandey *et al.* 2020)
Bletilla striata	NA	Whole plant	Polysaccharide	50 µg/mL	16.67	(Zhang *et al.* 2015)
Calycophyllum spruceanum	Tree of youth	Stem bark	Aqueous	300 µg/mL	16.00	(Peixoto *et al.* 2018)
Citrus medica	Finger citron	Fruit	Flavonoids	200 µg/mL	31.26	(Luo *et al.* 2020)
Cordyceps militaris	NA	Whole plant	Polysaccharide	250 µg/mL	16.58	(Liu *et al.* 2016)
Cuscuta chinensis	Chinese dodder	Seed	Methanol	30 µg/mL	24.35	(Sayed *et al.* 2021b)
Damnacathus officinarum	DOH	Root	n-butanol	800 µg/mL	17.24	(Yang *et al.* 2012)
Eucommia ulmoides	Chinese rubber	Bark	Methanol	30 µg/mL	9.28	(Sayed *et al.* 2021b)
Eugenia uniflora L.	Purple pitanga	Fruit	Phenolics	500 µg/mL	16.67	(Tambara *et al.* 2018)
Fagopyrum esculentum	Buckwheat	Seed	Trypsin inhibitor	10 µM	21.20	(Li *et al.* 2015)
Glochidon zeylanicum	Man pu	Leaf	Methanol	100 µg/mL	10.01	(Duangjan *et al.* 2019)
Glycine max	Soybean	Seed	Fermented	500 µg/mL	16.44	(Ibe *et al.* 2013)
Glycyrrhizae radix	NA	Whole plant	Aqueous	240 µg/mL	11.76	(Ruan *et al.* 2016)
Juniperus communis	Juniper berry	Fruit	Oil	10 µg/mL	18.54	(Pandey *et al.* 2018)
Lithocarpus polystachyrus	NA	Leaf	Trilobatin	250 µM	22.10	(Li *et al.* 2021b)

Malus domestica	Apple	Whole plant	Acetone	10000 μg/mL	39.60	(Vayndorf, Lee and Liu 2013)
Olea europea L.	Olive	Fruit	Oil	250 μM	21.13	(Cañuelo *et al.* 2012)
Paeonia suffruticosa And.	Tree peony	Flower	Ethanol	150 μg/mL	16.47	(Wang *et al.* 2020b)
Panax notoginseng	Notoginseng	Root	Polysaccharides	500 μg/mL	21.70	(Feng *et al.* 2019)
Phyllantus emblica	NA	Fruit	Polyphenols	800 μg/mL	18.53	(Wu *et al.* 2022)
Pinus densiflora	Pinus	Leaf	Dehydroabietic acid	10 μM	15.50	(Kim *et al.* 2015)
Platycladus orientalis L.	Chinese thuja	Seed	n-butanol	500 μg/mL	24.54	(Liu *et al.* 2013)
Polygonum multiflorum	NA	Whole plant	Aqueous	1000 μg/mL	18.60	(Saier *et al.* 2018)
Portulaca oleracea	Global panacea	Whole plant	Ethyl acetate	1000 μg/mL	16.47	(Zhang *et al.* 2020)
Ribes fasciculatum	NA	Stem	Ethyl acetate	500 μg/mL	16.30	(Jeon and Cha 2016)
Rosa rugosa	NA	Flower	Tea	200 μg/mL	38.10	(Zhang *et al.* 2019)
Scutellaria baicalensis	Baical skullcap	Leaf	Baicalein	100 μM	15.78	(Havermann, Humpf and Wätjen 2016)
Sesamum indicum L	Sesame	Seed	Peptide	12.5 μg/mL	15.60	(Wang *et al.* 2016)
Silybum marianum	Milk thistle	Fruit	2,3-dehydrosilybin	10 μM	16.09	(Filippopoulou *et al.* 2017)
Sophora moocroftiana	NA	Seed	Polysaccharides	4000 μg/mL	66.90	(Zhang *et al.* 2018)
Syzygium cumini	NA	Leaf	Beta-caryophyllene	50 μM	22.70	(Pant *et al.* 2014)
Stereospermum suaveolens	NA	Aerial part	Verminoside	25 μM	20.79	(Pant *et al.* 2015)
Streblus asper	NA	Leaf	Ethanol	50 μg/mL	3.49	(Prasansuklab *et al.* 2017)
Trachyspermum ammi	Carom	Seed	Oil	10 μg/mL	12.45	(Rathor *et al.* 2017)
Zanthoxylum aromatum	Indian thorny ash	Fruit	Tambulin	50 μM	16.80	(Pandey *et al.* 2019)

Evaluation of the anti-ageing properties of lignans (Fig. 2.3) isolated from *Arctium lappa* seeds revealed that the six isolated compounds have varying anti-ageing effects (Su and Wink 2015). While the lifespan-enhancing effect of arctigenin, arctiin, iso-lappaol A, lappaol C, and lappaol F ranges from 11.2 to 15.2%, and are not significantly different from one another, matairesinol elicited a 25% increase in the lifespan of *C. elegans*. Further study also showed that these lignans upregulated the expression of both Dauer abnormal formation-16 (DAF-160) and c-Jun N-terminal kinase 1 (JNK-1), thereby promoting stress resistance and longevity (Su and Wink 2015). Calycosin (isolated from *Mongholicus bunge*) (Lu *et al.* 2017) (Fig. 2.4a), trilobatin (isolated from *Lithocarpus polystachyrus*) (Li *et al.* 2021b) (Fig. 2.4b), beta-caryophyllene (isolated from *Syzygium cumini*) (Pant *et al.* 2014) (Fig. 2.4f) and verminoside (isolated from *Stereospermum suaveolens*) (Pant *et al.* 2015) (Fig. 2.4g) caused a similar extension (about 22%) in the lifespan of the worm via modulation of the DAF-16 pathway. A decreased effect (about 16%) in the lifespan change of the worms resulted from the influence of dehydroabietic acid (Fig. 2.4c) (Kim *et al.* 2015), baicalein (Fig. 2.4d) (Havermann, Humpf and Wätjen 2016), 2,3-dehydrosilybin (Fig. 2.4e) (Filippopoulou *et al.* 2017) and tambulin (Fig. 2.4h) (Pandey *et al.* 2019) by affecting the sirtuin 1 (SIRT1), Skinhead-1 (SKN-1) and DAF-16 respectively. Phenolic extracts from *Eugenia uniflora* (Tambara *et al.* 2018) and *Phyllantus emblica* (Wu *et al.* 2022) elicited 16.67 and 18.53% extension in the lifespan of the worm, respectively, while that of *Citrus medica* (Luo *et al.* 2020) prolonged their lifespan by 31.26%.

It is noteworthy that of all the samples tested for their anti-ageing properties, polysaccharides extracted from the seeds of *Sophora moocroftiana* elicited the highest increase (67%) in the lifespan of the worms. This is then followed by the duo of acetone extract of *Malus domestica* (40%) and tea made from the flowers of *Rosa rugosa* (38%), respectively. The anti-ageing activities of these plants were attributed to many mechanisms, including the antioxidant effect (Ibe *et al.* 2013; Luo *et al.* 2020), heat shock resistance (Park *et al.* 2014; Wu *et al.* 2022), hormesis (Cañuelo *et al.* 2012; Sayed *et al.* 2021a), neuroprotection (Yang *et al.* 2012) and upregulation of the insulin-like signaling pathway (Li *et al.* 2015; Ruan *et al.* 2016).

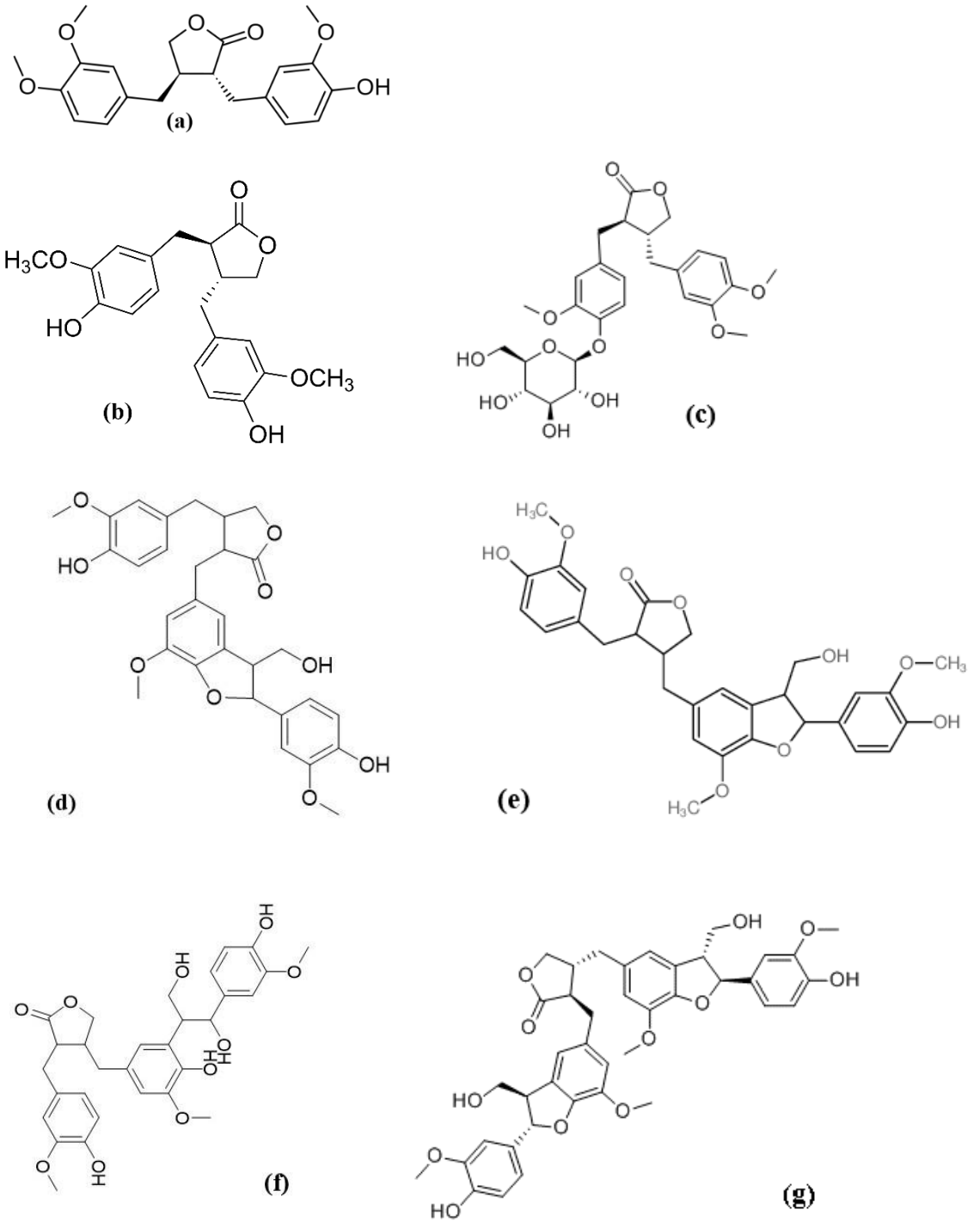

Figure 2.3. Structures of anti-ageing chemical compounds isolated from *Arctium lappa* seeds (a) Arctigenin (b) Matairesinol (c) Arctiin (d) Iso-lappaol A (e) Lappaol A (f) Lappaol C and (g) Lappaol F (Su and Wink, 2015).

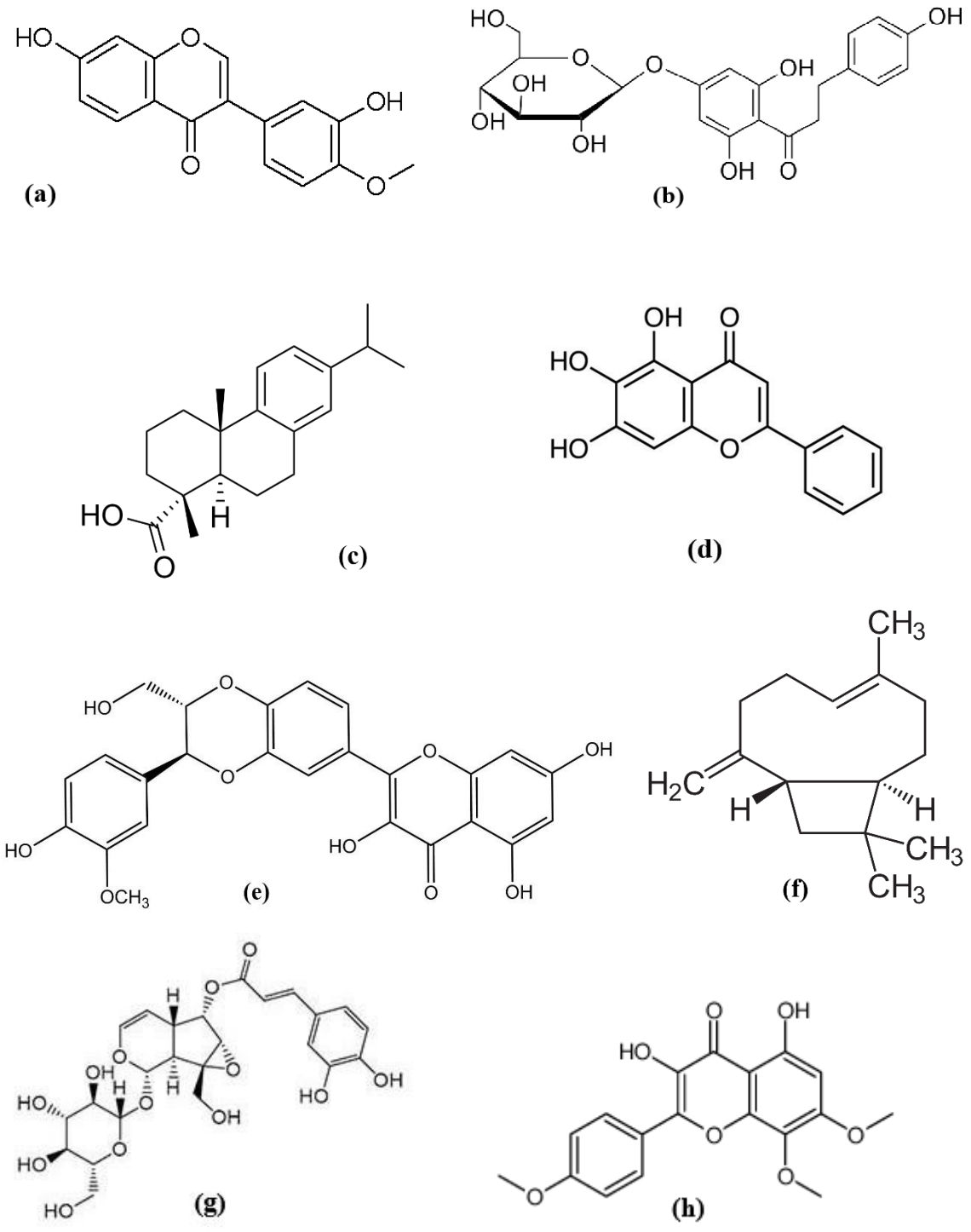

Figure 2.4. Structures of chemical compounds tested for anti-ageing properties in *Caenorhabditis elegans* model. (a) Calycosin (b) Trilobatin (c) Dehydroabietic acid (d) Baicalein (e) 2, 3-dehydrosilybin (f) Beta-caryophyllene (g) Verminoside and (h) Tambulin.

2.1.4.4 Drosophila melanogaster (fruit fly) model

Drosophila melanogaster, commonly known as the fruit fly, is a small fly characterized by compound eyes and wings (Jennings 2011). It has a lifespan of approximately 40 – 120 days, depending on its diet and environment, while it has a generation time of about 10 – 12 days (Abolaji *et al.* 2013). Though humans and fruit flies are not similar, important biological mechanisms that regulate development and survival are conserved between the species (Jennings 2011). Similarly, about 65% of human disease-associated genes have a homolog in Drosophila, making it easy to study genetic pathways in humans (Bilder and Irvine 2017). *Drosophila melanogaster* is a veritable model for the study of ageing with ease of use and manipulation, simple genome, short generation time at room temperature, cheap and easy to maintain as a result of the small body size and lifespan (Abolaji *et al.* 2013).

Table 2.4 reveals the anti-ageing properties of medicinal foods and plants in *Drosophila melanogaster*. Inclusion of aqueous extract of *Ipomoea batata* (Han *et al.* 2021) and *Panax notoginseng* (Han *et al.* 2021) in the diet of *D. melanogaster*, increased their longevity by more than 14%. Similarly, 3% ethanol extract of *Ganoderma sinense* fruits and *Panax notoginseng* caused a minute (2.7%) rise in the longevity of the flies (Teseo *et al.* 2021). Supplementation of the fruit fly diet with *Lycium barbarum* polysaccharide (Tang *et al.* 2019) and *Ludwigia octovalvis* ethanol extract (Lin *et al.* 2014) extended their lifespan by about 16%. Further analysis revealed that both samples displayed their anti-ageing potential through their antioxidant capacities. Ethanol extracts of *Lasia spinosa* stem (Men *et al.* 2021) and *Zingiber officinale* rhizome (Zhou *et al.* 2018) when included in the diet of the fruit fly also increased the longevity of the flies by 23% and 7%, respectively.

Supplementation of the fruit fly diet with 0.5 mg/mL of xanthohumol (isolated from *Humulus lupulus* Linn.) (Fig. 2.5a) increased the lifespan of the flies by 15% (Wongchum and Dechakhamphu 2021). It also increased the survival of the flies after exposure to toxicants (hydrogen peroxide and paraquat). Bioassay-guided isolation of the anti-ageing bioactive compounds from *Platanus orientalis* (Chatzigeorgiou *et al.* 2017) yielded two compounds, namely tiliroside (Fig. 2.5b) and platanoside (Fig. 2.5c). Enrichment of the fruit fly diet with both compounds decreased oxidative stress, while tiliroside increased their longevity by about 15% and mitigated the age-related reduction in locomotive activity. Further study revealed that tiliroside

upregulated genes involved UPS, chaperone, and antioxidant responses (Chatzigeorgiou *et al.* 2017).

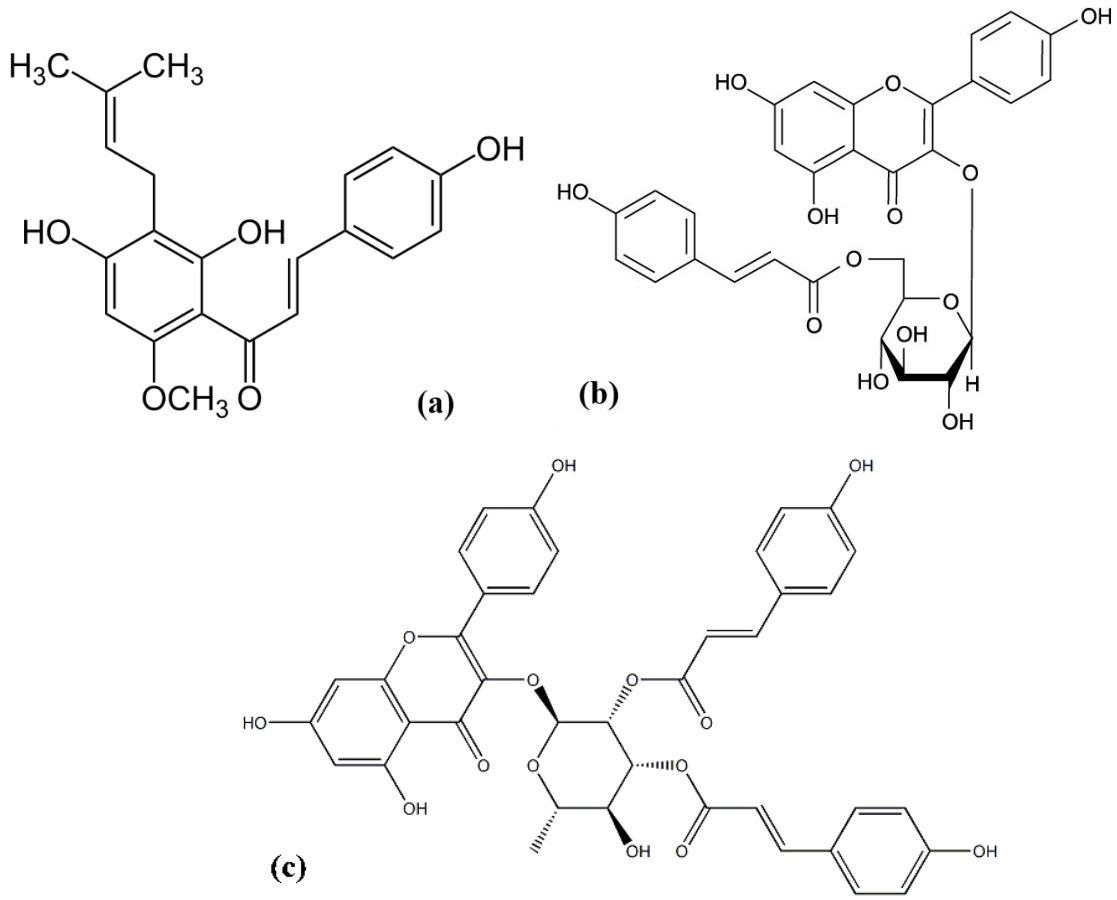

Figure 2.5. Structures of chemical compounds tested for anti-ageing properties in *Drosophila melanogaster*. (a) Xanthohumol (b) Tiliroside and (c) Platanoside (Chartzigeorgiou et al., 2017).

Table 2.4. Anti-ageing properties of medicinal foods and plants in *Drosophila melanogaster*

Scientific name	Common name	Parts	Extract/Compound	Concentration	ΔLongevity (%)		Reference
					Male	Female	
Euterpe oleracea Mart	Acai palm	Fruit	Water	2.0%	22.00	ND	(Sun *et al.* 2010)
Ganoderma sinense	NA	Fruit	Ethanol.	3.0%	2.70	ND	(Teseo *et al.* 2021)
Humulus lupulus Linn.	NA	Whole plant	Xanthohumol	0.5 mg/mL	14.89	ND	(Wongchum and Dechakhamphu 2021)
Ipomoea batata Linn.	Purple sweet potato	Tuber	Water	2 mg/mL	14.50	ND	(Han *et al.* 2021)
Lasia spinosa	NA	Stem	Ethanol	0.5 mg/mL	22.90	ND	(Men *et al.* 2021)
Ludwigia octovalvis	NA	Whole plant	Ethanol	0.1 mg/mL	16.10	24.20	(Lin *et al.* 2014)
Lycium barbarum	NA	Fruit	Polysaccharide	0.04%	16.20	19.20	(Tang *et al.* 2019)
Panax notoginseng	Red ginseng	Root	Water	0.025 mg/mL	14.35	8.18	(Lee *et al.* 2019)
Panax notoginseng	Red ginseng	Root	Ethanol	3.0%	2.70	ND	(Teseo *et al.* 2021)
Platanus orientalis	Plane tree	Fruit	Tiliroside	0.1 mg/mL	14.71	ND	(Chatzigeorgiou *et al.* 2017)
Zingiber officinale	Ginger	Rhizome	Ethanol	2 mg/mL	7.30	ND	(Zhou *et al.* 2018)

NA: Not available, ND: Not determined

2.1.4.5. In vitro cell culture model

The anti-ageing effects of medicinal foods and plants using cell culture are depicted in Table 2.5. Aqueous extracts of *Haberlea rhodopensis* (Dell'Acqua and Schweikert 2012) and *Terminalia chebula* (Manosroi *et al.* 2010) as well as the methanol extract of *Tagetes erecta* (Kang, Rhie and Kim 2018) displayed anti-ageing properties in a fibroblast by increasing the collagen content and reducing matrix metalloproteinase-2 activity. Aqueous extract of *Camellia japonica* (Mizutani and Masaki 2014a) and ethanol extract of *Sambucus nigra* (Lin *et al.* 2019) also reduced ageing in the keratinocyte by decreasing reactive oxygen species (ROS) and matrix metalloproteinase-1 activity, respectively. In addition, *Citrus bergamia* juice reduced cellular senescence in the cardiomyocyte (Da Pozzo *et al.* 2018) while ethanol extracts of *Andrographis paniculata* increased the level of proliferation of the human epidermal skin stem cells (You *et al.* 2015).

Six compounds (antcin A, antcin B, antcin C, antcin H, antcin K and antcin M), isolated from *Antrodia salmonea* (Fig. 2.6a-f), were subjected to anti-ageing assays (Senthil *et al.* 2016). Preliminary toxicity screening revealed that antcin A, antcin C and antcin M showed no significant cytotoxicity towards the human normal dermal fibroblast (HNDF). However, treatment of antcin A, antcin C and antcin M in high-glucose-induced cellular senescence in the HNDF revealed that only antcin M (Fig. 2.6f) displayed significant protection while others showed moderate inhibition. The study also showed that the mechanism of anti-ageing action of antcin M is the activation of Nrf-2 and Sirt-1 pathways (Senthil *et al.* 2016). Similarly, rutin (Fig. 2.7a), halleridone (Fig. 2.7b) and hydroxytyrosol (Fig. 2.7c) isolated from *Cornus sanguinea* counteracted hydrogen peroxide-induced cellular senescence in both human dermal and gingival fibroblasts (Iannuzzi *et al.* 2021). However, only halleridone reduced the gene expression of pro-inflammatory cytokine, IL-6 in the cells.

Three polymethoxyflavones [5,7-dimethoxyflavone (Fig. 7e), 5,7,4′-trimethoxyflavone (Fig. 2.7f), and 3,5,7,3′,4′-pentamethoxyflavone (Fig. 7g)] isolated from *Kaemferia parviflora* rhizome suppressed cellular senescence and ROS in primary human dermal fibroblasts by upregulating the expression of lamin B1 (Klinngam *et al.* 2022). Isoparvifuran (Fig. 2.7d) purified from *Dalbergia odorifera* also mitigated cellular senescence while encouraging cell proliferation in the fibroblast by activating SIRT1 and inhibiting Akt/mTOR signalling pathway (Yin, Park and Choi 2020). In another study, β-sitosterol (Fig. 2.7h) and vermicularin (Fig. 2.7i) isolated from *Thamnolia*

vermicularis displayed anti-ageing property (Haiyuan *et al.* 2019b). While β-sitosterol promoted the biosynthesis of hyaluronic acid by increasing the expression of hyaluronic acid synthase, vermicularin reduced the ROS and matrix metalloproteinase-1 activity.

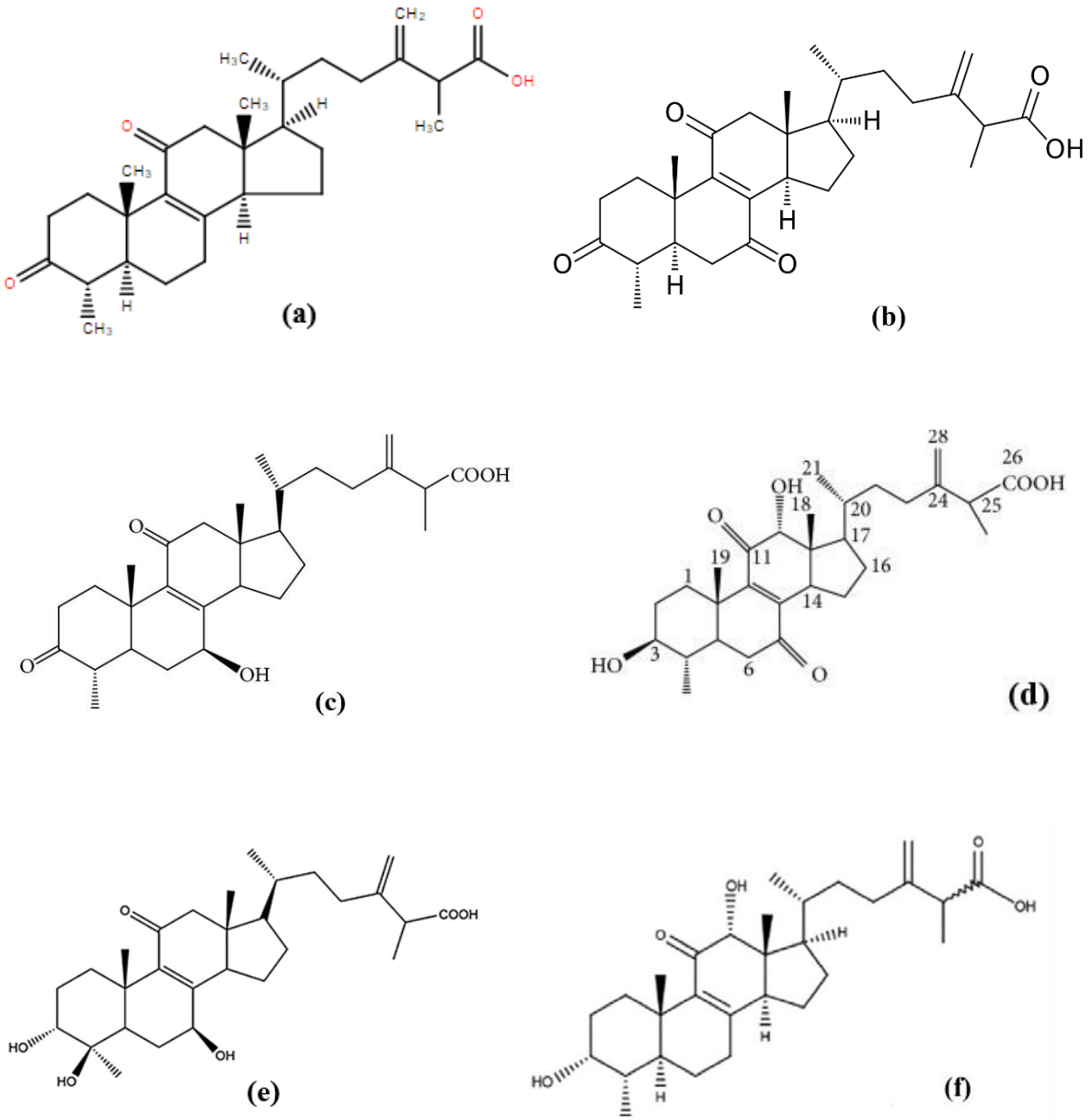

Figure 2.6. Structures of anti-ageing chemical compounds isolated from *Antrodia cinnamomea.* (a) Antcin A (b) Antcin B (c) Antcin C (d) Antcin H (e) Antcin K and (f) Antcin M (Senthil et al., 2016).

Table 2.5. Anti-ageing properties of medicinal foods and plants in cell line models

Scientific name	Common name	Parts	Extract/Compound	Cell type	Effects	Reference
Andrographis paniculata	King of bitters	Whole plant	Ethanol	EpSC	↑Proliferation; ↑Integrin β1	(You *et al.* 2015)
Antrodia salmonea	NA	Whole plant	Antcins	Fibroblast	↑Proliferation; ↓ROS	(Senthil *et al.* 2016)
Camellia japonica	Yabu-tsubaki	Leaf	Water	Keratinocyte	↓ROS; ↓Cell damage	(Mizutani and Masaki 2014b)
Citrus bergamia	Bergamot	Fruit	Juice	Cardiomyocyte	↓Cellular Senescence	(Da Pozzo *et al.* 2018)
Cornus sanguinea	Common dogwood	Drupe	Rutin	Fibroblasts	↓ROS; ↓Cellular Senescence	(Iannuzzi *et al.* 2021)
		Drupe	Halleridone	Fibroblasts	↓Cellular Senescence; ↓IL6	
		Drupe	Hydroxytyrosol	Fibroblasts	↓Cellular Senescence	
Dalbergia odorifera	Chinese rosewood	Heartwood	Isoparvifuran	Fibroblast	↓Senescence; ↑Proliferation	(Yin, Park and Choi 2020)
Haberlea rhodopensis	Resurrection plant	Whole plant	Water	Fibroblast	↑Collagen; ↑Elastin	(Dell'Acqua and Schweikert 2012)
Kaemferia parviflora	Thai black ginger	Rhizome	Polymethoxyflavones	Fibroblast	↓Senescence; ↓ROS	(Klinngam *et al.* 2022)
Sambucus nigra	Elderberry	Fruit	Ethanol	Keratinocyte	↓MMP-1; ↓Inflammation	(Lin *et al.* 2019)
Tagetes erecta	Marigold	Whole plant	Methanol	Fibroblast	↑Collagen; ↓MMP-2	(Kang, Rhie and Kim 2018)
Terminalia chebula	NA	Gall	Water	Fibroblast	↑Proliferation; ↓MMP-2	(Manosroi *et al.* 2010)
Thamnolia vermicularis	NA	Whole plant	β-sitosterol	Fibroblast	↑Hyaluronic acid synthase	(Haiyuan *et al.* 2019a)
Thamnolia vermicularis	NA	Whole plant	Vermicularin	Fibroblast	↓ROS; ↓MMP-1	

↑: Increase, ↓: Decrease, NA: Not available, EpSC: Epidermal skin cell, ROS: Reactive oxygen species, IL-6: Interleukin-6, MMP-1: Matrix metalloproteinase-1, MMP-2: Matrix metalloproteinase-2

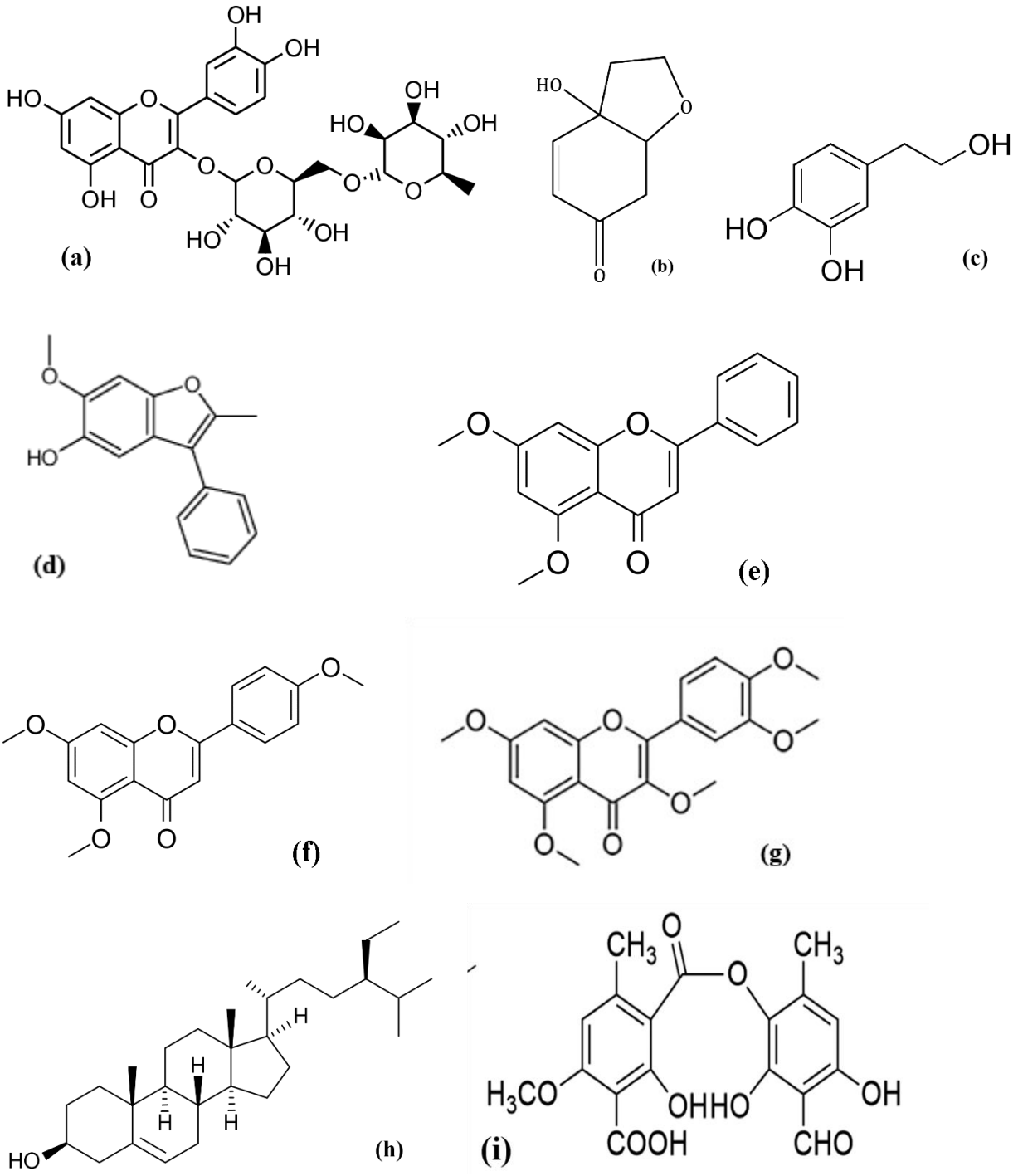

Figure 2.7. Structures of chemical compounds tested for anti-ageing properties in cell line models. (a) Rutin (b) Halleridone (c) Hydroxytyrosol (d) Isoparvifuran (e) 5,7-dimethoxyflavone (f) 5,7,4'-trimethoxyflavone (g) 3,4,5,7,4'-pentamethoxyflavone (h) β-sitosterol (i) Vermicularin.

2.1.4.6. Mouse model

The therapeutic potentials of medicinal foods and plants in galactose-induced ageing in mice are depicted in Table 6. Administration of 1.0% aqueous extract of *Hibiscus syriacus* (Yang *et al.* 2019) and ethanol extract of *Alchemilla mollis* (Hwang *et al.* 2018b) to UVB-induced photoaging in hairless mice improved the erythema index and melanin content while reducing the level of wrinkles, respectively. Supplementation of diets with *Prunus domestica* and *Aronia melanocarpa* fruits for 8 weeks reduced the levels of both advanced glycation end products (AGE) and malondialdehyde (MDA) while they increased the expression of Nuclear factor erythroid-2-related factor-2 (Nrf2) and Nuclear factor kappa B (Nf-κB) in D-galactose-induced aged mice (Jeong, Liu and Kim 2017). Administration of *Anectochilus roxburghii* ethanol extract (490 mg/kg) also improved memory and antioxidant enzymes (superoxide dismutase and glutathione peroxidase) levels in D-galactose-induced aged mice (Wang *et al.* 2020a).

Phenolic extract (200 mg/kg) of *Nephelium lappaceum* peels boosted the antioxidant status of the D-galactose-induced aged mice (Zhuang *et al.* 2017) while aqueous extract (300 mg/kg) of *Caulerpa racemose* increased the Peroxisome proliferator-activated receptor-gamma coactivator-1 alpha (PGC-1α) of the animals (Permatasari *et al.* 2021). Increased serum PGC-1α is correlated with improved antioxidant capacity and anti-ageing capacity. Administration of both *Coeloglossum viride* aqueous extract and fermented wheat to chemically induced aged rats improved the memory of the animals (Zhong *et al.* 2019b; Zhao *et al.* 2021). Long-term administration of both the phenolic extract of *Olea europaea* fruit and *Morus alba* ethanol extract improved the memory and neuronal function in the treated mice (Kim and Oh 2013; Luceri *et al.* 2017). Expectedly, *Syzygium aromaticum* ethanol extract reduced the wrinkles of the hairless mice's skin and improved skin parameters such as elastin (Hwang *et al.* 2018a).

Besides extracts and plant formulations, secondary metabolites such as dioscorin (Fig. 2.8a) isolated from *Dioscorea alata* were tested for anti-ageing properties in D-galactose-induced ageing in mice (Han *et al.* 2014). Five-week administration of dioscorin (80 mg/kg) reduced the latency of the animals as well as the concentration of AGE and MDA (Han *et al.* 2014). Thirty-day oral administration of 20 μM tetrahydrostilbene glucoside (TSG) (Fig. 2.8b) isolated from *Polygonatum multiflorum* improved the memory and lifespan of SAMP8 mice and reduced the level of insulin receptors (Zhou *et al.* 2015). Molecular analysis revealed that the anti-ageing

activity of TSG is due to the modulation of the neural insulin and insulin-like growth factor-1 signalling. Oral administration of aloin (Fig. 2.8c) improved the memory of D-galactose-induced aged mice as well as attenuated the levels of oxidative stress and inflammation caused by ageing (Zhong *et al.* 2019a). This is mediated by down-regulation of the ERK, p38 and NF-κB sigalling pathway. Dietary supplementation of Cyanidin-3-diglucoside-5-glucoside (CY3D5G) (Fig. 2.8d) obtained from *Brassica oleracea* leaf improved the antioxidant status of D-galactose-induced aged mice after 6 weeks of treatment (Zhang *et al.* 2021) by elevating the expression of proteins in glycolysis, Citric acid cycle and actin cytoskeleton. Nordihydroguaiaretic acid (NDGA) (Fig. 2.8e) supplemented in the diet of aged mice, extended the lifespan of the animals, reduced tumour growth rate while it increased tumour formation (Spindler *et al.* 2015).

Table 2.6. Anti-ageing properties of medicinal foods and plants in galactose-induced ageing in mice

Scientific name	Common name	Parts	Extract	Dose (Duration)	Effects	Reference
Alchemilla mollis	Lady's mantle	Leaf	Ethanol	1.0% (70 d)	↓Erythema index; ↓Wrinkle	(Hwang *et al.* 2018b)
Aloe sp.	NA	Leaf	Aloin	30 mg/kg bw (56 d)	↑Memory; ↓MDA; ↓TNF-α	(Zhong *et al.* 2019a)
Anectochilus roxburghii	King of medicines	Whole plant	Ethanol	490 mg/kg bw (30 d)	↑Memory; ↑GSH-Px; ↑SOD	(Wang *et al.* 2020a)
Aronia melanocarapa	Chokeberry	Fruit	Diet	1.0% (56 d)	↓AGE; ↓MDA; ↑Nrf2; ↑Nf-κB	(Jeong, Liu and Kim 2017)
Brassica oleracea	Red cabbage	Leaf	CY3D5G	150 mg/kg bw (42 d)	↓MDA; ↑T-AOC; ↑GSH-Px	(Zhang *et al.* 2021)
Caulerpa racemose	Seagrape	Fruit	Water	300 mg/kg bw (28 d)	↓Glucose; ↑PGC-1α	(Permatasari *et al.* 2021)
Coeloglossum viride	Zangla wangla	Tuber	Water	5 mg/kg bw (15 d)	↑Memory; ↑BDNF; ↓TNF-α	(Zhong *et al.* 2019b)
Dioscorea alata Linn	Yam	Tuber	Dioscorin	80 mg/kg bw (42 d)	↓AGE; ↓Latency; ↓MDA	(Han *et al.* 2014)
Hibiscus syriacus Linn.	Rose of Sharon	Root	Water	1.0% (28 d)	↑Erythema index; ↑Melanin	(Yang *et al.* 2019)
Larrea tridentate	Creosote bush	Leaf	NDGA	3.5 mg/kg bw (1400 d)	↑Lifespan; ↑Tumourigenesis	(Spindler *et al.* 2015)
Morus alba Linn.	Mulberry	Fruit	Ethanol	500 mg/kg bw (7 d)	↑Memory; ↑Neuronal function	(Kim and Oh 2013)
Nephelium lappaceum	Rambutan	Peel	Phenolics	200 mg/kg bw (45 d)	↓MDA; ↑T-AOC; ↑GSH-Px	(Zhuang *et al.* 2017)
Olea europaea	Olive	Fruit	Phenolics	6 mg/kg bw (180 d)	↑Memory; ↑Neuronal function	(Luceri *et al.* 2017)
Polygonatum multiflorum	NA	Whole plant	TSG	20 μM (30 d)	↑Memory; ↑Lifespan; ↓Klotho	(Zhou *et al.* 2015)
Prunus domestuca Linn.	Plum	Fruit	Diet	10% (56 d)	↓AGE; ↓MDA; ↑Nrf2; ↑Nf-κB	(Jeong, Liu and Kim 2017)
Syzygium aromaticum	Clove	Fruit	Ethanol	1.0% (56 d)	↓Wrinkle; ↑TGF-β1; ↑Elastin	(Hwang *et al.* 2018a)
Triticum aestivum	Wheat	Seed	Fermented wheat	20 mg/kg bw (42 d)	↑Memory; ↓TG; ↓TC; ↓MDA	(Zhao *et al.* 2021)

↑: Increase, ↓: Decrease, NA: Not available, TSG: Tetrahydrostilbene glucoside, CY3D5G: Cyanidin-3-diglucoside-5-glucoside, NDGA: Nordihydroguaiaretic acid, AGE: Advanced glycation endproduct, MDA: Malondialdehyde, GSH-Px: Reduced glutathione, SOD: Superoxide dismutase, T-AOC: Total antioxidant capacity, Nrf2: Nuclear factor erythroid-2-related factor-2, Nf-κB: Nuclear factor kappa B, TNF-α: Tumour necrosis factor alpha, BDNF: Brain-derived neutrotrophic factor, TG: Triglyceride, TC: Total cholesterol, TGF-β1: Transforming growth factor beta-1, PGC-1α: Peroxisome proliferator-activated receptor-gamma coactivator-1alpha, GPx: Glutathione peroxidase.

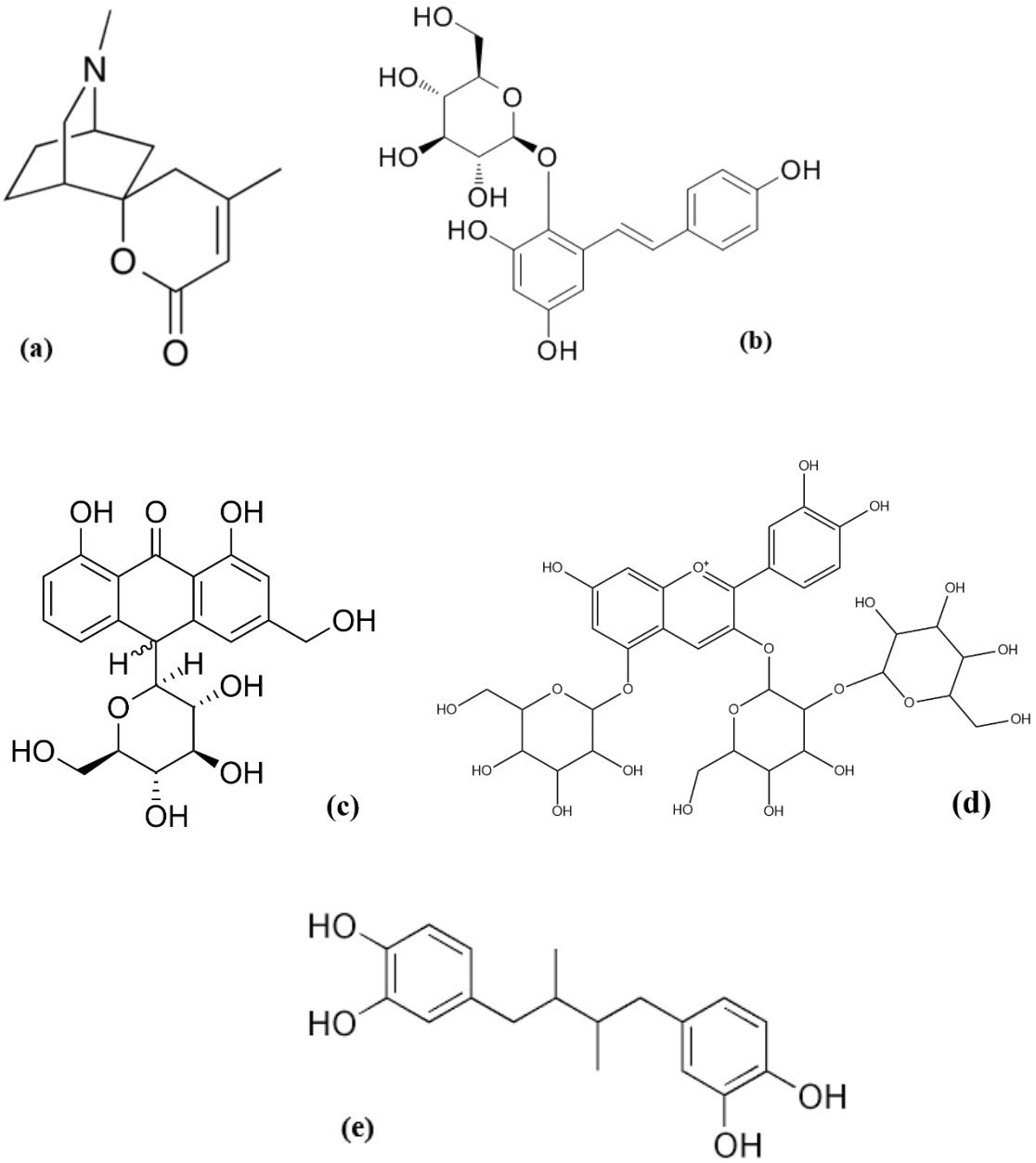

Figure 2.8. Structures of chemical compounds tested for anti-ageing properties in mice. (a) Dioscorin (b) Tetrahydrostilbene glucoside (c) Aloin (d) Cyanidin-3-diglucoside-5-glucoside (e) Nordihydroguaiaretic acid.

2.1.4.7. Rat model

Table 2.7 shows the ameliorative properties of medicinal foods and plants in galactose-induced aged rats. Administration of the aqueous extract of *Alpinia oxyphylla* fruit to D-galactose-induced aged male Wistar rats improved the longevity and survival of the animals, while decreasing the senescence-related features (Chang *et al.* 2021). Protocatechuic acid (Fig. 2.9a) isolated from the *Alpinia oxyphylla* fruit also restored the endogenous antioxidant status and normalized ageing-related alterations in aged rats after treatment for seven days (Zhang *et al.* 2011). Guilingji, a traditional Chinese medicine made from *Panax ginseng*, when administered to aged rats for 28 days, improved the memory and cholinergic system of the animals while reducing their oxidative stress status (Zhao *et al.* 2020). Supplementation of aged rats' diet with *Bactris setosa* fruits for 12 weeks elevated the antioxidant enzyme activity and upregulated the expression of hepatic SIRT1 and Nrf2, thereby ameliorating oxidative stress associated with ageing (Da Cunha and Arruda 2017).

Oral administration of total saponin from *Aralia taibaiensis* root to D-galactose-induced aged rats improved the memory of the animals and increased the total antioxidant capacity, while it decreased the product of lipid peroxidation (MDA) (Li *et al.* 2021a). Similarly, saponins isolated from *Trillium tschonoschii*, otherwise called diosgenin glucoside (Fig. 2.9b), enhanced the learning as well as the memory of galactose-induced aged rats and reduced dysfunctional autophagy associated with ageing by modulating Rheb-mTOR signalling (Wang *et al.* 2018). Bacoside (Fig. 2.9c) isolated from the crude saponin extract of *Bacopa monnieri* ameliorated neuroinflammation associated with ageing by attenuating inflammatory cytokines (TNF-α and IL-1β) and iNOS after three months of treatment in galactose-induced ageing in rats (Rastogi *et al.* 2012).

Table 2.7. Anti-ageing properties of medicinal foods and plants in galactose-induced ageing in rats

Scientific name	Common name	Parts	Extract/Compound	Dose	Effects	Reference
Alpinia oxyfylla Miq.	NA	Fruit	Protocatechuic acid	10 mg/kg	↓MDA; ↑GPx; ↑Catalase	(Zhang *et al.* 2011)
Alpinia oxyphylla Miq.	NA	Fruit	Water	100 mg/kg	↑Longevity; ↓Senescence	(Chang *et al.* 2021)
Aralia taibaiensis	NA	Root	Saponin	200 mg/kg	↑Memory; ↓MDA; ↑T-AOC	(Li *et al.* 2021a)
Bacopa monnieri Linn.	NA	Whole plant	Bacoside	200 mg/kg	↓IL-1β, ↓TNF-α; ↓iNOS	(Rastogi *et al.* 2012)
Bactris setosa Mart.	Tucum-do-cerrado	Fruit	Feed supplement	15%	↑SOD; ↑SIRT1; ↑Nrf2	(Da Cunha and Arruda 2017)
Panax notoginseng	Ginseng	Rhizome	Water	150 mg/kg	↑Memory; ↓MDA; ↓AChE	(Zhao *et al.* 2020)
Trillium tschonoschii Max.	NA	Rhizome	Diosgenin glucoside	100 mg/kg	↑Memory; ↓Autophagy	(Wang *et al.* 2018)

↑: Increase, ↓: Decrease, NA: Not available, MDA: Malondialdehyde, AChE: Acetylcholinesterase, MDA: Malondialdehyde, T-AOC: Total antioxidant capacity, SOD: Superoxide dismutase, TNF-α: Tumour necrosis factor alpha, IL-6: Interleukin-6, Nrf2: Nuclear factor erythroid-2-related factor-2, IL-1β: Interleukin-1 beta, iNOS: Inducible nitric oxide synthase.

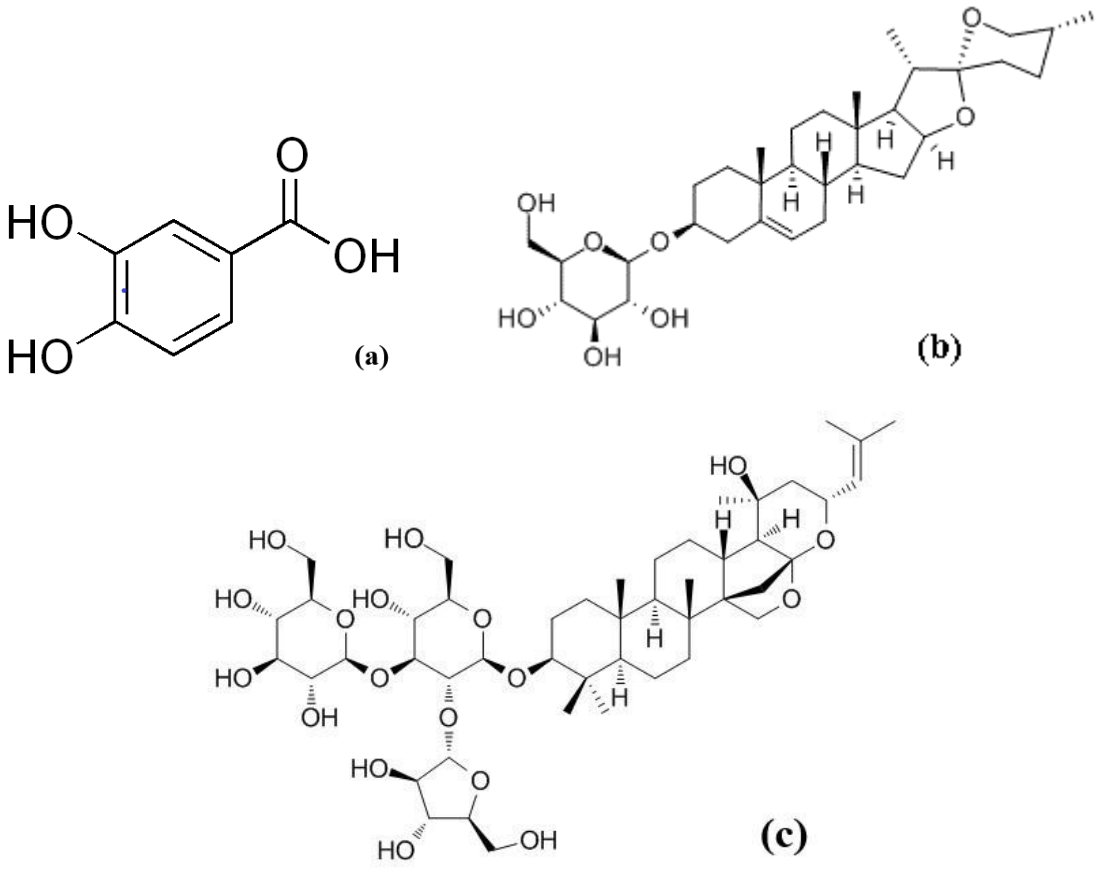

Figure 2. 9. Structures of chemical compounds tested for anti-ageing properties in rats. (a) Protocatechuic acid (b) Diosgenin glucoside and (c) Bacoside.

2.1.5. Conclusion

Ageing is a natural and inevitable process that occurs in all living organisms. This phenomenon is associated with the incidence of chronic diseases like diabetes, hypertension, and neurological disorders. Due to its importance, many studies have been conducted on the anti-ageing properties of medicinal plants and foods using different models. This study summarizes the use of different models (enzyme inhibition, yeast, cell lines, invertebrate, and vertebrate) for testing the efficacy of medicinal plants and foods in ameliorating ageing and its associated disorders. A total of 119 medicinal plants and 50 isolated compounds were reported in this study. Of all the studies reported in this paper, most of them were performed in *C. elegans*, and this is followed by the inhibition of ageing-related enzymes. While only two of the models are *in vitro* (enzyme inhibition and cell lines), five others (*C. elegans*, *D. melanogaster*, mice, rats, and yeast) are *in vivo* studies. Of these *in vivo* studies, *C. elegans* and *D. melanogaster* are more proficient than others due to the extensive generation of relevant data and are devoid of any ethical or regulatory concerns. Our study also revealed that the results of anti-ageing properties of medicinal foods and plants using different models are complementary and corroboratory.

Though most of the reports originated from Asia, especially China, these studies revealed that most medicinal plants and foods tested have anti-ageing properties. Some of the studies also reported the molecular mechanisms underlying the anti-ageing potential of some medicinal plants and isolated phytochemicals. However, there is a need to perform mechanistic and *in silico* studies on the other plants evaluated. The ultimate aim of any study is to improve the lives of man and enable them to live healthy in old age. Therefore, clinical trials should be conducted on some of these plants and phytochemicals that displayed strong anti-ageing effects in animal models. While further research is advocated on these anti-ageing medicinal plants, more attention should be focused on the consumption of the edible ones among them.

References

Abbasi, B. H., Siddiquah, A., Tungmunnithum, D., Bose, S., Younas, M., Garros, L., Drouet, S., Giglioli-Guivarc'h, N. and Hano, C. 2019. *Isodon rugosus* (Wall. ex Benth.) codd *in vitro* cultures: Establishment, phytochemical characterization and *in vitro* antioxidant and anti-aging activities. *International Journal of Molecular Sciences*, 20 (2): 452.

Abolaji, A., Kamdem, J., Farombi, E. and Rocha, J. 2013. *Drosophila melanogaster* as a promising model organism in toxicological studies. *Archives of Basic and Applied Medicine*, 1 (1): 33-38.

Amari, N. O., Razafimandimby, B., Auberon, F., Azoulay, S., Fernandez, X., Berkani, A., Bouchara, J.-P. and Landreau, A. 2021. Antifungal and antiaging evaluation of aerial part extracts of *Thymelaea hirsuta* (L.) Endl. *Natural Product Communications*, 16 (2): 1-10.

Bhullar, K. S. and Wu, J. 2020. Dietary peptides in aging: Evidence and prospects. *Food Science and Human Wellness*, 9 (1): 1-7.

Bilder, D. and Irvine, K. D. 2017. Taking stock of the Drosophila research ecosystem. *Genetics*, 206 (3): 1227-1236.

Boran, R. 2018. Investigations of anti-aging potential of *Hypericum origanifolium* Willd. for skincare formulations. *Industrial Crops and Products*, 118: 290-295.

Bose, B., Choudhury, H., Tandon, P. and Kumaria, S. 2017. Studies on secondary metabolite profiling, anti-inflammatory potential, *in vitro* photoprotective and skin-aging related enzyme inhibitory activities of *Malaxis acuminata*, a threatened orchid of nutraceutical importance. *Journal of Photochemistry and Photobiology B: Biology*, 173: 686-695.

Cañuelo, A., Gilbert-López, B., Pacheco-Liñán, P., Martínez-Lara, E., Siles, E. and Miranda-Vizuete, A. 2012. Tyrosol, a main phenol present in extra virgin olive oil, increases lifespan and

stress resistance in *Caenorhabditis elegans*. *Mechanisms of Ageing and Development*, 133 (8): 563-574.

Chaiyana, W., Anuchapreeda, S., Punyoyai, C., Neimkhum, W., Lee, K.-H., Lin, W.-C., Lue, S.-C., Viernstein, H. and Mueller, M. 2019. *Ocimum sanctum* Linn. as a natural source of skin anti-ageing compounds. *Industrial Crops and Products*, 127: 217-224.

Chang, Y.-M., Shibu, M. A., Chen, C.-S., Tamilselvi, S., Tsai, C.-T., Tsai, C.-C., Kumar, K. A., Lin, H.-J., Mahalakshmi, B. and Kuo, W.-W. 2021. Adipose derived mesenchymal stem cells along with *Alpinia oxyphylla* extract alleviate mitochondria-mediated cardiac apoptosis in aging models and cardiac function in aging rats. *Journal of Ethnopharmacology*, 264: 113297.

Chatzigeorgiou, S., Thai, Q. D., Tchoumtchoua, J., Tallas, K., Tsakiri, E. N., Papassideri, I., Halabalaki, M., Skaltsounis, A.-L. and Trougakos, I. P. 2017. Isolation of natural products with anti-ageing activity from the fruits of *Platanus orientalis*. *Phytomedicine*, 33: 53-61.

Chen, J.-C., Wang, R. and Wei, C.-C. 2022. Anti-aging effects of dietary phytochemicals: From *Caenorhabditis elegans*, *Drosophila melanogaster*, rodents to clinical studies. *Critical Reviews in Food Science and Nutrition*, 62: 5958-5983.

Chen, Q., Xu, B., Huang, W., Amrouche, A. T., Maurizio, B., Simal-Gandara, J., Tundis, R., Xiao, J., Zou, L. and Lu, B. 2020. Edible flowers as functional raw materials: A review on anti-aging properties. *Trends in Food science & Technology*, 106: 30-47.

Da Cunha, M. D. S. B. and Arruda, S. F. 2017. Tucum-do-Cerrado (*Bactris setosa* Mart.) may promote anti-aging effect by upregulating SIRT1-Nrf2 pathway and attenuating oxidative stress and inflammation. *Nutrients*, 9 (11): 1243.

Da Pozzo, E., De Leo, M., Faraone, I., Milella, L., Cavallini, C., Piragine, E., Testai, L., Calderone, V., Pistelli, L. and Braca, A. 2018. Antioxidant and antisenescence effects of bergamot juice. *Oxidative Medicine and Cellular Longevity*, 2018(1): 9395804.

Dell'Acqua, G. and Schweikert, K. 2012. Skin benefits of a myconoside-rich extract from resurrection plant *Haberlea rhodopensis*. *International Journal of Cosmetic Science*, 34 (2): 132-139.

Dhanjal, D. S., Bhardwaj, S., Sharma, R., Bhardwaj, K., Kumar, D., Chopra, C., Nepovimova, E., Singh, R. and Kuca, K. 2020. Plant fortification of the diet for anti-ageing effects: A review. *Nutrients*, 12 (10): 3008.

Duangjan, C., Rangsinth, P., Gu, X., Zhang, S., Wink, M. and Tencomnao, T. 2019. *Glochidion zeylanicum* leaf extracts exhibit lifespan-extending and oxidative stress resistance properties in *Caenorhabditis elegans* via DAF-16/FoxO and SKN-1/Nrf-2 signaling pathways. *Phytomedicine*, 64: 153061.

Eaknai, W., Bunwatcharaphansakun, P., Phungbun, C., Jantimaporn, A., Chaisri, S., Boonrungsiman, S., Nimmannit, U. and Khongkow, M. 2022. Ethanolic fenugreek extract: Its molecular mechanisms against skin aging and the enhanced functions by nanoencapsulation. *Pharmaceuticals*, 15 (2): 254.

Elgamal, A. M., Ahmed, R. F., Abd-ElGawad, A. M., El Gendy, A. E.-N. G., Elshamy, A. I. and Nassar, M. I. 2021. Chemical profiles, anticancer, and anti-aging activities of essential oils of *Pluchea dioscoridis* (L.) DC. and *Erigeron bonariensis* L. *Plants*, 10 (4): 667.

Ersoy, E., Ozkan, E. E., Boga, M., Yilmaz, M. A. and Mat, A. 2019. Anti-aging potential and anti-tyrosinase activity of three Hypericum species with focus on phytochemical composition by LC–MS/MS. *Industrial Crops and Products*, 141: 111735.

Farooq, U., Pan, Y., Disasa, D. and Qi, J. 2019. Novel anti-aging benzoquinone derivatives from *Onosma bracteatum* Wall. *Molecules*, 24 (7): 1428.

Feng, S., Cheng, H., Xu, Z., Feng, S., Yuan, M., Huang, Y., Liao, J. and Ding, C. 2019. Antioxidant and anti-aging activities and structural elucidation of polysaccharides from *Panax notoginseng* root. *Process Biochemistry*, 78: 189-199.

Filippopoulou, K., Papaevgeniou, N., Lefaki, M., Paraskevopoulou, A., Biedermann, D., Křen, V. and Chondrogianni, N. 2017. 2, 3-Dehydrosilybin A/B as a pro-longevity and anti-aggregation compound. *Free Radical Biology and Medicine*, 103: 256-267.

Georgieva, M., Moyankova, D., Djilianov, D., Uzunova, K. and Miloshev, G. 2015. Methanol extracts from the resurrection plant *Haberlea rhodopensis* ameliorate cellular vitality in chronologically ageing Saccharomyces cerevisiae cells. *Biogerontology*, 16 (4): 461-472.

German-Baez, L., Valdez-Flores, M., Figueroa-Perez, M., Garduno-Felix, K., Valdez-Ortiz, R., Meza-Ayala, K. and Valdez-Ortiz, A. 2017. Anti-aging and nutraceutical characterization of plant infusions used in traditional medicine. *Pakistan Journal of Nutrition*, 16 (4): 285-292.

Giunti, S., Andersen, N., Rayes, D. and De Rosa, M. J. 2021. Drug discovery: Insights from the invertebrate *Caenorhabditis elegans*. *Pharmacology Research & Perspectives*, 9 (2): e00721.

Haiyuan, Y., Shen, X., Liu, D., Hong, M. and Lu, Y. 2019. The protective effects of β-sitosterol and vermicularin from *Thamnolia vermicularis* (Sw.) Ach. against skin aging *in vitro*. *Anais da Academia Brasileira de Ciências*, 91 (4): e20181088.

Han, C.-H., Lin, Y.-F., Lin, Y.-S., Lee, T.-L., Huang, W.-J., Lin, S.-Y. and Hou, W.-C. 2014. Effects of yam tuber protein, dioscorin, on attenuating oxidative status and learning dysfunction in D-galactose-induced BALB/c mice. *Food and Chemical Toxicology*, 65: 356-363.

Han, Y., Guo, Y., Cui, S. W., Li, H., Shan, Y. and Wang, H. 2021. Purple sweet potato extract extends lifespan by activating autophagy pathway in male *Drosophila melanogaster*. *Experimental Gerontology*, 144: 111190.

Havermann, S., Humpf, H.-U. and Wätjen, W. 2016. Baicalein modulates stress-resistance and life span in *C. elegans* via SKN-1 but not DAF-16. *Fitoterapia*, 113: 123-127.

Hwang, E., Lin, P., Ngo, H. T. and Yi, T.-H. 2018a. Clove attenuates UVB-induced photodamage and repairs skin barrier function in hairless mice. *Food & Function*, 9 (9): 4936-4947.

Hwang, E., Ngo, H. T., Seo, S. A., Park, B., Zhang, M. and Yi, T.-H. 2018b. Protective effect of dietary *Alchemilla mollis* on UVB-irradiated premature skin aging through regulation of transcription factor NFATc1 and Nrf2/ARE pathways. *Phytomedicine*, 39: 125-136.

Iannuzzi, A. M., Giacomelli, C., De Leo, M., Russo, L., Camangi, F., De Tommasi, N., Braca, A., Martini, C. and Trincavelli, M. L. 2021. *Cornus sanguinea* fruits: A source of antioxidant and antisenescence compounds acting on aged human dermal and gingival fibroblasts. *Planta Medica*, 87 (10/11): 879-891.

Ibe, S., Kumada, K., Yoshida, K. and Otobe, K. 2013. Natto (fermented soybean) extract extends the adult lifespan of *Caenorhabditis elegans*. *Bioscience, Biotechnology, and Biochemistry*, 77 (2): 392-394.

Jan, H., Usman, H., Shah, M., Zaman, G., Mushtaq, S., Drouet, S., Hano, C. and Abbasi, B. H. 2021. Phytochemical analysis and versatile in vitro evaluation of antimicrobial, cytotoxic and enzyme inhibition potential of different extracts of traditionally used *Aquilegia pubiflora* Wall. Ex Royle. *BMC Complementary Medicine and Therapies*, 21 (1): 1-19.

Jaradat, N. A., Zaid, A. N., Hussen, F., Issa, L., Altamimi, M., Fuqaha, B., Nawahda, A. and Assadi, M. 2018. Phytoconstituents, antioxidant, sun protection and skin anti-wrinkle effects using four solvents fractions of the root bark of the traditional plant *Alkanna tinctoria* (L.). *European Journal of Integrative Medicine*, 21: 88-93.

Jennings, B. H. 2011. Drosophila–a versatile model in biology & medicine. *Materials Today*, 14 (5): 190-195.

Jeon, H. and Cha, D. S. 2016. Anti-aging properties of *Ribes fasciculatum* in *Caenorhabditis elegans*. *Chinese Journal of Natural Medicines*, 14 (5): 335-342.

Jeong, H., Liu, Y. and Kim, H. 2017. Dried plum and chokeberry ameliorate D-galactose-induced aging in mice by regulation of Pl3k/Akt-mediated Nrf2 and Nf-kB pathways. *Experimental Gerontology*, 95: 16-25.

Jiratchayamaethasakul, C., Ding, Y., Hwang, O., Im, S.-T., Jang, Y., Myung, S.-W., Lee, J. M., Kim, H.-S., Ko, S.-C. and Lee, S.-H. 2020. In vitro screening of elastase, collagenase, hyaluronidase, and tyrosinase inhibitory and antioxidant activities of 22 halophyte plant extracts for novel cosmeceuticals. *Fisheries and Aquatic Sciences*, 23 (1): 1-9.

Kang, C. H., Rhie, S. J. and Kim, Y. C. 2018. Antioxidant and skin anti-aging effects of marigold methanol extract. *Toxicological Research*, 34 (1): 31-39.

Kazeem, M., Bankole, H., Ogunrinola, O., Wusu, A. and Kappo, A. 2021. Functional foods with dipeptidyl peptidase-4 inhibitory potential and management of type 2 diabetes: A review. *Food Frontiers*, 2 (2): 153-162.

Kazeem, M. I. and Davies, T. C. 2016. Anti-diabetic functional foods as sources of insulin secreting, insulin sensitizing and insulin mimetic agents. *Journal of Functional Foods*, 20: 122-138.

Kim, H. G. and Oh, M. S. 2013. Memory-enhancing effect of *Mori fructus* via induction of nerve growth factor. *British Journal of Nutrition*, 110 (1): 86-94.

Kim, J., Kang, Y.-G., Lee, J.-y., Choi, D.-h., Cho, Y.-u., Shin, J.-M., Park, J. S., Lee, J. H., Kim, W. G. and Seo, D. B. 2015. The natural phytochemical dehydroabietic acid is an anti-aging reagent that mediates the direct activation of SIRT1. *Molecular and Cellular Endocrinology*, 412: 216-225.

Klinngam, W., Rungkamoltip, P., Thongin, S., Joothamongkhon, J., Khumkhrong, P., Khongkow, M., Namdee, K., Tepaamorndech, S., Chaikul, P. and Kanlayavattanakul, M. 2022. Polymethoxyflavones from *Kaempferia parviflora* ameliorate skin aging in primary human dermal fibroblasts and *ex vivo* human skin. *Biomedicine & Pharmacotherapy*, 145: 112461.

Kolakul, P. and Sripanidkulchai, B. 2017. Phytochemicals and anti-aging potentials of the extracts from *Lagerstroemia speciosa* and *Lagerstroemia floribunda*. *Industrial Crops and Products*, 109: 707-716.

Lee, K. K., Cho, J. J., Park, E. J. and Choi, J. D. 2001. Anti-elastase and anti-hyaluronidase of phenolic substance from *Areca catechu* as a new anti-ageing agent. *International Journal of Cosmetic Science*, 23 (6): 341-346.

Lee, S.-H., Lee, H.-Y., Yu, M., Yeom, E., Lee, J.-H., Yoon, A., Lee, K.-S. and Min, K.-J. 2019. Extension of drosophila lifespan by Korean red ginseng through a mechanism dependent on dSir2 and insulin/IGF-1 signaling. *Aging (albany NY)*, 11 (21): 9369.

Leung, M. C., Williams, P. L., Benedetto, A., Au, C., Helmcke, K. J., Aschner, M. and Meyer, J. N. 2008. *Caenorhabditis elegans*: An emerging model in biomedical and environmental toxicology. *Toxicological Sciences*, 106 (1): 5-28.

Li, H., Zhai, B., Sun, J., Fan, Y., Zou, J., Cheng, J., Zhang, X., Shi, Y. and Guo, D. 2021a. Antioxidant, anti-aging and organ protective effects of total saponins from *Aralia taibaiensis*. *Drug Design, Development and Therapy*, 15: 4025.

Li, J., Cui, X., Wang, Z. and Li, Y. 2015. rBTI extends *Caenorhabditis elegans* lifespan by mimicking calorie restriction. *Experimental Gerontology*, 67: 62-71.

Li, J., Lu, Y. R., Lin, I. F., Kang, W., Chen, H. b., Lu, H. F. and Wang, H. M. D. 2020. Reversing UVB-induced photoaging with *Hibiscus sabdariffa* calyx aqueous extract. *Journal of the Science of Food and Agriculture*, 100 (2): 672-681.

Li, N., Li, X., Shi, Y.-L., Gao, J.-M., He, Y.-Q., Li, F., Shi, J.-S. and Gong, Q.-H. 2021b. Trilobatin, a component from *Lithocarpus polystachyrus* Rehd., increases longevity in *C. elegans* through activating SKN1/SIRT3/DAF16 signaling pathway. *Frontiers in Pharmacology*, 12: 655045.

Lin, P., Hwang, E., Ngo, H. T., Seo, S. A. and Yi, T.-H. 2019. *Sambucus nigra* L. ameliorates UVB-induced photoaging and inflammatory response in human skin keratinocytes. *Cytotechnology*, 71 (5): 1003-1017.

Lin, W.-S., Chen, J.-Y., Wang, J.-C., Chen, L.-Y., Lin, C.-H., Hsieh, T.-R., Wang, M.-F., Fu, T.-F. and Wang, P.-Y. 2014. The anti-aging effects of *Ludwigia octovalvis* on *Drosophila melanogaster* and SAMP8 mice. *Age*, 36 (2): 689-703.

Liu, H., Liang, F., Su, W., Wang, N., Lv, M., Li, P., Pei, Z., Zhang, Y., Xie, X.-Q. and Wang, L. 2013. Lifespan extension by n-butanol extract from seed of *Platycladus orientalis* in *Caenorhabditis elegans*. *Journal of Ethnopharmacology*, 147 (2): 366-372.

Liu, X., Huang, Y., Chen, Y. and Cao, Y. 2016. Partial structural characterization, as well as immunomodulatory and anti-aging activities of CP2-c2-s2 polysaccharide from *Cordyceps militaris*. *RSC advances*, 6 (106): 104094-104103.

Lu, L., Zhao, X., Zhang, J., Li, M., Qi, Y. and Zhou, L. 2017. Calycosin promotes lifespan in *Caenorhabditis elegans* through insulin signaling pathway via DAF-16, AGE-1 and DAF-2. *Journal of Bioscience and Bioengineering*, 124 (1): 1-7.

Luceri, C., Bigagli, E., Pitozzi, V. and Giovannelli, L. 2017. A nutrigenomics approach for the study of anti-aging interventions: olive oil phenols and the modulation of gene and microRNA expression profiles in mouse brain. *European Journal of Nutrition*, 56 (2): 865-877.

Luo, J., Si, H., Jia, Z. and Liu, D. 2021. Dietary anti-aging polyphenols and potential mechanisms. *Antioxidants*, 10 (2): 283.

Luo, X., Wang, J., Chen, H., Zhou, A., Song, M., Zhong, Q., Chen, H. and Cao, Y. 2020. Identification of flavonoids from finger citron and evaluation of their antioxidative and antiaging activities. *Frontiers in Nutrition*, 7: 584900.

Manjia, J., Njayou, F., Joshi, A., Upadhyay, K., Shirsath, K., Devkar, R. and Moundipa, P. 2019a. The anti-aging potential of medicinal plants in Cameroon-*Harungana madagascariensis* Lam. and *Psorospermum aurantiacum* Engl. prevent in vitro ultraviolet B light-induced skin damage. *European Journal of Integrative Medicine*, 29: 100925.

Manosroi, A., Jantrawut, P., Akihisa, T., Manosroi, W. and Manosroi, J. 2010. *In vitro* anti-aging activities of *Terminalia chebula* gall extract. *Pharmaceutical Biology*, 48 (4): 469-481.

Manosroi, J., Chankhampan, C., Kumguan, K., Manosroi, W. and Manosroi, A. 2015. *In vitro* anti-aging activities of extracts from leaves of Ma Kiang (*Cleistocalyx nervosum* var. paniala). *Pharmaceutical Biology*, 53 (6): 862-869.

Markaki, M. and Tavernarakis, N. 2010. Modeling human diseases in *Caenorhabditis elegans*. *Biotechnology Journal*, 5 (12): 1261-1276.

Markaki, M. and Tavernarakis, N. 2020. *Caenorhabditis elegans* as a model system for human diseases. *Current Opinion in Biotechnology*, 63: 118-125.

Martel, J., Ojcius, D. M., Ko, Y. F., Chang, C. J. and Young, J. D. 2019. Antiaging effects of bioactive molecules isolated from plants and fungi. *Medicinal Research Reviews*, 39 (5): 1515-1552.

Meccariello, R. and D'Angelo, S. 2021. Impact of polyphenolic-food on longevity: An elixir of life. An overview. *Antioxidants*, 10 (4): 507.

Men, T. T., Khang, D. T., Tuan, N. T. and Trang, D. T. X. 2021. Anti-aging effects of *Lasia spinosa* L. stem extract on *Drosophila melanogaster*. *Food Science and Technology*, 42.

Mizutani, T. and Masaki, H. 2014a. Anti-photoaging capability of antioxidant extract from *Camellia japonica* leaf. *Experimental Dermatology*, 23: 23-26.

Nafiu, M. O., Salawu, M. O. and Kazeem, M. I. 2013. Antioxidant activity of African medicinal plants. In: *Medicinal Plant Research in Africa*. Elsevier, 787-803.

Napagoda, M. T., Kumari, M., Qader, M. M., De Soyza, S. G. and Jayasinghe, L. 2018. Evaluation of tyrosinase inhibitory potential in flowers of *Cassia auriculata* L. for the development of natural skin whitening formulation. *European Journal of Integrative Medicine*, 21: 39-42.

Okoro, N. O., Odiba, A. S., Osadebe, P. O., Omeje, E. O., Liao, G., Fang, W., Jin, C. and Wang, B. 2021. Bioactive phytochemicals with anti-aging and lifespan-extending potentials in *Caenorhabditis elegans*. *Molecules*, 26 (23): 7323.

Pandey, S., Phulara, S. C., Mishra, S. K., Bajpai, R., Kumar, A., Niranjan, A., Lehri, A., Upreti, D. K. and Chauhan, P. S. 2020. *Betula utilis* extract prolongs life expectancy, protects against amyloid-β toxicity and reduces alpha synuclien in *Caenorhabditis elegans* via DAF-16 and SKN-1. *Comparative Biochemistry and Physiology Part C: Toxicology & Pharmacology*, 228: 108647.

Pandey, S., Tiwari, S., Kumar, A., Niranjan, A., Chand, J., Lehri, A. and Chauhan, P. S. 2018. Antioxidant and anti-aging potential of Juniper berry (*Juniperus communis* L.) essential oil in *Caenorhabditis elegans* model system. *Industrial Crops and Products*, 120: 113-122.

Pandey, T., Sammi, S. R., Nooreen, Z., Mishra, A., Ahmad, A., Bhatta, R. S. and Pandey, R. 2019. Anti-ageing and anti-Parkinsonian effects of natural flavonol, tambulin from *Zanthoxyllum aromatum* promotes longevity in *Caenorhabditis elegans*. *Experimental Gerontology*, 120: 50-61.

Pant, A., Asthana, J., Yadav, A., Rathor, L., Srivastava, S., Gupta, M. and Pandey, R. 2015. Verminoside mediates life span extension and alleviates stress in *Caenorhabditis elegans*. *Free Radical Research*, 49 (11): 1384-1392.

Pant, A., Saikia, S. K., Shukla, V., Asthana, J., Akhoon, B. A. and Pandey, R. 2014. Beta-caryophyllene modulates expression of stress response genes and mediates longevity in *Caenorhabditis elegans*. *Experimental Gerontology*, 57: 81-95.

Park, J.-K., Kim, C.-K., Gong, S.-K., Yu, A.-R., Lee, M.-Y. and Park, S.-K. 2014. *Acanthopanax sessiliflorus* stem confers increased resistance to environmental stresses and lifespan extension in *Caenorhabditis elegans*. *Nutrition Research and Practice*, 8 (5): 526-532.

Peixoto, H., Roxo, M., Koolen, H., Da Silva, F., Silva, E., Braun, M. S., Wang, X. and Wink, M. 2018. *Calycophyllum spruceanum* (Benth.), the amazonian "tree of youth" prolongs longevity and enhances stress resistance in *Caenorhabditis elegans*. *Molecules*, 23 (3): 534.

Permatasari, H. K., Nurkolis, F., Augusta, P. S., Mayulu, N., Kuswari, M., Taslim, N. A., Wewengkang, D. S., Batubara, S. C. and Gunawan, W. B. 2021. Kombucha tea from seagrapes (*Caulerpa racemosa*) potential as a functional anti-ageing food: *in vitro* and *in vivo* study. *Heliyon*, 7 (9): e07944.

Pientaweeratch, S., Panapisal, V. and Tansirikongkol, A. 2016. Antioxidant, anti-collagenase and anti-elastase activities of *Phyllanthus emblica*, *Manilkara zapota* and silymarin: An in vitro comparative study for anti-aging applications. *Pharmaceutical Biology*, 54 (9): 1865-1872.

Prasansuklab, A., Meemon, K., Sobhon, P. and Tencomnao, T. 2017. Ethanolic extract of *Streblus asper* leaves protects against glutamate-induced toxicity in HT22 hippocampal neuronal cells and extends lifespan of *Caenorhabditis elegans*. *BMC Complementary and Alternative Medicine*, 17 (1): 1-14.

Prommaban, A., Sriyab, S., Marsup, P., Neimkhum, W., Sirithunyalug, J., Anuchapreeda, S., To-Anun, C. and Chaiyana, W. 2022. Comparison of chemical profiles, antioxidation, inhibition of skin extracellular matrix degradation, and anti-tyrosinase activity between mycelium and fruiting body of *Cordyceps militaris* and *Isaria tenuipes*. *Pharmaceutical Biology*, 60 (1): 225-234.

Rastogi, M., Ojha, R. P., Devi, B. P., Aggarwal, A., Agrawal, A. and Dubey, G. 2012. Amelioration of age-associated neuroinflammation on long-term bacosides treatment. *Neurochemical Research*, 37 (4): 869-874.

Rathor, L., Pant, A., Nagar, A., Tandon, S., Trivedi, S. and Pandey, R. 2017. *Trachyspermum ammi* L.(Carom) oil induces alterations in SOD-3, GST-4 expression and prolongs lifespan in *Caenorhabditis elegans*. *Proceedings of the National Academy of Sciences, India Section B: Biological Sciences*, 87 (4): 1355-1362.

Ruan, Q., Qiao, Y., Zhao, Y., Xu, Y., Wang, M., Duan, J. and Wang, D. 2016. Beneficial effects of *Glycyrrhizae radix* extract in preventing oxidative damage and extending the lifespan of *Caenorhabditis elegans*. *Journal of Ethnopharmacology*, 177: 101-110.

Rusu, M. E., Simedrea, R., Gheldiu, A.-M., Mocan, A., Vlase, L., Popa, D.-S. and Ferreira, I. C. 2019. Benefits of tree nut consumption on aging and age-related diseases: Mechanisms of actions. *Trends in Food Science & Technology*, 88: 104-120.

Sabiu, S. 2022. *Therapeutic use of plant secondary metabolites*. Bentham Science Publishers, pp. 390.

Saier, C., Büchter, C., Koch, K. and Wätjen, W. 2018. *Polygonum multiflorum* extract exerts antioxidative effects and increases life span and stress resistance in the model organism *Caenorhabditis elegans* via DAF-16 and SIR-2.1. *Plants*, 7 (3): 60.

Sayed, S. M., Siems, K., Schmitz-Linneweber, C., Luyten, W. and Saul, N. 2021b. Enhanced healthspan in *Caenorhabditis elegans* treated with extracts from the traditional Chinese medicine plants, *Cuscuta chinensis* Lam. and *Eucommia ulmoides* Oliv. *Frontiers in Pharmacology*, 12: 604435.

Senthil, K. K., Gokila, V. M., Mau, J.-L., Lin, C.-C., Chu, F.-H., Wei, C.-C., Liao, V. H.-C. and Wang, S.-Y. 2016. A steroid-like phytochemical Antcin M is an anti-aging reagent that eliminates

hyperglycemia-accelerated premature senescence in dermal fibroblasts by direct activation of Nrf2 and SIRT-1. *Oncotarget*, 7 (39): 62836.

Shoko, T., Maharaj, V. J., Naidoo, D., Tselanyane, M., Nthambeleni, R., Khorombi, E. and Apostolides, Z. 2018. Anti-aging potential of extracts from *Sclerocarya birrea* (A. Rich.) Hochst and its chemical profiling by UPLC-Q-TOF-MS. *BMC Complementary and Alternative Medicine*, 18 (1): 1-14.

Spindler, S. R., Mote, P. L., Lublin, A. L., Flegal, J. M., Dhahbi, J. M. and Li, R. 2015. Nordihydroguaiaretic acid extends the lifespan of drosophila and mice, increases mortality-related tumors and hemorrhagic diathesis, and alters energy homeostasis in mice. *Journals of Gerontology Series A: Biomedical Sciences and Medical Sciences*, 70 (12): 1479-1489.

Su, S. and Wink, M. 2015. Natural lignans from *Arctium lappa* as antiaging agents in *Caenorhabditis elegans*. *Phytochemistry*, 117: 340-350.

Sun, K., Xiang, L., Ishihara, S., Matsuura, A., Sakagami, Y. and Qi, J. 2012. Anti-aging effects of hesperidin on *Saccharomyces cerevisiae* via inhibition of reactive oxygen species and UTH1 gene expression. *Bioscience, Biotechnology, and Biochemistry*, 76 (4): 640-645.

Sun, X., Seeberger, J., Alberico, T., Wang, C., Wheeler, C. T., Schauss, A. G. and Zou, S. 2010. Açai palm fruit (*Euterpe oleracea* Mart.) pulp improves survival of flies on a high fat diet. *Experimental Gerontology*, 45 (3): 243-251.

Sung, B., Chung, J. W., Bae, H. R., Choi, J. S., Kim, C. M. and Kim, N. D. 2015. *Humulus japonicus* extract exhibits antioxidative and anti-aging effects via modulation of the AMPK-SIRT1 pathway. *Experimental and Therapeutic Medicine*, 9 (5): 1819-1826.

Szewczyk, K., Pietrzak, W., Klimek, K., Miazga-Karska, M., Firlej, A., Flisiński, M. and Grzywa-Celińska, A. 2021. Flavonoid and phenolic acids content and in vitro study of the potential anti-

aging properties of *Eutrema japonicum* (Miq.) Koidz cultivated in Wasabi Farm Poland. *International Journal of Molecular Sciences*, 22 (12): 6219.

Tambara, A. L., Moraes, L. d. L. S., Dal Forno, A. H., Boldori, J. R., Soares, A. T. G., de Freitas Rodrigues, C., Mariutti, L. R. B., Mercadante, A. Z., de Ávila, D. S. and Denardin, C. C. 2018. Purple pitanga fruit (*Eugenia uniflora* L.) protects against oxidative stress and increase the lifespan in *Caenorhabditis elegans* via the DAF-16/FOXO pathway. *Food and Chemical Toxicology*, 120: 639-650.

Tang, R., Chen, X., Dang, T., Deng, Y., Zou, Z., Liu, Q., Gong, G., Song, S., Ma, F. and Huang, L. 2019. *Lycium barbarum* polysaccharides extend the mean lifespan of *Drosophila melanogaster*. *Food & Function*, 10 (7): 4231-4241.

Teseo, S., Houot, B., Yang, K., Monnier, V., Liu, G. and Tricoire, H. 2021. *G. sinense* and *P. notoginseng* extracts improve healthspan of aging flies and provide protection in a Huntington disease model. *Aging and Disease*, 12 (2): 425.

Tlili, N., Kirkan, B. and Sarikurkcu, C. 2019. LC–ESI–MS/MS characterization, antioxidant power and inhibitory effects on α-amylase and tyrosinase of bioactive compounds from hulls of *Amygdalus communis*: The influence of the extracting solvents. *Industrial Crops and Products*, 128: 147-152.

Tungmunnithum, D., Drouet, S. and Hano, C. 2022. Validation of a high-performance liquid chromatography with photodiode array detection method for the separation and quantification of antioxidant and skin anti-aging flavonoids from *Nelumbo nucifera* Gaertn. stamen extract. *Molecules*, 27 (3): 1102.

UN. 2022. *World Population Prospects 2022: Summary of Results*. New York:

Utami, S., Sachrowardi, Q. R., Damayanti, N. A., Wardhana, A., Syarif, I., Nafik, S., Arrahman, B. C., Kusuma, H. S. W. and Widowati, W. 2018. Antioxidants, anticollagenase and antielastase

potentials of ethanolic extract of ripe sesoot (*Garcinia picrorrhiza* Miq.) fruit as antiaging. *Journal of Herbmed Pharmacology*, 7 (2): 88-93.

Vayndorf, E. M., Lee, S. S. and Liu, R. H. 2013. Whole apple extracts increase lifespan, healthspan and resistance to stress in *Caenorhabditis elegans*. *Journal of Functional Foods*, 5 (3): 1235-1243.

Wang, L., Chen, Q., Zhuang, S., Wen, Y., Cheng, W., Zeng, Z., Jiang, T. and Tang, C. 2020a. Effect of *Anoectochilus roxburghii* flavonoids extract on H_2O_2-Induced oxidative stress in LO2 cells and D-gal induced aging mice model. *Journal of Ethnopharmacology*, 254: 112670.

Wang, L., Du, J., Zhao, F., Chen, Z., Chang, J., Qin, F., Wang, Z., Wang, F., Chen, X. and Chen, N. 2018. *Trillium tschonoskii* maxim saponin mitigates D-galactose-induced brain aging of rats through rescuing dysfunctional autophagy mediated by Rheb-mTOR signal pathway. *Biomedicine & Pharmacotherapy*, 98: 516-522.

Wang, S., Xue, J., Zhang, S., Zheng, S., Xue, Y., Xu, D. and Zhang, X. 2020. Composition of peony petal fatty acids and flavonoids and their effect on *Caenorhabditis elegans* lifespan. *Plant Physiology and Biochemistry*, 155: 1-12.

Wang, Y., Lin, Y., Xiang, L., Osada, H. and Qi, J. 2017. Sesquiterpene glucosides from Shenzhou honey peach fruit showed the anti-aging activity in the evaluation system using yeasts. *Bioscience, Biotechnology, and Biochemistry*, 81 (8): 1586-1590.

Wang, Z., Ma, X., Li, J. and Cui, X. 2016. Peptides from sesame cake extend healthspan of *Caenorhabditis elegans* via upregulation of skn-1 and inhibition of intracellular ROS levels. *Experimental Gerontology*, 82: 139-149.

WHO. 2002. *WHO Traditional Medicine Strategy 2002 - 2005*. Geneva: World Health Organization.

WHO. 2022. *World Health Statistics 2022: Monitoring health for the SDGs, Sustainable Development Goals*. Geneva: World Health Organization.

Wongchum, N. and Dechakhamphu, A. 2021. Xanthohumol prolongs lifespan and decreases stress-induced mortality in *Drosophila melanogaster*. *Comparative Biochemistry and Physiology Part C: Toxicology & Pharmacology*, 244: 108994.

Wu, M., Cai, J., Fang, Z., Li, S., Huang, Z., Tang, Z., Luo, Q. and Chen, H. 2022. The composition and anti-aging activities of polyphenol extract from *Phyllanthus emblica* L. fruit. *Nutrients*, 14 (4): 857.

Wu, S., Li, J., Wang, Q., Cao, J., Yu, H., Cao, H. and Xiao, J. 2017. Chemical composition, antioxidant and anti-tyrosinase activities of fractions from *Stenoloma chusanum*. *Industrial Crops and Products*, 107: 539-545.

Yang, J.-E., Ngo, H. T., Hwang, E., Seo, S. A., Park, S. W. and Yi, T.-H. 2019. Dietary enzyme-treated *Hibiscus syriacus* L. protects skin against chronic UVB-induced photoaging via enhancement of skin hydration and collagen synthesis. *Archives of Biochemistry and Biophysics*, 662: 190-200.

Yang, X., Zhang, P., Wu, J., Xiong, S., Jin, N. and Huang, Z. 2012. The neuroprotective and lifespan-extension activities of *Damnacanthus officinarum* extracts in *Caenorhabditis elegans*. *Journal of Ethnopharmacology*, 141 (1): 41-47.

Yin, Z., Park, R. and Choi, B.-M. 2020. Isoparvifuran isolated from *Dalbergia odorifera* attenuates H_2O_2-induced senescence of BJ cells through SIRT1 activation and AKT/mTOR pathway inhibition. *Biochemical and Biophysical Research Communications*, 533 (4): 925-931.

You, J., Roh, K.-B., Li, Z., Liu, G., Tang, J., Shin, S., Park, D. and Jung, E. 2015. The antiaging properties of *Andrographis paniculata* by activation epidermal cell stemness. *Molecules*, 20 (9): 17557-17569.

Zhang, J., Xiao, Y., Guan, Y., Rui, X., Zhang, Y., Dong, M. and Ma, W. 2019. An aqueous polyphenol extract from *Rosa rugosa* tea has antiaging effects on *Caenorhabditis elegans*. *Journal of Food Biochemistry*, 43 (4): e12796.

Zhang, N., Zhang, Z., Xu, W. and Jing, P. 2021. TMT-based quantitative proteomic analysis of hepatic tissue reveals the effects of dietary cyanidin-3-diglucoside-5-glucoside-rich extract on alleviating D-galactose-induced aging in mice. *Journal of Proteomics*, 232: 104042.

Zhang, W., Zheng, B., Deng, N., Wang, H., Li, T. and Liu, R. H. 2020. Effects of ethyl acetate fractional extract from *Portulaca oleracea* L.(PO-EA) on lifespan and healthspan in *Caenorhabditis elegans*. *Journal of Food Science*, 85 (12): 4367-4376.

Zhang, X., Shi, G. F., Liu, X. z., An, L. j. and Guan, S. 2011. Anti-ageing effects of protocatechuic acid from Alpinia on spleen and liver antioxidative system of senescent mice. *Cell Biochemistry and Function*, 29 (4): 342-347.

Zhang, Y., Dan-Yang, M., Jin, W., Yan-Ping, L., Xu, Y., Shi, D., Xing-Ming, M. and Kai-Zhong, D. 2018. Constituent and effects of polysaccharides isolated from *Sophora moorcroftiana* seeds on lifespan, reproduction, stress resistance, and antimicrobial capacity in *Caenorhabditis elegans*. *Chinese Journal of Natural Medicines*, 16 (4): 252-260.

Zhang, Y., Lv, T., Li, M., Xue, T., Liu, H., Zhang, W., Ding, X. and Zhuang, Z. 2015. Anti-aging effect of polysaccharide from *Bletilla striata* on nematode *Caenorhabditis elegans*. *Pharmacognosy Magazine*, 11 (43): 449.

Zhao, S.-j., Liu, X.-j., Tian, J.-s., Gao, X.-x., Liu, H.-l., Du, G.-h. and Qin, X.-m. 2020. Effects of guilingji on aging rats and its underlying mechanisms. *Rejuvenation Research*, 23 (2): 138-149.

Zhao, Y., Liao, A.-M., Liu, N., Huang, J.-H., Lv, X., Yang, C.-R., Chen, W.-J., Hou, Y.-C., Ma, L.-J. and Hui, M. 2021. Potential anti-aging effects of fermented wheat germ in aging mice. *Food Bioscience*, 42: 101182.

Zheng, J. and Greenway, F. 2012. *Caenorhabditis elegans* as a model for obesity research. *International Journal of Obesity*, 36 (2): 186-194.

Zhong, J., Wang, F., Wang, Z., Shen, C., Zheng, Y., Ma, F., Zhu, T., Chen, L., Tang, Q. and Zhu, J. 2019a. Aloin attenuates cognitive impairment and inflammation induced by d-galactose via down-regulating ERK, p38 and NF-κB signaling pathway. *International Immunopharmacology*, 72: 48-54.

Zhong, S.-J., Wang, L., Wu, H.-T., Lan, R. and Qin, X.-Y. 2019b. *Coeloglossum viride* var. *bracteatum* extract improves learning and memory of chemically-induced aging mice through upregulating neurotrophins BDNF and FGF2 and sequestering neuroinflammation. *Journal of Functional Foods*, 57: 40-47.

Zhou, X., Yang, Q., Xie, Y., Sun, J., Hu, J., Qiu, P., Cao, W. and Wang, S. 2015. Tetrahydroxystilbene glucoside extends mouse life span via upregulating neural klotho and downregulating neural insulin or insulin-like growth factor 1. *Neurobiology of Aging*, 36 (3): 1462-1470.

Zhou, Y.-z., Xue, L.-y., Gao, L., Qin, X.-m. and Du, G.-h. 2018. Ginger extract extends the lifespan of *Drosophila melanogaster* through antioxidation and ameliorating metabolic dysfunction. *Journal of Functional Foods*, 49: 295-305.

Zhuang, Y., Ma, Q., Guo, Y. and Sun, L. 2017. Protective effects of rambutan (*Nephelium lappaceum*) peel phenolics on H_2O_2-induced oxidative damages in HepG2 cells and D-galactose-induced aging mice. *Food and Chemical Toxicology*, 108: 554-562.

2.2. *Cymbopogon citratus* (DC) Stapf (lemongrass) as a source of nutrients and pharmacological agents for the management of diseases

Mutiu Idowu Kazeem, John Jason Mellem and Saheed Sabiu

Department of Biotechnology and Food Science, Durban University of Technology, P. O. Box 1334, Durban 4000, South Africa

Preface: This article reviews studies that report the nutritional and phytochemical composition of lemongrass. It also presented the pharmacological properties of lemongrass against several diseases. The manuscript is submitted to the journal, *Vegetos*.

2.2.1. Abstract

Cymbopogon citratus (lemongrass) is a tropical grass found in Africa, Asia, and South America. It is commonly consumed as a beverage (just like green tea) or herbal tea to manage several diseases, including abdominal disturbance, inflammation, and infection. It is also used as a flavouring for food and beverages. This study reviewed the nutritional composition, phytochemical composition, and pharmacological properties of lemongrass. Relevant information was obtained from different electronic databases, including Web of Science, PubMed, Scopus, and Google Scholar. This study revealed that the plant is rich in many nutrients, including carbohydrates, protein, fats, minerals, and vitamins. It also showed that lemongrass contains numerous phytochemical compounds such as phenolics (e.g, chlorogenic acid), flavonoids (e.g, luteolin), and terpenoids (e.g, citral). Lemongrass extract and its essential oil also possess numerous pharmacological activities such as antioxidant, anticancer, antidiabetic, anti-inflammatory, and antimicrobial properties. It can be concluded that lemongrass is a valuable botanical resource with rich nutritional and phytochemical composition and extensive pharmacological properties. However, further studies are required to isolate the plant's bioactive compounds and provide possible mechanisms for its pharmacological actions.

Keywords: Lemongrass, amino acid, phytochemicals, infections, diabetes, cancer

2.2.2. Introduction

The genus Cymbopogon belongs to the Poaceae (Gramineae) botanical family. It comprises around 180 species, subspecies, varieties, and subvarieties with a wide geographical distribution in tropical and temperate regions of the world (Negrelle and Gomes 2007). The name Cymbopogon is of Greek origin and derives from the words kymbe (i.e., boat) and pogon (i.e., beard), which relates to the flower spike arrangement of the species of this genus (Tibenda *et al.* 2022). The genus Cymbopogon contains several species, including *C. citratus*, *C. flexuosus*, *C. pendulus*, *C. winterianus*, *C. martinii*, *C. nardus*, and *C. refractus* (Tazi et al. 2024). Three extensively distributed species include *C. citratus* (West Indian grass), *C. flexuosus* (Malabar grass, also known as East Indian grass), and *C. pendulus* (the Jammu grass) (Lawal *et al.* 2017).

Cymbopogon citratus (DC) Stapf., commonly known as West Indian, American lemongrass, or just lemongrass, is the most studied of all the species due to its extensive traditional usage in medicine (Ekpenyong, Akpan and Nyoh 2015). Lemongrass is a tall grass that originated from the South Asia region and is now found in many regions of the globe, including Africa, South America, and Europe (Kiani *et al.* 2022). It is a perennial and fast-growing herb displaying a tuft of leaves that sprout from annulate and sparingly branched rhizomes (Kusuma *et al.* 2024). It has many bulbous stems that increase the bulk size of the plant as it grows and can reach a height greater than 2 m and a width of around 1 m (Mukarram *et al.* 2021). The leaves are distinctively bluish-green, lemon-scented (justifying the name of the herb), with a width of 5–15 mm, and do not produce seeds (Ashaq *et al.* 2024).

The multiple resources of lemongrass include the fibre, leaves, and essential oils of the plant. Leaves are the most important product since they can be used as a flavouring for food and beverages; however, it is presently cultivated as a condiment and essential oil (Adhikary *et al.* 2024). The leaves are used in traditional medicine as antiemetics, antispasmodics, and antirheumatic remedies (Ekpenyong and Akpan 2017). They are also useful in nutrition and are functional components of food, possessing antioxidant and anticancer characteristics (Oladeji *et al.* 2019). Lemongrass tea is also prepared from either fresh or dried leaves and used as medicine in various countries (Silva and Bárbara 2022). Lemongrass leaves contain bioactive compounds that can act as antioxidants. Another attractive potential is their ability to be used as a lemon flavour in herbal teas developed either by extraction, infusion, or other formulations.

There are different reviews on lemongrass, maybe as a result of its wide usage among the populace. However, some of these studies are old and outdated (Negrelle and Gomes 2007; Ekpenyong, Akpan and Nyoh 2015), some reviewed their usage in the treatment of specific diseases (Silva and Bárbara 2022; Falcon *et al.* 2024), while some presented general information on the genus, Cymbogon (Tibenda *et al.* 2022). Some studies reviewed lemongrass essential oil or its extract alone (Mukarram *et al.* 2021; Adhikary *et al.* 2024; Ashaq *et al.* 2024) while others only reported its industrial applications (Kamaruddin *et al.* 2022). This study attempts to integrate all available information on the nutritional composition, phytochemical composition, and pharmacological properties of *Cymbopogon citratus* (lemongrass).

2.2.3. Methodology

The available information on the nutritional composition, phytochemical composition and pharmacological properties of lemongrass was collected via electronic search (using Web of Science, PubMed, Scopus, and Google Scholar) using keywords such as 'Cymbopogon citratus', 'lemongrass', 'lemongrass and diseases', 'lemongrass essential oil', and 'lemongrass nutrients'. A library search for articles published in books, including review articles and specific ethnomedical research articles, was also used as a source of information. Reference lists of published research articles were also consulted for relevant data. A total of 159 articles covering between years 2004 and 2024 were obtained from the electronic and manual searches. After eliminating duplications and irrelevant ones, 111 articles were used for this study. This paper excludes all studies that are not within the scope of providing information on the nutrients and phytochemicals present in lemongrass, and the pharmacological properties of its extracts, essential oil, or phytochemicals.

2.2.4. Nutritional composition of lemongrass

The consumption of lemongrass in the form of teas, infusions, or oils contains different nutrients that provide nutritional benefits to consumers (Soares *et al.* 2013). The nutrients include carbohydrates, protein, lipids, moisture, dietary fibre, and ash (Fagbohun Emmanuel *et al.* 2010; Akande *et al.* 2011). Table 2.8 presents several reports on the proximate composition of lemongrass

leaves (Asaolu, Oyeyemi and Olanlokun 2009; Uraku *et al.* 2016; Nimenibo-Uadia and Nwosu 2020).

Table 2.8. Proximate composition (%) of lemongrass

Reference	Carbohydrate	Protein	Fats	Fibre	Moisture	Ash
Nimenibo-Uadia & Nwosu (2020)	66.00 ± 1.11	15.86 ± 0.15	6.90 ± 0.10	1.00 ± 0.06	72.95 ± 0.03	9.40 ± 0.23
Uraku *et al*. (2016)	19.64 ± 0.91	22.59 ± 0.01	2.43 ± 0.04	37.53 ± 0.67	11.35 ± 0.01	7.15 ± 0.21
Asaolu *et al*. (2009)	9.28	4.56	3.60	55.00	5.76	22.30
Akande *et al*. (2011)	ND	0.34 ± 0.00	0.98 ± 0.04	78.43 ± 0.74	10.12 ± 0.11	5.01 ± 0.02
Fagbohun *et al*. (2010)	15.30 ± 2.60	12.00 ± 7.40	20.4 ± 5.30	31.40 ± 1.30	3.20 ± 1.20	20.10 ± 3.40
Soares *et al*. (2013)	62.60	19.79	4.98	ND	8.52	4.11

ND: Not determined

Some studies have also reported the mineral composition of lemongrass (Table 2.9). These revealed the presence of a variety of important minerals in the lemongrass (Uraku *et al.* 2016; Nimenibo-Uadia and Nwosu 2020). These included sodium, potassium, calcium, phosphorus, magnesium, and manganese. Other minerals present in lemongrass are zinc, copper, iron, and selenium (Asaolu, Oyeyemi and Olanlokun 2009; Fagbohun Emmanuel *et al.* 2010).

2.2.5. Phytochemical composition of lemongrass

Lemongrass represents one of the most sourced plants globally because of its distribution and application. Different extracts of lemongrass have shown diverse pharmacological activities that are generally attributed to its chemical composition. These include phenolic acids, flavonoids, terpenoids, triterpenoids, and tannins. There are many phenolic acids identified in lemongrass, such as chlorogenic acid, caffeic acid, p-coumaric acid, and elemicin (Figure 2.10). Examples of the flavonoids found in lemongrass are luteolin, quercetin, kaempferol, and orientin (Figure 2.11). Terpenoids have the largest presence in lemongrass and contribute significantly to its medicinal properties. These terpenoids include citral, myrecene, geranial, geraniol, and limonene (Figure 2.12).

Table 2.9. Mineral composition of lemongrass

Mineral (mg/100 g)	Nimenibo-Uadia & Nwosu (2020)	Uraku *et al*. (2016)	Asaolu *et al*. (2009)	Fagbohun *et al*. (2010)
Sodium	0.027	0.41 ± 0.01	3.23	54.80
Potassium	0.385	0.64 ± 0.01	2.98	59.50
Phosphorus	0.112	ND	12.45	89.30
Calcium	0.401	2.14 ± 0.02	2.42	39.50
Magnesium	0.138	ND	2.26	70.00
Manganese	ND	2.57 ± 0.04	0.25	0.95
Zinc	ND	0.03 ± 0.00	0.16	121.00
Iron	0.0075	0.11 ± 0.02	0.43	0.02
Copper	0.0045	0.39 ± 0.01	ND	ND
Selenium	ND	ND	0.02	ND
Cobalt	ND	0.39 ± 0.01	ND	ND

ND: Not determined

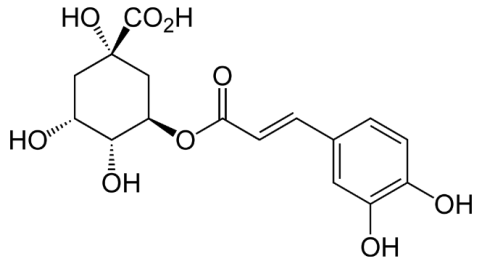

Chlorogenic acid

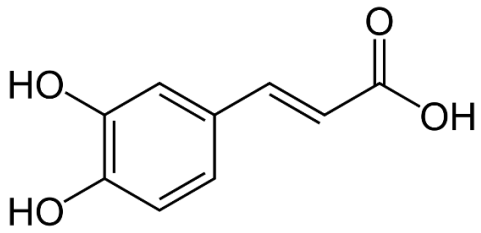

Caffeic acid

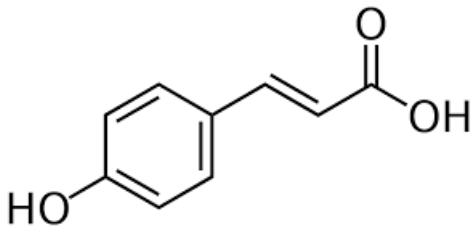

p-coumaric acid

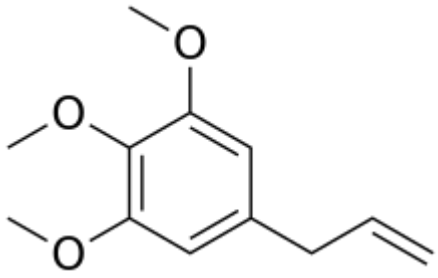

Elemicin

Figure 2.10. Structures of some phenolic acids from lemongrass.

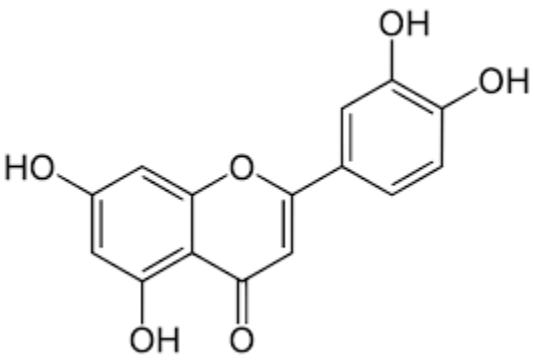

Luteolin

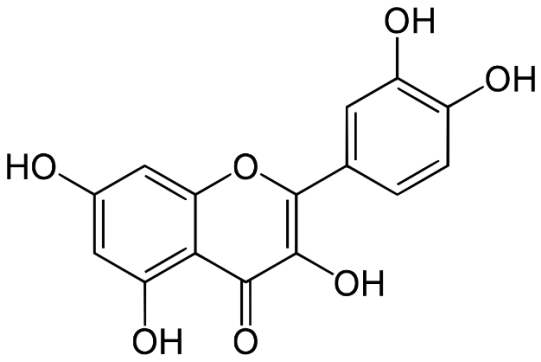

Quercetin

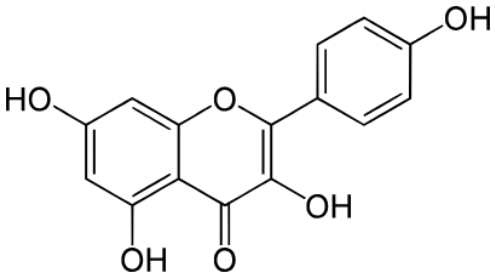

Kaempferol

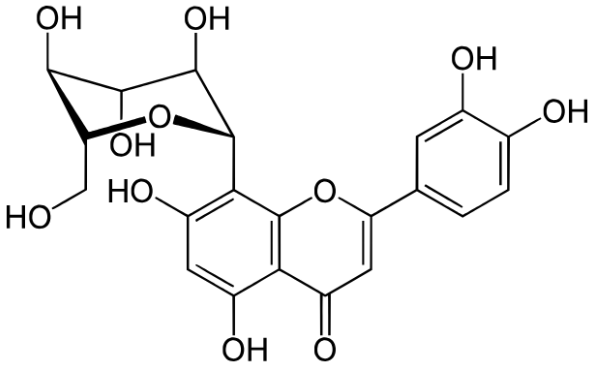

Orientin

Figure 2.11. Structures of some **f**lavonoids in lemongrass.

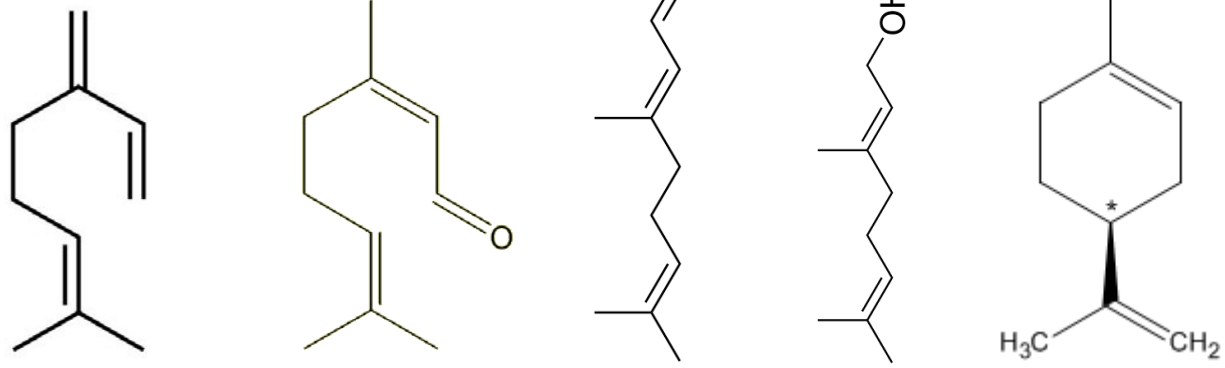

Myrecene Citral Geranial Geraniol Limonene

Figure 2.12. Structures of some terpenoids from lemongrass.

2.2.6. Pharmacological properties of lemongrass

2.2.6.1. Antioxidant activities of lemongrass

Normal physiological processes continuously generate reactive oxygen species that are mopped up by the natural antioxidant defence system, including reduced glutathione, superoxide dismutase, and catalase (Bankole *et al.* 2024). However, when the level of reactive oxygen species overwhelms the antioxidant system, oxidative stress results. Oxidative stress is implicated in many diseases such as diabetes mellitus, cancers, cardiovascular disorders, and neurodegenerative diseases (Kazeem and Tom Ashafa 2016). To counteract the harmful effects of oxidative stress, medicinal plants such as lemongrass are consumed due to their antioxidant potential. The *in vitro* antioxidant potential of lemongrass is presented in Table 2.10. Ethanol extracts of lemongrass displayed DPPH-free radical scavenging ability with IC_{50} values of 0.89 mg/mL (Boeira *et al.* 2018), 64.17 ppm (Fitria, Komariah and Kusuma 2022) and 191.97 µg/mL (Sah *et al.* 2012) respectively. Dichloromethane and ethyl acetate extracts of the plant also scavenged DPPH-free radicals with IC_{50} values of 152.20 and 131.30 µg/mL, respectively (Cheel *et al.* 2005). One study also evaluated both the DPPH and ABTS free radical scavenging abilities of the fresh and dry extracts of lemongrass (Guleria and Sehgal 2020). The wide variation in the antioxidant activities of the lemongrass extracts may be due to the difference in the extracting solvents.

Table 2.10. Antioxidant potential of lemongrass

Sample	Extract	Design	Method	EC_{50} values	Reference
Dry	Hydroethanol	*In-vitro*	DPPH	890 µg/mL	Boeira *et al*. (2018)
Fresh	Boiled water	*In-vitro*	DPPH/ABTS	10020/9970 µg/mL	Guleria & Sehgal (2020)
Dry	Boiled water	*In-vitro*	DPPH/ABTS	9540/10780 µg/mL	
Dry	70% Ethanol	*In-vitro*	DPPH	64.17 µg/mL	Fitria *et al* (2022)
Dry	40% Ethanol	*In-vitro*	DPPH	191.97 µg/mL	Sah *et al*. (2012)
Dry	Dichloromethane	*In-vitro*	DPPH	152.20 µg/mL	Cheel *et al* (2005)
	Ethylacetate	*In-vitro*	DPPH	131.30 µg/mL	

DPPH: 2,2-diphenyl-1-picrylhydrazyl, ABTS: 2,2-azino-bis(3-ethylbenzothiazoline-6-sulfonic acid

2.2.6.2 Anticancer activities of lemongrass

Cancer is responsible for the death of many people globally, killing 10 million people in 2020. Cancer-related death is projected to increase by 45% between 2008 and 2030, thereby worsening this situation. The most frequent cancers are breast, lung, colorectal, hepatic, ovarian, prostate, skin, and stomach. Due to a lack of therapeutic specificity, current chemotherapies, radiotherapies, and surgical procedures are associated with deleterious adverse effects and are not advised for long-term use. This calls for alternative therapies from natural products. Many studies have reported the anticancer activities of lemongrass using different cancer cell lines as presented in Table 2.11. Essential oil from fresh lemongrass is cytotoxic to H3B43 neck cancer cells (Yen *et al.* 2016), epithelial Vero cells (Salsabila *et al.* 2023) fibroblast, lung cancer cells (A549 and H1299) (Trang *et al.* 2020), liver cancer cells HepG2, and breast cancer cell MCF-7 (Mukhtar *et al.* 2023). Essential oil from dry lemongrass also inhibits the growth of Colorectal cancer HCT116 (Anton *et al.* 2022), cervical cancer cells (HeLa and ME-180) (Ghosh 2013), and breast cancer cells (SKBR3 and MCF-7) (Nagata *et al.* 2024). Ethanol extract from dry lemongrass is cytotoxic to prostate cancer cell PC3 (Nguyen *et al.* 2019), lymphoma cell U937 (Philion *et al.* 2017), and colon cancer cells (HT29 and HCT116) (Ruvinov *et al.* 2019).

2.2.6.3. Antidiabetic potential of lemongrass

Diabetes mellitus is a metabolic disorder characterized by hyperglycemia due to defects in insulin secretion and/or action. Its symptoms include polyuria, polydipsia and polyphagia and it can lead to serious complications such as nephropathy, neuropathy and retinopathy (Bankole *et al.* 2021). The goal of diabetes treatment is to sustain the blood glucose within the normal range (70 and 100 mg/dL). As such, diabetic patients manage this condition throughout their lives through physical activity, prescribed diets, and antidiabetic drugs (Kazeem *et al.* 2023). The consumption of lemongrass tea could be part of the diet to achieve glycemic control (Table 2.12). Essential oil from lemongrass inhibited α-amylase activity (Jumepaeng *et al.* 2013) and significantly reduced blood glucose levels in poloxamer-407 (Bharti *et al.* 2013) and fructose-induced hyperglycemia in rats (Dobhal *et al.* 2022). Ethanol extract of lemongrass inhibits α-glucosidase activity (Gunawan-Puteri *et al.* 2020), and the methanol extract reduced hyperglycemia in STZ-induced diabetic rats (Elekofehinti, Onunkun and Olaleye 2020). Dietary fibre from lemongrass (Villalobos, Nicolas

and Trinidad 2021) and aqueous extract (Garba *et al.* 2020) also reduced hyperglycemia in high-sugar diet-fed and STZ-fructose-induced diabetic rats.

Table 2.11. Anticancer activities of lemongrass

Sample	Extract	Method	Activity	Reference
Fresh	Oil	Neck cancer cell (H3B43)	15.42 ± 6.10 µg/mL	Yen *et al*. (2016)
Fresh	Oil	Vero cell (epithelial)	40 µg/mL	Salsabila *et al*. (2023)
		Fibroblast (NIH-3T3)	80 µg/mL	
Commercial	Oil	Colorectal cancer (HCT116)	7.8% at 75 µg/mL	Anton *et al*. (2022)
Fresh	Oil	Lung cancer cell (A549)	1.73 – 5.28 µg/mL	Trang *et al*. (2020)
	Oil	Lung cancer cell (H1299)	2.45 – 8.93 µg/mL	
Dry	Ethanol	Prostate cancer cell (PC3)	0.05 mg/mL	Nguyen *et al*. (2019)
Dry	Polysacch	Breast cancer cell (MDA)	600 µg/mL	Chen *et al*. (2022)
Fresh	Oil	Liver cancer cell (HepG2)	129.70 ± 11.40 µg/mL	Muktar *et al*. (2023)
		Breast cancer cell (MCF-7)	126.80 ± 10.90 µg/mL	
Dry	Hot water	Lymphoma cell (U-937)	0.39 ± 0.19 mg/mL	Philion *et al*. (2017)
	Ethanol	Lymphoma cell (U-937)	0.19 ± 0.05 mg/mL	
Dry	Oil	Cervical cancer cell (HeLa)	200 µg/mL	Ghosh (2023)
		Cervical cancer cell (ME-180)	200 µg/mL	
Dry	Methanol	Colon cancer cell (HCT116)	73.07 ± 2.42 µg/mL	Almutairi *et al*. (2024)
		Colon cancer cell (Caco-2)	40.37 ± 2.09 µg/mL	
Dry	Ethanol	Colon cancer cell (HT-29)	Reduce cell viability	Ruvinov *et al*. (2019)
		Colon cancer cell (HCT116)	Reduce cell viability	
Dry	Oil	Breast cancer cell (SKBR3)	18.40 µg/mL	Nagata *et al*. (2024)
		Breast cancer cell (MCF7)	12.40 µg/mL	

Polysacch: Polysaccharide

2.2.6.4. Anti-inflammatory potentials of lemongrass

Inflammation is a crucial phenomenon in the development of chronic diseases, namely diabetes, hypertension, and cancer. During an inflammatory response, macrophages release several

inflammatory mediators, such as cytokines, whose expression is regulated by different intracellular signalling pathways. Several medicinal plants have been evaluated for their ability to treat inflammation, and one of such plants is lemongrass (Table 2.13). Aqueous extract of lemongrass caused a 64.89% decrease in TNF-α expression (Francisco *et al.* 2013) and a 28.95% reduction in iNOS (Francisco *et al.* 2011) in lipopolysaccharide-induced cytokine production in macrophages. Luteolin isolated from lemongrass also reduced expression of the TNF-α in the macrophages by 33 (Tiwari, Dwivedi and Kakkar 2010) and 44% (Francisco *et al.* 2014) depending on concentration. Boiled water extract and essential oil of lemongrass caused about 43% (Costa *et al.* 2016) and 69% decrease (Boukhatem *et al.* 2014) in the eodema, respectively in carrageenan-induced paw oedema in rats. Lemongrass essential oil also significantly inhibited egg albumin denaturation with an IC_{50} of 29.71 µg/mL (Salaria *et al.* 2022). The oil also facilitated an 86% reduction in iNOS in lipopolysaccharide-induced dendritic cells (Figueirinha *et al.* 2010) and a 57% reduction in neutrophils in the zebrafish (Duarte da Silva *et al.* 2024). Finally, geraniol (100 µg/mL) isolated from lemongrass reduced the TNF-α expression by 68% in an Ox-LDL endothelial cell (Ben Ammar *et al.* 2022).

Table 2.12. Antidiabetic properties of lemongrass

Sample	Extract	Experimental design	Dose	FBG/IC_{50}	Reference
Fresh	Oil	Poloxamer-407 DM rats	800 mg/kg	323.96 mg/dL	Bharti *et al*. (2013)
Dry	Oil	α-amylase inhibition	NA	6.97 mg/dL	Jumapaeng *et al*. (2013)
Dry	Ethanol	α-glucosidase inhibition	NA	18.93 mg/mL	Gunawan-Puteri *et al* (2020)
Dry	Methanol	STZ-induced DM rats	400 mg/kg	82.57 mg/dL	Elekofehinti *et al*. (2020)
Dry	Aqueous	Fructose-induced MS in rats	250 mg/kg	127.50 mg/dL	Dobhal *et al*. (2022)
	Ethanol	Fructose-induced MS in rats	200 mg/kg	111.80 mg/dL	
	Oil	Fructose-induced MS in rat	300 mg/kg	111.60 mg/dL	
Dry	Boiled water	STZ fructose-induced DM rats	25%	170.00 mg/dL	Garba *et al*. (2020)
		STZ fructose-induced DM rats	50%	120.00 mg/dL	
Dry	Dietary fibre	α-amylase inhibition	NA	5.15 mg/mL	Villalobos *et al*. (2021)
		High sugar and fat diet rats	400 mg/kg	6.85 mmol/L	

FBG: Fasting blood glucose, NA: Not applicable, STZ: Streptozotocin, DM: Diabetes mellitus, MS: Metabolic syndrome

Table 2.13. Anti-inflammatory potentials of lemongrass

Sample	Extract	Experimental design	Dose	Results (Decrease)	Reference
Dry	Aqueous	LPS-induced TNF-α	1.12 mg/mL	64.89%	Francisco *et al*. (2013)
Dry	Luteolin	LPS-induced macrophages	50 µM	44%	Francisco *et al*. (2014)
Dry	Luteolin	LPS-induced macrophages	5 µg/mL	33%	Tiwari *et al*. (2010)
			10 µg/mL	56%	
Dry	Aqueous	LPS-induced macrophages	1.12 mg/mL	28.95% iNOS	Francisco *et al*. (2011)
Dry	Boil water	Caragenan-induced edema	1.0%	30%	Costa *et al*. (2016)
			4.0%	43% edema	
Dry	Oil	Egg albumin denaturation	NA	IC_{50}: 29.71 µg/mL	Salaria *et al*. (2021)
Dry	Oil	Caragenan-induced edema	40 mg/kg	95.56%	Boukhatem *et al*. (2014)
			100 mg/kg	69.23%	
Dry	Oil	Neutrophil in zebrafish	6.25 µg/mL	57%	Duarte Da Silva *et al*. (2024)
Dry	Oil	LPS-induced dendritic cell	1.12 mg/mL	85.7% NOS	Figuerinha *et al*. (2010)
Dry	Geraniol	Ox-LDL endothelial cell	100 µg/mL	68% TNF	Ben Ammar *et al*. (2022)

LPS: Lipopolysaccharide, TNF-α: Tumor necrosis factor-alpha, NA: Not applicable, iNOS: Inducible nitric oxide synthase, Ox-LDL: Oxidised low-density lipoprotein)

2.2.6.5. Antimicrobial activities of lemongrass

The prevalence of infections in all categories of individuals across the globe is on the increase, and all efforts to combat them prove abortive. The onset of multidrug-resistant strains of some microorganisms also thwarted the ongoing efforts at alleviating infections. As such, a great deal of attention has shifted to using natural products as alternative sources of antimicrobial agents (Table 2.14). Essential oils from dry lemongrass inhibited the growth of *Salmonella Heidelberg* (Dewi *et al.* 2021), *Candida dubliniensis* (MIC: 0.43 mg/mL) (Taweechaisupapong *et al.* 2012), and *Salmonella enterica* (Peichel *et al.* 2019). The oil also inhibited the growth of *Kytococcus sedentarius* (MIC: 0.10 mg/mL), *Dermatophilus congolensis* (MIC: 0.15 mg/mL), *Bacillus*

thuringiensis (Schweitzer *et al.* 2022), *Streptococcus mutans*, *Staphylococcus epidermidis*, and *Lactobacillus* spp (Ilango *et al.* 2019). Fresh lemongrass essential oil inhibited the growth of *Klebsiella pneumoniae* (MIC: 0.5%) (Naik *et al.* 2010), *Escherichia coli* (Dangkulwanich and Charaslertrangsi 2020), *Salmonella enterica* (MIC: 0.063%) (De Silva *et al.* 2017), and *Bacillus cereus* (MIC: 0.13 µL/mL) (Aiemsaard *et al.* 2011). Ethanol extract of lemongrass inhibited the growth of *Staphylococcus aureus* (ZI: 10 mm) (Elchaghaby, Abd El-Kader and Aly 2022) and *Salmonella typhi* (MIC: 24 µg/mL) (Ewansiha *et al.* 2012), while the methanol extract inhibited the growth of *Lactobacillus* spp. (ZI: 22.33 mm) (Owusu-Ansah *et al.* 2023) and *Staphylococcus aureus* (ZI:17.40 mm) (Ranjah *et al.* 2022).

Table 2.14. Antimicrobial activities of lemongrass

Sample	Extract	Experimental design	Dose	Effect	Reference
Dry	Oil	MDR *Salmonella* Heidelberg	0.15 – 1.5%	60% red pathogen	Dewi *et al*. (2021)
Dry	Oil	*Candida dubliniensis*	NA	MIC: 0.43 mg/mL	Taweechaisupapong et al. (2012)
	Oil	*Salmonella enterica*	0.03 – 0.5%	> 6 $\log_{10}$ CFU/mL	Peichel *et al*. (2019)
Dry	Ethanol	*Staphylococcus aureus*	20 mg/mL	ZI: 12.00 mm	Elchagaby *et al*. (2022)
		Streptococcus mutans	20 mg/mL	ZI: 11.00 mm	
		Enterococcus faecalis	20 mg/mL	ZI: 11.00 mm	
Fresh	Oil	*Staphylococcus aureus*	NA	MIC: 0.06%	Naik *et al*. (2010)
		Bacillus subtilis	NA	MIC: 0.06%	
		Klebsiella pneumoniae	NA	MIC: 0.50%	
Dry	Methanol	*Lactobacillus spp*	100%	ZI: 22.33 mm	Owusu-Ansah *et al*. (2023)
Dry	Methanol	*Staphylococcus aureus*	150 ppm	ZI: 17.40 mm	Ranjah *et al*. (2021)
		Escherichia coli	150 ppm	ZI: 16.00 mm	
		Salmonella ssp	150 ppm	ZI: 11.40 mm	
Dry	Ethanol	*Salmonella typhi*	NA	MIC: 24.00 µg/mL	Ewansiha *et al*. (2012)
		Escherichia coli	NA	MIC: 14.00 µg/mL	
		Candida albicans	NA	MIC: 32.00 µg/mL	
Fresh	Oil	*Escherichia coli*	NA	ZI: 1.47 cm	Dangkulwanich & Charaslertrangsi (2019)

		Staphylococcus aureus	NA	ZI: 2.30 cm	
		Bacillus subtilis	NA	ZI: 4.14 cm	
Fresh	Oil	*Pseudomonas aeruginosa*		MIC: 2.00% (v/v)	De Silva *et al*. (2017)
		Proteus mirabilis		MIC: 0.125% (v/v)	
		Salmonella enterica		MIC: 0.063% (v/v)	
Dry	Oil	*Kytococcus sedentarius*		MIC: 0.10 mg/mL	Shweitzer *et al*. (2022)
		Dermatophilus congolensis		MIC: 0.15 mg/mL	
		Bacillus thuringiensis		MIC: 0.15 mg/mL	
Dry	Oil	*Streptococcus mutans*	10 µL	ZI: 46.20 mm	Ilango *et al*. (2019)
		Staphylococcus epidermidis	10 µL	ZI: 30.00 mm	
		Lactobacillus spp	10 µL	ZI: 13.80 mm	
Fresh	Oil	*Staphylococcus aureus*		MIC: 0.54 µL/mL	Aiemsaard *et al*. (2011)
		Bacillus cereus		MIC: 0.13 µL/mL	
		Escherichia coli		MIC: 0.54 µL/mL	

MDR: Multi-drug resistant, MIC: Minimum inhibitory concentration, ZI: Zone of inhibition, CFU: Colony-forming unit, NA: Not applicable

2.2.7. Conclusion

Using medicinal foods and plants to manage diseases is a fruitful endeavour, as they mostly elicit their desired effect with minimal side effects. Lemongrass (*Cymbopogon citratus*) is one such plant that is consumed for recreation and medicinal benefits. This study provides integrated information on the nutritional composition, phytochemical composition, and pharmacological properties of lemongrass. This study revealed that lemongrass is rich in both nutrients and phytochemical compounds like phenolics, flavonoids, and terpenoids. It also showed that several studies had reported the antioxidant, anticancer, antidiabetic, anti-inflammatory, and antimicrobial properties of the plant, which may be due to its rich phytochemical profile. Though some compounds have been isolated from lemongrass, such as citral, there is a need to isolate other compounds and evaluate their pharmacological activities.

References

Adhikary, K., Banerjee, P., Barman, S., Bandyopadhyay, B. and Bagchi, D. 2024. Nutritional aspects, chemistry profile, extraction techniques of lemongrass essential oil and it's physiological benefits. *Journal of the American Nutrition Association*, 43 (2): 183-200.

Aiemsaard, J., Aiumlamai, S., Aromdee, C., Taweechaisupapong, S. and Khunkitti, W. 2011. The effect of lemongrass oil and its major components on clinical isolate mastitis pathogens and their mechanisms of action on *Staphylococcus aureus* DMST 4745. *Research in Veterinary Science*, 91 (3): e31-e37.

Akande, I., Samuel, T., Agbazue, U. and Olowolagba, B. 2011. Comparative proximate analysis of ethanolic and water extracts of *Cymbopogon citratus* (lemon grass) and four tea brands. *Plant Science Research*, 3 (4): 29-35.

Anton, A., Moacă, E. A., Sarau, C. A., Dinu, Ș., Semenescu, A. D., Macașoi, I. G. and Dehelean, C. A. 2022. Antioxidant and in vitro cytotoxic activity of commercial lemongrass, sea buckthorn and basil essential oils, against colorectal cancer cell line HCT 116. *Farmacia*, 1 (70): 683-689.

Asaolu, M., Oyeyemi, O. and Olanlokun, J. 2009. Chemical compositions, phytochemical constituents and in vitro biological activity of various extracts of *Cymbopogon citratus*. *Pakistan Journal of Nutrition*, 8 (12): 1920-1922.

Ashaq, B., Rasool, K., Habib, S., Bashir, I., Nisar, N., Mustafa, S., Ayaz, Q., Nayik, G. A., Uddin, J. and Ramniwas, S. 2024. Insights into chemistry, extraction and industrial application of lemon grass essential oil-A review of recent advances. *Food Chemistry: X*, Article ID: 101521.

Bankole, H. A., Fatai, A. A., Aleshe, S. M., Kazeem, M. I. and Kappo, A. P. 2021. *Laurus nobilis* Linn. inhibits polyol pathway enzymes: Strategy for managing diabetic complications. *Current Enzyme Inhibition*, 17 (2): 120-126.

Bankole, H. A., Kazeem, M. I., Fatai, A. A., Lawal, R. A., Lawanson, S. O., Ogunyemi, R. T., Ajiboye, T. O. and Olayemi, R. O. 2024. *Citrus aurantifolia* (Christm.) swingle extract ameliorates oxidative stress, dyslipidemia, and inflammation in galactose-induced aging in female rats. *South African Journal of Botany*, 168: 221-226.

Ben Ammar, R., Mohamed, M. E., Alfwuaires, M., Abdulaziz Alamer, S., Bani Ismail, M., Veeraraghavan, V. P., Sekar, A. K., Ksouri, R. and Rajendran, P. 2022. Anti-inflammatory activity of geraniol isolated from lemon grass on Ox-LDL-stimulated endothelial cells by upregulation of Heme Oxygenase-1 via PI3K/Akt and Nrf-2 signaling pathways. *Nutrients*, 14 (22): 4817.

Bharti, S., Kumar, A., Prakash, O., Krishnan, S. and Gupta, A. 2013. Essential oil of *Cymbopogon citratus* against diabetes: Validation by *in-vivo* experiment and computational studies. *Journal of Bioanalysis and Biomedicine*, 5(5): 194-203.

Boeira, C. P., Piovesan, N., Soquetta, M. B., Flores, D. C. B., Lucas, B. N., Rosa, C. S. d. and Terra, N. N. 2018. Extraction of bioactive compounds of lemongrass, antioxidant activity and evaluation of antimicrobial activity in fresh chicken sausage. *Ciência Rural*, 48 (11): e20180477.

Boukhatem, M. N., Ferhat, M. A., Kameli, A., Saidi, F. and Kebir, H. T. 2014. Lemon grass (*Cymbopogon citratus*) essential oil as a potent anti-inflammatory and antifungal drugs. *Libyan Journal of Medicine*, 9 (1): 25431.

Cheel, J., Theoduloz, C., Rodríguez, J. and Schmeda-Hirschmann, G. 2005. Free radical scavengers and antioxidants from Lemongrass (*Cymbopogon citratus* (DC.) Stapf.). *Journal of Agricultural and Food Chemistry*, 53 (7): 2511-2517.

Costa, G., Ferreira, J. P., Vitorino, C., Pina, M. E., Sousa, J. J., Figueiredo, I. V. and Batista, M. T. 2016. Polyphenols from *Cymbopogon citratus* leaves as topical anti-inflammatory agents. *Journal of Ethnopharmacology*, 178: 222-228.

Dangkulwanich, M. and Charaslertrangsi, T. 2020. Hydrodistillation and antimicrobial properties of lemongrass oil (*Cymbopogon citratus*, Stapf): An undergraduate laboratory exercise bridging chemistry and microbiology. *Journal of Food Science Education*, 19 (2): 41-48.

De Silva, B., Jung, W.-G., Hossain, S., Wimalasena, S., Pathirana, H. and Heo, G.-J. 2017. Antimicrobial property of lemongrass (*Cymbopogon citratus*) oil against pathogenic bacteria isolated from pet turtles. *Laboratory Animal Research*, 33: 84-91.

Dewi, G., Nair, D. V., Peichel, C., Johnson, T. J., Noll, S. and Johny, A. K. 2021. Effect of lemongrass essential oil against multidrug-resistant *Salmonella Heidelberg* and its attachment to chicken skin and meat. *Poultry Science*, 100 (7): 101116.

Dobhal, S., Singh, M. F., Setya, S. and Bisht, S. 2022. Comparative assessment of the effect of lemongrass (*Cymbopogon citratus*) ethanolic extract, aqueous extract and essential oil in high-fat diet and fructose-induced metabolic syndrome in rats. *Indian Journal of Pharmaceutical Education Research*, 56: s281-s293.

Duarte da Silva, K. C., Carneiro, W. F., Virote, B. d. C. R., Santos, M. d. F., de Oliveira, J. P. L., Castro, T. F. D., Bertolucci, S. K. V. and Murgas, L. D. S. 2024. Evaluation of the anti-inflammatory and antioxidant potential of *Cymbopogon citratus* essential oil in zebrafish. *Animals*, 14 (4): 581.

Ekpenyong, C. E., Akpan, E. and Nyoh, A. 2015. Ethnopharmacology, phytochemistry, and biological activities of *Cymbopogon citratus* (DC.) Stapf extracts. *Chinese Journal of Natural Medicines*, 13 (5): 321-337.

Ekpenyong, C. E. and Akpan, E. E. 2017. Use of *Cymbopogon citratus* essential oil in food preservation: Recent advances and future perspectives. *Critical Reviews in Food Science and Nutrition*, 57 (12): 2541-2559.

Elchaghaby, M. A., Abd El-Kader, S. F. and Aly, M. M. 2022. Bioactive composition and antibacterial activity of three herbal extracts (lemongrass, sage, and guava leaf) against oral bacteria: An *in vitro* study. *Journal of Oral Biosciences*, 64 (1): 114-119.

Elekofehinti, O. O., Onunkun, A. T. and Olaleye, T. M. 2020. *Cymbopogon citratus* (DC.) Stapf mitigates ER-stress induced by streptozotocin in rats via down-regulation of GRP78 and up-regulation of Nrf2 signaling. *Journal of Ethnopharmacology*, 262: 113130.

Ewansiha, J., Garba, S., Mawak, J. and Oyewole, O. 2012. Antimicrobial activity of *Cymbopogon citratus* (Lemon grass) and it's phytochemical properties. *Frontiers in Science*, 2(6): 214-220.

Fagbohun Emmanuel, D., David Oluwole, M., Adeyeye Emmanuel, I. and Oyedele, O. 2010. Chemical composition and antibacterial activities of some selected traditional medicinal plants used in the treatment of gastrointestinal infections in Nigeria. *International Journal of Pharmaceutical Science Review and Research*, 5 (3): 192-197.

Falcon, R. M. G., Fahrenbach, S. U., Feliciano, J. F., Flores, B. M. B., Dida-Agun, A. S., Domingo, E. J. V., Domingo, F. K. S., Duran, H. E. T., Dungala, D. B. and Dychiao, G. R. K. 2024. Antifungal properties of *Cymbopogon citratus* (DC.) Stapf—A scoping review. *South African Journal of Botany*, 170: 425-442.

Figueirinha, A., Cruz, M. T., Francisco, V., Lopes, M. C. and Batista, M. T. 2010. Anti-inflammatory activity of *Cymbopogon citratus* leaf infusion in lipopolysaccharide-stimulated dendritic cells: contribution of the polyphenols. *Journal of Medicinal Food*, 13 (3): 681-690.

Fitria, N., Komariah, K. and Kusuma, I. 2022. The antioxidant activity of lemongrass leaves extract against fibroblasts oxidative stress. *Brazilian Dental Science*, 25 (4): e3434.

Francisco, V., Costa, G., Figueirinha, A., Marques, C., Pereira, P., Neves, B. M., Lopes, M. C., García-Rodríguez, C., Cruz, M. T. and Batista, M. T. 2013. Anti-inflammatory activity of

Cymbopogon citratus leaves infusion via proteasome and nuclear factor-κB pathway inhibition: Contribution of chlorogenic acid. *Journal of Ethnopharmacology*, 148 (1): 126-134.

Francisco, V., Figueirinha, A., Costa, G., Liberal, J., Lopes, M. C., García-Rodríguez, C., Geraldes, C. F., Cruz, M. T. and Batista, M. T. 2014. Chemical characterization and anti-inflammatory activity of luteolin glycosides isolated from lemongrass. *Journal of Functional Foods*, 10: 436-443.

Francisco, V., Figueirinha, A., Neves, B. M., García-Rodríguez, C., Lopes, M. C., Cruz, M. T. and Batista, M. T. 2011. *Cymbopogon citratus* as source of new and safe anti-inflammatory drugs: bio-guided assay using lipopolysaccharide-stimulated macrophages. *Journal of Ethnopharmacology*, 133 (2): 818-827.

Garba, H. A., Mohammed, A., Ibrahim, M. A. and Shuaibu, M. N. 2020. Effect of lemongrass (*Cymbopogon citratus* Stapf) tea in a type 2 diabetes rat model. *Clinical Phytoscience*, 6: 1-10.

Ghosh, K. 2013. Anticancer effect of lemongrass oil and citral on cervical cancer cell lines. *Pharmacognosy Communications*, 3 (4). DOI: 10.5530/pc.2013.4.6

Guleria, K. and Sehgal, A. 2020. Appraisal of antioxidant effect of fresh and dried leaves of lemongrass (*Cymbopogon citratus*). *Plant Archives*, 20 (2): 2554-2557.

Gunawan-Puteri, M. D. P. T., Tjiptadi, F. M., Hendra, P., Santoso, F., Udin, Z., Artanti, N. and Ignatia, F. 2020. Lemongrass (*Cymbopogon citratus*) ethanolic extract exhibited activities that inhibit glucosidase enzymes and postprandial blood glucose elevation. *Makara Journal of Science*, 24 (4): 217-228.

Ilango, P., Suresh, V., Vummidi, A. V., Ravel, V., Chandran, V., Mahalingam, A. and Reddy, V. K. 2019. Evaluation of antibacterial activity of lemongrass oil against oral clinical isolates–an in vitro study. *Pharmacognosy Journal*, 11 (5): 1023-1028.

Jumepaeng, T., Prachakool, S., Luthria, D. L. and Chanthai, S. 2013. Determination of antioxidant capacity and [alpha]-amylase inhibitory activity of the essential oils from citronella grass and lemongrass. *International Food Research Journal*, 20 (1): 481.

Kamaruddin, Z. H., Jumaidin, R., Selamat, M. Z. and Ilyas, R. 2022. Characteristics and properties of lemongrass (*Cymbopogan citratus*): a comprehensive review. *Journal of Natural Fibers*, 19 (14): 8101-8118.

Kazeem, M. I., Bankole, H. A., Fatai, A. A., Oguntubi, T. S. and Kappo, A. P. 2023. Uncompetitive inhibition of polyol pathway enzymes by *Daucus carota* Linn. extract and management of diabetes mellitus. *Current Enzyme Inhibition*, 19 (3): 195-201.

Kazeem, M. I. and Tom Ashafa, A. O. 2016. Antioxidant and inhibitory properties of *Dombeya burgessiae* leaf extracts on enzymes linked to diabetes mellitus. *Transactions of the Royal Society of South Africa*, 71 (2): 167-174.

Kiani, H. S., Ali, A., Zahra, S., Hassan, Z. U., Kubra, K. T., Azam, M. and Zahid, H. F. 2022. Phytochemical composition and pharmacological potential of lemongrass (cymbopogon) and impact on gut microbiota. *AppliedChem*, 2 (4): 229-246.

Kusuma, I. Y., Perdana, M. I., Vágvölgyi, C., Csupor, D. and Takó, M. 2024. Exploring the Clinical Applications of Lemongrass Essential Oil: A Scoping Review. *Pharmaceuticals*, 17 (2): 159.

Lawal, O., Ogundajo, A., Avoseh, N. and Ogunwande, I. 2017. *Cymbopogon citratus*. In: *Medicinal spices and vegetables from Africa*. Elsevier, 397-423.

Mukarram, M., Choudhary, S., Khan, M. A., Poltronieri, P., Khan, M. M. A., Ali, J., Kurjak, D. and Shahid, M. 2021. Lemongrass essential oil components with antimicrobial and anticancer activities. *Antioxidants*, 11 (1): 20.

Mukhtar, M. H., El-Readi, M. Z., Elzubier, M. E., Fatani, S. H., Refaat, B., Shaheen, U., Adam Khidir, E. B., Taha, H. H. and Eid, S. Y. 2023. *Cymbopogon citratus* and citral overcome doxorubicin resistance in cancer cells via modulating the drug's metabolism, toxicity, and multidrug transporters. *Molecules*, 28 (8): 3415.

Nagata, T., Satou, T., Hayashi, S., Satyal, P., Watanabe, M., Riggs, B. and Saida, Y. 2024. Citral in lemon myrtle, lemongrass, litsea, and melissa essential oils suppress the growth and invasion of breast cancer cells. *BMC Complementary Medicine and Therapies*, 24 (1): 211.

Naik, M. I., Fomda, B. A., Jaykumar, E. and Bhat, J. A. 2010. Antibacterial activity of lemongrass (*Cymbopogon citratus*) oil against some selected pathogenic bacterias. *Asian Pacific Journal of Tropical Medicine*, 3 (7): 535-538.

Negrelle, R. and Gomes, E. 2007. *Cymbopogon citratus* (DC.) Stapf: Chemical composition and biological activities. *Revista Brasileira de Plantas Medicinais*, 9 (1): 80-92.

Nguyen, C., Mehaidli, A., Baskaran, K., Grewal, S., Pupulin, A., Ruvinov, I., Scaria, B., Parashar, K., Vegh, C. and Pandey, S. 2019. Dandelion root and lemongrass extracts induce apoptosis, enhance chemotherapeutic efficacy, and reduce tumour xenograft growth in vivo in prostate cancer. *Evidence-Based Complementary and Alternative Medicine*, 2019 (1): 2951428.

Nimenibo-Uadia, R. and Nwosu, E. 2020. Phytochemical, proximate and mineral elements composition of lemongrass (*Cymbopogon citratus* (DC) stapf) grown in ekosodin, Benin city, Nigeria. *Nigerian Journal of Pharmaceutical and Applied Science Research*, 9 (2): 52-56.

Oladeji, O. S., Adelowo, F. E., Ayodele, D. T. and Odelade, K. A. 2019. Phytochemistry and pharmacological activities of *Cymbopogon citratus*: A review. *Scientific African*, 6: e00137.

Owusu-Ansah, P., Alhassan, A. R., Ayamgama, A. A., Adzaworlu, E. G., Afoakwah, N. A., Mahunu, G. K. and Amagloh, F. K. 2023. Phytochemical analysis, enumeration, isolation, and

antimicrobial activity of lemongrass and moringa leaves extracts. *Journal of Agriculture and food Research*, 12: 100579.

Peichel, C., Nair, D., Dewi, G., Donoghue, A., Reed, K. and Johny, A. K. 2019. Effect of lemongrass (*Cymbopogon citratus*) essential oil on the survival of multidrug-resistant *Salmonella enterica* serovar Heidelberg in contaminated poultry drinking water. *Journal of Applied Poultry Research*, 28 (4): 1121-1130.

Philion, C., Ma, D., Ruvinov, I., Mansour, F., Pignanelli, C., Noel, M., Saleem, A., Arnason, J., Rodrigues, M. and Singh, I. 2017. *Cymbopogon citratus* and *Camellia sinensis* extracts selectively induce apoptosis in cancer cells and reduce growth of lymphoma xenografts in vivo. *Oncotarget*, 8 (67): 110756.

Ranjah, M. A., Ismail, A., Waseem, M., Tanweer, S., Ahmad, B., Mehmood, T., Shah, F.-U.-H., Ahmad, Z., Hussain, M. and Ismail, T. 2022. Comparative study of antioxidant and antimicrobial activity of different parts of lemongrass leaves and their application in the functional drink. *Nutrition & Food Science*, 52 (4): 657-669.

Ruvinov, I., Nguyen, C., Scaria, B., Vegh, C., Zaitoon, O., Baskaran, K., Mehaidli, A., Nunes, M. and Pandey, S. 2019. Lemongrass extract possesses potent anticancer activity against human colon cancers, inhibits tumorigenesis, enhances efficacy of FOLFOX, and reduces its adverse effects. *Integrative Cancer Therapies*, 18: 1534735419889150.

Sah, S. Y., Sia, C. M., Chang, S. K., Ang, Y. K. and Yim, H. S. 2012. Antioxidant capacity and total phenolic content of lemon grass (*Cymbopogon citratus*) leave. *Annals of Food Science and Technology*, 13 (2): 150-155.

Salaria, D., Rolta, R., Sharma, N., Patel, C. N., Ghosh, A., Dev, K., Sourirajan, A. and Kumar, V. 2022. *In vitro* and *in silico* antioxidant and anti-inflammatory potential of essential oil of *Cymbopogon citratus* (DC.) Stapf. of North-Western Himalaya. *Journal of Biomolecular Structure and Dynamics*, 40 (24): 14131-14145.

Salsabila, D. U., Wardani, R. K., Hasanah, N. U., Tafrihani, A. S., Zulfin, U. M. and Meiyanto, E. 2023. Cytoprotective properties of citronella oil (*Cymbopogon nardus* (L.) Rendl.) and lemongrass oil (*Cymbopogon citratus* (DC.) Stapf) through attenuation of senescent-induced chemotherapeutic agent doxorubicin on Vero and NIH-3T3 Cells. *Asian Pacific Journal of Cancer Prevention: APJCP*, 24 (5): 1667.

Schweitzer, B., Balázs, V. L., Molnár, S., Szögi-Tatár, B., Böszörményi, A., Palkovics, T., Horváth, G. and Schneider, G. 2022. Antibacterial effect of lemongrass (*Cymbopogon citratus*) against the aetiological agents of pitted keratolyis. *Molecules*, 27 (4): 1423.

Silva, H. and Bárbara, R. 2022. Exploring the anti-hypertensive potential of lemongrass—a comprehensive review. *Biology*, 11 (10): 1382.

Soares, M. O., Alves, R. C., Pires, P. C., Oliveira, M. B. P. and Vinha, A. F. 2013. Angolan *Cymbopogon citratus* used for therapeutic benefits: Nutritional composition and influence of solvents in phytochemicals content and antioxidant activity of leaf extracts. *Food and Chemical Toxicology*, 60: 413-418.

Taweechaisupapong, S., Ngaonee, P., Patsuk, P., Pitiphat, W. and Khunkitti, W. 2012. Antibiofilm activity and post antifungal effect of lemongrass oil on clinical *Candida dubliniensis* isolate. *South African Journal of Botany*, 78: 37-43.

Tazi, A., Zinedine, A., Rocha, J. M. and Errachidi, F. 2024. Review on the pharmacological properties of lemongrass (*Cymbopogon citratus*) as a promising source of bioactive compounds. *Pharmacological Research-Natural Products*, Article ID: 100046.

Tibenda, J. J., Yi, Q., Wang, X. and Zhao, Q. 2022. Review of phytomedicine, phytochemistry, ethnopharmacology, toxicology, and pharmacological activities of Cymbopogon genus. *Frontiers in Pharmacology*, 13: 997918.

Tiwari, M., Dwivedi, U. and Kakkar, P. 2010. Suppression of oxidative stress and pro-inflammatory mediators by *Cymbopogon citratus* D. Stapf extract in lipopolysaccharide stimulated murine alveolar macrophages. *Food and Chemical Toxicology*, 48 (10): 2913-2919.

Trang, D. T., Hoang, T. K. V., Nguyen, T. T. M., Van Cuong, P., Dang, N. H., Dang, H. D., Nguyen Quang, T. and Dat, N. T. 2020. Essential oils of lemongrass (*Cymbopogon citratus* Stapf) induces apoptosis and cell cycle arrest in A549 lung cancer cells. *BioMed Research International*, 2020 (1): 5924856.

Uraku, A., Okaka, A., Ogbanshi, M. and Onuoha, S. 2016. Nutritive and anti-nutritive potentials of *Cymbopopgon citratus* leaves. *American Journal of Food and Nutrition*, 6: 14-22.

Villalobos, M. C., Nicolas, M. G. and Trinidad, T. P. 2021. Antihyperglycemic and cholesterol-lowering potential of dietary fibre from lemongrass (*Cymbopogon citratus* Stapf.). *Mediterranean Journal of Nutrition and Metabolism*, 14 (4): 453-467.

Yen, N., Zainah, A., Arapoc, D. J., Mohamed, Z. A. M. A. and Shafii, K. 2016. Anticancer effect and apoptosis induction of *Cymbopogon citratus* plant on head and neck HTB43 cancer cell lines. *International Atomic Energy Agency*, Article ID: 48050355.

CHAPTER 3

3. Influence of drying on the nutritional composition, phytochemical constituents and *in vitro* antioxidant properties of *Cymbopogon citratus* (lemongrass) infusions

Mutiu Idowu Kazeem, John Jason Mellem and Saheed Sabiu

Department of Biotechnology and Food Science, Faculty of Applied Sciences, Durban University of Technology, P. O. Box 1334, Durban 4000, South Africa

Preface: This article evaluated the impact of drying on the proximate, mineral, amino acid, phytochemical composition, and the antioxidant properties of lemongrass infusions. The manuscript is submitted to the journal, *Food and Humanity*.

3.1. Abstract

This study evaluated the influence of drying on the phytochemical and nutritional composition of lemongrass teas and their antioxidant properties. Infusions made from fresh and dry lemongrass leaves were subjected to proximate, mineral, amino-acid, and phytochemical analysis using standard methods. The antioxidant properties of the infusions were assessed using 1,1-diphenyl-2-picrylhydrazyl (DPPH), hydroxyl, and superoxide anion radical scavenging abilities as well as the iron chelation assay. The results revealed that fresh infusion has a higher ($p < 0.05$) quantity of protein (20.27%) and fibre (26.39%) than dry tea, while dry tea is richer in ash (10.97%) and carbohydrate (40.01%) content. Both infusions have similar macroelement composition, but the fresh tea is richer in the microelements. While the general amino acid profiles are similar in both the fresh and dry infusions, arginine (0.16 g/100 g), leucine (0.18 g/100 g), and proline (3.75 g/100 g) are higher in the fresh infusion. Both infusions have similar phytochemical constituents; however, the percentage composition of corymboside, veranisatin C, chamaemeloside, and herbarumin II is higher in the dry sample. The EC_{50} value for the inhibition of DPPH (44.60 µg/mL), hydroxyl (55.05 µg/mL), and superoxide anion (37.48 µg/mL) radicals is lower ($p < 0.05$) in the dry infusion compared to the fresh one, while the fresh infusion has a lower EC_{50} for iron chelation. It can be concluded that both fresh and dry lemongrass infusions are rich in nutrients, minerals, amino acids, as well as phytochemicals, and exhibit potential antioxidant properties.

However, the dry tea displayed better antioxidant properties than the fresh one, and this may be due to its richer phytochemical composition compared to the fresh tea.

Keywords: Lemongrass tea, *Cymbopogon citratus*, nutrients, non-communicable diseases, medicinal foods, phytochemical composition

3.2. Introduction

Non-communicable diseases constitute the most prominent cause of death globally (Gouda *et al.* 2019). Seven of the top 10 causes of mortality are NCDs, including Ischaemic heart disease, cancers, and diabetes mellitus (Bigna and Noubiap 2019). These diseases are chronic and are managed for a long period with the aid of orthodox drugs. However, there are some concerns regarding the efficacy, safety, and compliance with the treatment regimen (Stein, Lamos and Davis 2013). Consequently, about 8 out of 10 people around the globe now use medicinal foods and plants to treat their ailments (Gurib-Fakim 2006). Every region of the globe is blessed with several plants that can be therapeutic for many ailments.

In Africa, the use of plants in traditional medicine has been in place since time immemorial, and our fathers depend solely on them for their cure (Gurib-Fakim 2006). They are used to treat many ailments, including malaria, inflammation, cough, diabetes, infertility, and kidney and liver diseases (Prasathkumar *et al.* 2021). Prominent among the plants used as medicine are *Ageratum conyzoides* (billygoat weed), *Azadirachta indica* (neem), *Carica papaya* (pawpaw), *Ficus exasperata* (white fig tree), *Khaya senegalensis* (African mahogany), *Viscum album* (mistletoe), and *Cymbopogon citratus* (lemongrass) (Mohammed, Ibrahim and Islam 2014). The efficacy and safety of these medicinal plants have been reported in several articles.

Cymbopogon citratus (lemongrass) is a perennial grass that belongs to the family Poaceae and is found in the tropical parts of the globe (Avoseh *et al.* 2015). Due to its aroma, it is widely taken as tea or decoction in Africa, Asia, and South America (Oladeji *et al.* 2019). It is also used in folk medicine to treat malaria, pain, inflammation, infection, cough, and stomach ache. Scientific studies have revealed that the plant has antimicrobial, anti-inflammatory, antimalarial, antilipidemic, antioxidant, and antitumor properties (Oladeji *et al.* 2019; Kamaruddin *et al.* 2022). Traditionally, two types of infusions are made from this plant: one from the fresh leaves and the other from the dry ones. However, there is no report in the literature on whether there are

differences in the chemical composition and antioxidant potential of both the fresh and dry infusions of lemongrass. Consequently, we evaluated the effect of drying on the phytochemical and nutritional composition of lemongrass teas and their *in vitro* antioxidant properties.

3.3. Materials and methods

3.3.1. Preparation of lemongrass infusion

Leaves of lemongrass were harvested from farmland in the Iba area of Lagos in October 2021. It was identified and authenticated at the Department of Botany, Lagos State University, and was assigned the voucher number: LSH/21/1055. The leaves were gently rinsed in tap water to remove soil and dirt. A portion was cut into pieces, spread on foil paper and dried to constant weight at 25 °C. After drying, the sample was pulverized using an electric blender (Silver Crest, Germany). One litre of boiled distilled water was poured on a 100 g milled sample, shaken, and left to steep for 24 h to produce an infusion. An additional 1.0 L of boiled distilled water was poured on the second portion (100 g) of the fresh lemongrass and left to steep for 24 h. Both infusions were filtered and dried in a freeze-dryer (Virtis BenchTop, SP Scientific Series, USA). The freeze-dried teas were used for subsequent analysis.

3.3.2. Nutritional composition

3.3.2.1. Proximate composition

The moisture content of samples was evaluated by drying them in a hot air oven at 105 °C, while ash content was determined by incineration in a muffle furnace at 600 °C. Total protein was quantified using the Kjeldahl method (F = 6.25), total fat using the Soxhlet extraction method and total dietary fibre via the AOAC method (AOAC 2012). The carbohydrate content was calculated by the difference method [100 – (ash + fat + fibre + moisture + protein)].

3.3.2.2. Mineral composition

The minerals were determined in the samples by digesting in a diffused microwave system (MLS 1200 Mega; Milestone S.r.L., Sorisole, Italy) using polytetrafluoroethylene digestion vessels. Minerals in the digested samples were estimated by Inductively Coupled Plasma Mass Spectrometry (ICP-MS 7700 series, Agilent Technology International Pvt. Ltd).

3.3.2.3. Amino acid composition

The amino acid analysis was performed using the previous method (Zhang *et al.* 2017). Hydrochloric acid (6N) and 6 N NaOH were used to hydrolyze and neutralize the samples, respectively, before derivatization. The derivatized samples were injected into high-performance liquid chromatography (HPLC) (Perkin Elmer, USA) equipped with a C18 RP column and a fluorescence detector. The amino acids were identified and quantified by comparing them with the retention times and peak areas of standards (WAT088122, Waters).

3.3.3. Phytochemical composition

3.3.3.1. Total phenolic content

The total phenolic content (TPC) was determined by adding 0.5 mL of the samples to 2.5 mL of 10% Folin-Ciocalteu's reagent (v/v), and 2.0 mL of 7.5% sodium carbonate was added (Liu *et al.* 2017). The mixture was incubated at 45 °C for 40 min, and the absorbance was measured at 765 nm in a spectrophotometer using gallic acid as a standard.

3.3.3.2. Total flavonoid content

The total flavonoid content (TFC) was estimated by mixing 0.5 mL of the samples with 0.5 mL methanol, 50 µL 10% $AlCl_3$, 50 µL 1 M potassium acetate, and 1.4 mL water, and the mixture was incubated at room temperature for 30 min (Zhishen, Mengcheng and Jianming 1999). The absorbance of the reaction mixture was measured at 415 nm, and the total flavonoid content was calculated using quercetin as a standard.

3.3.3.3. LC-MS analysis

The phytochemical composition of the teas obtained from fresh and dry lemongrass leaves was assessed using a previous method (Suleria, Barrow and Dunshea 2020). Agilent 6520 Accurate-Mass QTOF was applied in a positive and negative mode. Synergi Hydro-RP (4 µm particle size, 4.6 mm internal diameter, and 250 mm length with 80 Å pore size were used to separate phenolic compounds, and the flow rate was set at 800 µL/min. An aliquot of 10 µL from each sample was injected while gradient was 0–5 min (0–10%), 5–25 min (10–25% B), 25–35 min (25–35% B), 35–45 min (40–60% B) 45–75 min (40–55% B), 75–80 min (55–88% B) (80–82 min (80–90% B), 82–85 min (90–100% B), 85–90 min (0% B). Mobile phase A was 0.1% formic acid in wate,r and mobile phase B was 95% acetonitrile with 0.1% formic acid. A full scan mode was achieved in

the range of 100–1000 amu with the following conditions: Capillary voltage (3500 V), nozzle voltage (500 V), nitrogen gas flow rate (9 L/min) at 325 °C and nebulization was set as 45 psi while 10, 20 and 30 eV collision energies were used. Acquisition of data was performed through the employment of MassLynx4.1 software, while detection and confirmation of metabolites were processed using the MS-DIAL software and MS-FINDER (RIKEN Centre for Sustainable Resource Science: Metabolome Informatics Research Team, Kanagawa, Japan). For further confirmation, identification of the profiled metabolites was also performed by comparing the respective mass spectra obtained against the National Institute of Standards and Technology (NIST) library (Wallace and Moorthy, 2023).

3.3.4. Antioxidant properties

3.3.4.1. DPPH free radical scavenging ability

The ability of the teas to scavenge DPPH (1,1-diphenyl-2-picrylhydrazyl) free radicals was evaluated by adding different concentrations (3.13 – 100 µg/mL) of the lemongrass infusions (150 µL) to 150 µL of 0.4 mmol/L methanol solution containing DPPH radicals (Saha *et al.* 2008). The mixture was incubated in the dark for 30 min, and the absorbance was determined at 516 nm. The concentration of infusion or standard (gallic acid) that scavenged 50% of DPPH radicals (EC_{50}) was evaluated using Microsoft Excel (2010).

3.3.4.2. Hydroxyl radical scavenging ability

The ability of the teas to scavenge hydroxyl radicals was performed by adding 40 µL freshly prepared infusions (3.13 – 100 µg/mL) to a reaction mixture containing 20 µL 20 mM deoxyribose, 80 µL 0.1 M phosphate buffer, 10 µL 20 mM hydrogen peroxide, and 10 µL 500 mM $FeSO_4$ (Oboh and Rocha 2007). The reaction mixture was incubated at 37 °C for 30 min, followed by the addition of 50 µL of 2.8% TCA (trichloroacetic acid) and 50 µL of 0.6% thiobarbituric acid (TBA) solution. The mixtures were then incubated for 20 min, and the absorbance was taken at 532 nm in a microplate reader (Model 680, BIO-RAD). The concentration of infusion or standard (gallic acid) that scavenged 50% of hydroxyl radicals (EC_{50}) was evaluated using Microsoft Excel (2010).

3.3.4.3. Iron chelation assay

The chelation of ferrous ions by the teas was evaluated by adding 200 µL of 0.2 mM $FeCl_2$ to 40 µL aliquots of infusions (3.13 – 100 µg/mL) (Kazeem and Ashafa 2015). This is followed by the addition of 5 mM ferrozine (80 µL), and the mixture was vigorously shaken and left to stand at room temperature for 10 min. The absorbance was then measured at 562 nm in a microplate reader (Model 680, BIO-RAD, USA). The concentration of infusion or standard (EDTA) that chelated 50% of iron (EC_{50}) was evaluated using Microsoft Excel (2010).

3.3.4.4. Superoxide anion radical scavenging ability

The superoxide anion scavenging activity of the lemongrass teas was accomplished by generating superoxide radicals first by adding 50 µL of Tris-HCl buffer (16 mM, pH 8.0) containing 50 µL of NBT (50 mM) solution, 50 µL NADH (78 mM) solution, and different concentrations (3.13 – 100 µg/mL) of lemongrass infusions (100 µL) together (Liu, Ooi and Chang 1997). This was followed by the addition of 1 mL of phenazine methosulphate (PMS) solution (10 mM) to the mixture. The reaction mixture was incubated at 25 °C for 5 min, and the absorbance was measured at 560 nm. The concentration of infusion or standard (gallic acid) that scavenged 50% of superoxide anion radicals (EC_{50}) was evaluated using Microsoft Excel (2010).

3.3.5. Statistical analysis

Nutritional composition and antioxidant analyses were conducted in triplicate, and data were expressed as mean ± standard error of the mean (SEM). Student's t-test was used to assess differences in the percentage scavenging abilities and IC_{50} values of the samples using the GraphPad Prism statistical package (GraphPad Software, USA). Statistical significance was considered at $p < 0.05$.

3.4. Results and discussion

The effect of drying on the nutritional composition, phytochemical constituents, and antioxidant properties of teas obtained from fresh and dry lemongrass leaves was evaluated.

3.4.1. Effect of drying on proximate composition

Table 3.1 shows the results of the proximate composition of infusions obtained from fresh and dry samples of lemongrass. The fresh infusion has significantly higher ($p < 0.05$) protein (20.27%) and

fibre content (26.39%) compared to the dry sample. These values are similar to the ones reported earlier (Soares *et al.* 2013; Unuigbe *et al.* 2019). Conversely, the dry infusion exhibited significantly higher carbohydrate (40.01%) and ash content (10.97%) than the fresh one. The ash content of the dry infusion is similar to the report of (Nimenibo-Uadia and Nwosu 2020). The moisture and fat content are similar in the two samples. While the fat content is identical to the report of (Nimenibo-Uadia and Nwosu 2020), the moisture content is higher than that of (Soares *et al.* 2013).

Table 3.1. Proximate composition of teas obtained from fresh and dry lemongrass leaves

Nutrients	Fresh (%)	Dry (%)
Protein	20.27 ± 1.12	13.16 ± 0.60*
Moisture	11.79 ± 0.24	10.17 ± 0.22
Ash	6.99 ± 0.72	10.97 ± 0.60*
Fat	6.26 ± 0.66	7.77 ± 0.52
Fibre	26.39 ± 0.74	17.94 ± 0.69*
Carbohydrate	28.31 ± 0.56	40.01 ± 0.82*

Values are expressed as mean ± SEM of triplicate determinations. *Significant difference at $p<0.05$.

The high content of carbohydrates in both lemongrass infusions, especially the dry sample, may imply that they are a good source of energy for the consumers (Devi, Bains and Kaur 2019). The higher composition of protein in the fresh sample suggests that the proteins and enzymes present in it were preserved from denaturation, which may hitherto occurred by drying (Devi, Bains and Kaur 2019). This provides support for the body by engendering the growth and repair of worn-out tissues. A similar concentration of fat in the two infusions may signify that they maintain the integrity of the cellular membranes, thereby preventing the consumers from undue attack arising from membrane damage (Li *et al.* 2024). The lower fibre content in dry infusion may be due to the loss of moisture, which makes it less efficient in maintaining the health of the digestive system of its consumers (Garba and Oviosa 2019).

3.4.2. Effect of drying on mineral composition

Table 3.2 shows the mineral composition of infusions obtained from fresh and dry samples of lemongrass. The essential mineral (sodium, magnesium, potassium, and calcium) composition of the two samples is similar ($p > 0.05$) but is higher than the previous report (Asaolu, Oyeyemi and Olanlokun 2009), which may be due to the impact of hot water used in preparing the infusions. The content of the essential minerals (especially potassium and calcium) is also very high compared to the trace minerals. However, the fresh infusion has a higher content ($p < 0.05$) of trace minerals (manganese, copper, and zinc) while iron is more in the dry tea. However, the micronutrient level in both samples is higher than Cornelian cherry (Bayram *et al.* 2024). Both the fresh and dry infusions are rich in macro-elements (sodium, potassium, calcium, and magnesium). Sodium contributes to the extracellular osmolality of water, while potassium contributes to intracellular osmotic activity (Ahmed *et al.* 2024; Hwang *et al.* 2024). Potassium also helps to excrete sodium in the kidneys and regulate blood pressure (Hwang *et al.* 2024). Calcium plays a key role in bone and teeth structure, blood coagulation, endocrine function, and the physiology of the heart and smooth muscles (Ahmed *et al.* 2024). Magnesium serves as a cofactor of many enzymatic reactions and some hormones. It also helps in muscle contraction as well as the maintenance of the structures and integrity of biological membranes.

The higher concentration of manganese, copper, and zinc in the fresh infusion suggests that it is richer in the microelements than in the dry sample. Zinc plays a catalytic role by being a component of metalloenzymes and maintaining the structure of zinc-finger proteins (Hwang *et al.* 2024). It also regulates cell signalling pathways and the transmission of nerve impulses. Copper, on the other hand, helps in bone and connective tissue formation, as well as in brain, cardiac, and immune function (Jomova *et al.* 2022). Both samples are rich in iron, which suggests that they may play a role in the transport of oxygen and other useful entities in the body. Though selenium is present in minute amounts in both infusions, it may play a significant role in the transmission of nerve impulses, the immune system, endocrine function, and male reproduction.

Table 3.2. Mineral composition of teas obtained from fresh and dry lemongrass leaves.

Minerals	Fresh (ppm)	Dry (ppm)
Sodium	2757.40 ± 5.87	2487.70 ± 3.52
Magnesium	8721.90 ± 7.40	7574.90 ± 5.85
Potassium	75688.10 ± 10.05	66127.50 ± 9.27
Calcium	33443.90 ± 9.10	28238.70 ± 8.80
Manganese	146.70 ± 4.30	112.93 ± 2.25*
Iron	143.80 ± 3.50	162.81 ± 4.20*
Copper	34.41 ± 1.30	13.51 ± 1.10*
Zinc	58.79 ± 2.50	35.27 ± 1.50*
Selenium	0.20 ± 0.00	0.18 ± 0.00

Values are expressed as mean ± SEM of triplicate determinations. *Significant difference at $p<0.05$.

3.4.3. Effect of drying on amino acid composition

The amino acid composition of the infusion obtained from fresh and dry samples of lemongrass is shown in Table 3.3. The fresh infusion has a significantly higher ($p < 0.05$) concentration of arginine, lysine, leucine, and proline than the dry sample, while the dry infusion has more aspartic acid content. In both samples, the concentrations of proline and aspartic acid are more than 60% of the whole sample. The concentration of other amino acids is also similar in both the fresh and dry infusions. The higher abundance of proline and aspartic acid in both samples implies their biological importance to consumers. Both proline and aspartic acid are non-essential amino acids that are present in proteins. While proline plays a key role in protein function and maintenance of cellular redox homeostasis (Vettore, Westbrook and Tennant 2021), aspartic acid is involved in urea synthesis, gluconeogenesis, and transmission of nerve impulses (Holeček 2023). The concentrations of arginine, lysine, and leucine are higher in the fresh infusion compared to the dry sample. Consumption of arginine-rich fresh infusion improves immune function, helps in the healing of wounds, and increases insulin sensitivity (Mustafa *et al.* 2013). Lysine is essential for optimal growth of cells, while leucine encourages protein synthesis (Mohanty *et al.* 2014).

Consequently, the trio of arginine, lysine, and leucine in the fresh infusion may encourage normal growth, heal wounds, and regulate blood glucose levels.

Table 3.3. Amino-acid composition of teas obtained from fresh and dry lemongrass leaves.

Amino acid	Fresh (g/100g)	Dry (g/100g)
Histidine	0.10 ± 0.01	0.10 ± 0.00
Arginine	0.16 ± 0.01	0.08 ± 0.00*
Threonine	0.25 ± 0.01	0.24 ± 0.01
Lysine	0.18 ± 0.01	0.10 ± 0.01*
Valine	0.23 ± 0.01	0.23 ±0.01
Isoleucine	0.10 ± 0.00	0.07 ± 0.00
Leucine	0.18 ± 0.01	0.08 ± 0.00*
Phenylalanine	0.17 ± 0.00	0.15 ± 0.00
Serine	0.17 ± 0.01	0.29 ± 0.01
Glycine	0.23 ± 0.01	0.18 ± 0.01
Aspartic acid	1.35 ± 0.05	2.02 ± 0.07*
Glutamic acid	0.91 ± 0.03	0.90 ± 0.04
Alanine	0.54 ± 0.02	0.44 ± 0.02
Proline	3.75 ± 0.09	3.40 ± 0.08*
Tyrosine	0.10 ± 0.00	0.07 ± 0.00

Values are expressed as mean ± SEM of triplicate determinations. *Significant difference at $p<0.05$.

3.4.4. Effect of drying on the antioxidant activities

Figure 3.1 shows the free-radical scavenging abilities of infusions obtained from fresh and dry samples of lemongrass. At higher concentrations (50 – 100 µg/mL), the dry infusion has higher ($p < 0.05$) DPPH (Fig. 3.1a) and superoxide anion (Fig. 3.1d) radical scavenging abilities, while they are similar at other doses. The dry infusion also displayed better hydroxyl radical scavenging ability, especially at 6.25 and 50 µg/mL, than the fresh sample (Fig. 3.1b). However, the fresh infusion has a significantly higher ($p < 0.05$) iron chelation activity compared to the dry one (Fig.

3.1c). The EC_{50} values for the free radical scavenging abilities of the infusions obtained from fresh and dry samples of lemongrass are shown in Table 3.4. The dry infusion exhibited significantly lower ($p < 0.05$) EC_{50} for the DPPH, hydroxyl, and superoxide anion radical scavenging abilities compared to the fresh sample. However, the fresh infusion displayed a lower EC_{50} value for the iron chelation activity, and this is comparable to the standard, EDTA.

Previous reports have revealed that oxidative stress is implicated in the pathogenesis and progression of many pathological conditions (Liguori *et al.* 2018; Dubois-Deruy *et al.* 2020). The fact that dry infusion exhibited a lower EC_{50} for the DPPH, hydroxyl, and superoxide anion radical scavenging activities suggests that it possessed better antioxidant activity (Mbhele *et al.* 2015). However, the fresh sample displayed a lower EC_{50} for the iron chelation assay, which may imply that the fresh tea is better at chelating oxidative-stress-induced cellular iron production. It eventually decreases the concentration of transition metals, which catalyzes lipid peroxidation (Kazeem and Davies 2016). While the dry infusion is more potent at scavenging free radicals generated in oxidative stress, the fresh sample chelates transition metals more and prevents lipid peroxidation.

3.4.5. Effect of drying on phytochemical composition

The results of the total phenolic content (TPC) and total flavonoid content (TFC) are shown in Figure 3.2. The dry infusion had a higher TPC (16.84 mg/g) than the fresh one (11.30 mg/g). These values are higher than those reported for aqueous, ethanolic, and methanolic extracts of lemongrass (Soares *et al.* 2013), and chrysanthemum teas (Li *et al.* 2019). This may be due to the differences in the nature and temperature of the solvent used. The higher TPC of the dry infusion may be due to the formation of new and more bioactive compounds at high temperatures (Alkaltham, Salamatullah and Hayat 2020). This may also contribute to its better antioxidant activity because phenolics protect the cells from free radical formation. However, the TFCs of both infusions are similar but are lower than those of pu-erh (Lu *et al.* 2019) green, oolong, and red tea (Chai *et al.* 2020). This suggests that though the lemongrass teas may be rich in phenolic compounds, it is low in flavonoid compounds.

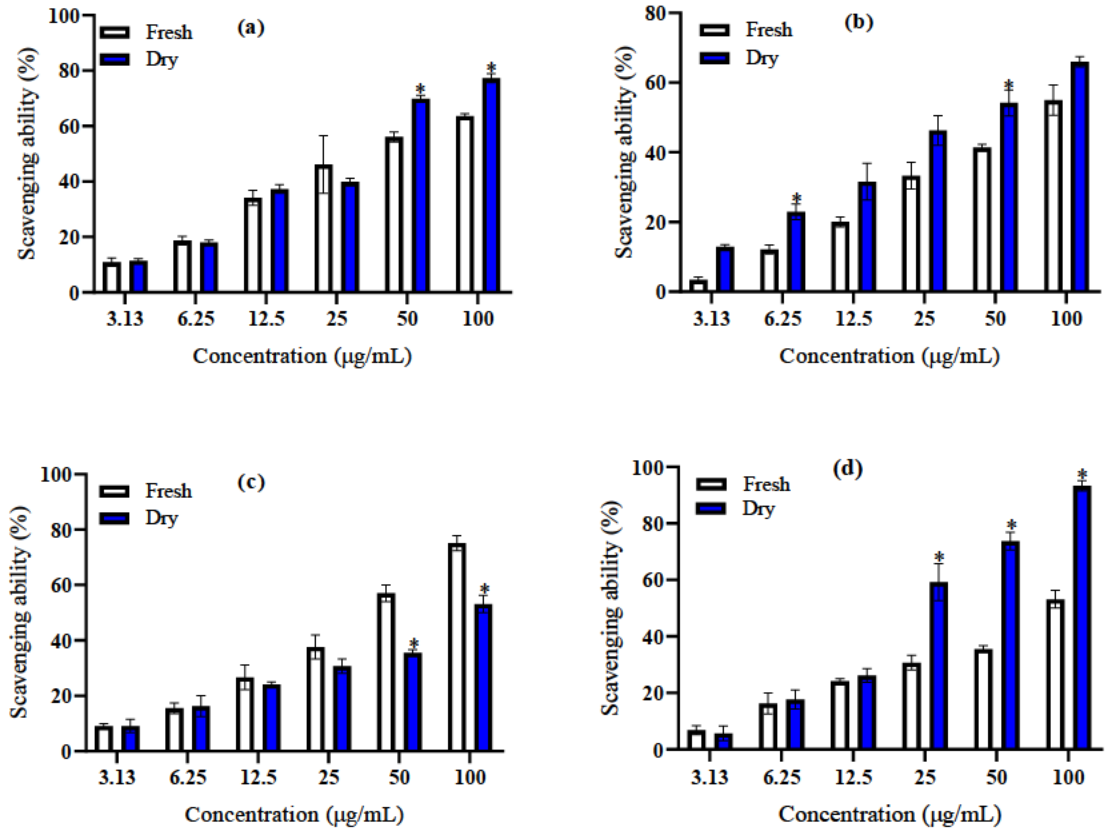

Figure 3.1. Scavenging abilities of teas obtained from fresh and dry *Cymbopogon citratus* leaf on (a) 1,1-diphenyl-2-picrylhydrazyl (DPPH) radical (b) hydroxyl radical (c) iron chelation and (d) superoxide anion radical. Values are expressed as mean ± SEM of triplicate determinations. *Significant difference at $p<0.05$.

Table 3.4. EC_{50} values for the free radical scavenging activities of teas from fresh and dry lemongrass leaves

Samples	EC_{50}			
	DPPH	Hydroxyl	Iron chelation	Superoxide
Fresh infusion	56.52 ± 5.42^{a}	80.10 ± 5.33^{a}	52.88 ± 0.41^{a}	87.67 ± 4.52^{a}
Dry infusion	44.60 ± 1.72^{b}	55.05 ± 3.32^{b}	88.16 ± 4.86^{b}	37.48 ± 3.80^{b}
Gallic acid	58.66 ± 1.34^{a}	52.06 ± 2.54^{b}	ND	45.84 ± 0.68^{b}
EDTA	ND	ND	59.59 ± 1.10^{a}	ND

ND: Not determined. The values are expressed as means ± SEM of triplicate determinations. Means down vertical columns not sharing a common letter are significantly different ($P < 0.05$).

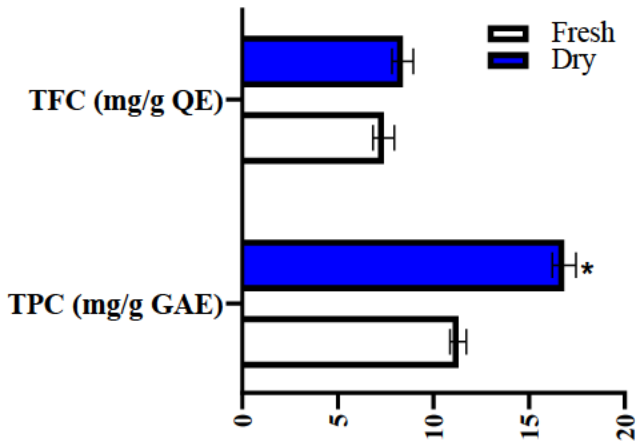

Figure 3.2. Total phenolic content (TPC) and total flavonoid content (TFC) of teas obtained from fresh and dry lemongrass. *Significant difference at $p<0.05$

Table 3.5 shows the results of the LC-MS profile of the infusions obtained from fresh and dry samples of lemongrass. A total of 23 chemical compounds were found in both samples, but at different concentrations. The top three compounds with high peak height intensity in the dry infusion are corymboside (7432), veranisatin C (7356), and chamaemeloside (7251), while the fresh infusion also has corymboside (6526), herbarumin II (4882), and chamaemeloside (3856) as the top three compounds. The observed potent antioxidant activity of both the fresh and dry infusions may be due to the presence of phytochemical compounds in lemongrass, especially corymboside, chamaemeloside, veranisatin C, and herbarumin II. Previous studies revealed that corymboside (Fig. 3.3a), a component of matcha green tea (*Camellia sinensis*), has antioxidant, anti-inflammatory, and antiproliferative properties (Christina *et al.* 2022; Zhao *et al.* 2022). Chamaemeloside (Fig. 3.3b), which is a flavonoid glycoside first isolated from *Chamaemelum nobile* (Tschan *et al.* 1996), is reported to have hypoglycemic potential (König *et al.* 1998). While herbarumin II (a nonelide) (Fig. 3.3c) displayed calmodulin inhibitory properties (Rivero-Cruz *et al.* 2003), thereby preventing unregulated cell growth, veranisatin C (Fig. 3.3d) exhibited a neurotoxic effect (Jin *et al.* 2023). This suggests that these phytochemicals confer antioxidant, anti-inflammatory, hypoglycemic, and antitumor properties on the lemongrass infusions.

Table 3.5. LC-MS profiling of phenolic compounds of infusions obtained from fresh and dry lemongrass leaves.

Average RT (min)	Average *m/z*	Compound	Peak height intensity	
			Fresh	Dry
9.125	203.0922	Phellodendric acid A	1009	1111
12.012	239.0542	Eucomic acid	3824	3631
12.170	353.0867	Chlorogenic acid	49	53
12.365	517.1571	Sibiricose A5	1244	6
12.532	367.1029	4-*O*-feruloyl-D-quinic acid	1522	4259
12.828	179.0334	Caffeic acid	1432	1542
13.058	417.1778	Ascleposide B	716	148
13.555	431.1867	Aspulvinone H	538	45
14.363	415.1598	Phenylethyl primeveroside	3233	5661
14.801	579.1349	Rustoside	1623	3038
14.995	371.0976	Veranisatin C	3765	7356
15.675	163.0399	2-hydroxycinnamic acid	299	45
15.859	563.1393	Corymboside	6526	7432
16.048	593.1495	Lonicerin	534	2763
16.520	549.1240	Limocitrin-7-(6”-acetylglucoside)	2876	2763
17.728	401.1809	Glochidionionoside A	2806	5436
18.062	399.1639	Corchoionoside B	1315	2251
18.421	447.0910	Quercitrin	155	39
20.830	243.1231	Herbarumin II	4882	6668
21.017	575.1404	Chamaemeloside	3856	7251
21.630	577.1546	Kaempferitrin	1661	2998
22.659	692.2037	Neocuscutoside C	47	1273
23.088	373.1305	Wikstromol	1285	213

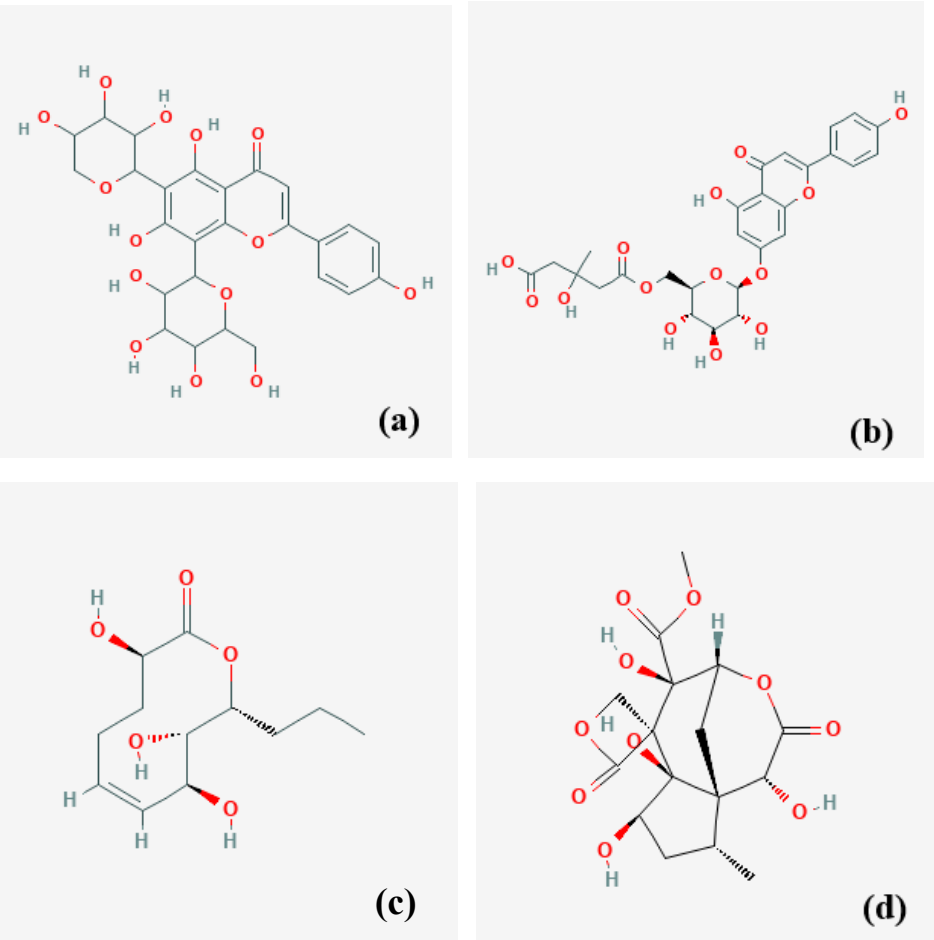

Figure 3.3. Chemical structure of (a) corymboside (b) chamaemeloside (c) herbarumin II and (d) veranisatin C found in *Cymbopogon citratus* (lemongrass) teas.

3.5. Conclusion

It is customary in Africa to prepare infusions from either fresh or dry leaves of lemongrass for pleasure or medicinal purposes. This study revealed fresh and dry lemongrass infusions are rich in nutrients, minerals, amino acids and phytochemicals. While fresh tea is richer in nutritional properties, the dry tea contains more phytochemicals. The dry lemongrass tea possessed lower EC_{50} values for the DPPH, hydroxyl and superoxide radical scavenging abilities, thereby displaying better antioxidant activity. This may be attributed to the phytochemical composition of the dry tea as it is richer in corymboside, veranisatin C, chamaemeloside and herbarumin II. These phytochemicals are reported to have antioxidant, anti-inflammatory and anticancer properties.

3.6. References

Ahmed, M., Sanaullah, M., Sarfraz, S., Zahra, M., Tanveer, M., Sohail, A., Qamar, S., Ahmad, W., Kundi, I. A. and Feroz, M. 2024. Essential and non-essential metals in coconut milk: Determination, chemometric analysis, and risk assessment study. *Journal of Food Composition and Analysis*, 127: 105943.

Alkaltham, M. S., Salamatullah, A. and Hayat, K. 2020. Determination of coffee fruit antioxidants cultivated in Saudi Arabia under different drying conditions. *Journal of Food Measurement and Characterization*, 14: 1306-1313.

AOAC. 2012. *Official Methods of Analysis of AOAC International* Washington DC, USA:

Asaolu, M., Oyeyemi, O. and Olanlokun, J. 2009. Chemical compositions, phytochemical constituents and in vitro biological activity of various extracts of *Cymbopogon citratus*. *Pakistan Journal of Nutrition*, 8 (12): 1920-1922.

Avoseh, O., Oyedeji, O., Rungqu, P., Nkeh-Chungag, B. and Oyedeji, A. 2015. Cymbopogon species; ethnopharmacology, phytochemistry and the pharmacological importance. *Molecules*, 20 (5): 7438-7453.

Bayram, H. M., Ozkan, K., Ozturkcan, A., Sagdic, O., Gunes, E. and Karadag, A. 2024. Effect of drying methods on free and bound phenolic compounds, antioxidant capacities, and bioaccessibility of Cornelian cherry. *European Food Research and Technology*, Article ID: 1-18.

Bigna, J. J. and Noubiap, J. J. 2019. The rising burden of non-communicable diseases in sub-Saharan Africa. *The Lancet Global Health*, 7 (10): e1295-e1296.

Chai, Z., Tian, L., Yu, H., Zhang, L., Zeng, Q., Wu, H., Yan, Z., Li, D., Hutabarat, R. P. and Huang, W. 2020. Comparison on chemical compositions and antioxidant capacities of the green, oolong, and red tea from blueberry leaves. *Food Science & Nutrition*, 8 (3): 1688-1699.

Christina, Y. I., Rifa'i, M., Widodo, N. and Djati, M. S. 2022. Comparative study of antiproliferative activity in different plant parts of *Phaleria macrocarpa* and the underlying mechanism of action. *The Scientific World Journal*, 2022 (1): 3992660.

Devi, C. B., Bains, K. and Kaur, H. 2019. Effect of drying procedures on nutritional composition, bioactive compounds and antioxidant activity of wheatgrass (*Triticum aestivum* L). *Journal of Food Science and Technology*, 56: 491-496.

Dubois-Deruy, E., Peugnet, V., Turkieh, A. and Pinet, F. 2020. Oxidative stress in cardiovascular diseases. *Antioxidants*, 9 (9): 864.

Garba, Z. N. and Oviosa, S. 2019. The effect of different drying methods on the elemental and nutritional composition of *Vernonia amygdalina* (bitter leaf). *Journal of Taibah University for Science*, 13 (1): 396-401.

Gouda, H. N., Charlson, F., Sorsdahl, K., Ahmadzada, S., Ferrari, A. J., Erskine, H., Leung, J., Santamauro, D., Lund, C. and Aminde, L. N. 2019. Burden of non-communicable diseases in sub-Saharan Africa, 1990–2017: Results from the Global Burden of Disease Study 2017. *The Lancet Global Health*, 7 (10): e1375-e1387.

Gurib-Fakim, A. 2006. Medicinal plants: traditions of yesterday and drugs of tomorrow. *Molecular aspects of Medicine*, 27 (1): 1-93.

Holeček, M. 2023. Aspartic acid in health and disease. *Nutrients*, 15 (18): 4023.

Hwang, I. M., Jeong, J. Y., Kim, M. J., Jung, S., Choi, J. Y. and Lee, J.-H. 2024. Elemental analysis of three types of *Raphanus sativus* kimchi and their potential health impact in South Korea. *Journal of Food Composition and Analysis*, 127: 105970.

Jin, Y., Xie, Y., Zhang, P., Khan, A., Zhou, Z. and Liu, L. 2023. Chemical composition and pharmacological activity of seco-prezizaane-type sesquiterpenes. *Chinese Herbal Medicines*, 16(1): 70-81.

Jomova, K., Makova, M., Alomar, S. Y., Alwasel, S. H., Nepovimova, E., Kuca, K., Rhodes, C. J. and Valko, M. 2022. Essential metals in health and disease. *Chemico-biological interactions*, 367: 110173.

Kamaruddin, Z. H., Jumaidin, R., Selamat, M. Z. and Ilyas, R. 2022. Characteristics and properties of lemongrass (*Cymbopogan citratus*): A comprehensive review. *Journal of Natural Fibers*, 19 (14): 8101-8118.

Kazeem, M. I. and Ashafa, A. O. T. 2015. In-vitro antioxidant and antidiabetic potentials of *Dianthus basuticus* Burtt Davy whole plant extracts. *Journal of Herbal Medicine*, 5 (3): 158-164.

Kazeem, M. I. and Davies, T. C. 2016. Hypoglycaemic potential of leaf extracts of *Lonchocarpus cyanescens* (Schum. and Thonn) Benth. *Transactions of the Royal Society of South Africa*, 71 (1): 1-6.

König, G. M., Wright, A. D., Keller, W. J., Judd, R. L., Bates, S. and Day, C. 1998. Hypoglycaemic activity of an HMG-containing flavonoid glucoside, chamaemeloside, from *Chamaemelum nobile*. *Planta medica*, 64 (07): 612-614.

Li, Y., Yang, P., Luo, Y., Gao, B., Sun, J., Lu, W., Liu, J., Chen, P., Zhang, Y. and Yu, L. L. 2019. Chemical compositions of chrysanthemum teas and their anti-inflammatory and antioxidant properties. *Food Chemistry*, 286: 8-16.

Li, Z., Shen, G., Hong, T., Yu, M., Li, B., Gu, Y., Guo, Y. and Han, J. 2024. The nutritive quality comparison of the processed fresh sweet-waxy corn from three regions in China. *Journal of Food Composition and Analysis*, 126: 105872.

Liguori, I., Russo, G., Curcio, F., Bulli, G., Aran, L., Della-Morte, D., Gargiulo, G., Testa, G., Cacciatore, F. and Bonaduce, D. 2018. Oxidative stress, aging, and diseases. *Clinical Interventions in Aging*, 13: 757-772.

Liu, F., Ooi, V. and Chang, S. 1997. Free radical scavenging activities of mushroom polysaccharide extracts. *Life Sciences*, 60 (10): 763-771.

Liu, S., Ai, Z., Qu, F., Chen, Y. and Ni, D. 2017. Effect of steeping temperature on antioxidant and inhibitory activities of green tea extracts against α-amylase, α-glucosidase and intestinal glucose uptake. *Food Chemistry*, 234: 168-173.

Lu, X., Liu, J., Zhang, N., Fu, Y., Zhang, Z., Li, Y., Wang, W., Li, Y., Shen, P. and Cao, Y. 2019. Ripened Pu-erh tea extract protects mice from obesity by modulating gut microbiota composition. *Journal of Agricultural and Food Chemistry*, 67 (25): 6978-6994.

Mbhele, N., Balogun, F. O., Kazeem, M. I. and Ashafa, T. 2015. In vitro studies on the antimicrobial, antioxidant and antidiabetic potential of *Cephalaria gigantea*. *Bangladesh Journal of Pharmacology*, 10 (1): 214-221.

Mohammed, A., Ibrahim, M. A. and Islam, M. S. 2014. African medicinal plants with antidiabetic potentials: A review. *Planta Medica*, 80 (05): 354-377.

Mohanty, B., Mahanty, A., Ganguly, S., Sankar, T., Chakraborty, K., Rangasamy, A., Paul, B., Sarma, D., Mathew, S. and Asha, K. K. 2014. Amino acid compositions of 27 food fishes and their importance in clinical nutrition. *Journal of Amino Acids*, 2014 (1): 269797.

Mustafa, A., Sujuti, H., Permatasari, N. and Widodo, M. A. 2013. Determination of nutrient contents and amino acid composition of *Pasuruan Channa* striata extract. *IEESE International Journal of Science and Technology*, 2 (4): 1.

Nimenibo-Uadia, R. and Nwosu, E. 2020. Phytochemical, proximate and mineral elements composition of lemongrass (*Cymbopogon citratus* (DC) stapf) grown in ekosodin, Benin city, Nigeria. *Nigerian Journal of Pharmaceutical and Applied Science Research*, 9 (2): 52-56.

Oboh, G. and Rocha, J. B. T. 2007. Polyphenols in red pepper [*Capsicum annuum* var. aviculare (Tepin)] and their protective effect on some pro-oxidants induced lipid peroxidation in brain and liver. *European Food Research and Technology*, 225: 239-247.

Oladeji, O. S., Adelowo, F. E., Ayodele, D. T. and Odelade, K. A. 2019. Phytochemistry and pharmacological activities of *Cymbopogon citratus*: A review. *Scientific African*, 6: e00137.

Prasathkumar, M., Anisha, S., Dhrisya, C., Becky, R. and Sadhasivam, S. 2021. Therapeutic and pharmacological efficacy of selective Indian medicinal plants–a review. *Phytomedicine Plus*, 1 (2): 100029.

Rivero-Cruz, J. F., Macías, M., Cerda-García-Rojas, C. M. and Mata, R. 2003. A New Phytotoxic Nonenolide from *Phoma herbarum*. *Journal of Natural Products*, 66 (4): 511-514.

Saha, M., Hasan, S., Akter, R., Hossain, M., Alam, M., Alam, M. and Mazumder, M. 2008. In vitro free radical scavenging activity of methanol extract of the leaves of *Mimusops elengi* Linn. *Bangladesh Journal of Veterinary Medicine*, 6(2): 197-202.

Soares, M. O., Alves, R. C., Pires, P. C., Oliveira, M. B. P. and Vinha, A. F. 2013. Angolan *Cymbopogon citratus* used for therapeutic benefits: Nutritional composition and influence of solvents in phytochemicals content and antioxidant activity of leaf extracts. *Food and Chemical Toxicology*, 60: 413-418.

Stein, S. A., Lamos, E. M. and Davis, S. N. 2013. A review of the efficacy and safety of oral antidiabetic drugs. *Expert Opinion on Drug Safety*, 12 (2): 153-175.

Suleria, H. A., Barrow, C. J. and Dunshea, F. R. 2020. Screening and characterization of phenolic compounds and their antioxidant capacity in different fruit peels. *Foods*, 9 (9): 1206.

Tschan, G. M., König, G. M., Wright, A. D. and Sticher, O. 1996. Chamaemeloside, a new flavonoid glycoside from *Chamaemelum nobile*. *Phytochemistry*, 41 (2): 643-646.

Unuigbe, C., Enahoro, J., Erharuyi, O. and Okeri, H. 2019. Phytochemical analysis and antioxidant evaluation of lemon grass (*Cymbopogon citratus* DC.) Stapf leaves. *Journal of Applied Sciences and Environmental Management*, 23 (2): 223-228.

Wallace, W. E., Moorthy, A. S. 2023. NIST mass spectrometry data center standard reference libraries and software tools: Application to seized drug analysis. *Journal of Forensic Sciences*, 68(5): 1484-1493.

Vettore, L. A., Westbrook, R. L. and Tennant, D. A. 2021. Proline metabolism and redox; maintaining a balance in health and disease. *Amino Acids*, 53 (12): 1779-1788.

Zhang, X., Lei, J., Zheng, D., Liu, Z., Li, G., Wang, S. and Ding, Y. 2017. Amino acid composition of leaf, grain and bracts of japonica rice (*Oryza Sativa* ssp. japonica) and its response to nitrogen fertilization. *Plant Growth Regulation*, 82: 1-9.

Zhao, M., Linghu, K.-G., Xiao, L., Hua, T., Zhao, G., Chen, Q., Xiong, S., Shen, L., Yu, J. and Hou, X. 2022. Anti-inflammatory/anti-oxidant properties and the UPLC-QTOF/MS-based metabolomics discrimination of three yellow camellia species. *Food Research International*, 160: 111628.

Zhishen, J., Mengcheng, T. and Jianming, W. 1999. The determination of flavonoid contents in mulberry and their scavenging effects on superoxide radicals. *Food Chemistry*, 64 (4): 555-559.

CHAPTER 4

4. Anti-ageing properties of lemongrass (*Cymbopogon citratus*) infusion: Insights from *in vitro* and computational studies

Mutiu Idowu Kazeem, Rukayat Abiola Abdulsalam, John Jason Mellem and Saheed Sabiu
Department of Biotechnology and Food Science, Faculty of Applied Sciences, Durban University of Technology, P. O. Box 1334, Durban 4000, South Africa

Preface: This study investigated the inhibitory effect of lemongrass infusions on ageing-related enzymes and determined the possible interaction of the lemongrass constituents with the enzymes. The manuscript is submitted to the journal, *Scientific African*.

4.1. Abstract

Ageing is a natural phenomenon in living organisms, leading to decreased functional capacities and increased exposure to diseases. This study evaluated the anti-ageing properties of lemongrass (*Cymbopogon citratus*) infusions using *in vitro* and *in silico* techniques. The inhibitory effect of the lemongrass infusions was tested on the activities of four ageing-related enzymes (collagenase, elastase, hyaluronidase and tyrosinase). Computational techniques, including molecular docking, molecular dynamics simulation and pharmacokinetic profiling, were employed to probe the possible mechanism of anti-ageing effects of the lemongrass infusion. The dry lemongrass infusion displayed a better inhibition of all the enzymes with lower IC_{50} values for collagenase (93.43 µg/mL), elastase (56.47 µg/mL), hyaluronidase (93.43 µg/mL) and tyrosinase (65.55 µg/mL). Molecular docking showed that lonicerin had the lowest docking score for collagenase (-9.7 kcal/mol) and hyaluronidase (-8.3 kcal/mol), while limocitrin-7-(6”-acetylglucoside) and isovitexin-2”-O-arabinoside exhibited the lowest docking scores for elastase (-7.4 kcal/mol) and tyrosinase (-9.2 kcal/mol), respectively. However, kaempferitrin had the lowest binding energy for collagenase (-41.57 kcal/mol) and hyaluronidase (-52.09 kcal/mol), while lonicerin and isovitexin-2”-O-arabinoside possessed the lowest binding energies for elastase and tyrosinase, respectively. This may imply that more stable interactions exist between the ligands and proteins. Kaempferitrin had the highest number of stable interactions with collagenase and hyaluronidase, while limocitrin-

7-(6”-acetylglucoside) and isovitexin-2”-O-arabinoside interacted more with elastase and tyrosinase, respectively. Pharmacokinetic profiling revealed that all the lead compounds are safe except chamaemeloside and kaempferol-3,4-dixyloside, which may cause hepatotoxicity and nephrotoxicity, respectively. It can be concluded that lemongrass infusions exhibit anti-ageing properties, and this may be due to the presence of phytochemicals (such as kaempferitrin, limocitrin-7-(6”-acetylglucoside) and isovitexin-2”-O-arabinoside) in it. Further study is required to evaluate the *in vivo* anti-ageing properties of these compounds.

Keywords: Ageing, collagenase, elastase, hyaluronidase, Kaempferitrin, lemongrass

4.2. Introduction

Ageing is a complex biological process characterized by a gradual loss of physiological integrity, leading to decreased biological functions and increased vulnerability to death (Martel *et al.* 2019). It is typified by a gradual reduction in the efficiency of the cellular machinery and physiological processes, leading to a decline in functional capabilities, ultimately impacting an organism’s health and overall function (Cătană, Atanasov and Berindan-Neagoe 2018). This progressive impairment constitutes the primary risk factor for many human pathologies, such as cancer, diabetes, cardiovascular disorders, as well as neurodegenerative diseases (Luo *et al.* 2021). The prevalence of old people (aged 60 years and above) is 12% and is projected to rise to 22% by the year 2050 (Grinin, Grinin and Korotayev 2023). Due to the increasing population of old people, there is a need for management strategies to promote healthy ageing and mitigate most of the diseases associated with ageing.

One of these strategies is the consumption of medicinal foods and plants. These are plants that provide medicinal benefits in addition to their nutritional role (Kazeem, Mellem and Sabiu 2024). Due to the severity and complications of ageing, several medicinal plants are traditionally used to manage ageing. These include *Moringa oleifera* (drumstick), *Murayya koenigii* (curry), *Citrus medica* (finger citron), *Olea europaea* (olive), and *Cymbopogon citratus* (lemongrass) (Chen, Wang and Wei 2024). Lemongrass is a perennial grass found in the tropical regions of the globe, including South America, Asia and Africa (Ekpenyong, Akpan and Nyoh 2015). It is used as an additive in preparing foods, cuisines, and beverages. A fresh or dry sample of the lemongrass leaves is also used to prepare infusions taken as teas for recreational and therapeutic purposes.

While there are several reports on the pharmacological potentials of lemongrass, including antioxidant, antidiabetic, antimicrobial and anti-inflammatory properties (Oladeji *et al.* 2019), there is a shortage of information on its effect on ageing.

Many proteins and enzymes, such as collagenase, elastase, hyaluronidase and tyrosinase, mediate the ageing process. Collagenase and elastase are involved in the breakdown of collagen (which gives tensile strength) and elastin (which promotes elasticity), respectively, thereby causing wrinkles and severe atrophy on the skin (Jiratchayamaethasakul *et al.* 2020). Hyaluronidase destroys hyaluronic acid (which promotes skin rejuvenation) while tyrosinase plays a crucial role as a rate-limiting step during melanin production (Martel *et al.* 2019). The inhibition of one or more of these enzymes may be an effective approach to prevent or ameliorate the deleterious effects of ageing (Jiratchayamaethasakul *et al.* 2020). Therefore, there is an urgent need to increase understanding of the underlying mechanisms of the ageing process and to find effective anti-ageing therapeutic interventions, so that the continual increase in the proportion of older persons in the population will be beneficial rather than detrimental to future societies.

Though lemongrass infusions are consumed for refreshment and medicinal purposes, there is a dearth of information on the protective and ameliorative roles of lemongrass infusion on ageing and its associated complications. Therefore, this study evaluated the inhibitory properties of lemongrass infusions on ageing-related enzymes (collagenase, elastase, hyaluronidase and tyrosinase) and molecular interaction between its secondary metabolites and the target enzymes using computational techniques (molecular docking, molecular dynamic simulation and pharmacokinetic considerations). This is aimed at providing information on the possible bioactive compounds that contribute to the anti-ageing properties of the infusions and the possible mechanisms of action.

4.3. Materials and methods

4.3.1. Materials

All the enzymes and their substrates, namely collagenase from *Clostridium histolyticum*, porcine pancreatic elastase, bovine hyaluronidase, mushroom tyrosinase, L-tyrosine, N-[3-(2-furyl) acryloyl]-Leu-Gly-Pro-Ala (FALGPA), N-Succinyl-Ala-Ala-Ala-p-nitroanilide (SANA),

hyaluronic acid sodium salt, are obtained from Merck, St. Louis, USA. All other chemicals are of analytical grade, and the water used is glass-distilled.

4.3.2. Preparation of lemongrass teas

Leaves of lemongrass were harvested from farmland in the Iba area of Lagos in October 2021. It was identified and authenticated at the Department of Botany, Lagos State University, Nigeria, and was assigned the voucher number: LSH/21/1055. The leaves were gently rinsed in tap water to remove soil and dirt. A portion was cut into pieces using a stainless-steel kitchen knife, spread on foil paper and dried to constant weight on the laboratory table at room temperature. After drying, the sample was milled using an electric grinder (Silver Crest, Germany). One litre of boiled distilled water was poured on a 100 g milled sample, shaken, and left to steep for 24 h to produce an infusion. Another 1.0 L of boiled distilled water was poured on the second portion (100 g) of the fresh lemongrass and left to steep for 24 h. Both infusions were filtered and concentrated in a lyophilizer (Virtis BenchTop, SP Scientific Series, USA). The lyophilized infusions were used for subsequent analysis by dissolving in distilled water to give stock solutions of 1.0 mg/mL and different concentrations (3.13, 6.25, 12.5, 25, 50, and 100 µg/mL). All infusions were stored at 4 °C before analysis.

4.3.3. Metabolite profiling using Liquid Chromatography-Mass Spectrometry (LC-MS)

The phytochemical composition of the teas obtained from fresh and dry lemongrass leaves was assessed using a previous method (Taamalli *et al.* 2015). The phytochemical composition of the teas obtained from fresh and dry lemongrass leaves was assessed using a previous method (Suleria, Barrow and Dunshea 2020). Agilent 6520 Accurate-Mass QTOF was applied in a positive and negative mode. Synergi Hydro-RP (4 µm particle size, 4.6 mm internal diameter, and 250 mm length with 80 Å pore size were used to separate phenolic compounds, and the flow rate was set at 800 µL/min. An aliquot of 10 µL from each sample was injected while gradient was 0–5 min (0–10%), 5–25 min (10–25% B), 25–35 min (25–35% B), 35–45 min (40–60% B) 45–75 min (40–55% B), 75–80 min (55–88% B) (80–82 min (80–90% B), 82–85 min (90–100% B), 85–90 min (0% B). Mobile phase A was 0.1% formic acid in water, and mobile phase B was 95% acetonitrile with 0.1% formic acid. A full scan mode was achieved in the range of 100–1000 amu with the following conditions: Capillary voltage (3500 V), nozzle voltage (500 V), nitrogen gas flow rate (9 L/min) at 325 °C and nebulization was set as 45 psi while 10, 20 and 30 eV collision energies

were used. Acquisition of data was performed through the employment of MassLynx4.1 software, while detection and confirmation of metabolites were processed using the MS-DIAL software and MS-FINDER (RIKEN Centre for Sustainable Resource Science: Metabolome Informatics Research Team, Kanagawa, Japan). For detailed confirmation, identification of the profiled metabolites was also performed by comparing the respective mass spectra obtained against the National Institute of Standards and Technology (NIST) library (Wallace and Moorthy, 2023).

4.3.4. In vitro inhibitory studies

4.3.4.1. Collagenase inhibitory assay

Collagenase (E.C.3.4.24.3) (1.1 U/mL) from *Clostridium histolyticum* and the synthetic substrate N-[3-(2-furyl) acryloyl]-Leu-Gly-Pro-Ala (FALGPA) (1 mM) were dissolved in 0.05 M tricine buffer (pH=7.5 with 0.4 M NaCl and 0.01 M $CaCl_2$) (Thring, Hili and Naughton 2009). To adjust the pH of the solution, 1 M NaOH was added. Before adding the substrate, the lemon grass extracts were incubated in tricine buffer with collagenase for 15 min. The total volume of the final reaction mixture was 125 µL, which contained 25 µL buffer solution, 50 µL of the substrate (FALGPA), 25 µL of the enzyme, and 25 µL of lemongrass extracts (3.13 – 100 µg/mL). Oleanolic acid was used as the standard (3.13 – 100 µg/mL). After adding the substrate, absorbance was measured immediately at 335 nm and 2-min intervals for 20 min using a Thermo Scientific Multiskan Microplate Reader. Percentage inhibitory activity was calculated as percentage inhibition, thus;

$$\% \text{ Inhibition} = [(\Delta Abs_{control} - \Delta Abs_{extract})/\Delta Abs_{control}] \times 100$$

The concentration of sample or standard that inhibited 50% of collagenase activity (IC_{50}) was evaluated using Microsoft Excel (2010).

4.3.4.2. Elastase inhibitory assay

This assay was performed by a spectrophotometric method (Lee and Choi 1999). Porcine pancreatic elastase (E.C. 3.4.21.36) (3.33 mg/mL) was used as the enzyme and dissolved in 0.2 mM Tris−HCl buffer (pH=8.0). The substrate, N-Succinyl-Ala-Ala-Ala-p-nitroanilide (SANA) was also dissolved in the buffer solution at 1.6 mM. 50 µL buffer, 25 µL enzyme with 50 µL lemongrass extracts (3.13 – 100 µg/mL) were preincubated at room temperature for 15 min before SANA was added. Oleanolic acid was used as the standard (3.13 – 100 µg/mL). To start the

reaction, 125 µL substrate solution was added to the reaction mixture and incubated at room temperature for 20 min. The absorbance was measured at 410 nm. Percentage inhibitory activity was calculated as percentage inhibition, thus;

$$\% \text{ Inhibition} = [(\Delta Abs_{control} - \Delta Abs_{extract})/\Delta Abs_{control}] \times 100$$

The concentration of sample or standard that inhibited 50% of elastase activity (IC_{50}) was evaluated using Microsoft Excel (2010).

4.3.4.3. Hyaluronidase inhibitory assay

Briefly, 5 µL of lemongrass extracts (3.13 – 100 µg/mL) were incubated for 10 min at 37 °C with bovine hyaluronidase (1.50 U) in 100 µL of 20 mM sodium phosphate buffer solution (pH 7.0), sodium chloride (77 mM), in addition to 0.01% bovine serum albumin (BSA). The assay reaction was initiated by adding the hyaluronic acid sodium salt (100 µL) from the rooster comb (0.03% in 300 mM sodium phosphate, pH 5.35) to the incubation mixture, then the mixture was incubated at 37 °C for 45 min. The precipitation of undigested hyaluronic acid was carried out by 1 mL acidic solution of albumin, involving 0.1% BSA in sodium acetate (24 mM) and acetic acid (79 mM, pH 3.75). The reaction was incubated for 10 min at room temperature, and fluorescence was detected using a Tecan Infinite microplate reader at 545 nm excitation and 612 nm emission (Takahashi *et al.* 2003). Oleanolic acid was used as the standard (3.13 – 100 µg/mL). Percentage inhibitory activity was calculated as percentage inhibition, thus;

$$\% \text{ Inhibition} = [(\Delta Abs_{control} - \Delta Abs_{extract})/\Delta Abs_{control}] \times 100$$

The concentration of sample or standard that inhibited 50% of hyaluronidase activity (IC_{50}) was evaluated using Microsoft Excel (2010).

4.3.4.4. Tyrosinase inhibitory assay

Tyrosinase inhibitory activity was assayed using the method described by (Manosroi *et al.* 2010) with some slight modifications. The reaction was carried out in 500 µL of phosphate buffer (pH 6.8, 0.1 M), and 250 µL of L-tyrosine (1.5 mM). After preincubation for 15 min at 37 °C, 50 µL of lemongrass extract (3.13 – 100 µg/mL) and 100 µL of mushroom tyrosinase (31 units/mL) maintained at 37 °C were added. The blank contained the buffer instead of the enzyme, and ascorbic acid was used as the standard (3.13 – 100 µg/mL). The mixture was incubated for 45 min

at 25 °C. The absorbance of the mixture was read at 490 nm against a blank. Percentage inhibitory activity was calculated as percentage inhibition, thus;

% Inhibition = $[(\Delta Abs_{control}-\Delta Abs_{extract})/\Delta Abs_{control}] \times 100$

The concentration of sample or standard that inhibited 50% of tyrosinase activity (IC_{50}) was evaluated using Microsoft Excel (2010).

4.3.5. In silico studies

4.3.5.1. Collection and preparation of the identified metabolites

The 3D structures of the 49 identified compounds from *Cymbopogon citratus* and those of the reference compounds [oleanolic acid with ID 10494 (standard for collagenase, elastase and hyaluronidase)], and [ascorbic acid with ID 54670067 (standard for tyrosinase)], were obtained from PubChem (https://pubchem.ncbi.nlm.nih.gov/) and then optimized via the additions of nonpolar hydrogen atoms and charges using the Avogadro software (Aribisala *et al.* 2022). The optimized ligands were saved in Mol2 format for subsequent molecular docking.

4.3.5.2. Collection and preparation of therapeutic targets

The X-ray crystal structures of collagenase (ID: 1CGL, sequence length: 169), elastase (ID: 1H1B, sequence length: 218), hyaluronidase (ID: 1FCV, sequence length: 350), and tyrosinase (ID: 5M8P, sequence length: 446) were acquired from the Protein Data Bank (https://www.rcsb.orgs/) and prepared through the removal of non-standard amino acids and water molecules using UCSF chimera software v 1.14 (Branden, Sjogren, Schnecke and Xue 2014). The cleaned structures were then saved in PDB format for molecular docking.

4.3.5.3. Molecular docking and validation of C. citratus metabolites

The docking procedure entailed the selection of amino residues at the active site of the protein whose grid box coordinates coincide with the established x-y-z coordinates: Collagenase [centre (X: 19.76, Y: 24.46, Z: 23.64)], elastase [centre (X: 19.39, Y: 9.78, Z: 20.87)], hyaluronidase [centre (X: 54.21, Y: 26.81, Z: 5.65)], and tyrosinase [centre (X: -36.70, Y: 7.03, Z: -19.11)]. Subsequent docking at the active site of the proteins was ensured by dragging the grid box to fit the established, well-defined x-y-z coordinates. Thereafter, the optimized 3D structures of the ligands (*C. citratus* metabolites and reference compounds) and cleaned proteins were subjected to

molecular docking using the Autodock vina package on Python Prescription v 0.9.5 (PyRx), which allows for multiple docking of ligands (Onder *et al.* 2022). Finally, the ligands were ranked based on their binding affinity, and the top five docked complexes with the best pose were saved in PDB format and subjected to MD simulations.

To validate the docking conformation, the superimposition and redocking techniques were employed, where the appropriate root-mean-square deviation (RMSD) of a docked compound from its reference point (position of native inhibitors) in each target was calculated (Al-Khodairy *et al.* 2013). The best conformations from this dock were ranked based on the RMSD between their docked position and the ligand's experimentally determined position (Al-Khodairy *et al.* 2013).

4.3.5.4. Molecular dynamics simulation

The MD simulation was performed on the complexes formed by the top five compounds with the proteins, as previously described (Nair and Miners 2014). Succinctly, the simulations were performed over a 200 ns period using the AMBER 18 package of the in-house program (HEAL1361) resident at the Centre for High-Performance Computing (CHPC), South Africa. The FF18SB variant of the AMBER force field was adopted to describe the operating systems. The ANTECHAMBER was employed to create the ligands' atomic partial charges by exploiting the general amber force field (GAFF) procedures and restrained electrostatic potential (RESP). The hydrogen atoms, Na^+, and Cl^- counter ions of the Leap module were used to neutralise the systems. In each case of the simulation, the numbering of the amino acid residues was done accordingly, and the systems were suspended inside an orthorhombic box of TIP3P water molecules in such a way that all atoms were within 8 Å of any box edge. The bonds of hydrogen atoms in each case of the simulation were constrained using the SHAKE algorithm. Each simulation had a 2 fs step size, which corresponded to the isobaric–isothermal ensemble (NPT) with randomised seeding, a temperature of 300 K, constant pressure of 1 bar, and a Langevin thermostat with a 1.0 ps collision frequency and a pressure-coupling constant of 2 ps. Following that, the results of the 120 ns MD simulation were examined and regarded as post-dynamic data.

4.3.5.5. Post-MD simulation

The post-MD simulation was carried out as earlier described (Basconi and Shirts 2013). Briefly, after the simulation, the systems' coordinates were combined and analyzed using the AMBER 14 PTRAJ module of CHPC. After this, the root mean square fluctuation (RMSF), the radius of gyration (RoG), root mean square deviation (RMSD), and solvent accessibility surface area (SASA) were analyzed using the CPPTRAJ module of the same package, and their raw data were generated using Origin V6 (Seifert 2014). Similarly, using the Molecular Mechanics/GB Surface Area approach, the free binding energy (ΔG) in each case of the simulation was calculated using the expression ΔG bind = Gcomplex – (G Receptor + G ligand) by averaging among 120,000 snapshots taken from a 120 ns MD simulation trajectory. The complexes' interactions in each simulation case were visualized and analyzed post-MD simulation using Discovery Studio version 21.1.0 (BIOVIA 2021).

4.3.5.6 Determination of pharmacokinetic properties

The ADMETlab 3.0 web (https://admetlab3.scbdd.com/) was used to forecast the adsorption, distribution, metabolism, excretion and toxicological properties of the compounds with the top docking score. This is done by entering the Simplified Molecular Input Line Entry System (SMILES) of the compounds onto the platform and submitting them for ADMET screening. The outcome generated was critically examined to determine the status of the compounds.

4.3.6. Statistical analysis

The *in vitro* enzyme inhibitory studies were performed in triplicate, and data were expressed as mean ± standard error of the mean (SEM). IC_{50} values were obtained from percentage inhibitions using Microsoft Excel software (Microsoft, 2010). Student's t-test was used to assess differences in the percentage inhibitory activities and mean values of the samples using the GraphPad Prism statistical package (GraphPad Software, USA). Statistical significance was considered at $p < 0.05$. Except otherwise stated, the raw data plots for the in-silico evaluations were generated using the Origin data analysis software V18 (OriginLab, Northampton, MA, USA).

4.4. Results and discussion

This study evaluated the anti-ageing properties of lemongrass teas by evaluating their inhibitory effect on the activities of ageing-related enzymes (collagenase, elastase, hyaluronidase and tyrosinase) and the interaction of their secondary metabolites with the enzymes using molecular docking, molecular dynamics simulation and ADMET evaluation.

4.4.1. In vitro study

Some processes, including cellular senescence, mitochondrial dysfunction, telomere attrition and oxidative stress, facilitate ageing progression. Oxidative stress involves the production of excessive reactive oxygen species (ROS) and promotes the increased expression of matrix metalloproteinases (Abdelfattah *et al.* 2022). Matrix metalloproteinase is a group of enzymes responsible for breaking down the extracellular matrix fibrous proteins, such as collagen, elastin and hyaluronic acid (Deniz *et al.* 2020). These enzymes include collagenase, elastase and hyaluronidase.

Figure 4.1 shows the inhibitory properties of fresh and dry tea of lemongrass leaves on the activities of ageing-related enzymes. The dry lemongrass tea significantly inhibited ($p < 0.05$) the activity of collagenase at all concentrations tested except at the concentration of 3.13 µg/mL (Fig. 4.1a). Though there are differences in the percentage inhibition of elastase by the fresh and dry infusions of lemongrass, they are not significant (Fig. 4.1b). The dry lemongrass tea had a significantly higher ($p < 0.05$) inhibition of hyaluronidase than the fresh one at all concentrations tested (Fig. 4.1c). While both infusions similarly inhibited tyrosinase at lower concentrations (3.13 – 12.5 µg/mL), the dry tea significantly inhibited the enzyme at higher concentrations (25 – 100 µg/mL).

The dry lemongrass tea exhibited significantly lowered ($p < 0.05$) IC_{50} values for the inhibition of collagenase, hyaluronidase and tyrosinase, while both infusions had similar IC_{50} values for the inhibition of elastase (Table 4.1).

The potent inhibition of these enzymes by dry lemongrass tea suggests that it is richer in secondary metabolites than the fresh tea, thereby mitigating the undesirable action of the enzymes. This will prevent collagenase and elastase from hydrolyzing collagen and elastin, thereby promoting the tensile strength and elasticity of the skin (Figueiredo *et al.* 2023). Hyaluronic acid is one of the

important components of the extracellular matrix, which improves skin moisture and tissue repair (Elgamal *et al.* 2021), while tyrosinase plays a significant role in melanin synthesis (Abdelfattah *et al.* 2022). The effective inhibition of hyaluronidase (which hydrolyzes hyaluronic acid) and tyrosinase by the lemongrass tea suggests that their actions promote skin rejuvenation and adequate production of melanin (Elgamal *et al.* 2021; Bras *et al.* 2024). Consequently, symptoms of ageing such as skin wrinkles, dryness, and hyperpigmentation may be mitigated by phytochemicals present in lemongrass teas.

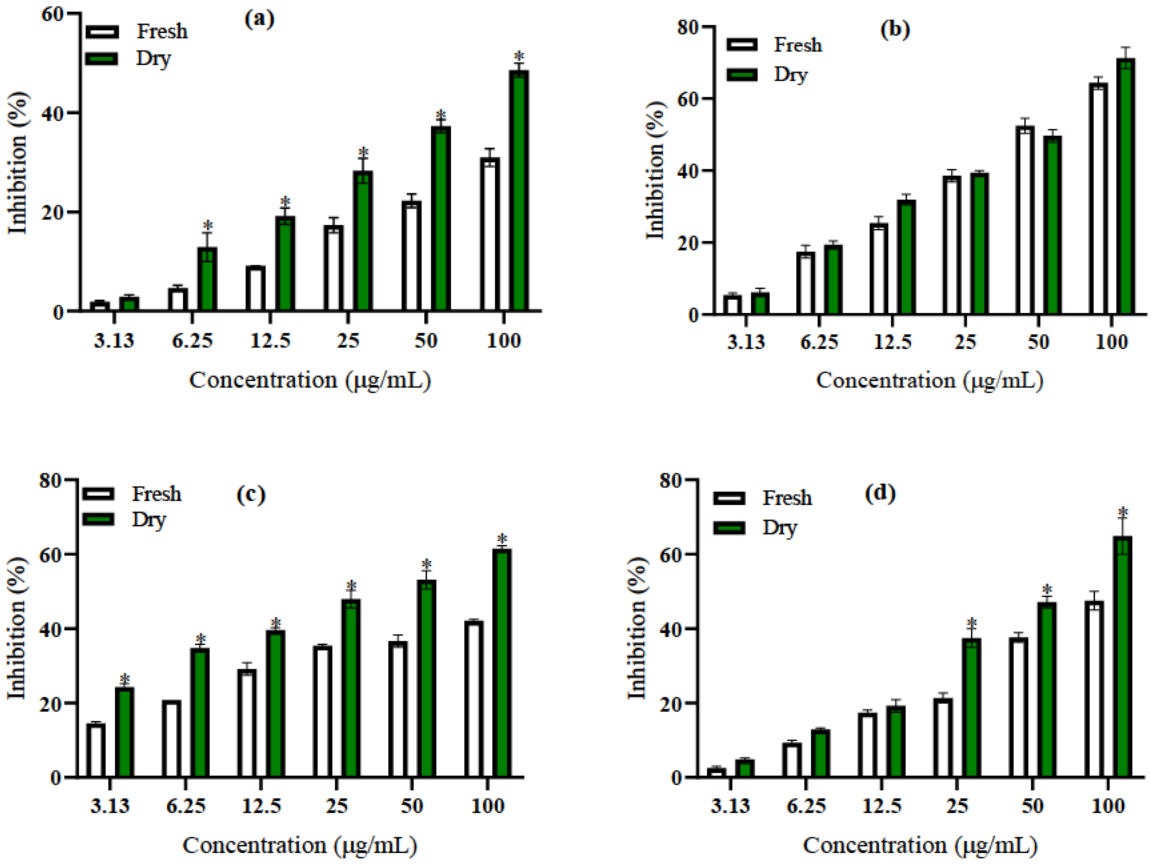

Figure 4.1. Inhibitory properties of fresh and dry lemongrass tea on the activities of ageing-related enzymes (a) collagenase (b) elastase (c) hyaluronidase and (d) tyrosinase. Values are expressed as mean ± SEM of triplicate determinations. *Values are significantly different at ($p < 0.05$).

Table 4.1. IC_{50} values for the inhibition of activities of ageing-related enzymes by infusions of fresh and dry lemongrass

Samples	IC_{50}			
	Collagenase	Elastase	Hyaluronidase	Tyrosinase
Fresh tea	158.50 ± 11.84^{a}	62.10 ± 2.26^{a}	119.80 ± 5.45^{a}	95.85 ± 3.53^{a}
Dry tea	93.43 ± 4.80^{b}	56.47 ± 0.94^{ab}	93.43 ± 4.80^{b}	65.55 ± 2.64^{b}
Oleanolic acid	74.69 ± 1.30^{c}	47.86 ± 3.33^{b}	74.69 ± 1.30^{c}	ND
Ascorbic acid	ND	ND	ND	51.12 ± 4.20^{bc}

ND: Not determined.

The values are expressed as means ± SEM of triplicate determinations. Means down vertical columns not sharing a common letter are significantly different ($P < 0.05$) from each other.

4.4.2. Molecular docking

Molecular docking was performed to determine how the secondary metabolites from the lemongrass teas interact with the ageing-related enzymes. Appendix 4.1 reveals the docking scores of the 49 compounds found in lemongrass teas against collagenase, elastase, hyaluronidase and tyrosinase. Table 2 shows the docking scores of the top five compounds and standards against ageing-related targets. While lonicerin has the lowest docking scores for both collagenase (-9.7 kcal/mol) and hyaluronidase (-8.3 kcal/mol), limocitrin-7-(6''-acetylglucoside) and isovitexin-2''-O-arabinoside had the lowest docking score for elastase (-7.4 kcal/mol) and tyrosinase (-9.2 kcal/mol), respectively. Except chamaemeloside (-7.0 kcal/mol), which has a higher docking score for elastase than oleanolic acid (-7.2 kcal/mol), all the other compounds possessed lower docking scores than their respective standard drugs. Molecular docking is a technique used to elucidate how ligands associate with molecular targets (Khojah *et al.* 2024). The possession of the lowest docking scores by lonicerin (for collagenase and hyaluronidase), limocitrin-7-(6''-acetylglucoside) (for elastase) and isovitexin-2''-O-arabinoside (for tyrosinase) signifies that they have the best affinities for the enzymes than other compounds (Fikry *et al.* 2023). The outcome of the docking validation exercise is presented in Appendix 4.2, and the superimposition demonstrated that the top-hit compounds, the reference standards, and the docked native inhibitors in each case had relative binding orientation at the receptor binding domains of each target with RMSD values of 0.5 Å. These findings supported the validity of the docking scores obtained in the study.

Table 4. 2. Docking scores of the top five compounds of lemongrass infusions and standards with ageing-related enzymes

Targets	Compound/Standard	PubChem ID	Docking score (kcal/mol)
Collagenase	Chamaemeloside	101688668	-9.0
	Isovitexin-2”-O-arabinoside	44468060	-9.3
	Kaempferitrin	5486199	-9.4
	Lonicerin	5282152	**-9.7**
	Quercitrin	5280459	-9.1
	Oleanolic acid*	10494	-7.1
Elastase	Chamaemeloside	101688668	-7.0
	Kaempferol-3,4-dixyloside	44258938	-7.3
	Limocitrin-7-(6”-acetylglucoside)	44260014	**-7.4**
	Lonicerin	5282152	-7.3
	Rustoside	74977996	-7.2
	Oleanolic acid*	10494	-7.2
Hyaluronidase	Isocarlinoside	21576182	-7.9
	Isovitexin-2”-O-arabinoside	44468060	-7.7
	Kaempferitrin	5486199	-8.0
	Limocitrin-7-(6”-acetylglucoside)	44260014	-7.7
	Lonicerin	5282152	**-8.3**
	Oleanolic acid*	10494	-7.5
Tyrosinase	Chamaemeloside	101688668	-8.7
	Isocarlinoside	21576182	-8.6
	Isovitexin-2”-O-arabinoside	44468060	**-9.2**
	Kaempferitrin	5486199	-8.6
	Lonicerin	5282152	-9.1
	Ascorbic acid*	54670067	-6.3

*Reference standards

4.4.3. Molecular dynamics simulation

To determine the behaviour of the secondary metabolites while interacting with the anti-ageing targets, binding energies were obtained during molecular dynamics simulation. Table 4.3 shows the energy component profile of the topmost compounds of lemongrass teas against ageing-related enzymes. All the top five compounds that interacted with collagenase had lower free binding energies (-41.57 to -34.19 kcal/mol) than the standard (oleanolic acid) (-24.67 kcal/mol). This aligns with their docking score which was also lower than that of oleanolic acid, which implies they interacted more effectively with collagenase (Yepes *et al.* 2021). While four of the top five compounds displayed higher free binding energies when they interacted with elastase and hyaluronidase, lonicerin and kaempferitrin had lower binding energy for elastase (-35.55 kcal/mol) and hyaluronidase (-52.09 kcal/mol) than oleanolic acid, respectively. This suggests that lonicerin and kaempferitrin had more binding affinities for elastase and hyaluronidase respectively (Haider *et al.* 2021). This is because the lower the binding energy, the stronger the interaction between the ligands and molecular targets. In the case of tyrosinase, one of the top five compounds, isocarlinoside (-11.01 kcal/mol), had higher free binding energy than the standard drug (ascorbic acid) (-19.27 kcal/mol) while the other four compounds displayed lower free binding energies than ascorbic acid. This agrees with the higher docking score isocarlinoside has for tyrosinase than other top compounds (Yepes *et al.* 2021).

Table 4.3. Energy component profiles of the top five compounds of lemongrass teas and standards against ageing-related enzymes

Complex	ΔEvdW	ΔEelec	ΔGgas	ΔGsolv	ΔEsur	ΔGbind
Collagenase						
Chamaemeloside	-45.49 ± 5.73	-41.09 ± 19.06	-86.59 ± 17.24	46.74 ± 13.26	-5.63 ± 0.48	-39.85 ± 6.12
Isovitexin 2"-O-arabinoside	-39.79 ± 4.20	-56.99 ± 13.09	-96.79 ± 12.11	56.46 ± 9.39	-5.64 ± 0.28	-40.33 ± 5.38
Kaempferitrin	-44.61 ± 3.53	-46.15 ± 23.95	-90.77 ± 23.82	49.19 ± 15.87	-5.91 ± 0.52	-41.57 ± 9.09
Lonicerin	-33.79 ± 7.14	-62.72 ± 18.19	-96.52 ± 18.51	62.33 ± 14.66	-4.71 ± 0.88	-34.19 ± 6.54
Quercitrin	-36.63 ± 4.73	-49.88 ± 11.90	-86.51 ± 12.63	46.79 ± 10.85	-4.86 ± 0.25	-39.72 ± 5.10
Oleanolic acid	-21.11 ± 9.19	-7.79 ± 7.13	-35.26 ± 14.45	10.59 ± 6.08	-2.58 ± 1.14	-24.67 ± 9.59
Elastase						
Chamaemeloside	-32.39 ± 6.07	-17.17 ± 9.81	-49.56 ± 12.02	25.99 ± 7.98	-4.19 ± 0.78	-23.57 ± 6.03
Kaempferol 3,4'-dixyloside	-41.09 ± 6.84	-36.10 ± 11.82	-77.19 ± 15.85	42.19 ± 8.02	-5.09 ± 0.67	-35.00 ± 9.38
Limocitrin 7-(6"-acetylglucoside)	-41.31 ± 4.43	-18.49 ± 7.37	-59.79 ± 28.3	28.32 ± 5.45	-4.32 ± 0.51	-31.47 ± 4.37
Lonicerin	-46.24 ± 85.6	-24.31 ± 9.45	-70.54 ± 12.44	34.99 ± 7.44	-5.82 ± 0.67	-35.55 ± 6.78
Rustoside	-34.56 ± 5.84	-28.72 ± 10.89	-63.28 ± 12.85	37.10 ± 8.62	-4.70 ± 0.65	-26.17 ± 5.69
Oleanolic acid	-31.46 ± 3.78	-8.95 ± 4.13	-46.47 ± 5.96	11.38 ± 3.35	-3.79 ± 0.47	-35.09 ± 4.82
Hyaluronidase						
Isocarlinoside	-45.93 ± 4.66	-75.17 ± 12.42	-121.10 ± 11.26	73.96 ± 8.72	-6.51 ± 0.42	-47.14 ± 4.66
Isovitexin 2"-O-arabinoside	-39.79 ± 4.20	-56.99 ± 13.09	-96.79 ± 12.11	56.46 ± 9.39	-5.64 ± 0.28	-40.33 ± 5.38
Kaempferitrin	-49.93 ± 3.98	-52.79 ± 8.56	-102.72 ± 8.98	50.62 ± 5.63	-6.44 ± 0.28	-52.09 ± 5.28
Limocitrin 7-(6"-acetylglucoside)	-37.78 ± 6.17	-45.16 ± 29.06	-82.94 ± 29.73	48.81 ± 21.30	-5.25 ± 0.85	-34.13 ± 9.33
Lonicerin	-35.47 ± 4.93	-75.10 ± 21.79	-110.57 ± 19.85	64.66 ± 14.28	-5.77 ± 0.38	-45.92 ± 7.10
Oleanolic acid	-50.13 ± 3.65	-8.71 ± 6.71	-64.83 ± 8.49	13.26 ± 5.88	-5.86 ± 0.38	-51.57 ± 4.32

Tyrosinase						
Chamaemeloside	-46.02 ± 4.59	-49.44 ± 15.71	-95.46 ± 14.98	59.71 ± 12.77	-6.11 ± 0.39	-35.75 ± 4.87
Isocarlinoside	-35.93 ± 3.89	0.99 ± 21.25	-34.94 ± 21.80	23.93 ± 17.09	-4.94 ± 0.50	-11.01 ± 7.13
Isovitexin 2"-O-arabinoside	-46.59 ± 4.79	-76.33 ± 14.05	-122.93 ± 14.25	69.84 ± 9.85	-7.08 ± 0.28	-53.09 ± 6.94
Kaempferitrin	-37.12 ± 4.96	-47.27 ± 19.80	-84.39 ± 20.02	57.61 ± 14.78	-5.18 ± 0.54	-26.78 ± 8.75
Lonicerin	-37.86 ± 5.13	-52.11 ± 17.20	-89.97 ± 17.41	57.88 ± 12.17	-4.96 ± 0.60	-32.09 ± 7.77
Ascorbic acid	-19.71 ± 2.71	-34.38 ± 7.43	-54.09 ± 7.69	34.82 ± 5.39	-3.24 ± 0.20	-19.27 ± 5.63

ΔEvdW: Van der Waals energy, ΔEelec: Electrostatic energy, ΔGgas: Gas-phase free energy, ΔGsolv: Solvation free energy, ΔGbind: Total binding free energy

4.4.4. Post-molecular dynamics simulation

The formation of an enzyme-ligand complex may cause conformational changes and alter the biological activity of the enzymes. Consequently, post-molecular dynamics simulation was conducted to determine the stability, flexibility, and compactness of the resulting complexes. The results of the post-MD simulation of the topmost compounds while interacting with their respective enzymes are presented in Table 4.4 and Figures 4.2 – 4.5.

4.4.4.1. Root mean square deviation (RMSD)

The collagenase complexes first equilibrated around 20 ns after which they diverged throughout the simulation period except isovitexin-2''-O-arabinoside which swayed at 100 ns till the end of the simulation (Figure 4.2a). This might have accounted for the lowest RMSD value (1.88 Å) of the collagenase-isovitexin-2''-O-arabinoside complex (Table 4.4). While only the isovitexin-2''-O-arabinoside and kaempferitrin complexes had lower RMSD values than the free enzyme, all the resulting complexes of the tested compounds had lower RMSD values than that of the standard (oleanolic acid). All the elastase complexes initially converged up to about 40 ns after which they diverged throughout the simulation period (Figure 4.2b). However, all the complexes formed from the compounds and the standard had lower RMSD values than the free enzyme (Table 4.4). This suggests that all the complexes formed from the interactions are more stable than the free enzyme (Aribisala *et al.* 2022). The hyaluronidase system witnessed equilibration of up to 20 ns followed by incessant fluctuations which were more prominent between 70 and 120 ns (Figure 4.2c). This is reflected in the diversity of their RMSD values. Though, isovitexin-2''-O-arabinoside displayed the lowest RMSD value (1.85 Å), isocarlinoside (3.15 Å) and kaempferitrin (2.97 Å) had higher RMSD values than the standard and the free enzyme (Table 4.4). The fact that the isocarlinoside-hyaluronidase complex has an RMSD value greater than 3.0 depicts that the complex is not stable (Balogun *et al.* 2022). All the enzyme complexes formed in the tyrosinase system appeared to converge at around 170 ns where the kaempferitrin swayed briefly (Figure 4.2d). This may explain why the kaempferitrin complex had the highest RMSD value (1.91 Å). Notably, isovitexin-2-O''-arabinoside displayed the lowest RMSD values for collagenase, hyaluronidase and tyrosinase (Table 4.4), which suggests that the complexes resulting from these interactions are the most stable.

Table 4.4. Post-molecular dynamics simulation parameters of the top five compounds of lemongrass teas with ageing-related enzymes

	RMSD (Å)	RMSF(Å)	ROG (Å)	SASA (Å)	No of H-bonds	Distance of H bonds(Å)	Angle (°) of H-bonds
Collagenase							
Unbound	2.14 ± 0.33	1.31 ± 0.71	15.09 ± 0.09	8584.55 ± 243.72	63.15 ± 5.72	2.86 ± 0.06	151.70 ± 7.45
Chamaemeloside	2.27 ± 0.56	1.69 ± 0.96	15.32 ± 0.24	8902.15 ± 513.16	64.39 ± 6.29	2.86 ± 0.06	151.72 ± 7.41
Isovitexin 2"-O-arabinoside	1.88 ± 0.18	1.18 ± 0.61	15.04 ± 0.08	8486.61 ± 219.66	70.54 ± 5.68	2.86 ± 0.06	151.49 ± 7.52
Kaempferitrin	2.04 ± 0.29	1.27 ± 0.79	14.98 ± 0.08	8208.65 ± 231.39	68.27 ± 6.25	2.86 ± 0.06	151.45 ± 7.59
Lonicerin	2.44 ± 0.64	1.55 ± 1.18	15.22 ± 0.14	8798.91 ± 299.70	66.14 ± 5.85	2.86 ± 0.07	151.49 ± 7.41
Quercitrin	2.50 ± 0.40	1.41 ± 0.81	15.12 ± 0.09	8581.29 ± 252.80	67.99 ± 5.86	2.86 ± 0.06	151.53 ± 7.53
Oleanolic acid	2.68 ± 0.42	1.56 ± 1.46	15.45 ± 0.29	8877.86 ± 294.82	66.52 ± 6.13	2.86 ± 0.06	151.79 ± 7.39
Elastase							
Unbound	2.26 ± 0.29	1.42 ± 0.89	16.43 ± 0.08	11238.01 ± 335.38	90.61 ± 7.30	2.87 ± 0.05	151.32 ± 7.38
Chamaemeloside	1.84 ± 0.16	1.31 ± 0.88	16.44 ± 0.08	11109.18 ± 302.01	93.51 ± 6.33	2.87 ± 0.06	151.29 ± 7.32
Kaempferol 3,4'-dixyloside	1.79 ± 0.21	1.22 ± 0.71	16.49 ± 0.08	11102.01 ± 284.87	90.76 ± 6.37	2.87 ± 0.06	151.10 ± 7.23
Limocitrin 7-(6"-acetylglucoside)	1.82 ± 0.25	1.19 ± 0.81	16.46 ± 0.08	11011.67 ± 265.26	94.58 ± 6.48	2.87 ± 0.06	151.07 ± 7.24
Lonicerin	2.19 ± 0.39	1.29 ± 0.84	16.24 ± 0.06	10845.55 ± 276.01	95.13 ± 6.73	2.87 ± 0.06	151.32 ± 7.36
Rustoside	2.07 ± 0.32	1.27 ± 0.79	16.41 ± 0.08	10984.38 ± 286.82	97.88 ± 7.10	2.87 ± 0.06	151.18 ± 7.43
Oleanolic acid	2.04 ± 0.17	1.27 ± 0.72	16.49 ± 0.09	11006.24 ± 249.63	93.36 ± 6.60	2.87 ± 0.05	151.29 ± 7.39
Hyaluronidase							
Unbound	2.67 ± 0.58	1.48 ± 1.33	22.82 ± 0.15	19980.17 ± 366.56	189.75 ± 9.41	2.86 ± 0.06	151.26 ± 7.49
Isocarlinoside	3.15 ± 0.56	1.41 ± 1.24	22.46 ± 0.09	19531.04 ± 295.64	195.18 ± 9.27	2.86 ± 0.06	151.01 ± 7.65
Isovitexin 2"-O-arabinoside	1.85 ± 0.21	1.28 ± 0.69	22.61 ± 0.14	19666.41 ± 299.72	194.93 ± 9.16	2.86 ± 0.06	151.21 ± 7.68

Kaempferitrin	2.29 ± 0.32	1.35 ± 0.86	22.79 ± 0.11	20203.57 ± 404.82	194.49 ± 9.25	2.86 ± 0.06	151.02 ± 7.55
Limocitrin 7-(6"-acetylglucoside)	2.97 ± 0.47	1.37 ± 1.10	22.69 ± 0.12	19577.93 ± 331.23	197.84 ± 9.27	2.86 ± 0.06	150.95 ± 7.52
Lonicerin	2.17 ± 0.29	1.38 ± 1.00	22.67 ± 0.14	19694.08 ± 321.18	200.08 ± 9.77	2.86 ± 0.06	151.05 ± 7.57
Oleanolic acid	2.22 ± 0.23	1.22 ± 0.70	22.81 ± 0.08	19656.77 ± 314.75	186.58 ± 9.16	2.86 ± 0.06	151.13 ± 7.53
Tyrosinase							
Unbound	1.69 ± 0.16	1.10 ± 0.56	21.57 ± 0.06	19750.26 ± 438.04	215.97 ± 10.19	2.86 ± 0.06	151.45 ± 7.64
Chamaemeloside	1.74 ± 0.15	1.18 ± 0.58	21.57 ± 0.07	19383.64 ± 478.56	223.86 ± 10.17	2.86 ± 0.06	151.34 ± 7.77
Isocarlinoside	1.75 ± 0.18	1.12 ± 0.55	21.45 ± 0.07	19332.06 ± 488.43	218.08 ± 10.21	2.86 ± 0.06	151.38 ± 7.69
Isovitexin 2"-O-arabinoside	1.67 ± 0.20	1.15 ± 0.58	21.52 ± 0.07	19062.28 ± 432.22	228.19 ± 9.94	2.86 ± 0.06	151.38 ± 7.66
Kaempferitrin	1.91 ± 0.28	1.18 ± 0.59	21.49 ± 0.08	19364.69 ± 539.64	221.88 ± 10.18	2.86 ± 0.07	151.47 ± 7.66
Lonicerin	1.72 ± 0.16	1.21 ± 0.59	21.54 ± 0.09	19411.44 ± 446.41	221.34 ± 9.98	2.86 ± 0.06	151.40 ± 7.64
Ascorbic acid	1.79 ± 0.19	1.15 ± 0.66	21.52 ± 0.08	18711.59 ± 379.92	228.16 ± 9.82	2.86 ± 0.06	151.30 ± 7.72

RMSD: Root mean square deviation, RMSF: Root mean square fluctuation, ROG: Radius of gyration, SASA: Solvent accessible surface area

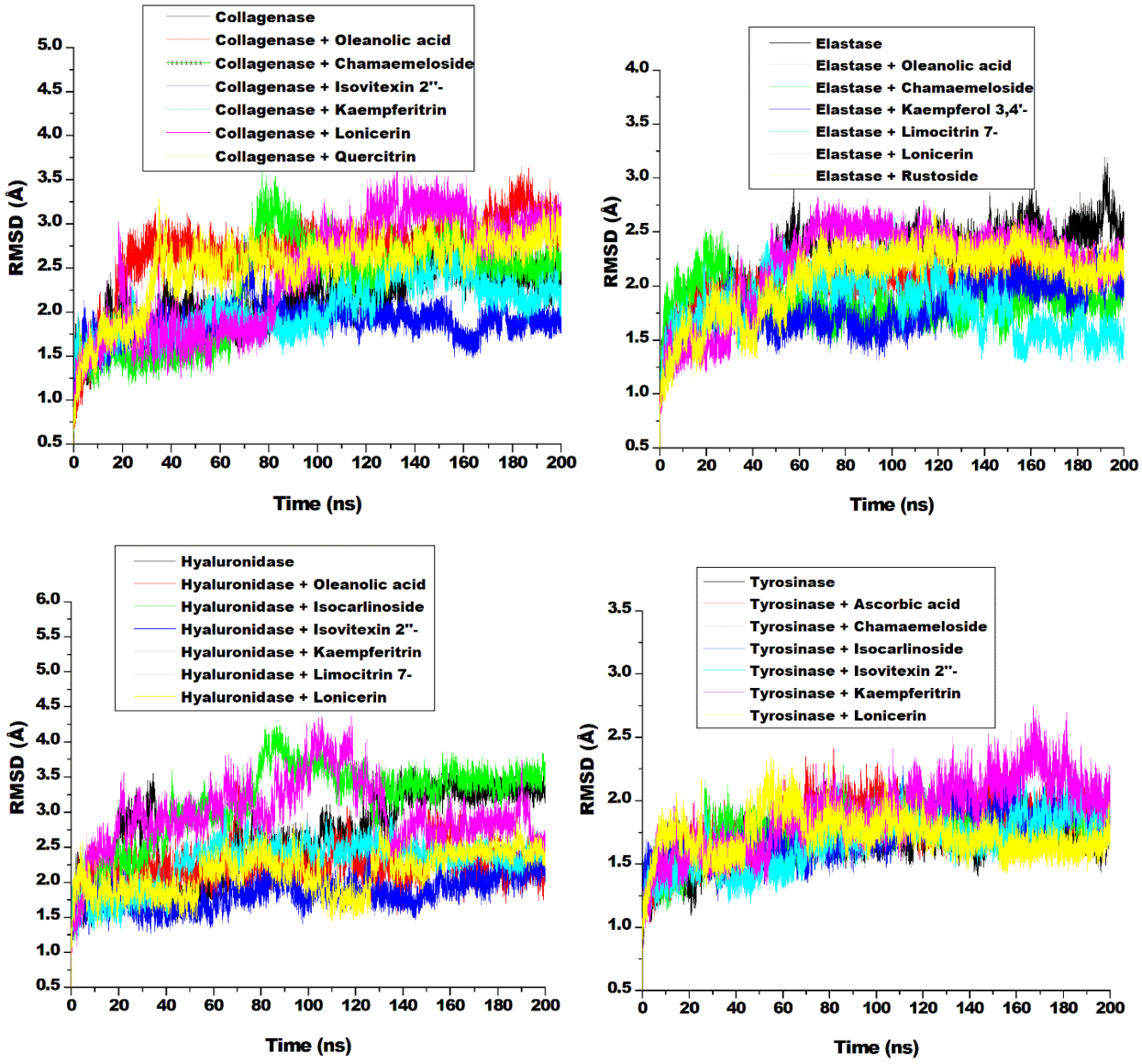

Figure 4.2. Comparative plots of alpha-carbon of (a) elastase (b) collagenase (c) hyaluronidase and (d) tyrosinase and top five compounds in lemongrass teas presented as root mean square deviation (RMSD) over 200 ns molecular dynamic simulation.

4.4.4.2. Root mean square fluctuation (RMSF)

The root mean square fluctuation quantifies the effect of a ligand on the active site of a molecular target, providing insight into the flexibility of the enzyme-ligand complex. There were fluctuations in the RMSF of the collagenase system at 160, 190 and 210 residues (Figure 4.3a). The isovitexin-

2''-O-arabinoside (1.18 Å) and kaempferitrin (1.27 Å) possessed lower RMSF values than other complexes and the free enzyme (Table 4.4). Fluctuations were also observed in the elastase complexes but were more prominent at the 150 residues (Figure 4.3b). However, all the complexes had lower RMSF values than the unbound enzyme, which implies that all the resulting complexes are more flexible and stable than the free enzyme (Bisht *et al.* 2024). There seems to be consistency in the RMSF pattern of the hyaluronidase complexes except at 400 residues (Figure 4.3c). All the complexes possessed lower RMSF values than the unbound enzyme, the standard (oleanolic acid) had the lowest RMSF value (1.22 Å) (Table 4.4), which indicates reduced fluctuation and better flexibility of the complexes. Fluctuations were observed in the RMSF of the tyrosinase complexes around 50 and 200 residues (Figure 4.3d) and the RMSF values of the complexes were higher than the free enzyme. This suggests that the resulting complexes are not stable and flexible, and may not be suitable ligands for tyrosinase (Gok, Budama-Kilinc and Kecel-Gunduz 2024).

4.4.4.3. Radius of gyration (ROG)

When the ligands and enzymes interact, the parameter that provides information on the compactness of their interaction is the radius of gyration (ROG) (Gok, Budama-Kilinc and Kecel-Gunduz 2024). All the collagenase complexes converged to around 120 ns when oleanolic acid diverged from the others (Figure 4.4a). Though all the complexes had lower ROG values than the standard, only kaempferitrin (14.98 Å) and isovitexin-2''-O-arabinoside (15.04 Å) exhibited lower ROG values than the free enzyme (15.09 Å) (Table 4.4). This suggests that the binding does not affect the structural compactness of the protein (Bisht *et al.* 2024). The elastase system was equilibrated throughout the simulation (Figure 4.4b) resulting in similar ROG values except for lonicerin (16.24 Å) with the lowest value compared to the unbound enzyme (16.43 Å). There is consistency in the pattern of the ROG for the hyaluronidase complexes (Figure 4.4c) but the metabolite complexes are lower than the standard and free enzyme (Table 4.4). This implies that the structure of hyaluronidase was not affected by the thermodynamic changes caused by binding of the metabolites (Nutho and Tungmunnithum 2023). The tyrosinase system diverged initially but equilibrated throughout the simulation (Figure 4.4d) resulting in similar ROG values for the complexes.

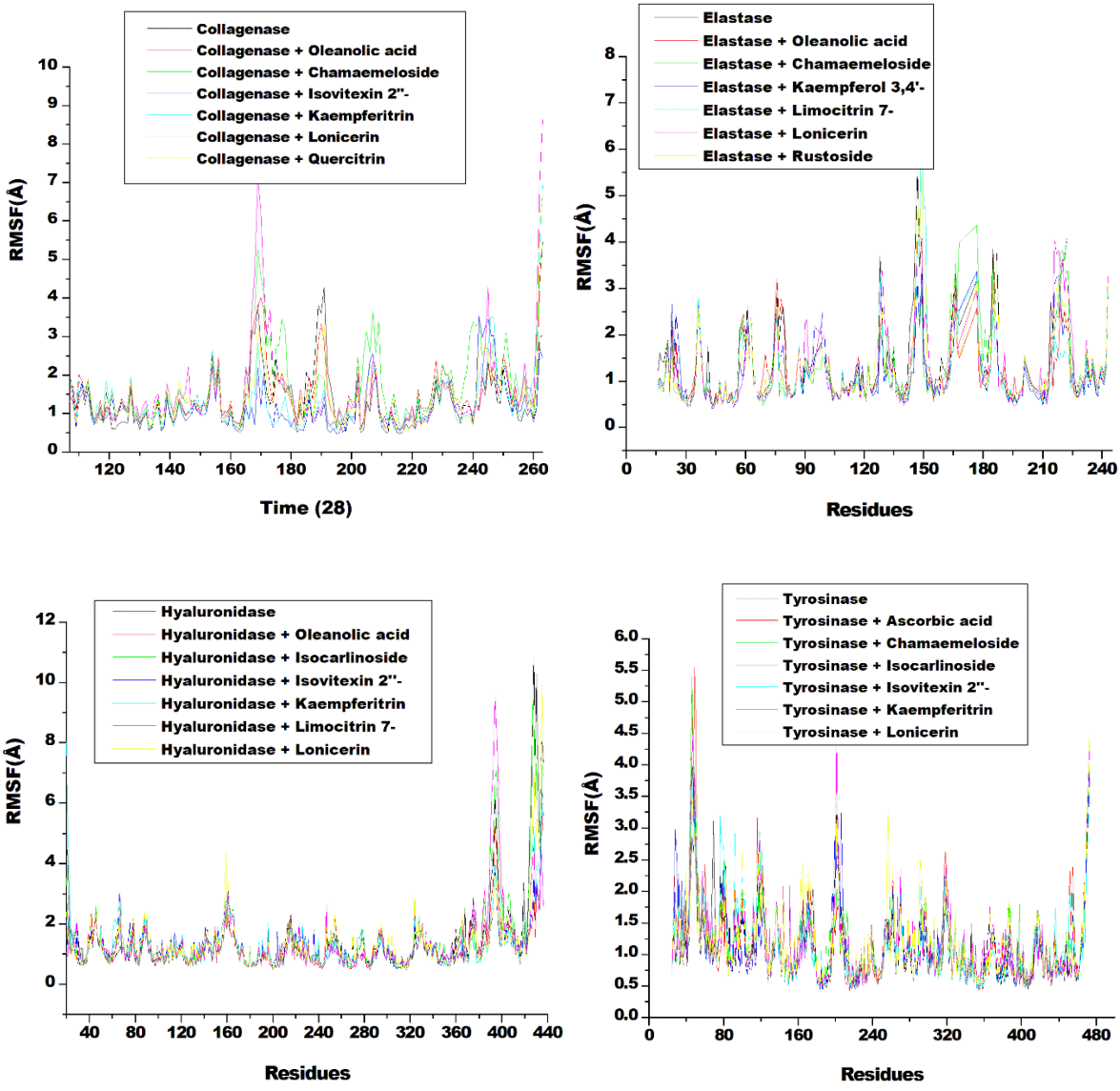

Figure 4.3. Comparative plots of alpha-carbon of (a) collagenase (b) elastase (c) hyaluronidase and (d) tyrosinase and top five compounds in lemongrass teas presented as root mean square fluctuations (RMSF) over 200 ns molecular dynamic simulation.

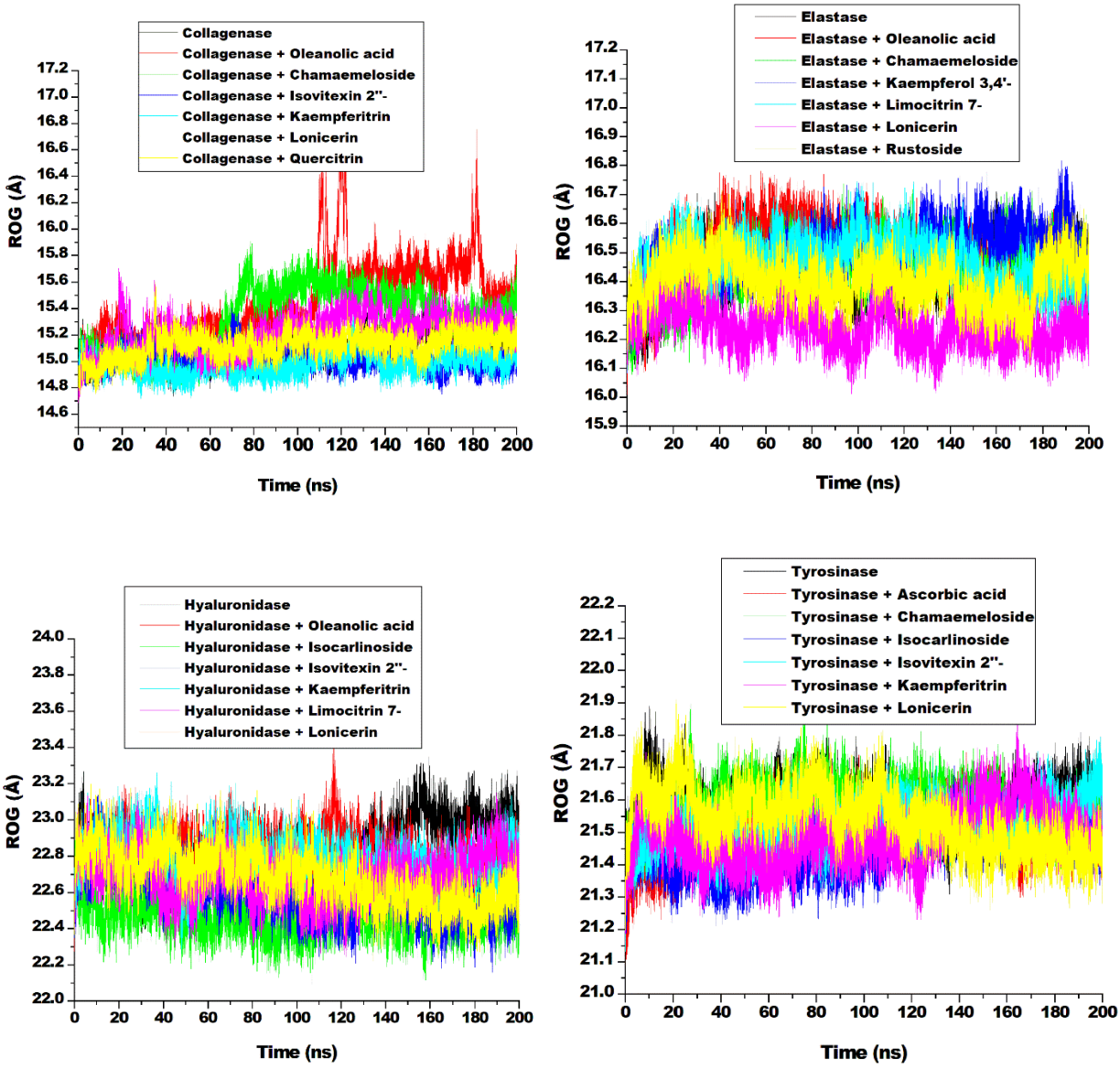

Figure 4.4. Comparative plots of alpha-carbon of (a) collagenase (b) elastase (c) hyaluronidase and (d) tyrosinase and the top five compounds in lemongrass teas presented as the radius of gyration (ROG) over 200 ns molecular dynamic simulation.

4.4.4.4. Solvent-accessible surface area (SASA)

The solvent-accessible surface area (SASA) evaluates protein folding and changes in its surface during simulation. It is determined by the hydrophilicity or hydrophobicity of the amino acid residues of the enzymes to solvents. The SASA plots for all the systems followed a consistent pattern (Figures 4.5a-d). All the complexes formed from the interaction with elastase and tyrosinase possessed lower SASA values than unbound enzymes (Table 4.4). This could indicate that the bound complexes have better stability than the unbound enzymes (Nutho and Tungmunnithum 2023). However, chamaemeloside (8902.15 Å) and lonicerin (8798.91 Å) had higher SASA values than unbound collagenase (8584.55 Å). This may be due to reduced solvent access for the non-polar residues, preventing their stability (Sabiu, Balogun and Amoo 2021). While other complexes had lower SASA values than the unbound enzyme, kaempferitrin (20203.57 Å) exhibited a higher SASA value than the free hyaluronidase (19980.17 Å). This suggests that while other hyaluronidase complexes increased solvent access to the amino acid residues of the protein, the kaempferitrin-hyaluronidase complex had reduced access, which resulted in reduced stability.

4.4.5. Forms and nature of interactions

The ability of a ligand to bind to a protein also depends on the type, number, and nature of the interactions between the ligand and amino acid residues of the protein (Sabiu, Balogun and Amoo 2021). Figure 4.6 shows the interaction plots of the topmost lemongrass compounds (kaempferitrin) and standard (oleanolic acid) with collagenase before and after 200 ns molecular dynamics simulation. This is because kaempferitrin had seventeen (17) interactions with the enzyme, which is the highest at the end of the simulation period. These interactions comprise 3 conventional hydrogen bonds (Asn74, Leu75, Ser133), one carbon-hydrogen bond (Hie77), 12 Van der Waals forces, and 2 other interactions compared to oleanolic acid, with just three interactions (2 Van der Waals forces and 1 attractive charge). Eleven of the interactions kaempferitrin had with collagenase were also conserved (Fig. 4.6A1 and 46A2) while none of the interactions were stable in oleanolic acid (Fig. 4.6B1 and 4.6B2). This is consistent with the lowest binding energy of the kaempferitrin-collagenase complex and a higher number of hydrogen bonds (Aribisala *et al.* 2022), which indicates that kaempferitrin has the best affinity for collagenase and forms a more stable complex than the standard, oleanolic acid.

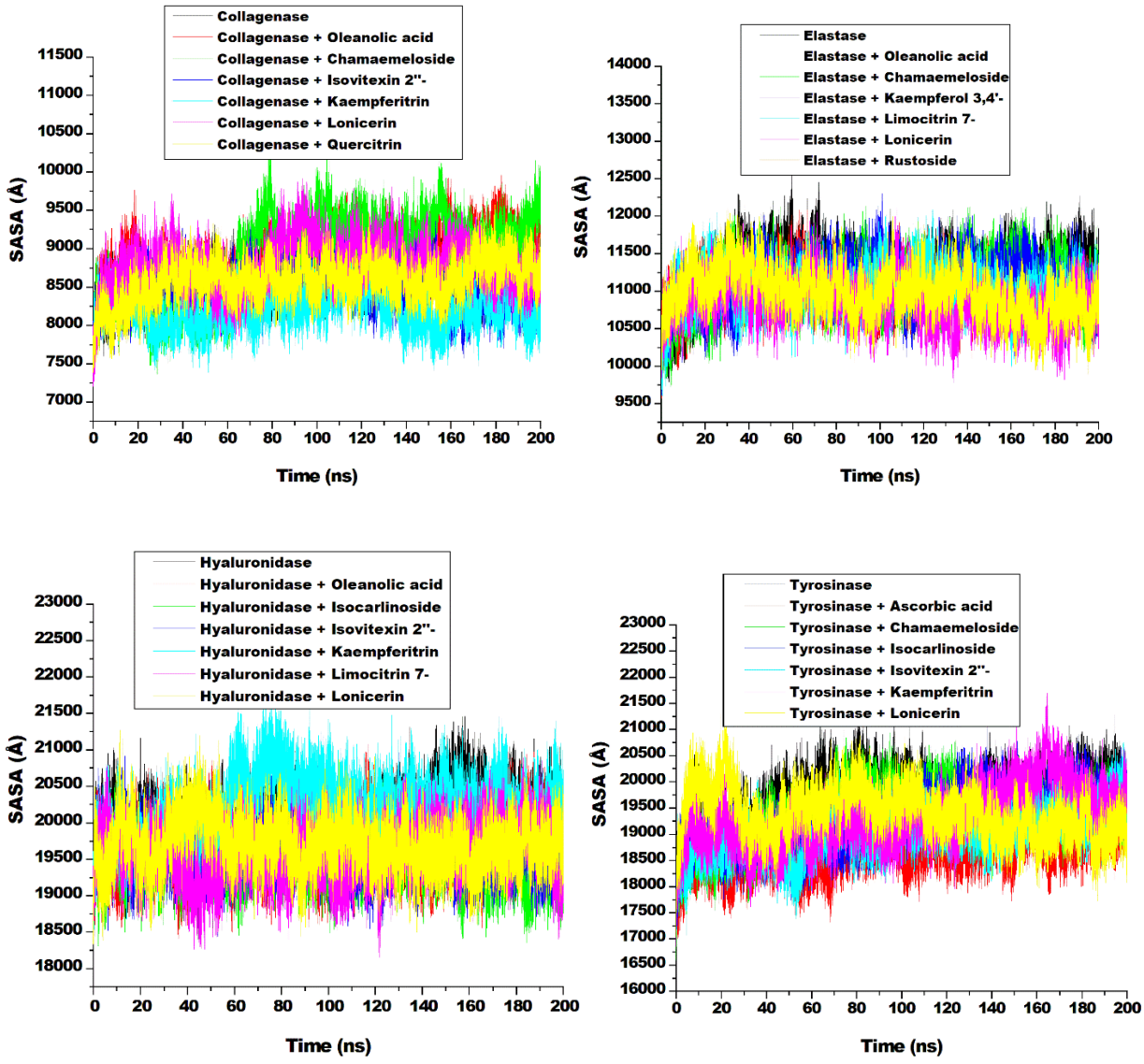

Figure 4.5. Comparative plots of alpha-carbon of (a) collagenase (b) elastase (c) hyaluronidase and (d) tyrosinase and top five compounds in lemongrass teas presented as solvent accessibility surface area (SASA) over 200 ns molecular dynamic simulation.

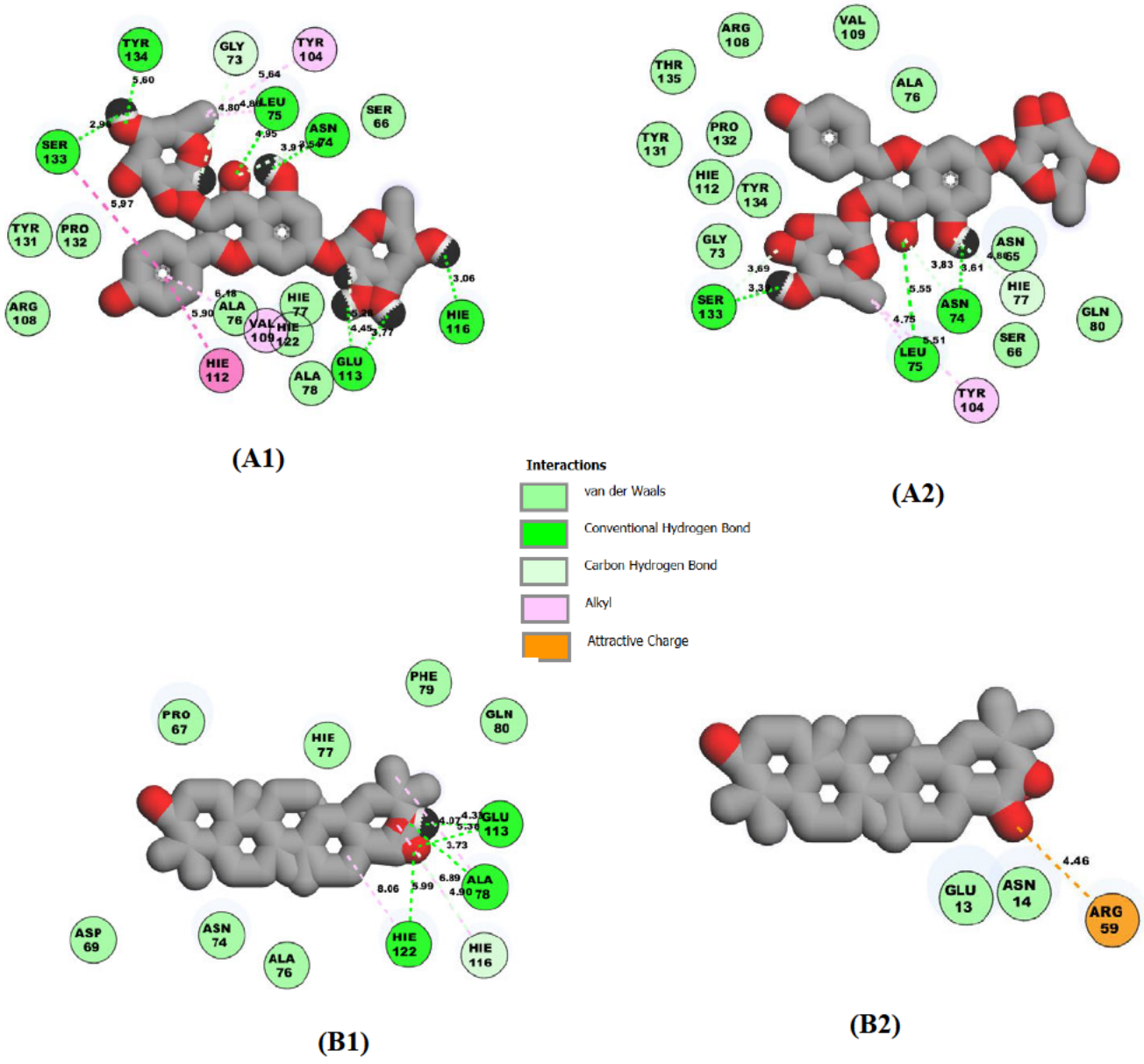

Figure 4.6. 2D interaction plots of (A) kaempferitrin and (B) oleanolic acid against collagenase before (A1, B1) and after (A2, B2) 200 ns molecular dynamics simulation.

At the end of the simulation period, limocitrin 7-(6''-acetylglucoside) (among the top five compounds) exhibited the highest number of viable interactions with elastase compared to the standard (oleanolic acid) (Figure 4.7). Limocitrin 7-(6''-acetylglucoside) had 17 interactions with the enzyme, comprising two conventional hydrogen bonds (Cys169 and Val190), three carbon-hydrogen bonds (Ser173, Ser188, and Phe189), twelve Van der Waals forces contrary to oleanolic acid with 12 interactions made up of two hydrogen bonds, five Van der Waals forces, and five other interactions. Twelve of the seventeen interactions possessed by limocitrin 7-(6''-acetylglucoside) were conserved throughout the simulation period (Fig. 4.7A1 and 4.7A2) while only eight were conserved in the standard (Fig. 4.7B1 and 4.7B2). The higher number of interactions, hydrogen bonds, and conserved interactions possessed by limocitrin 7-(6''-acetylglucoside) suggests that it forms a more stable complex than oleanolic acid and that it binds more closely to the protein (Nutho and Tungmunnithum 2023), which makes it more suitable for treatment.

The interaction plots of the topmost lemongrass metabolite (kaempferitrin) with hyaluronidase before and after 200 ns were presented in Figure 4.8. Kaempferitrin exhibited twenty (20) interactions before and after the simulation, and fifteen (15) of these interactions were stable throughout the experiment (Fig. 4.8A1 and 4.8A2). After a 200 ns simulation, kaempferitrin has seven conventional hydrogen bonds (Glu285, Thr324, Asn331, Hie356, Leu360, Phe368, and Glu396) (Fig. 4.8A2) compared to two hydrogen bonds (Leu362 and Asn364) possessed by oleanolic acid (Fig. 4.8B2). The higher the number of hydrogen bonds between a ligand and protein, the better the affinity of the ligand for the protein (Aguilar-Toalá *et al.* 2023). Therefore, kaempferitrin forms a better and more stable complex with hyaluronidase than oleanolic acid. This also agrees with the lowest binding energy of the kaempferitrin-hyaluronidase complex.

Of the top five compounds that interact with tyrosinase, isovitexin-2''-O-arabinoside had the highest number of interactions and, therefore, was selected for further evaluation. Figure 4.9 revealed that at the end of the 200 ns simulation period, isovitexin-2''-O-arabinoside exhibited eighteen (18) interactions with tyrosinase, comprising five conventional hydrogen bonds (Glu192, Glu336, Tyr338, Asn345, and Thr367), eleven Van der Waals forces, and two other interactions. The standard (ascorbic acid), on the other hand, had two conventional hydrogen bonds (Glu336 and Gly365), two carbon-hydrogen bonds (Gly364 and Thr367), and eight Van der Waals forces.

Fifteen of the interactions of isovitexin-2''-O-arabinoside were consistent throughout the simulation period (Fig. 4.9A1 and 4.9A2), while ascorbic acid had eleven stable interactions (Fig. 4.9B1 and 4.9B2). The higher number of interactions and the consistency of most of the interactions of isovitexin-2''-O-arabinoside with tyrosinase compared to the standard indicates the resulting complex is more stable and compact than the one formed by the standard (ascorbic acid) (Gok, Budama-Kilinc and Kecel-Gunduz 2024). This suggests that isovitexin-2''-O-arabinoside may be a better tyrosinase inhibitor.

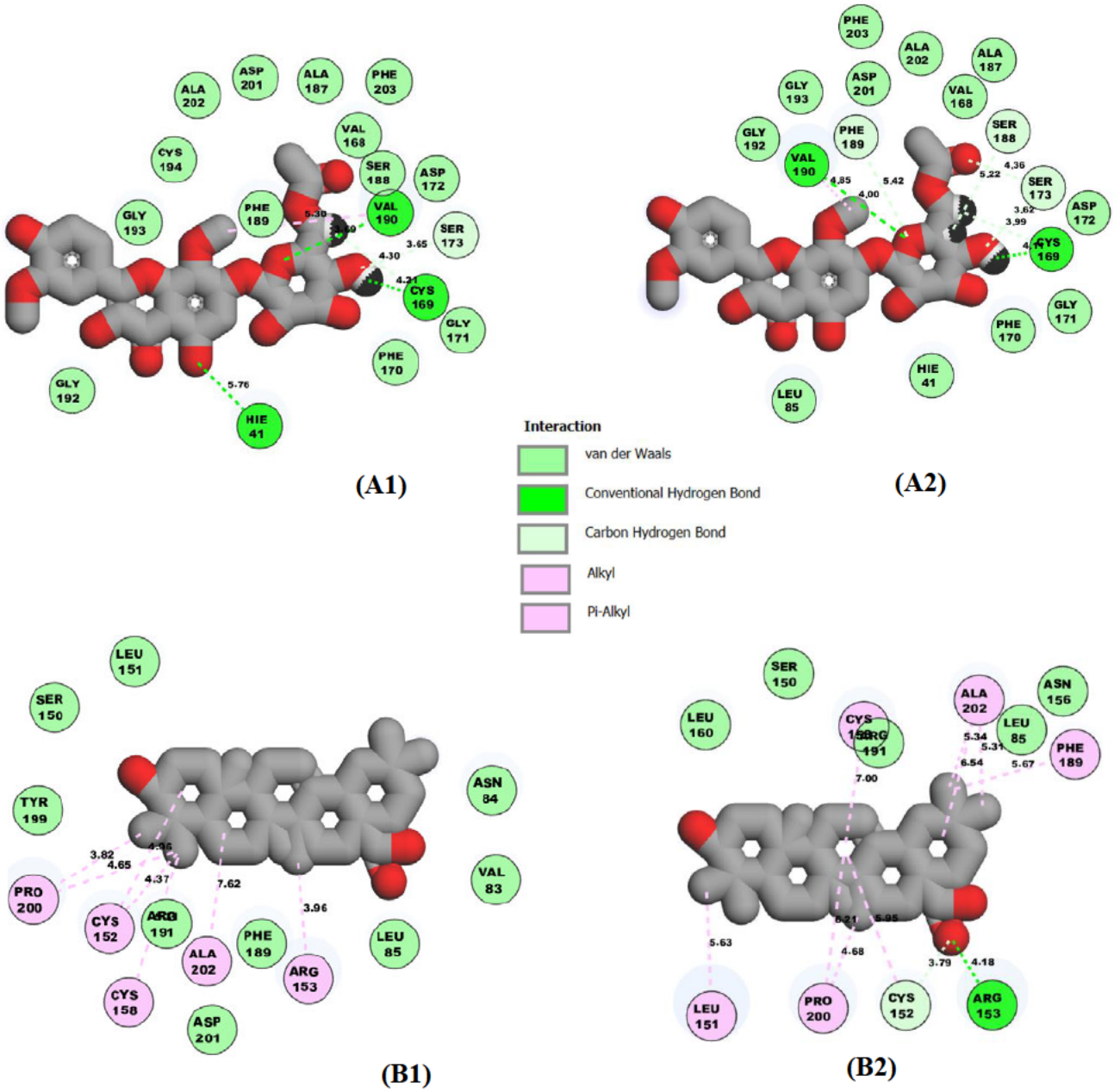

Figure 4.7. 2D interaction plots of (A) limocitrin-7-(6”-acetylglucoside) and (B) oleanolic acid against elastase before (A1, B1) and after (A2, B2) 200 ns molecular dynamics simulation.

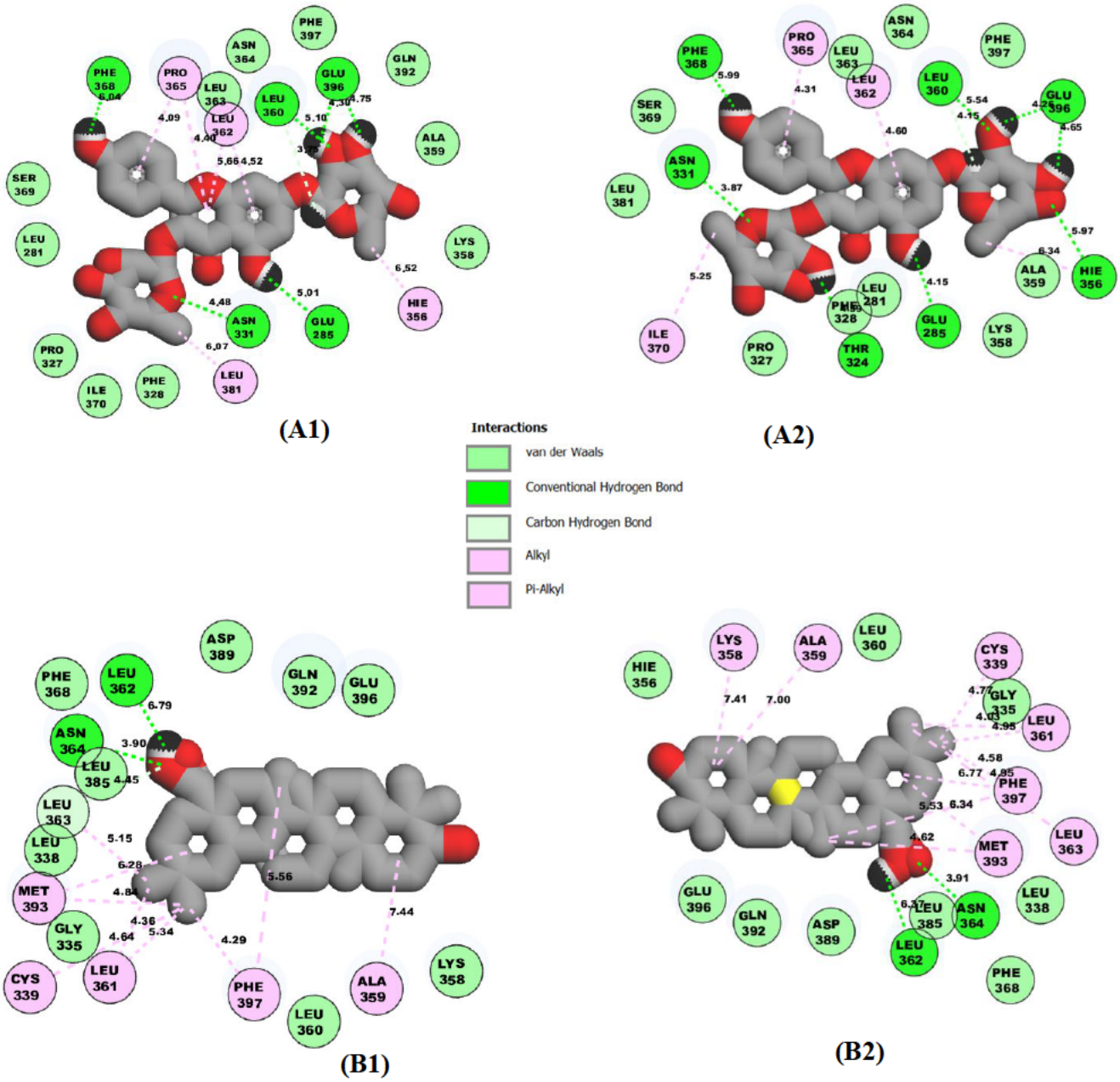

Figure 4.8. 2D interaction plots of (A) kaempferitrin and (B) oleanolic acid against hyaluronidase before (A1, B1) and after (A2, B2) 200 ns molecular dynamics simulation.

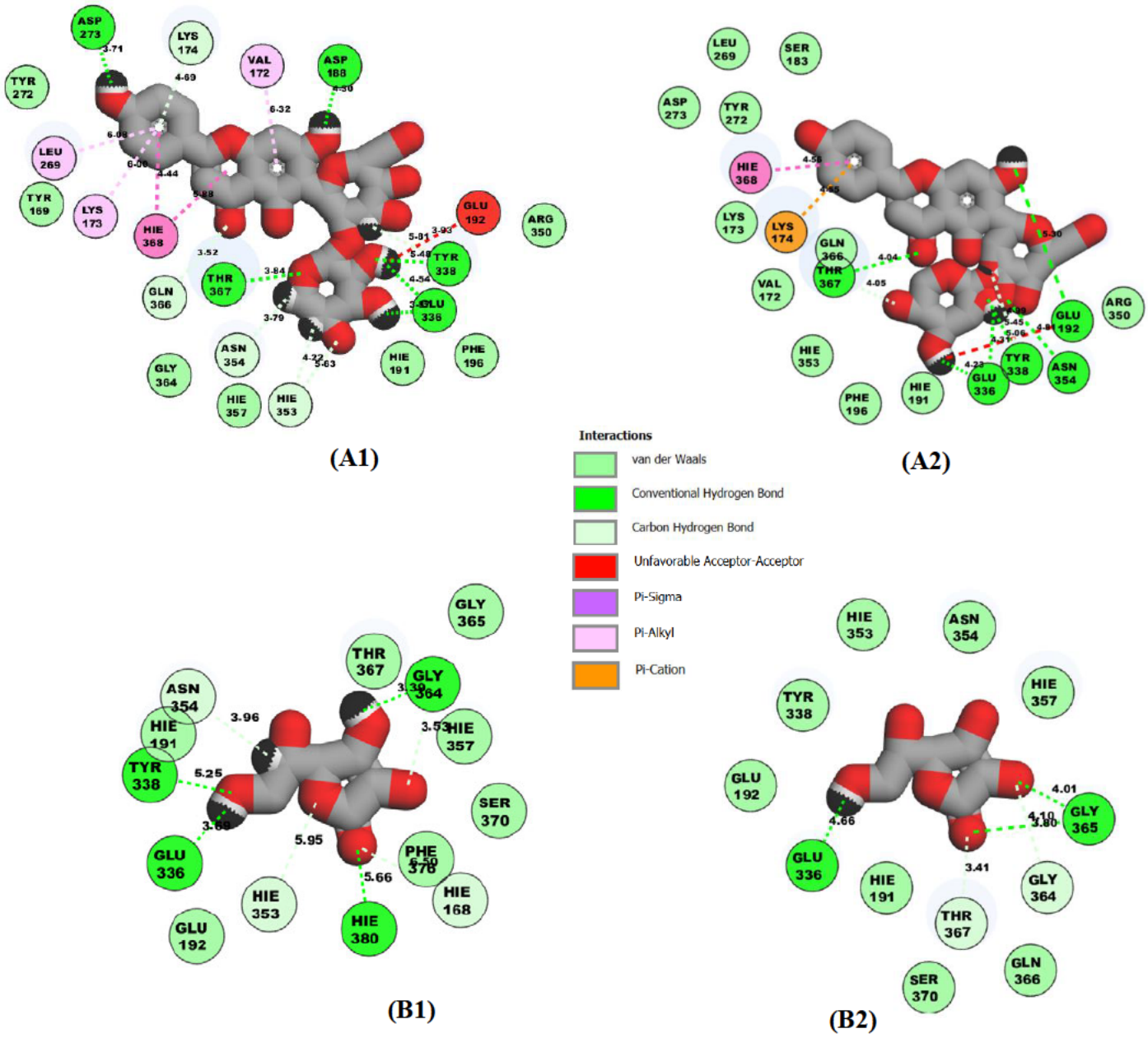

Figure 4.9. 2D interaction plots of (A) isovitexin-2”-O-arabinoside and (B) ascorbic acid against monoamine oxidase before (A1, B1) and after (A2, B2) 200 ns molecular dynamics simulation.

4.4.6. ADMET properties prediction

The drug development process requires the consideration of the pharmacokinetic and safety profile of the proposed therapeutic agent. This involves the determination of absorption, distribution, metabolism, excretion and toxicity (ADMET) properties of the agent. Table 4.5 shows the ADMET profile of top-hit compounds from lemongrass. The human intestinal absorption (HIA) index is an important requirement for the apparent efficacy of a drug, while 20% bioavailability (F20) measures the bioavailability of a drug for use at the site of action (Assaggaf *et al.* 2023). The trio of kaempferitrin, quercitrin, and kaempferol-3,4-dixyloside is classified as having excellent or moderate HIA and F20. Rustoside and limocitrin 7(6-''acetylglucoside) have moderate F20 while chamaemeloside has a moderate HIA index. This suggests that these compounds are safely delivered into the system and can be distributed appropriately.

To measure the distribution of the compounds in human circulation, the blood-brain barrier (BBB), plasma protein binding (PPB,) and unbound fraction in plasma (Fu) are evaluated. Notably, all nine compounds tested in this study performed excellently in the BBB, PPB, and Fu determination. This implies that all the compounds can cross the blood-brain barrier to reach their targets to elicit their pharmacological effects, and effectively bind to plasma protein, thereby improving the drug uptake and can traverse the cellular membranes efficiently (Salekeen *et al.* 2022). The cytochrome P450 system comprises 57 isozymes in humans, and many of them serve as major drug-metabolizing enzymes (Murali *et al.* 2023). The fact that none of the compounds inhibited the activity of CYP1A2 and CYP3A4 suggests that they cannot initiate drug-drug interaction within the circulation, thereby ensuring the appropriate metabolism of the compounds. However, only isovitexin-2''-O-arabinoside and quercitrin were successful in the human liver microsomal (HLM) stability test, which indicates that their clearance by the liver will be efficiently done (Balogun *et al.* 2022).

Plasma clearance (CL plasma) is the overall capacity of the body to eliminate a drug while half-life (T0.5) is the time it takes for the concentration of the drug to reduce by half (Toutain and Bousquet-mélou 2004). All the compounds evaluated possessed good CLplasma and T0.5 values, which suggest that when administered, they are excreted from the body at the appropriate time after eliciting their effects (Salekeen *et al.* 2022).

Table 4.5. ADMET properties of all the top compounds of lemongrass docked against ageing-related enzymes

Compounds	ABS			DIS			METAB			EXCR		TOX				
	Caco2	HIA	F20	BBB	PPB	Fu	CYP1A2	CYP.3A4	HLM	CLplas	T0.5	ROA	Can	Neuro	Hepato	Neph
Chamaemeloside	Po	Md	Po	Ex	Ex	Ex	No	No	Po	Ex	Md	Ex	Ex	Ex	Md	Po
Isovitexin-2”-O-arabinoside	Po	Po	Po	Ex	Ex	Ex	No	No	Md	Ex	Md	Ex	Ex	Ex	Md	Md
Kaempferitrin	Po	Md	Ex	Ex	Ex	Ex	No	No	Po	Ex	Md	Ex	Ex	Ex	Md	Md
Lonicerin	Po	Po	Po	Ex	Ex	Ex	No	No	Po	Ex	Md	Ex	Ex	Ex	Md	Md
Quercitrin	Po	Ex	Md	Ex	Ex	Ex	No	No	Ex	Ex	Md	Ex	Ex	Ex	Md	Ex
Kaempferol-3,4-dixyloside	Po	Ex	Ex	Ex	Ex	Ex	No	No	Po	Ex	Md	Ex	Ex	Ex	Po	Md
Limocitrin-7-(6”-acetylglucoside)	Po	Po	Md	Ex	Ex	Ex	No	No	Po	Ex	Md	Md	Md	Ex	Md	Ex
Rustoside	Po	Po	Md	Ex	Ex	Ex	No	No	Po	Ex	Md	Ex	Ex	Ex	Md	Ex
Isocarlinoside	Po	Po	Po	Ex	Ex	Ex	No	No	Po	Ex	Ex	Ex	Ex	Ex	Md	Md
Standard drugs																
Oleanolic acid	Po	Ex	Md	Md	Po	Po	No	No	Md	Ex	Po	Md	Po	Ex	Po	Po
Ascorbic acid	Po	Ex	Ex	Md	Ex	Ex	No	No	Po	Md	Md	Ex	Md	Ex	Po	Po

ABS: Absorption, DIS: Distribution, METAB: Metabolism, EXCR: Excretion, TOX: Toxicity, Caco-2: Caco-2 permeability, HIA: Human intestinal absorption, F20: 20% bioavailability, BBB: Blood-brain barrier, Fu: Fraction unbound in plasma, CYP1A2: CYP1A2 inhibitor, CYP2C9: CYP2C9 inhibitor, HLM: Human liver microsomal stability, CLplas: Plasma clearance, T0.5: Half-life, ROA: Rat oral toxicity, Can: Carcinogenicity, Neuro: Neurotoxicity, Neph: Nephrotoxicity, Hepato: Hepatotoxicity. Ex: Excellent, Md: Medium, Po: Poor

Since drugs are exogenous to the human body, they are foreign compounds that are likely to be toxic to the system. Consequently, new drugs are subjected to a variety of toxicity tests. All the compounds tested in this study are not orally toxic (ROA), carcinogenic (Can), or neurotoxic (Neuro). While chamaemeloside displayed the tendency to be nephrotoxic, kaempferol-3,4-dixyloside performed poorly in the hepatotoxicity test. This suggests that all the compounds studied are potentially safe for humans, while caution should be exercised in the use of chamaemeloside and kaempferol-3,4-dixyloside (Murali *et al.* 2023).

4.5. Conclusion

This study evaluated the inhibitory properties of lemongrass infusions on the activities of four ageing-related enzymes (collagenase, elastase, hyaluronidase, and tyrosinase) using *in vitro* and *in silico* approaches. Our study revealed that dry lemongrass infusion inhibited the enzymes more potently than the fresh one *in vitro*. The docking study showed that lonicerin had the lowest docking score for collagenase and hyaluronidase, while limocitrin-7-(6”-acetylglucoside) and isovitexin-2”-O-arabinoside exhibited the lowest docking scores for elastase and tyrosinase, respectively. Kaempferitrin had the highest number of stable interactions with collagenase and hyaluronidase, while limocitrin-7-(6”-acetylglucoside) and isovitexin-2”-O-arabinoside interacted more with elastase and tyrosinase, respectively. After subjecting the top-hit compounds to ADMET profiling, all the compounds exhibited good distribution, metabolism, and excretion properties. However, kaempferitrin, quercitrin, and kaempferol-3,4-dixyloside had the best absorption tendencies. All the compounds are also deemed safe except kaempferol-3,4-dixyloside (which is hepatotoxic) and chamaemeloside (which is nephrotoxic). It can therefore be concluded that lemongrass infusion exhibited anti-ageing properties by inhibiting ageing-related enzymes. This may be due to the presence of chemical compounds such as kaempferitrin, limocitrin-7-(6”-acetylglucoside), and isovitexin-2”-O-arabinoside. However, the fact that an entity possessed therapeutic properties during *in vitro* and *in silico* studies does not guarantee success. Hence, there is a need to evaluate the anti-ageing potential of lemongrass infusions in *in vivo* and/or clinical studies.

4.6. References

Abdelfattah, M. A., Dmirieh, M., Bakrim, W. B., Mouhtady, O., Ghareeb, M. A., Wink, M. and Sobeh, M. 2022. Antioxidant and anti-aging effects of *Warburgia salutaris* bark aqueous extract: Evidences from *in silico*, *in vitro* and *in vivo* studies. *Journal of Ethnopharmacology*, 292: 115187.

Aguilar-Toalá, J. E., Vidal-Limon, A., Liceaga, A. M., Zambrano-Zaragoza, M. L. and Quintanar-Guerrero, D. 2023. Application of molecular dynamics simulations to determine interactions between canary seed (*Phalaris canariensis* L.) bioactive peptides and skin-aging enzymes. *International Journal of Molecular Sciences*, 24 (17): 13420.

Al-Khodairy, F. M., Khan, M. K. A., Kunhi, M., Pulicat, M. S., Akhtar, S. and Arif, J. M. 2013. *In Silico* prediction of mechanism of erysolin-induced apoptosis in human breast cancer cell lines. *American Journal of Bioinformatics Research*, 3 (3): 62-71.

Aribisala, J. O., Abdulsalam, R. A., Dweba, Y., Madonsela, K. and Sabiu, S. 2022. Identification of secondary metabolites from *Crescentia cujete* as promising antibacterial therapeutics targeting type 2A topoisomerases through molecular dynamics simulation. *Computers in Biology and Medicine*, 145: 105432.

Assaggaf, H., El Hachlafi, N., El fadili, M., Elbouzidi, A., Ouassou, H., Jeddi, M., Alnasser, S. M., Qasem, A., Attar, A. and AL-Farga, A. 2023. GC/MS profiling, in vitro antidiabetic efficacy of *Origanum compactum* Benth. essential oil and in silico molecular docking of its major bioactive compounds. *Catalysts*, 13 (11): 1429.

Balogun, F. O., Naidoo, K., Aribisala, J. O., Pillay, C. and Sabiu, S. 2022. Cheminformatics Identification and validation of dipeptidyl peptidase-IV modulators from shikimate pathway-derived phenolic acids towards interventive type-2 diabetes therapy. *Metabolites*, 12 (10): 937.

Basconi, J. E., Shirts, M. R. 2013. Effects of temperature control algorithms on transport properties and kinetics in molecular dynamics simulations. *Journal of Chemical Theory and Computation*, 9: 2887–2899.

Bisht, A., Tewari, D., Kumar, S. and Chandra, S. 2024. Network pharmacology, molecular docking, and molecular dynamics simulation to elucidate the mechanism of anti-aging action of *Tinospora cordifolia*. *Molecular Diversity*, 28 (3): 1743-1763.

Branden, G., Sjogren, T., Schnecke, V., Xue, Y. 2014. Structure-based ligand design to overcome CYP inhibition in drug discovery projects. *Drug Discovery Today*, 19: 905–911.

Bras, B. S., do Nascimento Pereira, I., Zibordi, L. C., Rosatto, P. A. P., Santos, H. H., Granero, F. O., Figueiredo, C. C. M., de Faria, M. L., Ximenes, V. F. and de Moraes, R. O. 2024. Green synthesis of silver nanoparticles using food supplement from *Avena sativa* L., and their antioxidant, antiglycation, and anti-aging activities: *In vitro* and *in silico* studies. *Food and Bioproducts Processing*, 147: 175-188.

Cătană, C.-S., Atanasov, A. G. and Berindan-Neagoe, I. 2018. Natural products with anti-aging potential: Affected targets and molecular mechanisms. *Biotechnology Advances*, 36 (6): 1649-1656.

Chen, J.-C., Wang, R. and Wei, C.-C. 2024. Anti-aging effects of dietary phytochemicals: From *Caenorhabditis elegans*, *Drosophila melanogaster*, rodents to clinical studies. *Critical Reviews in Food Science and Nutrition*, 64 (17): 5958-5983.

Deniz, F. S. S., Salmas, R. E., Emerce, E., Cankaya, I. I. T., Yusufoglu, H. S. and Orhan, I. E. 2020. Evaluation of collagenase, elastase and tyrosinase inhibitory activities of Cotinus coggygria Scop. through in vitro and in silico approaches. *South African Journal of Botany*, 132: 277-288.

Ekpenyong, C. E., Akpan, E. and Nyoh, A. 2015. Ethnopharmacology, phytochemistry, and biological activities of *Cymbopogon citratus* (DC.) Stapf extracts. *Chinese Journal of Natural Medicines*, 13 (5): 321-337.

Elgamal, A. M., El Raey, M. A., Gaara, A., Abdelfattah, M. A. and Sobeh, M. 2021. Phytochemical profiling and anti-aging activities of *Euphorbia retusa* extract: *in silico* and *in vitro* studies. *Arabian Journal of Chemistry*, 14 (6): 103159.

Figueiredo, C. C. M., da Costa Gomes, A., Zibordi, L. C., Granero, F. O., Ximenes, V. F., Pavan, N. M., Silva, L. P., Sonvesso, C. d. S. M., Job, A. E. and Nicolau-Junior, N. 2023. Biosynthesis of silver nanoparticles of *Tribulus terrestris* food supplement and evaluated antioxidant activity and collagenase, elastase and tyrosinase enzyme inhibition: *In vitro* and *in silico* approaches. *Food and Bioproducts Processing*, 138: 150-161.

Fikry, E., Mahdi, I., Ortaakarsu, A. B., Tawfeek, N., Ochieng, M. A., Bakrim, W. B., Abdelfattah, M. A., Omari, K. W., Mahmoud, M. F. and Sobeh, M. 2023. Dermato-cosmeceutical properties of *Pseudobombax ellipticum* (Kunth) Dugand: Chemical profiling, *in vitro* and *in silico* studies. *Saudi Pharmaceutical Journal*, 31 (10): 101778.

Gok, B., Budama-Kilinc, Y. and Kecel-Gunduz, S. 2024. Anti-aging activity of Syn-Ake peptide by in silico approaches and in vitro tests. *Journal of Biomolecular Structure and Dynamics*, 42 (10): 5015-5029.

Grinin, L., Grinin, A. and Korotayev, A. 2023. Global Aging: An Integral Problem of the Future. How to Turn a Problem into a Development Driver? In: *Reconsidering the limits to growth: A report to the Russian association of the club of Rome*. Springer, 117-135.

Haider, M. S., Ashraf, W., Javaid, S., Rasool, M. F., Rahman, H. M. A., Saleem, H., Anjum, S. M. M., Siddique, F., Morales-Bayuelo, A. and Kaya, S. 2021. Chemical characterization and evaluation of the neuroprotective potential of *Indigofera sessiliflora* through in-silico studies and behavioral tests in scopolamine-induced memory compromised rats. *Saudi Journal of Biological Sciences*, 28 (8): 4384-4398.

Jiratchayamaethasakul, C., Ding, Y., Hwang, O., Im, S.-T., Jang, Y., Myung, S.-W., Lee, J. M., Kim, H.-S., Ko, S.-C. and Lee, S.-H. 2020. In vitro screening of elastase, collagenase,

hyaluronidase, and tyrosinase inhibitory and antioxidant activities of 22 halophyte plant extracts for novel cosmeceuticals. *Fisheries and Aquatic Sciences*, 23: 1-9.

Kazeem, M. I., Mellem, J. J. and Sabiu, S. 2024. Medicinal foods and plants with antiaging properties: A review of in vitro and in vivo studies. *Food Frontiers*, 5 (1): 24-45.

Khojah, H., Ahmed, S. R., Alharbi, S. Y., AlSabeelah, K. K., Alrayyes, H. Y., Almusayyab, K. B., Alrawiliy, S. R., Alshammari, R. M. and Qasim, S. 2024. Skin anti-aging potential of *Launaea procumbens* extract: Antioxidant and enzyme inhibition activities supported by ADMET and molecular docking studies. *Saudi Pharmaceutical Journal*, Article ID: 102107.

Lee, K. K. and Choi, J. D. 1999. The effects of *Areca catechu* L extract on anti-aging. *International journal of Cosmetic Science*, 21 (4): 285-295.

Luo, J., Si, H., Jia, Z. and Liu, D. 2021. Dietary anti-aging polyphenols and potential mechanisms. *Antioxidants*, 10 (2): 283.

Manosroi, A., Jantrawut, P., Akihisa, T., Manosroi, W. and Manosroi, J. 2010. In vitro anti-aging activities of *Terminalia chebula* gall extract. *Pharmaceutical Biology*, 48 (4): 469-481.

Martel, J., Ojcius, D. M., Ko, Y. F., Chang, C. J. and Young, J. D. 2019. Antiaging effects of bioactive molecules isolated from plants and fungi. *Medicinal Research Reviews*, 39 (5): 1515-1552.

Murali, M., Ahmed, F., Gowtham, H. G., Aribisala, J. O., Abdulsalam, R. A., Shati, A. A., Alfaifi, M. Y., Sayyed, R., Sabiu, S. and Amruthesh, K. N. 2023. Exploration of CviR-mediated quorum sensing inhibitors from Cladosporium spp. against *Chromobacterium violaceum* through computational studies. *Scientific Reports*, 13 (1): 15505.

Nair, P. C., Miners, J. O. 2014. Molecular dynamics simulations: From structure-function relationships to drug discovery. *In Silico Pharmacology*, 2, 1–4.

Nutho, B. and Tungmunnithum, D. 2023. Exploring major flavonoid phytochemicals from *Nelumbo nucifera* Gaertn. as potential skin anti-aging agents: In silico and in vitro evaluations. *International Journal of Molecular Sciences*, 24 (23): 16571.

Oladeji, O. S., Adelowo, F. E., Ayodele, D. T. and Odelade, K. A. 2019. Phytochemistry and pharmacological activities of *Cymbopogon citratus*: A review. *Scientific African*, 6: e00137.

Onder, F. C., Sahin, K., Senturk, M., Durdagi, S. and Ay, M. 2022. Identifying highly effective coumarin-based novel cholinesterase inhibitors by in silico and in vitro studies. *Journal of Molecular Graphics and Modelling*, 115: 108210.

Sabiu, S., Balogun, F. O. and Amoo, S. O. 2021. Phenolics profiling of *Carpobrotus edulis* (L.) NE Br. and insights into molecular dynamics of their significance in type 2 diabetes therapy and its retinopathy complication. *Molecules*, 26 (16): 4867.

Salekeen, R., Ahmed, A., Islam, M. E., Billah, M. M., Rahman, H. and Islam, K. M. D. 2022. In-silico screening of bioactive phytopeptides for novel anti-ageing therapeutics. *Journal of Biomolecular Structure and Dynamics*, 40 (10): 4475-4487.

Seifert, E. 2014. OriginPro 9.1: Scientific data analysis and graphing software-software review. *Journal of Chemical Information and Modelling*, 54: 1552.

Taamalli, A., Arráez-Román, D., Abaza, L., Iswaldi, I., Fernández-Gutiérrez, A., Zarrouk, M. and Segura-Carretero, A. 2015. LC-MS-based metabolite profiling of methanolic extracts from the medicinal and aromatic species *Mentha pulegium* and *Origanum majorana*. *Phytochemical analysis*, 26 (5): 320-330.

Takahashi, T., Ikegami-Kawai, M., Okuda, R. and Suzuki, K. 2003. A fluorimetric Morgan–Elson assay method for hyaluronidase activity. *Analytical Biochemistry*, 322 (2): 257-263.

Thring, T. S., Hili, P. and Naughton, D. P. 2009. Anti-collagenase, anti-elastase and anti-oxidant activities of extracts from 21 plants. *BMC Complementary and Alternative Medicine*, 9 (1): 1-11.

Toutain, P.-L. and Bousquet-mélou, A. 2004. Plasma clearance. *Journal of Veterinary Pharmacology and Therapeutics*, 27 (6): 415-425.

Wallace, W. E., Moorthy, A. S. 2023. NIST mass spectrometry data center standard reference libraries and software tools: Application to seized drug analysis. *Journal of Forensic Sciences*, 68(5): 1484-1493.

Yepes, A., Ochoa-Bautista, D., Murillo-Arango, W., Quintero-Saumeth, J., Bravo, K. and Osorio, E. 2021. Purple passion fruit seeds (*Passiflora edulis* f. edulis Sims) as a promising source of skin anti-aging agents: Enzymatic, antioxidant and multi-level computational studies. *Arabian Journal of Chemistry*, 14 (1): 102905.

CHAPTER 5

5. Lemongrass (*Cymbopogon citratus*) infusions exhibit neuroprotective properties: Evidence from *in vitro* and *in silico* studies

Mutiu Idowu Kazeem, Rukayat Abiola Abdulsalam, John Jason Mellem and Saheed Sabiu
Department of Biotechnology and Food Science, Faculty of Applied Sciences, Durban University of Technology, P. O. Box 1334, Durban 4000, South Africa

Preface: This manuscript investigated the neuroprotective potential of lemongrass infusions using *in vitro* and *in silico* techniques. It has been published in the journal: *Food Bioscience*, 68, 106355, https://doi.org/10.1016/j.fbio.2025.106355. (Appendix 8)

5.1. Abstract

The prevalence of neurological disorders is high, especially in the elderly, and current therapies only provide temporary relief and elicit serious adverse effects. This study evaluated the neuroprotective effect of *Cymbopogon citratus* (lemongrass) teas using *in vitro* and *in silico* techniques. The inhibitory effect of the infusions from fresh and dry lemongrass was tested against four enzymes implicated in neurological diseases, viz, acetylcholinesterase (AChE), butyrylcholinesterase (BChE), β-secretase (BACE-1), and monoamine oxidase (MAO). This was followed by molecular docking and molecular dynamics simulation studies to assess the interactions of the metabolites present in lemongrass with the selected enzymes. The fresh lemongrass tea displayed a better inhibitory effect on the activities of BACE-1 (IC_{50}: 38.24 µg/mL) and MAO (IC_{50}: 78.62 µg/mL), and is comparable to the standard drugs. Molecular docking revealed that resulting complexes from 4-oxo-3-phenyl-4H-chromen-7-yl 3-phenylprop-2-enoate (OPCPPE) as well as aspulvinone H (-10.6 kcal/mol), [1,1'-binaphthalen]-2-ol (-12.1 kcal/mol), neocuscutoside C (-10.5 kcal/mol) and aspulvinone H (-11.9 kcal/mol) had the lowest scores for AChE, BChE, BACE-1, and MAO, respectively. A further probe through a 120-ns molecular dynamics simulation on the top-performing metabolites showed that the resulting complexes formed with chamaemeloside (-66.59 kcal/mol), isocarlinoside (-65.79 kcal/mol), neocuscutoside C (-41.09 kcal/mol), and aspulvinone H (-72.28 kcal/mol) against AChE, BChE, BACE-1 and

MAO, respectively, had the lowest binding free energy values compared to the respective standards. In conclusion, the fresh lemongrass tea elicited better neuroprotective properties *in vitro*, and its phenolic constituents (especially aspulvinone H and neocuscutoside C) are potent inhibitors of neurological targets *in silico*. There is a need for further studies on the *in vivo* neuroprotective potential of these compounds.

Keywords: Alzheimer's disease, acetylcholinesterase, β-secretase, lemongrass, aspulvinone H

5.2. Introduction

Neurological disorders (NDs) are ailments that affect the nervous system, characterized by behavioral changes and cognitive deficits (Haider *et al.* 2021). These diseases cause continuous alterations in the neuronal structure and function, leading to cellular death (Paudel *et al.* 2019). Globally, more than 3 billion people are living with neurological disorders, and over 80% of neurological deaths and ill health occur in low and middle-income countries (Steinmetz *et al.* 2024). They are the leading cause of ill health and disability and cause severe hardship to individuals, families, and society at large (Gyebi *et al.* 2023). These pathologies (which include dementia, Alzheimer's, Parkinson's, and Huntington's disease) may differ in their etiology but share neural cell death, neuroinflammation, and brain damage (Paudel *et al.* 2019). The onset of these ailments may affect the mobility, memory, and speech of the patients, thereby causing lifelong disabilities and a socio-economic burden on society.

Approved therapies for the management of neurological disorders only achieve symptomatic relief and do not cure these diseases, while they also cause serious adverse effects (Santi *et al.* 2020). Consequently, there is an urgent need to search for neuroprotective agents from alternative sources like plants. About 80% of the global population relies on medicinal foods and plants for the treatment of diseases due to their accessibility, affordability, efficacy, and perceived safety (WHO 2002). Several medicinal plants have been validated for their various therapeutic properties, including antioxidant, antidiabetic, anticancer, hepatoprotective, cardioprotective, and neuroprotective agents (Kazeem and Davies 2016; Cancela *et al.* 2020). These therapeutic effects are attributed to the presence of phytochemical compounds including polyphenols, flavonoids, saponins, terpenes, and glycosides.

Cymbopogon citratus (Poaceae), commonly referred to as lemongrass, is a perennial grass that is native to Asia but widely distributed in all regions of the globe (Oladeji *et al.* 2019). Infusions prepared from the leaves are consumed for nutritional and/or therapeutic purposes, similar to other herbal teas like green or rooibos tea (Ekpenyong, Akpan and Nyoh 2015). Due to its aromatic nature, the leaf's essential oil is used in the food, soap, cosmetic, and pharmaceutical industries (Avoseh *et al.* 2015). It is used in traditional medicine for the treatment of cold, pain, fever, indigestion, and gastrointestinal disturbances (Ekpenyong, Akpan and Nyoh 2015). Several studies have reported the pharmacological properties of the plant, including antioxidant, antimicrobial, anti-inflammatory, antidiabetic, and antimalarial properties (Negrelle and Gomes 2007; Oladeji *et al.* 2019). Though there are some studies on the neuroprotective potential of lemongrass leaves in the literature (Umukoro *et al.* 2018; Madi *et al.* 2020; Hacke *et al.* 2021; Rojek *et al.* 2022; Fatima *et al.* 2024), there is a need to provide detailed information on the mechanism of neuroprotective activity of the lemongrass teas.

Previous studies have revealed that many enzymes serve as therapeutic targets for neurological disorders. These include [acetylcholinesterase (AChE), butyrylcholinesterase (BChE), β-secretase (BACE-1), and monoamine oxidase (MOA)]. AChE and BChE hydrolyze and inactivate acetylcholine, thereby controlling the concentration of the neurotransmitter at the synapse (Masondo *et al.* 2019). However, excessive inactivation of acetylcholine is implicated in the pathogenesis of Alzheimer's disease. Beta-site Amyloid Precursor Protein Cleaving Enzyme 1 (BACE-1), otherwise called β-secretase, catalyzes the initial cleavage of the amyloid precursor protein (APP), leading to the generation of amyloid-β (Aβ) peptides (Gyebi *et al.* 2023). Accumulation of amyloid-β in the brain causes Alzheimer's disease, and BACE-1 is a potential therapeutic target for the disease (Mazumder and Choudhury 2019; Mendes *et al.* 2023). Monoamine oxidase (MAO) is an enzyme that catalyzes the oxidative deamination of monoaminergic neurotransmitters such as serotonin, dopamine, epinephrine, and norepinephrine (Moorkoth *et al.* 2021). It is implicated in the pathogenesis of depression, Alzheimer's, and Parkinson's disease (Jalal *et al.* 2022).

Therefore, this study investigated the inhibitory properties of lemongrass infusions on neurological targets [acetylcholinesterase (AChE), butyrylcholinesterase (BChE), β-secretase (BACE-1), and monoamine oxidase (MAO)] *in vitro* and complemented the findings with computational studies

through establishment of intermolecular interactions between its metabolites and the target enzymes as a way of lending credence to its mechanism of neuroprotective action. This is hoped to contribute towards discovering novel therapeutic agents for managing neurological disorders.

5.3. Materials and methods

5.3.1. Materials

All the enzymes and their substrates, namely acetylcholinesterase (AChE) type V from electric eel, butyrylcholinesterase (BChE) from equine serum, acetylthiocholine iodide, butyrylcholine iodide, kynuramine, as well as β-secretase and monoamine oxidase from humans, are obtained from Sigma Aldrich, Missouri, USA. The reference drugs donepezil, AZD3293, and tranylcypromine were products of Pfizer Inc., New York, USA. All other chemicals are of analytical grade, and the water used is glass-distilled. All materials used in this study are properly stored and used within 3 months.

5.3.2. Preparation of lemongrass teas

Leaves of lemongrass were harvested from farmland in the Iba area of Lagos in October 2021. It was identified and authenticated at the Department of Botany, Lagos State University, Nigeria, and was assigned the voucher number: LSH/21/1055. The leaves were gently rinsed in tap water to remove soil and dirt. A portion was cut into pieces using a stainless-steel kitchen knife, spread on foil paper, and dried to constant weight on the laboratory table at ambient temperature (25 °C), while the second portion was used fresh. After drying, the sample was milled using an electric grinder (Silver Crest, Germany). One litre of boiled distilled water was poured on a 100 g milled sample, shaken, and left to steep for 24 h to produce an infusion. Another 1.0 L of boiled distilled water was poured on the second portion (100 g) of the fresh lemongrass and left to steep for 24 h. Both infusions were filtered and concentrated in a lyophilizer (Virtis BenchTop, SP Scientific Series, USA). The lyophilized infusions were used for subsequent analysis by dissolving in distilled water to give stock solutions of 1.0 mg/mL and different concentrations (3.13, 6.25, 12.5, 25, 50, and 100 µg/mL). All infusions were stored at 4 °C before analysis.

5.3.3. Metabolite profiling using Liquid Chromatography-Mass Spectrometry (LC-MS)

The phytochemical composition of the teas obtained from fresh and dry lemongrass leaves was assessed using a previous method (Suleria, Barrow and Dunshea 2020). Agilent 6520 Accurate-

Mass QTOF was applied in a positive and negative mode. Synergi Hydro-RP (4 µm particle size, 4.6 mm internal diameter, and 250 mm length with 80 Å pore size was used to separate phenolic compounds, and the flow rate was set at 800 µL/min. An aliquot of 10 µL from each sample was injected while gradient was 0–5 min (0–10%), 5–25 min (10–25% B), 25–35 min (25–35% B), 35–45 min (40–60% B) 45–75 min (40–55% B), 75–80 min (55–88% B) (80–82 min (80–90% B), 82–85 min (90–100% B), 85–90 min (0% B). Mobile phase A was 0.1% formic acid in water, and mobile phase B was 95% acetonitrile with 0.1% formic acid. A full scan mode was achieved in the range of 100–1000 amu with the following conditions: Capillary voltage (3500 V), nozzle voltage (500 V), nitrogen gas flow rate (9 L/min) at 325 °C, and nebulization was set as 45 psi while 10, 20, and 30 eV collision energies were used. Acquisition of data was performed through the employment of MassLynx4.1 software, while detection and confirmation of metabolites were processed using the MS-DIAL software and MS-FINDER (RIKEN Centre for Sustainable Resource Science: Metabolome Informatics Research Team, Kanagawa, Japan). For further confirmation, identification of the profiled metabolites was also performed by comparing the respective mass spectra obtained against the National Institute of Standards and Technology (NIST) library (Wallace and Moorthy, 2023).

5.3.4. In vitro inhibitory studies

5.3.4.1 Cholinesterase inhibition assay

The acetylcholinesterase (AChE) inhibitory activity of the lemongrass infusions was evaluated (Perry *et al.* 2001). Forty microliters of (0.28 U/ml) acetylcholinesterase, 140 µL of 3.3 mM of 5,5-dithiobis-(2-nitrobenzoic) acid (prepared in 0.1 M phosphate-buffered solution, pH 7.0, containing 6 mM $NaHCO_3$), lemongrass infusions (3.13 – 100 µg/mL), and 80 µl of phosphate buffer (pH 8.0) were added to each well of microplate. The solution was incubated for 20 min at 25 °C. Acetylthiocholine iodide (0.05 mM, 40 µl) was added to each well, and the absorbance was determined in a microtiter plate reader (Synergy MX Biotech) at 412 nm for 3 min immediately after the addition of the substrate. The same experiment was used to determine the butyrylcholinesterase (BChE) activity of the extracts using butyrylcholine iodide. The enzyme inhibitory activities were expressed as percentage inhibition. Donepezil was used as the positive control (3.13 – 100 µg/mL).

5.3.4.2. Beta-secretase inhibition assay

The β-secretase inhibitory property of the lemongrass infusions was performed using a standard method (Puksasook *et al.* 2017). Briefly, 20 µL of 0.1 U/mL β-secretase and 20 µL of lemongrass infusions (3.13 – 100 µg/mL) dissolved in 100 mM sodium acetate buffer, pH 4.5, were added to the 96-well plate and incubated at 37 °C for 10 min. Then 50 µL of 750 mM β-secretase substrate in 100 mM sodium acetate buffer pH 4.5 was added and incubated at 37 °C for 20 min. After that, 10 µL of stop buffer (2.5 M sodium acetate buffer, pH 4.5) was added to the 96-well plate. Then, the fluorescence was measured at 380 nm (excitation wavelength) and 510 nm (emission wavelength) using a microplate reader (Spectramax, USA). AZD3293 was used as the positive control (3.13 – 100 µg/mL).

5.3.4.3. Monoamine oxidase inhibitory assay

The monoamine oxidase inhibitory property of the samples was evaluated (Yang *et al.* 2020). Briefly, 50 µL of potassium phosphate buffer (0.1 M, pH 7.4) and 50 µL of monoamine oxidase solution (final protein concentration was 0.0006 mg/mL) were mixed with 50 µL of lemongrass infusions (prepared in potassium phosphate buffer) (3.13 – 100 µg/mL), followed by incubation at 37 °C for 30 min. Thereafter, 50 µL kynuramine (40 µM) was added to the mixture to initiate the reaction, followed by incubation at 37 °C for 20 min, and the reaction was terminated by the addition of 75 µL of 2 M NaOH. The fluorescence was subsequently measured at excitation and emission wavelengths of 310 and 380 nm, respectively. Tranylcypromine was used as a positive control (3.13 – 100 µg/mL).

5.3.5. In silico studies

5.3.5.1. Collection and preparation of the identified metabolites

The 3D structures of the 49 identified/annotated compounds from *Cymbopogon citratus* using MS-DIAL software and MS-FINDER coupled with further confirmation by comparing the respective mass spectra obtained against NIST library and those of the reference drugs [donepezil with ID 3152 (standard for acetylcholinesterase and butyrylcholinesterase)], [AZD3293 with ID 67979346 (standard for β-secretase)], and [tranylcypromine with ID 19493 (standard for monoamine oxidase)], were obtained from PubChem (https://pubchem.ncbi.nlm.nih.gov/) and then optimized

via the additions of nonpolar hydrogen atoms and charges using the Avogadro software (Aribisala *et al.* 2022). The optimized ligands were saved in Mol2 format for subsequent molecular docking.

5.3.5.2. Collection and preparation of therapeutic targets

The X-ray crystal structures of AChE (ID: 4PQE), BChE (ID: 1P0I), BACE (ID: 11SGZ), and MAO-A (ID: 2BXS) were acquired from the Protein Data Bank (https://www.rcsb.orgs/) and prepared through the removal of non-standard amino acids and water molecules using UCSF Chimera software v 1.14 (Gyebi *et al.* 2023). The cleaned structures were then saved in PDB format for molecular docking.

5.3.5.3. Molecular docking and validation of C. citratus metabolites

The docking procedure entailed the selection of amino residues at the active site of the protein whose grid box coordinates coincide with the established x-y-z coordinates; AChE [centre (X: 32.03; Y: 7.10; Z: 14.59) radius (22.20)], BChE [centre (X: 23.13; Y: -47.61; Z: −33.33), radius (5.0)], BACE-1 [centre (X: 32.67; Y: 6.14; Z: 12.66), radius (12.20)], and MOA [centre (X: − 4.85; Y: 35.25; Z: -17.94), radius (25.20)].

Subsequent docking at the active site of the proteins was ensured by dragging the grid box to fit the established, well-defined x-y-z coordinates. Thereafter, the optimized 3D structures of the ligands (*C. citratus* metabolites and reference drugs) and cleaned proteins (AChE, BChE, BACE, and MAO-A) were subjected to molecular docking using the Autodock vina package on Python Prescription v 0.9.5 (PyRx), which allows for multiple docking of ligands (Onder *et al.* 2022). Finally, the ligands were ranked based on their binding affinity, and the top five docked complexes with the best pose were saved in Protein Data Bank (PDB) format and subjected to MD simulations. To validate the docking conformation, the superimposition and redocking techniques were employed, where the appropriate root-mean-square deviation (RMSD) of a docked compound from its reference point (position of native inhibitors) in each target was calculated (Al-Khodairy *et al*., 2013). The best conformational clusters from this dock were ranked based on the RMSD between their docked position and the ligand's experimentally determined position.

5.3.5.4. Molecular dynamics simulation

The MD simulation was performed as previously described (Sabiu, Balogun and Amoo 2021). Succinctly, the simulations were performed over a 120 ns period using the AMBER 14 package of

the Centre for High-Performance Computing (CHPC), South Africa. The FF18SB variant of the AMBER force field was adopted to describe the operating systems. The ANTECHAMBER was employed to create the ligands' atomic partial charges by exploiting the general amber force field (GAFF) procedures and restrained electrostatic potential (RESP). The hydrogen atoms, Na^+, and Cl^- counter ions of the Leap module were used to neutralize the systems. In each case of the simulation, the numbering of the amino acid residues was done accordingly, and the systems were suspended inside an orthorhombic box of TIP3P water molecules in such a manner that all atoms were within 8 Å of any box edge. The bonds of hydrogen atoms in each case of the simulation were constrained using the SHAKE algorithm. Each simulation had a 2 fs step size, which corresponded to the isobaric–isothermal ensemble (NPT) with randomized seeding, a temperature of 300 K, constant pressure of 1 bar, and a Langevin thermostat with a 1.0 ps collision frequency and a pressure-coupling constant of 2 ps. Following that, the results of the 120 ns MD simulation were examined and regarded as post-dynamic data.

5.3.5.5. Post-MD simulation

The post-MD simulation was carried out as earlier described (Jalal *et al.* 2022). Briefly, after the simulation, the systems' coordinates were combined and analyzed using the AMBER 14 PTRAJ module of CHPC. After this, the root mean square fluctuation (RMSF), the radius of gyration (RoG), root mean square deviation (RMSD), and solvent accessibility surface area (SASA) were analyzed using the CPPTRAJ module of the same package, and their raw data were generated using Origin V6. Similarly, using the Molecular Mechanics/GB Surface Area approach, the free binding energy (ΔG) in each case of the simulation was calculated using the expression ΔG bind = Gcomplex – (G Receptor + G ligand) by averaging among 100,000 snapshots taken from a 120 ns MD simulation trajectory. The complexes' interactions in each simulation case were visualized and analyzed post-MD simulation using Discovery Studio version 21.1.0.

5.3.5.6. Determination of pharmacokinetic properties

The ADMETlab 3.0 web (https://admetlab3.scbdd.com/) was used to forecast the adsorption, distribution, metabolism, excretion, and toxicological properties of the compounds with the top docking score. This is done by entering the Simplified Molecular Input Line Entry System

(SMILES) of the compounds onto the platform and submitting them for ADMET screening. The outcome generated was critically examined to determine the status of the compounds.

5.3.6. Statistical analysis

The *in vitro* enzyme inhibitory studies were performed in triplicate, and data were expressed as mean ± standard error of the mean (SEM). IC_{50} values were obtained from percentage inhibitions using Microsoft Excel software (Microsoft, 2010). The student's t-test was used to assess differences in the percentage inhibitory activities and mean values of the samples using the GraphPad Prism statistical package (GraphPad Software, USA). Statistical significance was considered at $p < 0.05$. Except otherwise stated, the raw data plots for the *in-silico* evaluations were generated using the Origin data analysis software V18 (OriginLab, Northampton, MA, USA).

5.4. Results and discussion

5.4.1. Phytochemical composition

Table 5.1 and Appendix 5.1 show the results of the LC-MS profile of the infusions from fresh and dry lemongrass leaves. The chromatogram revealed the presence of 49 phytochemical compounds in all the samples tested. Corymboside, veranisatin C, chamaemeloside, neocuscutoside C, and herbarumin II had the highest peaks in the chromatogram, which suggests that they have the highest relative abundances.

5.4.2. In vitro study

One of the neurological disorders associated with aging is Alzheimer's disease, caused by a continuous deficiency in cholinergic neurotransmission, and affects about 10% of older people (Racchi *et al.* 2004). Hydrolysis of synaptic acetylcholine is important in cholinergic neurotransmission and is mediated by two enzymes – acetylcholinesterase (AChE) and butyrylcholinesterase (BChE) (Soreq and Seidman 2001). Figure 5.1 shows the percentage inhibition of neurological-related enzymes by fresh and dry infusions of lemongrass. Both fresh and dry infusions of lemongrass similarly inhibited acetylcholinesterase except at low concentration (6.25 µg/mL) where the dry infusion is higher (Fig. 5.1a). Butyrylcholinesterase was also inhibited in the same manner by the fresh and dry teas of lemongrass except at the

concentrations of 3.13 and 6.25 µg/mL (Fig. 5.1b). Table 5.2 shows that fresh and dry teas have similar IC_{50} values for both acetylcholinesterase and butyrylcholinesterase, though the standard donepezil has higher values for butyrylcholinesterase.

Table 5.1. LC-MS profiling of phytochemical compounds from fresh and dry lemongrass infusions

s/n	RT	*m/z*	Phytochemical compounds	PubChem D
1	7.302	249.06046	carboxyethylidene]-alpha-D-galactose	133960
2	7.302	249.06046	3,4-O-[(1S)-1-carboxyethylidene]-beta-D-galactose	51351726
3	9.125	203.09221	Phellodendric acid A	16088229
4	9.125	203.09221	diethyl 2-hydroxypentanedioate	13270883
5	12.012	239.05424	Eucomic acid	23757219
6	12.170	353.08673	Chlorogenic acid	1794427
7	12.170	353.08673	Scopolin	439514
8	12.271	367.09875	4-oxo-3-phenyl-4H-chromen-7-yl 3-phenylprop-2-enoate	133568962
9	12.365	517.15710	Sibiricose A5	6326020
10	12.532/15.188	367.10294	Caffeoyl-O-methylquinic acid	131752769
11	12.532/15.188	367.10294	4-O-feruloyl-D-quinic acid	10177048
12	12.828	179.03342	Caffeic acid	689043
13	12.828	179.03342	Aspirin	2244
14	13.058	417.17783	Ascleposide B	10740722
15	13.555	431.18668	Aspulvinone H	54675755
16	13.555	431.18668	Sinensol E	11796980
17	13.989	351.12982	5-[(6-ethoxy-3,4,5-trihydroxyoxan-2-yl) methoxy]-3-hydroxy-3-methyl-5-oxopentanoic acid	156602899
18	14.363	415.15979	Phenylethyl primeveroside	14704521
19	14.363	415.15979	Benzyl alcohol beta-D-rutinoside	10549806
20	14.801/15.480	579.13489	Rustoside	74977996
21	14.801/15.480	579.13489	Isocarlinoside	21576182
22	14.995	371.09760	Veranisatin C	10643000
23	14.995	371.09760	Dihydroferulic acid 4-O-glucuronide	190069
24	15.675	163.03993	2-Hydroxycinnamic acid	637540
25	15.675	163.03993	Phenylpyruvic acid	997
26	15.859/19.078	563.13928	Corymboside	13644660

27	15.859/19.078	563.13928	Isovitexin 2"-O-arabinoside	44468060
28	16.048	593.14948	Astragalin 7-rhamnoside	57390614
29	16.048	593.14948	Lonicerin	5282152
30	16.520	549.12396	Kaempferol 3,4'-dixyloside	44258938
31	16.520	549.12396	Limocitrin 7-(6"-acetylglucoside)	44260014
32	17.728	401.18091	Methyl 7-epi-12-hydroxyjasmonate glucoside	131751189
33	17.728	401.18091	Glochidionionoside A	11825585
34	18.062	399.16385	Corchoionoside B	131751110
35	18.421	447.09097	Quercitrin	5280459
36	18.421	447.09097	Trifolin	5282149
37	20.107	239.13066	(+)-7alpha,8alpha-Epoxyblumenol B	44559648
38	20.830/22.375	243.12306	Pandangolide 1a	11687387
39	20.830/22.375	243.12306	Herbarumin II	9992042
40	21.017	575.14044	Chamaemeloside	101688668
41	21.017	575.14044	Vitexin 6"-(3-hydroxy-3-methylglutarate)	44257690
42	21.630	577.15460	Kaempferitrin	5486199
43	21.630	577.15460	Vitexin 2"-O-rhamnoside	5874704
44	22.659	693.20367	Neocuscutoside C	131801689
45	22.659	693.20367	Sinocrassoside B3	NA
46	23.088	373.13046	8-Hydroxypinoresinol	3010930
47	23.088	373.13046	3',4',5,7,8-Pentamethoxyflavanone	72703226
48	23.287	269.09729	[1,1'-binaphthalen]-2-ol	136672961
49	23.287	269.09729	10-phenyl-9,10-dihydroanthracen-9-one	NA

The effective inhibition of both AChE and BChE activities, as depicted by the low IC_{50} values by both fresh and dry teas of lemongrass leaf, indicated that the infusions can diminish the undesirable inactivation of acetylcholine experienced in Alzheimer's disease (Sheeja Malar *et al.* 2017). This will, in turn, enhance the brain acetylcholine level, thereby improving the memory and cognitive deficits of the patients.

Many studies have reported the accumulation of amyloid-β in the brain as the main cause of Alzheimer's disease, and BACE-1 is a potential therapeutic target of the disease (Mazumder and Choudhury 2019; Mendes *et al.* 2023). MOA, on the other hand, serves as a therapeutic target for

the management of depression, as well as Alzheimer's and Parkinson's disease (Jalal *et al.* 2022). At all concentrations tested, the fresh lemongrass tea significantly ($p < 0.05$) inhibited β-secretase compared to the dry sample except at the lowest concentration (Fig. 5.1c). Both the fresh and dry lemongrass teas inhibited monoamine oxidase similarly at concentrations of 6.25 and 50 µg/mL but inhibition by the fresh tea was significantly higher than the dry one at other concentrations (Fig. 5.1d).

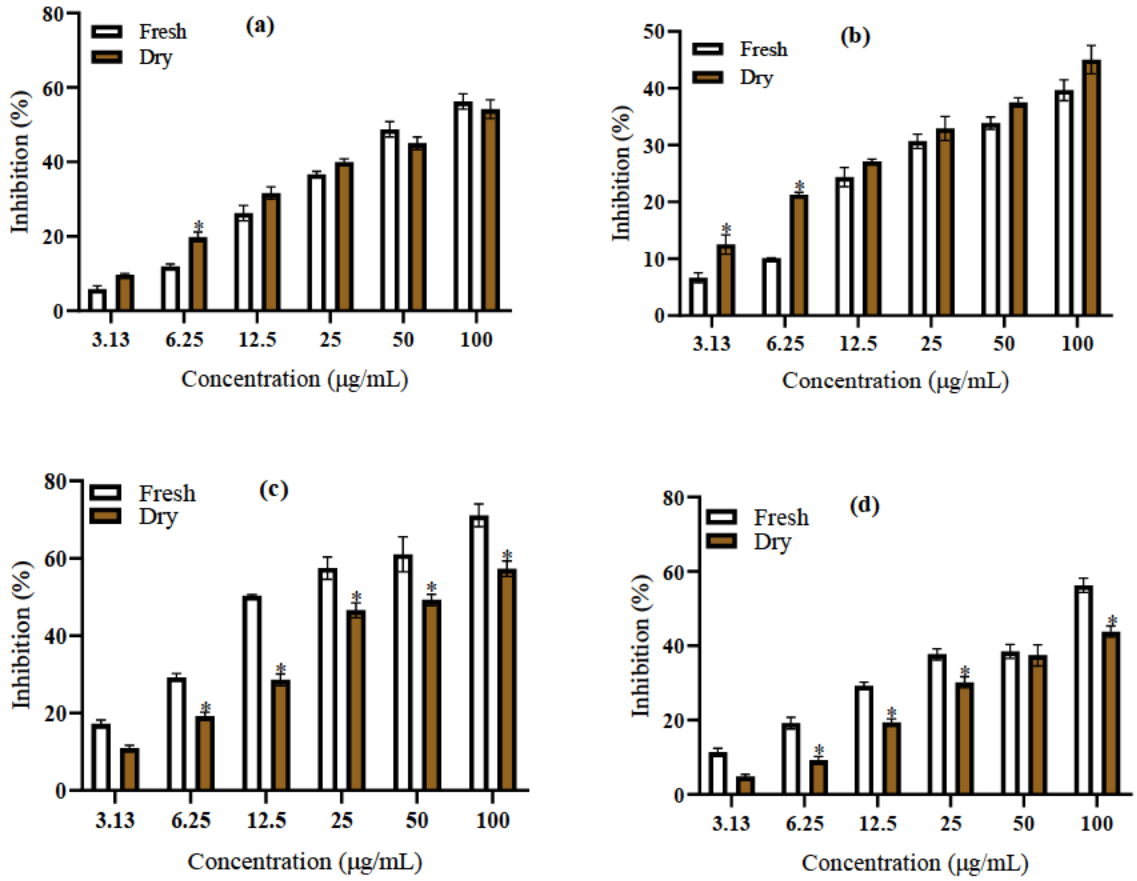

Figure 5.1. Inhibitory properties of lemongrass infusions on the activities of neurological-related enzymes (a) acetylcholinesterase and (b) butyrylcholinesterase (c) β-secretase and (d) monoamine oxidase. Values are expressed as mean ± SEM of triplicate determinations. *Values are significantly different at ($p < 0.05$).

The IC_{50} values for the inhibition of neurologically-related enzymes by the fresh and dry infusions of lemongrass are shown in Table 5.2. The fresh lemongrass tea has significantly lower IC_{50} values ($p < 0.05$) for the inhibition of β-secretase and monoamine oxidase than the dry infusion. While

the standard β-secretase inhibitor (AZD3293) has a similar IC_{50} value as the dry infusion, the standard monoamine oxidase inhibitor (tranylcypromine) has a lower IC_{50} value than both infusions. The significant inhibition of both β-secretase and monoamine oxidase by fresh lemongrass infusion may be due to the conservation of phytochemicals and nutrients, which might have been lost in the dry lemongrass due to drying (Duangupama *et al.* 2023). Previous studies revealed that drying may contribute to the loss of phytochemicals and nutrients in plants (Devi *et al*. 2019; Oliveira-Alves *et al*., 2021).

Table 5.2. IC_{50} values for the inhibitory activities of neurological-related enzymes by fresh and dry lemongrass teas

Samples	IC_{50} values			
	AChE	BChE	β-secretase	MAO
Fresh infusion	72.62 ± 3.53^{a}	119.70 ± 4.42^{a}	38.24 ± 4.21^{a}	78.62 ± 2.33^{a}
Dry infusion	76.27 ± 5.47^{a}	107.20 ± 7.14^{a}	67.50 ± 2.76^{b}	102.50 ± 6.74^{b}
Donepezil	71.66 ± 2.18^{a}	76.51 ± 2.05^{b}	ND	ND
AZD3293	ND	ND	56.47 ± 0.94^{b}	ND
Tranylcypromine	ND	ND	ND	65.55 ± 2.64^{c}

The values are expressed as means ± SEM of triplicate determinations. Means down vertical columns not sharing a common letter are significantly different ($P < 0.05$) from each other.
AChE: Acetylcholinesterase, BChE: Butyrylcholinesterase, MAO: Monoamine oxidase, ND: Not deterrmined.

5.4.3. Molecular docking

To determine the probable interactions between the phenolic compounds found in lemongrass and target enzymes evaluated in the *in vitro* study, computational analysis was performed using molecular docking and molecular dynamic simulation. Appendix 5.2 contains the docking scores of all 49 compounds and standards against acetylcholinesterase, butyrylcholinesterase, β-secretase and monoamine oxidase, as revealed by the LC-MS. The docking scores of the top five compounds of lemongrass tea and standard drugs against selected targets of neurodegeneration are presented

in Table 5.3. While both aspulvinone H and 4-oxo-3-phenyl-4H-chromen-7-yl 3-phenylprop-2-enoate (OPCPPE) had the lowest docking scores of -10.6 kcal/mol for AChE, [1,1'-binaphthalen]-2-ol has the lowest docking score of -12.1 kcal/mol for BChE. Neocuscutoside C and aspulvinone H exhibited the lowest docking scores of -10.5 and -11.9 kcal/mol for β-secretase and monoamine oxidase, respectively. All the standard drugs tested had higher docking scores than the profiled compounds. Molecular docking is a tool that predicts the mode of interaction of chemical compounds with the active sites of the enzymes (Wu *et al.* 2022). The lowest docking scores of OPCPPE (and aspulvinone H), [1,1'-binaphthalen]-2-ol, neocuscutoside C and chlorogenic acid for AChE, BChE, BACE-1 and MAO respectively, indicated that they have better affinities for these enzymes than other compounds and standards (Kim *et al.* 2018; Jalal *et al.* 2022). This is because the lower the docking score of a compound, the better the pose and affinity towards the enzyme. The outcome of the docking validation exercise is presented in Appendix 5.3, and the superimposition demonstrated that the top-hit compounds, the reference standards, and the docked native inhibitors in each case had relative binding orientation at the receptor binding domains of each target with RMSD values of 0.5 Å. These findings supported the validity of the docking scores obtained in the study.

Table 5.3. Docking scores of the top five compounds of lemongrass infusions and standards against enzymes implicated in neurodegeneration

Targets	Compound/Standard	PubChem ID	Docking score (kCal/mol)
Acetylcholinesterase	4-oxo-3-phenyl-4H-chromen-7-yl 3-phenylprop-2-enoate	133568962	**-10.6**
	Aspulvinone H	54675755	**-10.6**
	Astragalin 7-rhamnoside	57390614	-9.4
	Benzyl alcohol beta-D-rutinoside	10549806	-9.9
	Chamaemeloside	101688668	-10.0
	Donepezil*	3152	-9.7
Butyrylcholinesterase	[1,1'-binaphthalen]-2-ol	136672961	**-12.1**
	Isocarlinoside	21576182	-10.1
	Kaempferitrin	5486199	-10.5
	Lonicerin	5282152	-11.0
	Vitexin 6''-(3-hydroxy-3-methylglutarate)	44257690	-10.3
	Donepezil*	3152	-9.5
Beta-secretase	Neocuscutoside C	131801689	**-10.5**
	Lonicerin	5282152	-9.5
	Aspulvinone H	54675755	-9.2
	Isocarlinoside	21576182	-9.5
	Vitexin 6"-(3-hydroxy-3-methylglutarate)	44257690	-9.4
	AZD3293*	67979346	-8.8
Monoamine oxidase	Chlorogenic acid	1794427	-9.8
	Benzyl alcohol beta-D-rutinoside	10549806	-9.4
	Aspulvinone H	54675755	**-11.9**
	Phenylethyl primeveroside	14704521	-10.1
	4-O-feruloyl-D-quinic acid	10177048	-9.7
	Tranylcypromine*	19493	-6.5

*Reference standards

5.4.4. Molecular dynamics simulation

Since docking indicates the preliminary interaction of a ligand to the active site of a receptor, the behaviour of the compounds was subjected to binding energy calculations using molecular dynamics (MD) simulation. Table 5.4 shows the results of the thermodynamic profiles of the top compounds of lemongrass tea against each of the target enzymes. As for BACE-1 and MOA, the top five compounds had lower free binding energies (-72.28 to -31.42 kcal/mol) than the reference standards, AZD3293 (-23.56 kcal/mol) and tranylcypromine (-20.19 kcal/mol). This conforms with the docking scores obtained which implies that these compounds have stronger affinities for these enzymes and form more stable complexes (Moorkoth *et al.* 2021; Balogun *et al.* 2022). While four of the selected compounds displayed lower free binding energies (-46.10 to 66.59 kcal/mol) for acetylcholinesterase than the standard, donepezil (-40.17 kcal/mol), 4-oxo-3-phenyl-4H-chromen-7-yl 3-phenylprop-2-enoate (OPCPPE) had a higher free binding energy of -37.29 kcal/mol. Of the top five compounds, the duo of [1,1'-binaphthalen]-2-ol and Vitexin-6''-(3-hydroxyl-3-methylglutarate) possessed higher binding free energies of -29.85 and -40.89 kcal/mol, respectively, for BChE than the reference standard, donepezil (-45.82 kcal/mol). However, benzyl alcohol beta-D-rutinoside, isocarlinoside, neocuscutoside C, and aspulvinone H have the lowest binding energies for AChE, BChE, BACE-1 and MAO, respectively. This suggests that these compounds have the best affinity for the enzymes and are the best inhibitors of the targets (Sheeja Malar *et al.* 2017; Haider *et al.* 2021).

Table 5. 4. Energy component profiles of the top five compounds of lemongrass teas and standards against enzymes implicated in neurodegeneration

Complex	ΔEvdW	ΔEelec	ΔGgas	ΔGsolv	ΔEsur	ΔGbind
Acetylcholinesterase						
OPCPPE*	-51.36 ± 3.02	-4.68 ± 3.45	-56.05 ± 4.21	18.75 ± 2.35	-6.39 ± 0.36	-37.29 ± 3.35
Aspulvinone H	-53.5 ± 4.68	-26.15 ± 9.91	-79.67 ± 11.62	33.56 ± 5.39	-6.79 ± 0.35	-46.10 ± 7.70
Astragalin-7-rhamnoside	-57.94 ± 5.33	-44.86 ± 15.74	-102.79 ± 14.07	54.79 ± 9.56	-7.05 ± 0.36	-47.99 ± 6.34
Benzyl alcohol beta-D-rutinoside	-49.85 ± 5.49	-58.18 ± 12.51	-108.03 ± 12.16	55.29 ± 5.68	-7.08 ± 0.43	-52.75 ± 8.79
Chamaemeloside	-65.64 ± 4.95	-64.69 ± 11.89	-130.33 ± 9.64	63.74 ± 6.17	-8.81 ± 0.31	-66.59 ± 5.33
Donepezil	-51.10 ± 3.24	-249.54 ± 10.21	-300.66 ± 11.08	260.51 ± 10.72	-6.21 ± 0.30	-40.15 ± 3.63
Butyrylcholinesterase						
[1,1'-binaphthalen]-2-ol	-52.57 ± 4.40	-271.06 ± 17.79	-323.63 ± 19.72	293.78 ± 17.80	-6.53 ± 0.42	-29.85 ± 3.89
Isocarlinoside	-45.75 ± 7.19	-80.46 ± 20.01	-126.21 ± 16.71	60.42 ± 10.37	-6.50 ± 0.49	-65.79 ± 8.36
Kaempferitrin	-53.59 ± 5.23	-78.06 ± 11.76	-131.65 ± 10.79	68.16 ± 7.83	-7.69 ± 0.35	-63.49 ± 6.70
Lonicerin	-56.47 ± 4.94	-44.79 ± 10.49	-101.26 ± 9.42	47.45 ± 5.43	-7.36 ± 0.35	-53.80 ± 6.44
Vitexin-6''-(3-hydroxyl-3-methylglutarate)	-52.31 ± 5.79	-43.45 ± 15.36	-95.76 ± 16.82	54.87 ± 11.97	-6.58 ± 0.61	-40.89 ± 8.06
Donepezil	-51.98 ± 3.89	-131.1 ± 8.82	-183.10 ± 10.58	137.28 ± 8.55	-6.37 ± 0.36	-45.82 ± 5.64
Beta-secretase						
Neocuscutoside C	-56.40 ± 5.68	-42.65 ± 9.08	-99.05 ± 11.43	57.96 ± 7.13	-7.11 ± 0.64	-41.09 ± 6.36
Lonicerin	-46.15 ± 7.91	-33.01 ± 23.65	-79.16 ± 29.63	47.74 ± 16.12	-6.05 ± 1.08	-31.42 ± 14.75
Aspulvinone H	-44.12 ± 3.80	-38.44 ± 5.21	-82.56 ± 6.76	43.86 ± 3.96	-5.84 ± 0.47	-38.69 ± 4.37
Isocarlinoside	-46.54 ± 7.35	-54.88 ± 13.13	-101.42 ± 14.36	66.78 ± 7.50	-6.27 ± 1.12	-34.65 ± 9.56
Vitexin 6"-(3-hydroxy-3-methylglutarate)	-47.07 ± 4.66	-49.75 ± 16.82	-96.82 ± 17.60	57.64 ± 10.22	-6.77 ± 0.56	-39.18 ± 9.74

AZD3293	-34.16 ± 7.29	-173.71 ± 22.58	-207.85 ± 26.21	184.28 ± 20.97	-4.43 ± 0.86	-23.56 ± 7.36
Monoamine oxidase						
Chlorogenic acid	-55.10 ± 3.15	-38.49 ± 12.69	-93.60 ± 11.92	47.36 ± 6.72	-6.78 ± 0.13	-46.24 ± 7.26
Benzyl alcohol beta-D-rutinoside	-58.10 ± 3.85	-75.26 ± 13.08	-133.36 ± 12.90	62.80 ± 6.84	-7.67 ± 0.21	-70.56 ± 8.23
Aspulvinone H	-71.87 ± 3.39	-42.70 ± 5.75	-114.58 ± 5.30	42.29 ± 3.56	-8.59 ± 0.17	-72.28 ± 4.11
Phenylethyl primeveroside	-47.29 ± 3.18	-29.29 ± 8.76	-76.58 ± 10.06	32.26 ± 6.92	-6.18 ± 0.31	-44.32 ± 4.53
4-O-feruloyl-D-quinic acid	-57.14 ± 3.68	-45.72 ± 9.13	-102.85 ± 8.24	50.99 ± 5.09	-7.24 ± 0.18	-51.86 ± 5.73
Tranylcypromine	-19.33 ± 2.31	-73.51 ± 10.84	-92.84 ± 10.78	72.64 ± 9.68	-3.14 ± 0.11	-20.19 ± 2.86

*4-oxo-3-phenyl-4H-chromen-7-yl 3-phenylprop-2-enoate

ΔEvdW: Van der Waals energy, ΔEelec: Electrostatic energy, ΔGgas: Gas-phase free energy, ΔGsolv: Solvation free energy, ΔGbind: Total binding free energy

5.4.5. Post-molecular dynamics simulation

Enzyme-ligand complex is prone to conformational changes caused by the binding ligand, and this may modify the biological activity of the enzyme. This necessitated further evaluation of the stability, flexibility, and compactness of the resulting complex through post-MD simulation analysis. The results of the post-MD simulation of the interaction of the top five compounds with selected enzymes are shown in Table 5.5 and Figures 5.2 – 5.5.

5.4.5.1. Root mean square deviation (RMSD)

In the AChE complex, there was an initial convergence in the RMSD up to 20 ns after which they diverged throughout the simulation period (Figure 5.2a). The unbound AChE has a higher average RMSD value (1.65 Å) than the complexes except for aspulvinone H and donepezil. The system converged up to around 30 ns and 45 ns after which the unbound BChE, donepezil, and [1,1'-binaphthalen]-2-ol complexes diverged (Figure 5.2b). The mean RMSD value of the unbound BChE (2.40 Å) is higher than all the complexes while [1,1'-binaphthalen]-2-ol has the same RMSD value (1.59 Å) as donepezil. As for the BACE-1, convergence was achieved up to around 20 ns and 40 ns after which the aspulvinone H complex diverged throughout the simulation period (Figure 5.2c). The unbound BACE-1 has a lower RMSD value (1.49 Å) than all the complexes. The MOA system witnessed continuous divergence among all the complexes throughout the simulation period (Figure 5.2d). While all other complexes have higher RMSD values than the unbound MOA (3.89 Å), benzyl alcohol beta-D-rutinoside and 4-O-feruloyl-D-quinic acid had a lower RMSD value of 3.83 and 3.23 Å, respectively. The RMSD value depicts the stability of the protein-ligand complex and a low RMSD value signifies higher stability of the complex (Mendes *et al.* 2023). The fact that all the resulting complexes from BChE and AChE (except aspulvinone and donepezil) had lower RMSD indicated that the ligand complexes are more stable than the free enzymes (Murali *et al.* 2023). Conversely, the unbound β-secretase is more stable than all the ligand-complexes because it has the lowest RMSD value compared to the complexes (Jalal *et al.* 2022). However, the OPCPPE, kaempferitrin, and 4-O-feruloyl-D-quinic acid possessed the lowest RMSD values for acetylcholinesterase, butyrylcholinesterase and monoamine oxidase-bound complexes respectively, it implies they formed the most stable complexes with their respective enzymes (Othman *et al.* 2022; Gholami, Minai-Tehrani and Eriksson 2023).

Table 5.5. Post-molecular dynamics simulation of the interaction of top five compounds of lemongrass teas with enzymes implicated in neurodegeneration

	RMSD (Å)	RMSF(Å)	ROG (Å)	SASA (Å)	No of H-bonds	Distance of H bonds(Å)	Angle (°) of H-bonds
Acetylcholinesterase							
Unbound	1.65 ± 0.25	1.03 ± 0.58	22.92 ± 0.07	21663.24 ± 369.16	250.72 ± 10.85	2.86 ± 0.06	151.66 ± 7.53
OPCPPE*	1.24 ± 0.26	0.95 ± 0.48	22.86 ± 0.05	21217.75 ± 334.07	253.07 ± 10.59	2.86 ± 0.06	151.44 ± 7.62
Aspulvinone H	1.84 ± 0.20	1.08 ± 0.60	22.94 ± 0.07	21539.44 ± 462.15	252.83 ± 10.38	2.86 ± 0.06	151.67 ± 7.62
Astragalin-7-rhamnoside	1.44 ± 0.14	0.98 ± 0.49	22.99 ± 0.06	21560.89 ± 413.64	251.99 ± 10.56	2.86 ± 0.06	151.49 ± 7.71
Benzyl alcohol beta-D-rutinoside	1.49 ± 0.13	1.02 ± 0.56	22.88 ± 0.07	21226.43 ± 391.75	251.86 ± 10.23	2.86 ± 0.06	151.47 ± 7.62
Chamaemeloside	1.32 ± 0.18	1.02 ± 0.58	22.85 ± 0.06	21033.03 ± 342.62	256.47 ± 10.22	2.86 ± 0.06	151.57 ± 7.65
Donepezil	1.84 ± 0.10	0.99 ± 0.54	22.89 ± 0.06	21385.68 ± 354.78	255.04 ± 10.10	2.86 ± 0.06	151.49 ± 7.69
Butyrylcholinesterase							
Unbound	2.40 ± 0.49	1.33 ± 1.05	23.31 ± 0.12	21271.65 ± 502.71	249.38 ± 10.85	2.86 ± 0.06	152.14 ± 7.56
[1,1'-binaphthalen]-2-ol	1.59 ± 0.23	1.13 ± 0.68	23.11 ± 0.08	20315.76 ± 475.35	252.98 ± 11.15	2.86 ± 0.06	151.87 ± 7.61
Isocarlinoside	1.68 ± 017	1.12 ± 0.61	23.17 ± 0.07	20489.09 ± 415.42	265.27 ± 11.16	2.86 ± 0.06	151.88 ± 7.68
Kaempferitrin	1.45 ± 0.12	1.04 ± 0.55	23.02 ± 0.06	19912.06 ± 336.48	263.86 ± 10.47	2.86 ± 0.06	151.69 ± 7.69
Lonicerin	1.99 ± 0.30	1.12 ± 0.82	23.15 ± 0.07	20297.06 ± 415.39	258.73 ± 10.26	2.86 ± 0.06	151.92 ± 7.66
Vitexin-6''-(3-hydroxyl-3-methylglutarate)	2.14 ± 0.43	1.28 ± 0.76	23.23 ± 0.12	20852.46 ± 523.60	259.96 ± 10.46	2.86 ± 0.06	152.13 ± 7.59
Donepezil	1.59 ± 0.12	1.07 ± 0.57	23.16 ± 0.07	20514.45 ± 426.25	254.16 ± 10.33	2.86 ± 0.06	151.87 ± 7.57
Beta-secretase							
Unbound	1.49 ± 0.17	1.15 ± 0.64	21.17 ± 0.09	16437.93 ± 341.26	184.46 ± 8.67	2.85 ± 0.06	151.89 ± 7.71
Neocuscutoside C	2.00 ± 0.29	1.21 ± 0.58	21.44 ± 0.14	16503.24 ± 295.76	185.18 ± 8.76	2.85 ± 0.06	151.89 ± 7.58
Lonicerin	1.83 ± 0.28	1.23 ± 0.65	21.50 ± 0.13	16940.72 ± 402.13	186.16 ± 8.80	2.85 ± 0.06	152.02 ± 7.66

Aspulvinone H	2.49 ± 0.41	1.15 ± 0.65	21.44 ± 0.09	16677.27 ± 295.09	189.25 ± 9.13	2.85 ± 0.06	152.12 ± 7.58
Isocarlinoside	1.79 ± 0.29	1.16 ± 0.57	20.99 ± 0.12	16036.45 ± 329.44	193.06 ± 8.97	2.85 ± 0.06	151.92 ± 7.61
Vitexin 6"-(3-hydroxy-3-methylglutarate)	1.86 ± 0.29	1.43 ± 0.65	21.27 ± 0.31	16539.11 ± 425.75	189.17 ± 8.94	2.85 ± 0.06	152.17 ± 7.68
AZD3293	1.99 ± 0.21	1.16 ± 0.62	21.12 ± 0.14	16300.84 ± 313.36	192.07 ± 8.59	2.85 ± 0.06	151.92 ± 7.60
Monoamine oxidase							
Unbound	3.89 ± 1.42	1.89 ± 2.09	24.69 ± 0.51	21648.36 ± 516.29	254.63 ± 10.55	2.85 ± 0.06	152.03 ± 7.17
Chlorogenic acid	3.96 ± 0.65	1.56 ± 1.41	24.44 ± 0.27	21167.02 ± 445.95	254.36 ± 10.49	2.85 ± 0.06	152.01 ± 7.17
Benzyl alcohol beta-D-rutinoside	3.83 ± 0.74	1.45 ± 1.40	24.69 ± 0.21	21584.19 ± 454.64	253.02 ± 10.62	2.85 ± 0.06	151.82 ± 7.39
Aspulvinone H	4.29 ± 0.94	1.46 ± 1.46	24.22 ± 0.34	20647.14 ± 413.91	257.59 ± 10.77	2.86 ± 0.06	151.89 ± 7.30
Phenylethyl primeveroside	4.67 ± 1.06	1.82 ± 2.05	25.02 ± 0.40	21518.15 ± 470.35	252.45 ± 10.66	2.86 ± 0.06	151.89 ± 7.29
4-O-feruloyl-D-quinic acid	3.23 ± 0.70	1.51 ± 1.34	24.94 ± 0.28	21275.25 ± 391.14	252.09 ± 11.45	2.85 ± 0.06	151.89 ± 7.32
Tranylcypromine	4.98 ± 1.85	2.21 ± 2.68	24.48 ± 0.56	21602.32 ± 531.63	251.79 ± 11.81	2.86 ± 0.06	152.03 ± 7.15

*4-oxo-3-phenyl-4H-chromen-7-yl 3-phenylprop-2-enoate

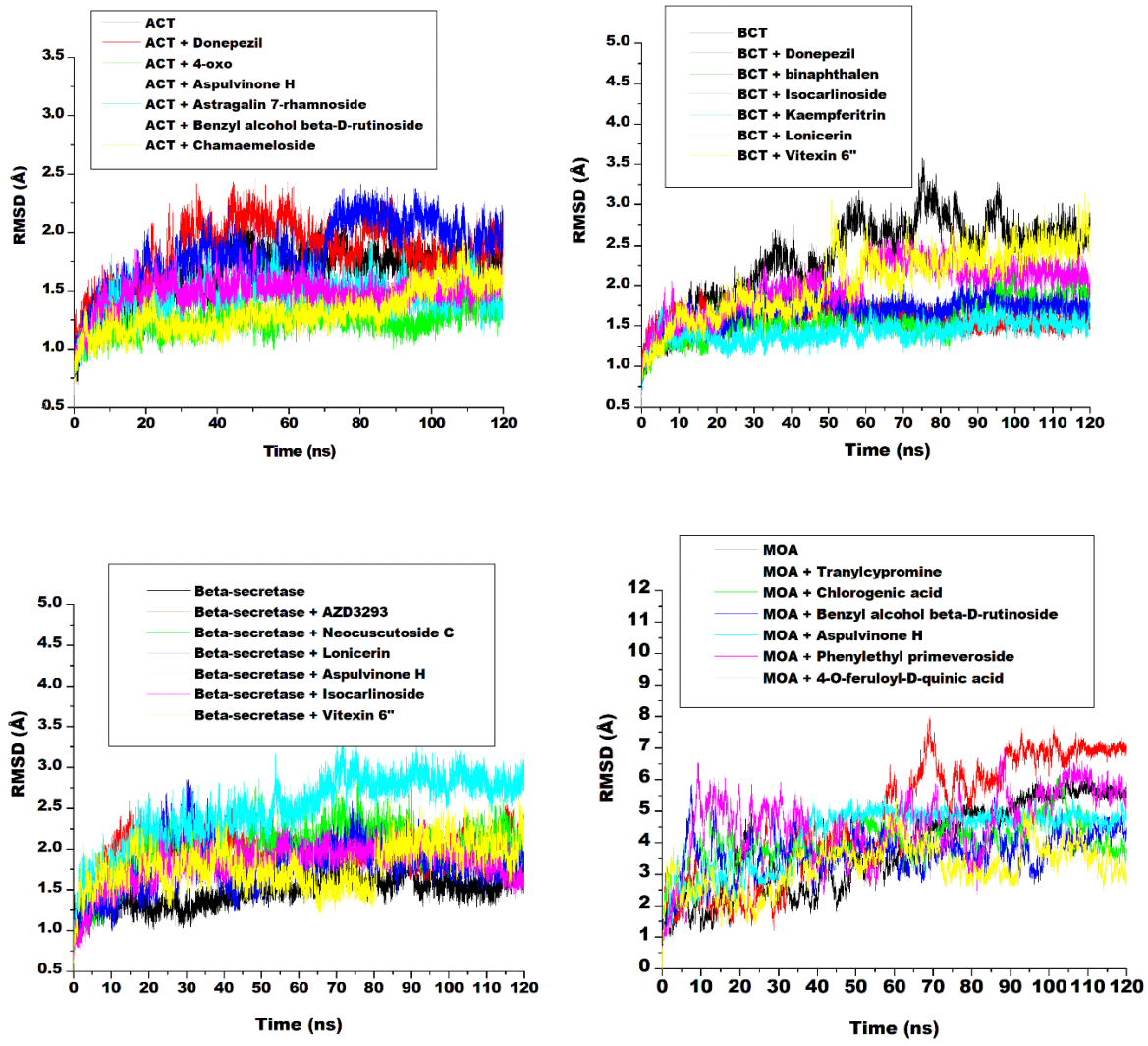

Figure 5.2. Comparative plots of alpha-carbon of (a) acetylcholinesterase (b) butyrylcholinesterase (c) beta-secretase and (d) monoamine oxidase and top five compounds in lemongrass teas presented as root mean square deviation (RMSD) over 120 ns molecular dynamic simulation.

5.4.5.2. Root mean square fluctuation (RMSF)

The root mean square fluctuation (RMSF) measures the effect of a binding compound on the active site of an enzyme, thereby providing information on the flexibility of the protein-ligand complex (Cancela *et al.* 2020), and is determined by the extent of fluctuations in the system. There were fluctuations in the AChE system especially at the 75, 250, 375 and 500 amino acid residues (Figure 5.3a). The RMSF value of the unbound AChE (1.03 Å) is higher than all the complexes except aspulvinone H (1.08 Å). The fluctuations among the BChE system followed a similar pattern and occurred mostly at 75, 275, and 375 amino acid residues (Figure 5.3b). The unbound BChE displayed the highest RMSF value (1.33 Å) than other complexes suggesting that the the complexes are more flexible and have better stability (Gupta *et al.* 2020). Both donepezil-acetylcholinesterase and donepezil-butyrylcholinesterase complexes had lower RMSF values compared to unbound enzymes, which indicates lower fluctuation and better flexibility of the complexes (Gyebi *et al.* 2023). Consistent fluctuations were observed throughout the β-secretase systems and are prominent at 60, 90, 270, and 300 amino acid residues (Figure 5.3c). Neocuscutoside C, lonicerin, and vitexin 6"-(3-hydroxy-3-methylglutarate) displayed higher RMSF values than the unbound β-secretase and AZD3293-β-secretase complex (1.15 Å), implying that AZD3293 may be more flexible and stable than some tested metabolites (Othman *et al.* 2022). The MOA system witnessed fewer fluctuations in the amino acid residues which occurred around 250 and 475 residues (Figure 5.3d). The unbound MOA has a higher RMSF value (3.89 Å) than other complexes, except tranylcypromine, which suggests that all the metabolite-monoamine oxidase complexes displayed lesser fluctuations and improved stability of the complexes (Cancela *et al.* 2020).

5.4.5.3. Radius of gyration (ROG)

The radius of gyration (ROG) measures the compactness of the resulting complex from the interaction of the ligand and enzymes, the lower the ROG value the better the compactness of the complex (Aribisala *et al.* 2022). Figure 5.4a revealed that there is a convergence of all the complexes in the AChE system throughout the simulation period. The unbound AChE as well as aspulvinone H and astragalin-7-rhamnoside complexes possessed higher radius of gyration (ROG) values than other complexes, which signifies that they are less compact and stable than other complexes (Kundu and Dubey 2021). Though there is a convergence in the ROG plot among the

complexes up to 50 ns, they diverged afterwards to the end of the simulation period (Figure 5.4b). The ROG value of the unbound butyrylcholinesterase (1.33 Å) is higher than all the complexes, which may imply that binding of the metabolites to the enzymes improved the compactness of the resulting complex. There is a similar pattern in the convergence in the ROG plot of the β-secretase and its complexes (Figure 5.4c). The unbound β-secretase has a lower ROG value (21.17 Å) than other complexes except for isocarlinoside (20.99 Å) and AZD3293 (21.12 Å), which suggests that isocarlinoside- β-secretase complex is the most compact and is better than the standard drug, AZD3293 (Gyebi *et al.* 2023). Throughout the simulation period, there is a consistent divergence in the ROG plot of the MOA and its complexes (Figure 5.4d). The ROG value of the unbound monoamine oxidase (24.69 Å) is the same as that of benzyl alcohol beta-D-rutinoside, and is higher than other complexes except phenylethyl primeveroside (25.02 Å) and 4-O-feruloyl-D-quinic acid (24.94 Å). This shows that the binding of benzyl alcohol beta-D-rutinoside to the monoamine oxidase does not affect the compactness of the unbound enzyme (Balogun *et al.* 2022). However, the binding of aspulvinone H to the MAO caused the best reduction in the ROG values compared to other complexes thereby eliciting more compactness and stability of the complex.

5.4.5.4. Solvent accessibility surface area (SASA)

The solvent accessibility surface area (SASA) value assesses the behaviour of the amino acid residues of the enzymes when exposed to solvents (Gyebi *et al.* 2023). When the SASA value is low, it indicates low surface area and better stability. There are consistent fluctuations in the SASA plot of all the investigated enzymes (Figures 5.5a-e). The SASA values for the unbound acetylcholinesterase (21663.24 Å), butyrylcholinesterase (21271.65 Å), and monoamine oxidase (21648.36 Å) are higher than all other complexes. This suggests that all the resulting complexes from these interactions are more stable than the unbound enzymes (Gholami, Minai-Tehrani and Eriksson 2023). As for β-secretase, the SASA value of the unbound form (16437.93 Å) is only higher than that of isocarlinoside complex (16036.45 Å) and the standard drug, AZD3293 (16300.84 Å), while other complexes have higher SASA values. This indicated that isocarlinoside has the lowest surface area and is more stable than all other complexes (Sabiu, Balogun and Amoo 2021). Chamamaeloside (21033.03 Å), kaempferitrin (19912.06 Å), isocarlinoside (16036.45 Å), and aspulvinone H (20647.14 Å) exhibited lowest SASA values for acetylcholinesterase, butyrylcholinesterase, β-secretase, and monoamine oxidase respectively. This signifies that these

complexes are the most stable and are more stable than the complexes resulting from all the standard drugs.

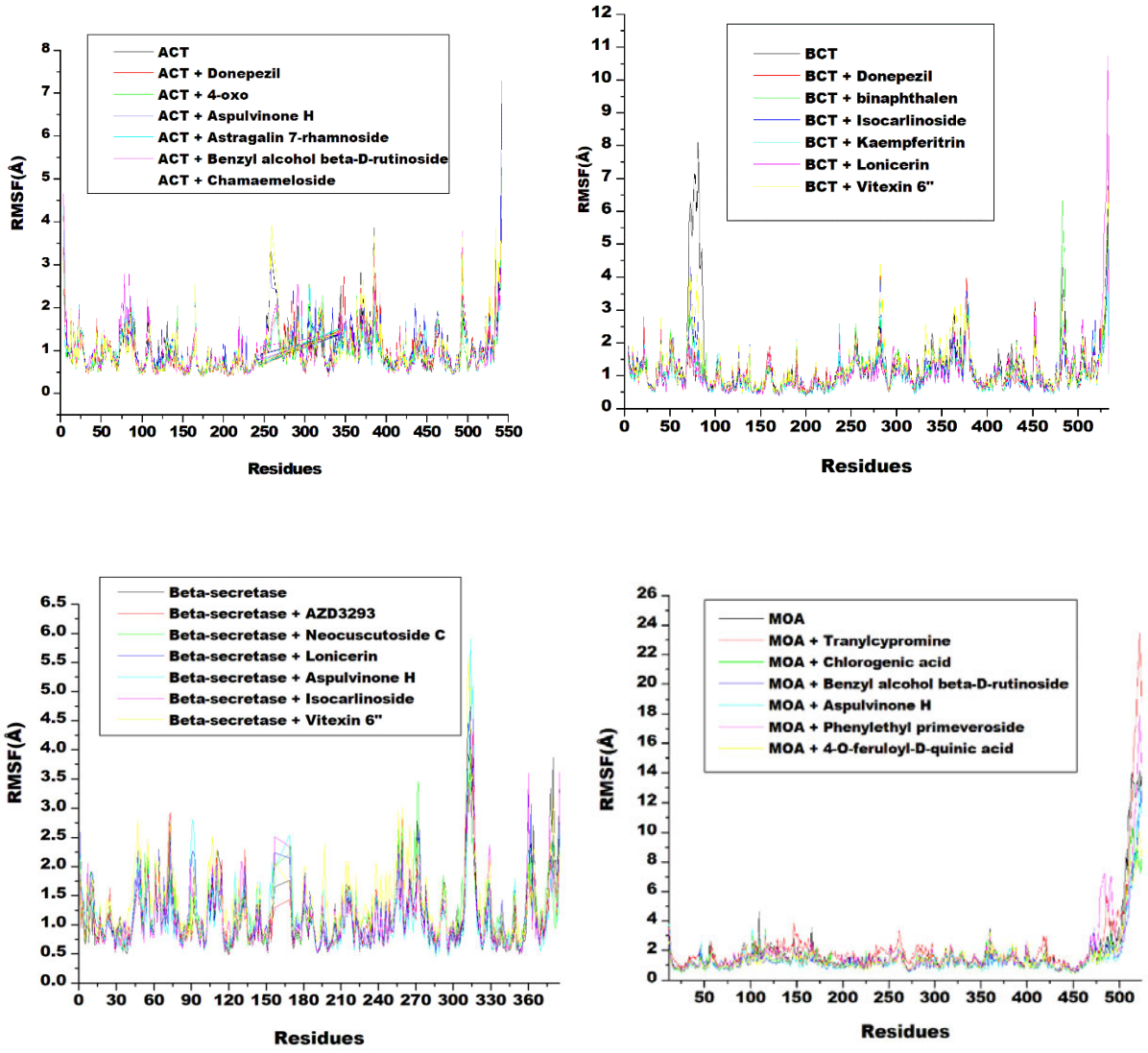

Figure 5.3. Comparative plots of alpha-carbon of (a) acetylcholinesterase (b) butyrylcholinesterase (c) beta-secretase and (d) monoamine oxidase and top five compounds in lemongrass teas presented as root mean square fluctuations (RMSF) over 120 ns molecular dynamic simulation.

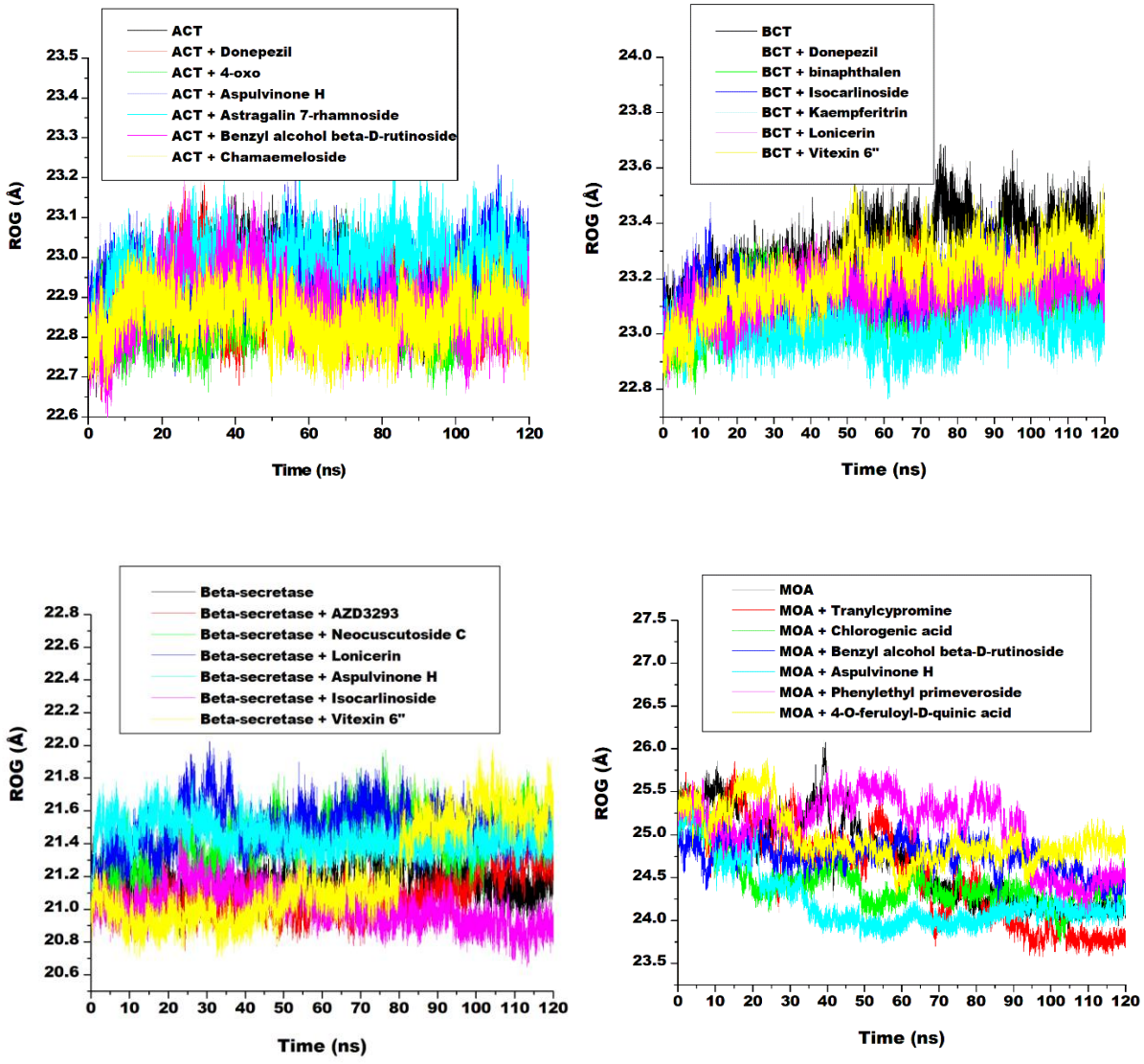

Figure 5.4. Comparative plots of alpha-carbon of (a) acetylcholinesterase (b) butyrylcholinesterase (c) beta-secretase and (d) monoamine oxidase and top five compounds in lemongrass teas presented as radius of gyration (ROG) over 120 ns molecular dynamic simulation.

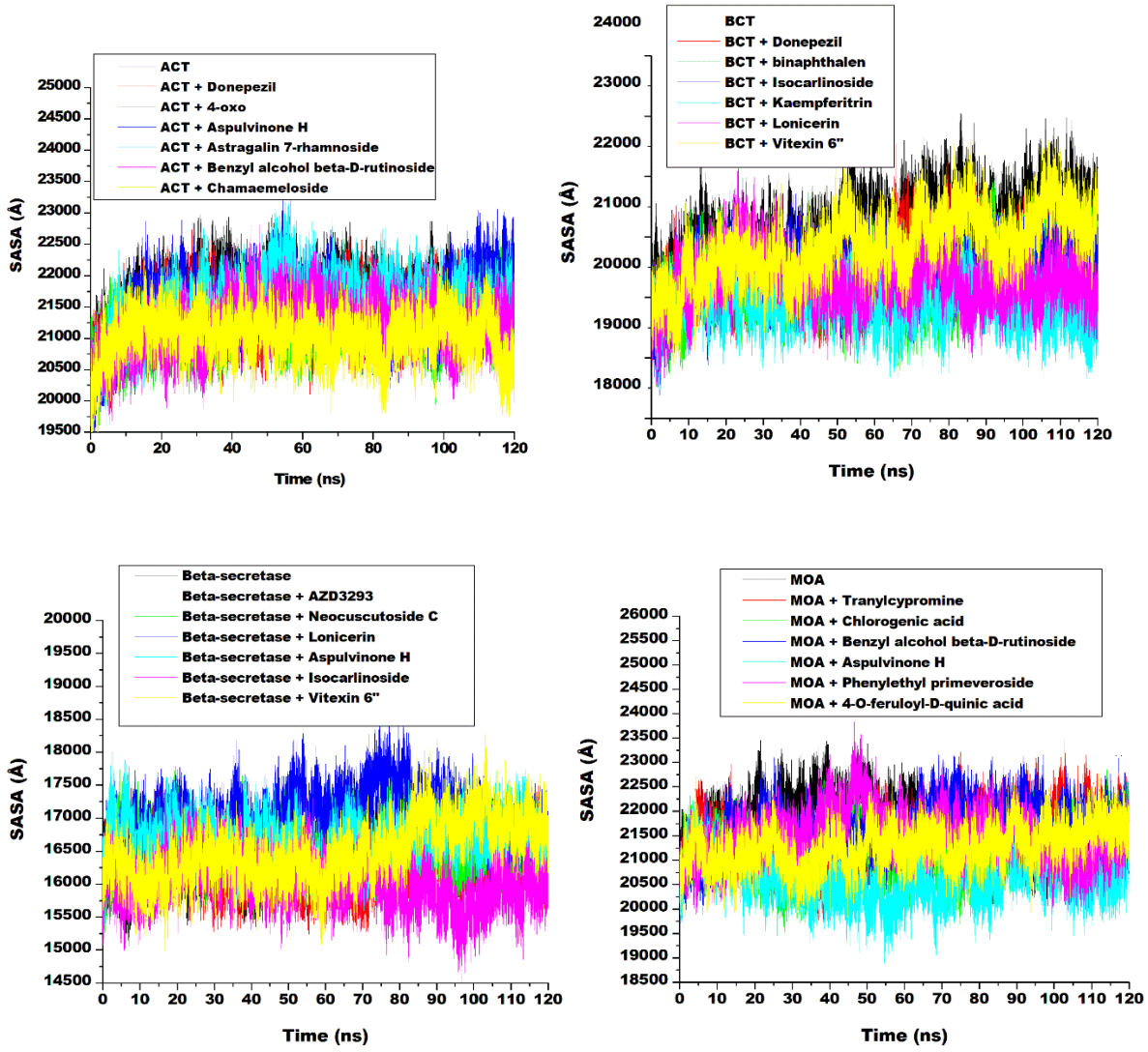

Figure 5.5. Comparative plots of alpha-carbon of (a) acetylcholinesterase (b) butyrylcholinesterase (c) beta-secretase and (d) monoamine oxidase and top five compounds in lemongrass teas presented as solvent accessibility surface area (SASA) over 120 ns molecular dynamic simulation.

5.4.5.5. Number, distance and angle of hydrogen bonds

Across all the enzymes that interacted with the ligands, the unbound enzymes exhibited the lowest number of hydrogen bonds because they are free enzymes (Table 4.4). Isovitexin 2"-O-arabinoside had the highest number of hydrogen bonds (70.54) when it interacted with collagenase, which is higher than the standard, oleanolic acid (66.52). Rustoside-elastase complex possessed the highest number of hydrogen bonds (97.88) compared to other complexes and is also higher than oleanolic acid (93.36). As for hyaluronidase, the complex formed from lonicerin exhibited the highest number of hydrogen bonds (200.08), while isovitexin 2"-O-arabinoside-tyrosinase complex displayed the highest number of hydrogen bonds (228.19). Notably, the complex tyrosinase formed with the standard ascorbic acid had a similar number of hydrogen bonds (228.16) with the isovitexin 2"-O-arabinoside-tyrosinase complex. However, the distance and angles of the hydrogen bonds of all the enzyme-ligand complexes were identical.

5.4.6. Forms and nature of interactions

The form and number of interactions between the enzymes and the ligands provide information on their compatibility and affect the binding energy of the resulting complex (Kundu and Dubey 2021). Figure 5.6 shows the interaction plots of the topmost lemongrass metabolite (benzyl alcohol beta-D-rutinoside) and standard drug (donepezil) with acetylcholinesterase before and after a 120 ns molecular dynamics simulation. Out of the top five compounds that formed complexes with acetylcholinesterase, benzyl alcohol beta-D-rutinoside has the highest number of interactions, comprising six hydrogen bonds (Trp83, Gly119, Ser122, Glu199, Ser200, and Tyr329), fifteen Van der Waals forces, and four other interactions (Val70, Pro85, Arg288, and Tyr333). Ten of these interactions were consistent before and after the simulation (Fig. 5.6A1 and 5.6A2). This is better than observation with the donepezil, which has 20 interactions comprising two hydrogen bonds (Ser122 and Tyr333), fourteen Van der Waals forces, and four other interactions (Val70, Asp71, Hie276, and Trp278), out of which only five were consistent (Fig. 5.6B1 and 5.6B2). This may be due to the low binding energy of the complex and a higher number of hydrogen bonds, which implies that benzyl alcohol beta-D-rutinoside has a better affinity for acetylcholinesterase than donepezil, and the resulting complex is also more stable.

All the top five compounds that interacted with butyrylcholinesterase had a higher number of interactions (19 – 26 bonds) than the standard drug, donepezil, with 18 interactions. Figure 5.7 shows the interaction plots of the topmost compound (kaempferitrin) with butyrylcholinesterase before and after molecular dynamic simulation. Kaempferitrin has twenty-six interactions with butyrylcholinesterase compared to the eighteen interactions donepezil (standard) has with the protein. Kaempferitrin has five hydrogen bonds (Gly114, Glu194, Ala196, Glu273 and Hie435), seventeen Van der Waal's forces and four others (Trp79, Val277, Pro282 and Tyr437) while donepezil has four hydrogen bonds (Gly113, Thr117, Ala325 and Hie435), ten Van der Waal's forces and four other interactions (Phe326, Tyr329, Trp427 and Met431). Thirteen of the interactions of the kaempferitrin-butyrylcholinesterase complex were stable throughout the simulation period (Fig. 5.7A1 and 5.7A2). Since the number of hydrogen bonds in a complex contributes to its stability and conformation, this study revealed kaempferitrin-butyrylcholinesterase complex is more stable than the donepezil-butyrylcholinesterase complex (Gyebi *et al.* 2023). This also conforms with the lower binding energy of the kaempferitrin complex.

The interaction of the topmost compound (neocuscutoside C) with β-secretase before and after a 120 ns molecular dynamics simulation is shown in Figure 5.8. Though all the compounds have a higher number of interactions with the protein than the standard drug (AZD3293), neocuscutoside has the highest number of interactions. Neocuscutoside C has twenty interactions with β-secretase comprising six hydrogen bonds (Gln15, Thr75, Gln76, Trp118, Asp220, and Arg227), ten Van der Waal's forces and four other interactions (Leu33, Tyr74, Phe111, and Ile121), out of which seven are consistent throughout the simulation period (Fig. 5.8A1 and 5.8A2). This is in contrast to the ten interactions of AZD3293 consisting of three hydrogen bonds (Ser13, Asn114, and Glu302), five Van der Waal's forces, and two other interactions (Asp303 and Val404), out of which only one was stable (Fig. 5.8B1 and 5.8B2). The fact that the number of interactions between the β-secretase and neocuscutoside C doubles that of β-secretase and AZD3293 signifies the formation of a more stable complex (Santi *et al.* 2020). The higher number of interactions and hydrogen bonds may imply neocuscutoside C has a better affinity for the enzyme and may result in better efficacy (Kumar and Patnaik 2016). This may be due to the lower docking score and binding energy of the neocuscutoside C compared to the AZD3293.

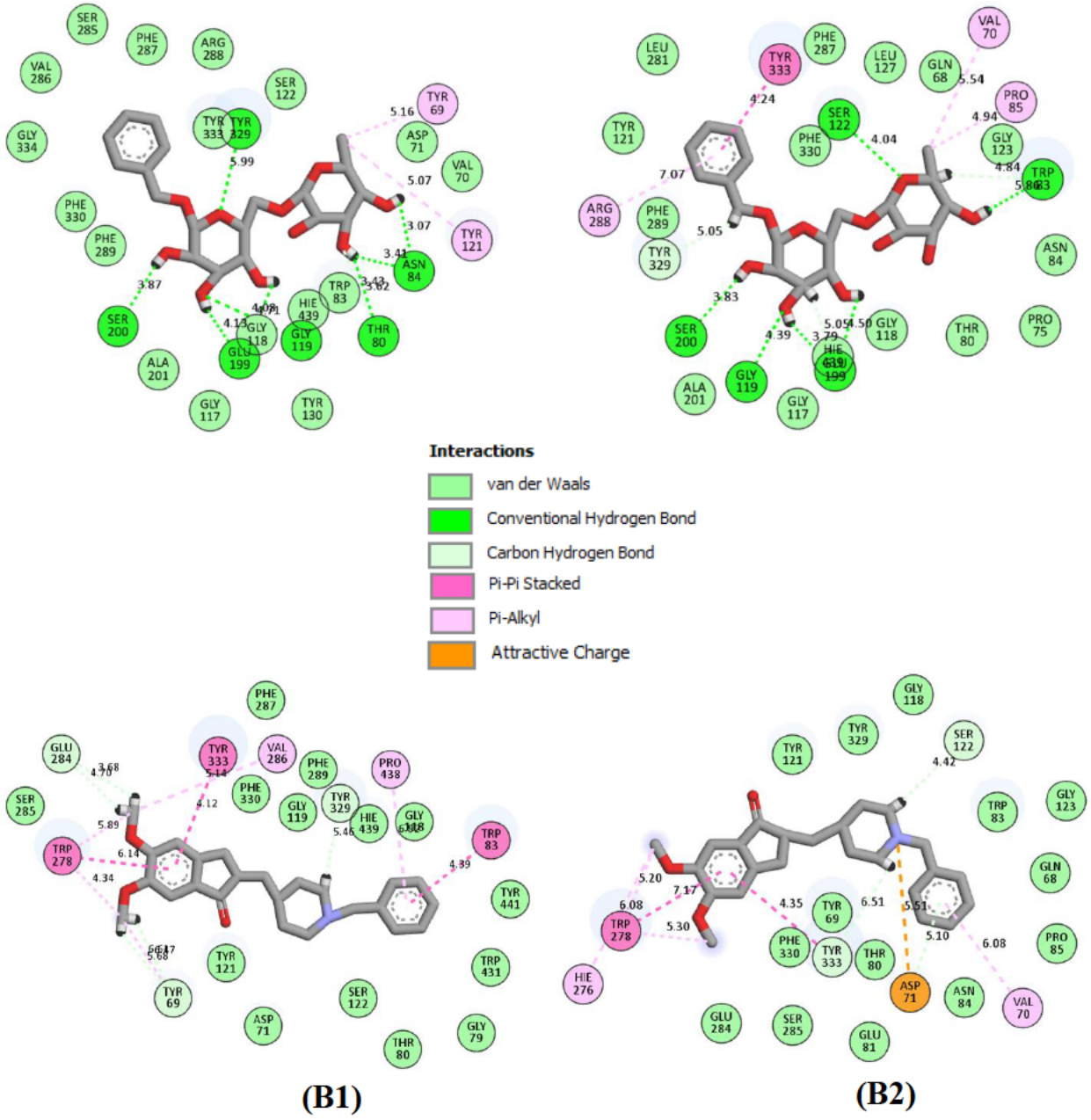

Figure 5.6. 2D interaction plots of (A) benzyl alcohol beta-D-rutinoside and (B) donepezil against acetylcholinesterase before (A1, B1) and after (A2, B2) 120 ns molecular dynamics simulation.

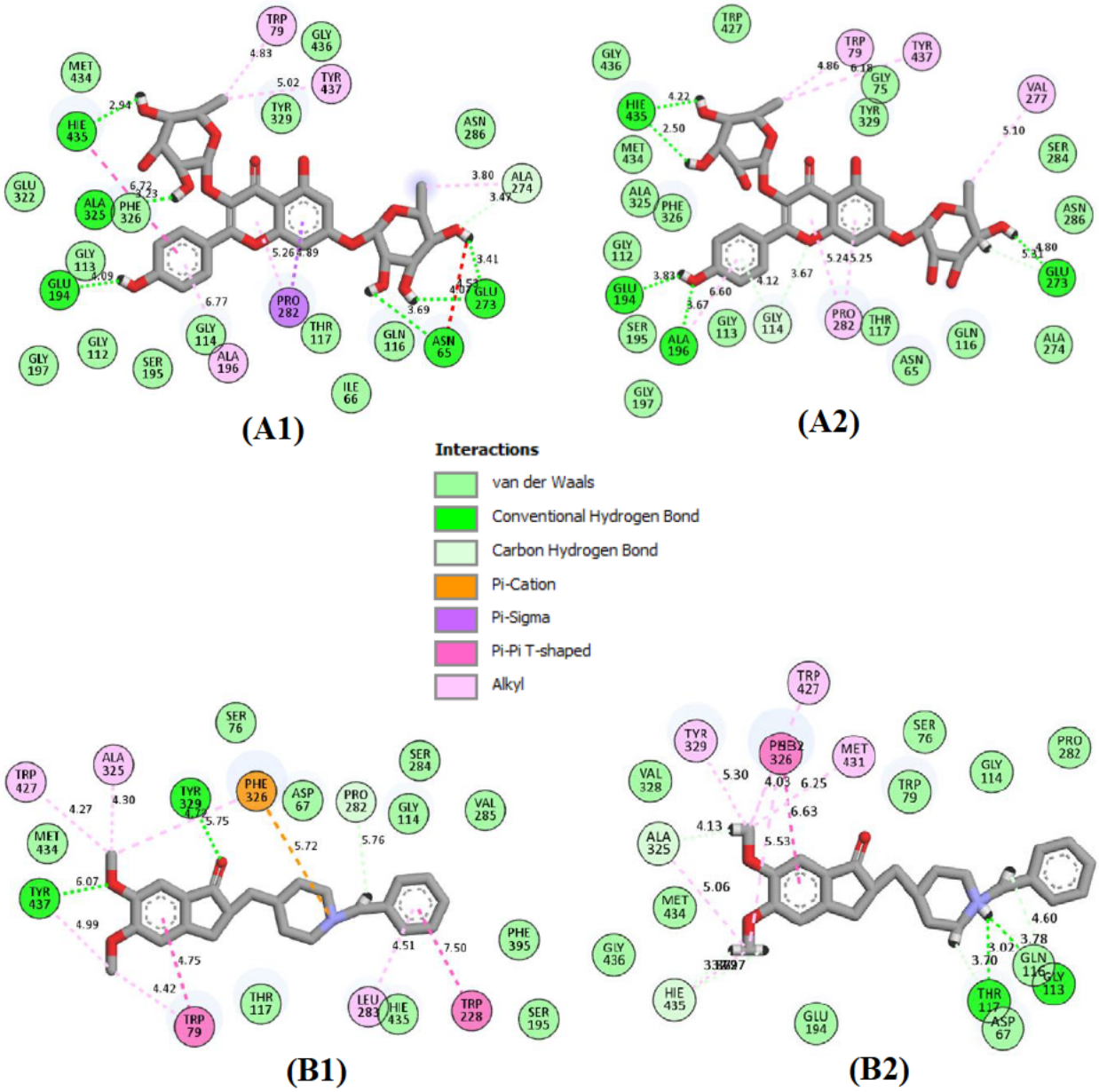

Figure 5.7. 2D interaction plots of (A) kaempferitrin and (B) donepezil against butyrylcholinesterase before (A1, B1) and after (A2, B2) 120 ns molecular dynamics simulation.

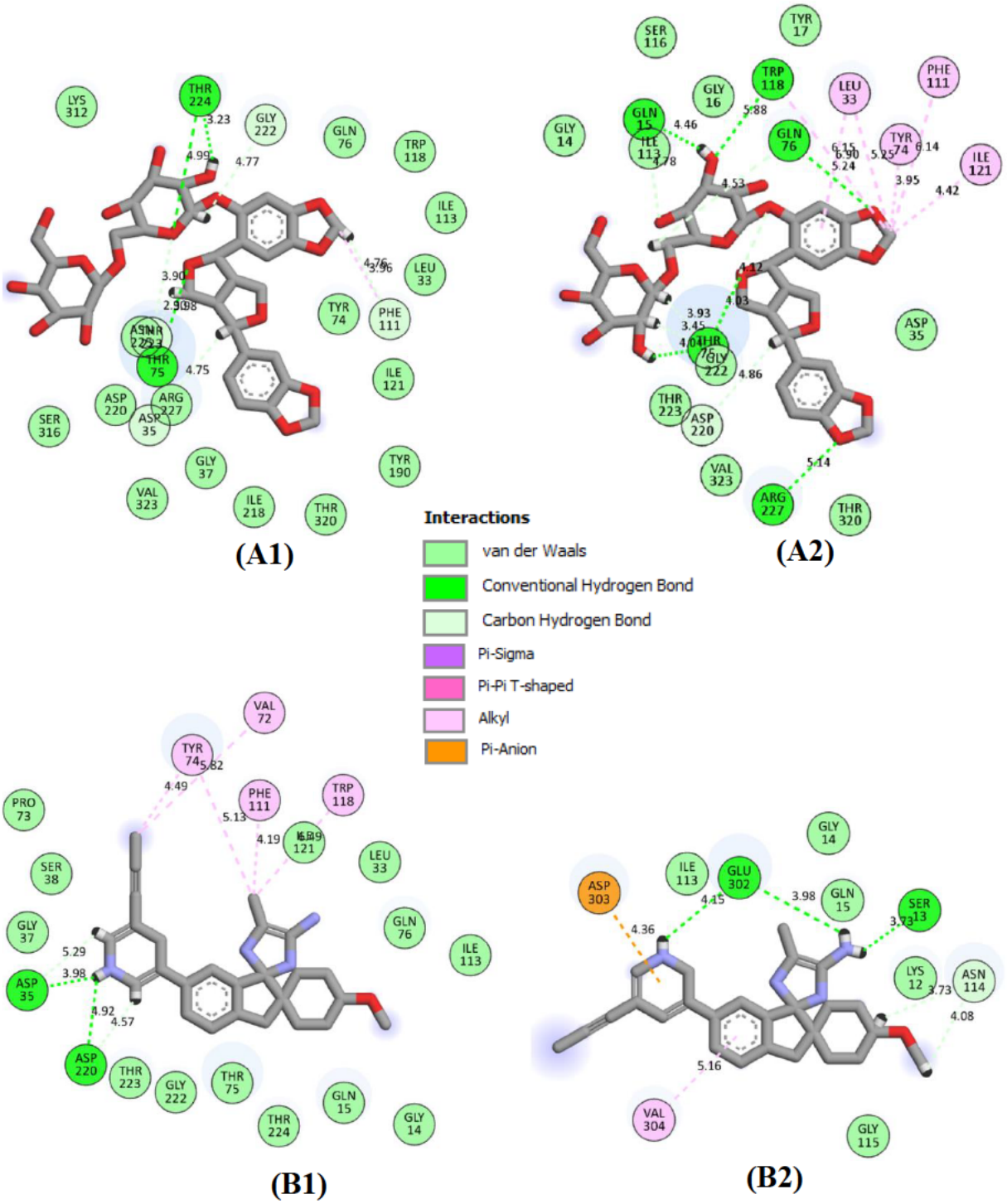

Figure 5.8. 2D interaction plots of (A) neocuscutoside C and (B) AZD3293 against beta-secretase before (A1, B1) and after (A2, B2) 120 ns molecular dynamics simulation.

Figure 5.9 shows the interaction plots of aspulvinone H and standard (tranylcypromine) with monoamine oxidase before and after molecular dynamics simulation. This is because of all the top five compounds, aspulvinone H possessed the highest number of interactions. All the top five compounds also have a higher number of interactions with the protein than tranylcypromine. Aspulvinone has thirty-five interactions with monoamine oxidase comprising five hydrogen bonds (Arg40, Tyr58, Ala261, Tyr396 and Met434), twenty-four Van der Waal's forces and six other interactions (Ser13, Ile196, Ile262, Pro263, Tyr433 and Ala436), seventeen of which were conserved throughout the simulation period (Fig. 9A1 and 9A2). Conversely, tranylcypromine has fifteen interactions consisting of eleven Van der Waal's forces and four other interactions (Gly10, Glu32, Ala33 and Ile262). The possession of a higher number of interactions (35) and hydrogen bonds (5) by aspulvinone H-monoamine oxidase complex than the tranylcypromine-monoamine oxidase complex may imply it has a better affinity for the enzyme (Das *et al.* 2024), which makes the complex more stable. This may be connected with the lower docking score (-11.9 kCal/mol) and binding energy (-72.28) of the complex compared to tranylcypromine.

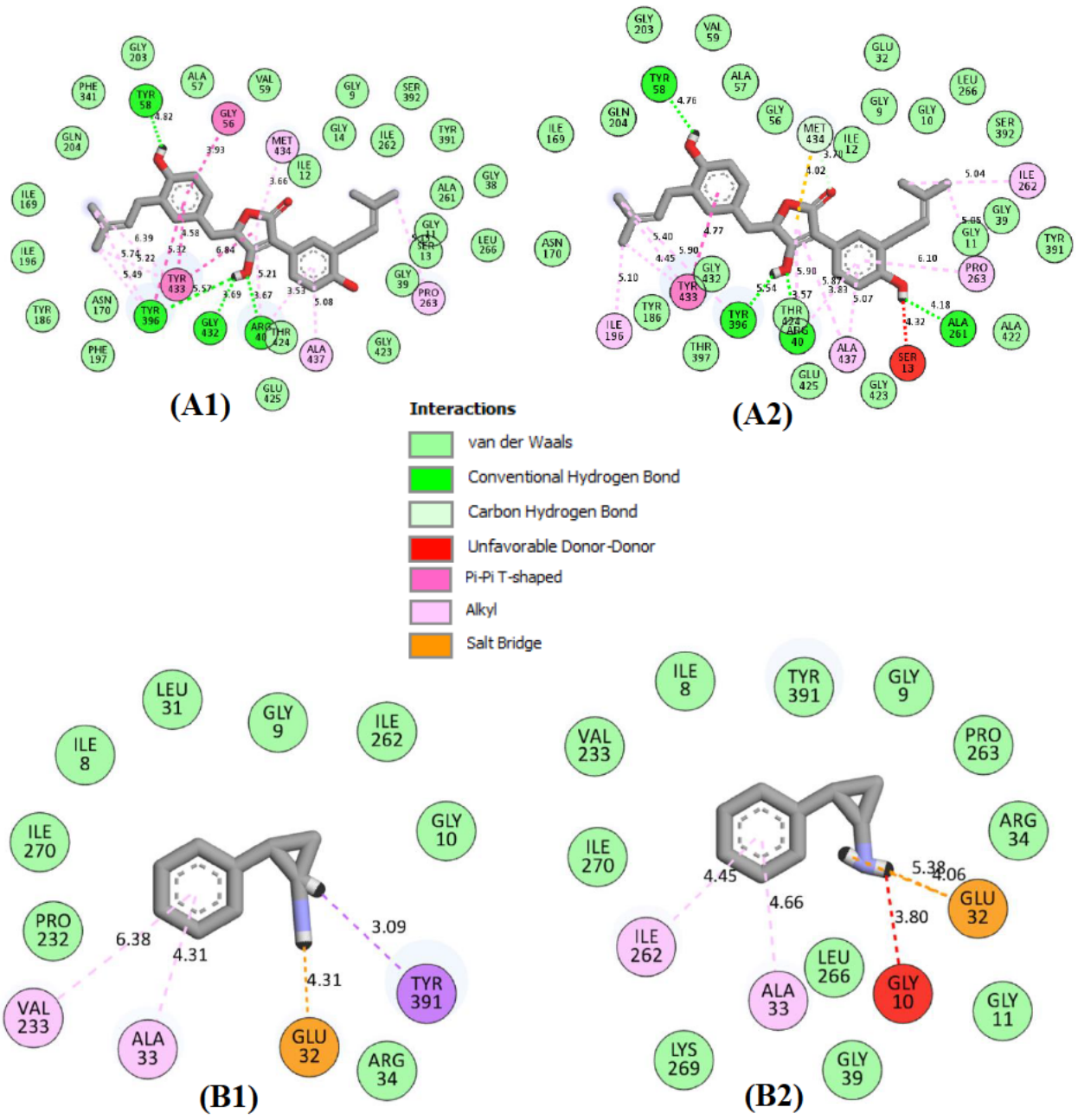

Figure 5.9. 2D interaction plots of (A) aspulvinone H and (B) tranylcypromine against monoamine oxidase before (A1, B1) and after (A2, B2) 120 ns molecular dynamics simulation.

5.4.7 ADMET properties prediction

The drug development process is a long and cumbersome one, but it may not yield the desired results in the end. To reduce this burden, the *in silico* determination of the desirable properties of would-be drugs can be performed. These include adsorption, distribution, metabolism, excretion, and toxicity, jointly referred to as ADMET properties. This provides information on drug-likeness, bioavailability, and safety of the compounds. Before an oral drug reaches the systemic circulation, it must pass through intestinal cell membranes, and this is adsorption. Table 5.6 shows the results obtained for the ADMET profiling of the top-hit compounds from lemongrass. All the compounds tested, except astragalin 7-rhamnoside, isocarlinoside, and phenylethyl primeveroside are easily adsorbed by the cell membranes, as determined by the Caco-2 permeability, human intestinal absorption (HIA), and F20 value. This suggests these compounds are safely delivered into the system and are available for distribution (Lanrewaju et al., 2023).

All the compounds tested displayed good activity in blood-brain barrier (BBB) penetration and volume of distribution at steady state (VDS). This implies that these compounds can cross the blood-brain barrier to reach their targets, and the compounds are distributed effectively in the body (Jongwachirachai et al., 2024). Drug toxicity, diminished pharmacological impact, and adverse drug effects can all result from drug interactions and metabolism. A significant determinant of such reactions is the use of the cytochrome P450 system (Verma et al., 2022). Except for 4-oxo-3-phenyl-4H-chromen-7-yl 3-phenylprop-2-enoate (OPCPPE), aspulvinone H, and [1,1'-binaphthalen]-2-ol, none of the compounds inhibited the activities of cytochrome P450 enzymes (CYP1A2, CYP2C19, and CYP3A4), indicating their inability to initiate drug-drug interaction when used alongside other drugs. Plasma clearance (CL plasma) is the overall capacity of the body to eliminate a drug, while half-life (T0.5) is the time it takes for the concentration of the drug to reduce by half (Shode et al., 2022). All the compounds evaluated possessed good CLplasma and T0.5 except OPCPPE and [1,1'-binaphthalen]-2-ol, which suggests that when ingested, they are excreted from the body at the appropriate time (Verma et al, 2022). While not all the compounds are toxic orally in rat oral acute toxicity (ROA) and are not carcinogenic (CC), both OPCPPE and [1,1'-binaphthalen]-2-ol performed poorly in the neurotoxicity (Neuro) prediction. Of all the compounds, aspulvinone H, astragalin, chamaemeloside, and [1,1'-binaphthalen]-2-ol displayed

poor values in terms of nephrotoxicity (Neph) and genotoxicity (GEN), which implies that the compounds are relatively safe.

Table 5.6. ADMET properties of all the top compounds of lemongrass docked against neurological-related enzymes

Compounds	ADS			DIS			METAB			EXCR		TOX				
	Caco2	HIA	F20	BBB	PPB	VDSS	CYP1A2	CYP2C19	CYP3A4	CLplas	T0.5	ROA	CC	Neuro	Neph	GEN
OPCPPE	Ex	Ex	Ex	Ex	Po	Ex	Yes	Yes	No	Md	Po	Ex	Md	Po	Md	Ex
Aspulvinone H	Ex	Po	Po	Ex	Po	Ex	No	Yes	No	Ex	Md	Md	Ex	Md	Po	Po
AS7RH	Po	Po	Po	Ex	Ex	Ex	No	No	No	Ex	Md	Ex	Ex	Ex	Po	Po
BABR	Po	Po	Md	Ex	Ex	Ex	No	No	No	Ex	Md	Ex	Ex	Ex	Po	Ex
Chamaemeloside	Po	Md	Po	Ex	Ex	Ex	No	No	No	Ex	Md	Ex	Ex	Ex	Po	Po
BN2OL	Ex	Ex	Ex	Md	Po	Ex	Yes	Yes	No	Ex	Po	Ex	Md	Po	Po	Po
Isocarlinoside	Po	Po	Po	Ex	Ex	Ex	No	No	No	Ex	Ex	Ex	Ex	Ex	Md	Po
Kaempferitrin	Po	Md	Po	Ex	Ex	Ex	No	No	No	Ex	Md	Ex	Ex	Ex	Md	Po
Lonicerin	Po	Po	Ex	Ex	Ex	Ex	No	No	No	Ex	Md	Ex	Ex	Ex	Md	Po
V6H3M	Po	Ex	Po	Ex	Ex	Ex	No	No	No	Ex	Md	Md	Ex	Ex	Md	Po
Neocuscutoside C	Po	Ex	Ex	Md	Ex	Ex	No	No	No	Ex	Md	Md	Md	Md	Ex	Po
Chlorogenic acid	Po	Ex	Po	Ex	Ex	Ex	No	No	No	Ex	Md	Ex	Ex	Ex	Md	Ex
PEPV	Po	Po	Po	Ex	Ex	Ex	No	No	No	Ex	Md	Ex	Ex	Md	Ex	Ex
4FQA	Po	Ex	Po	Ex	Ex	Ex	No	No	No	Ex	Md	Ex	Md	Md	Po	Ex
Standard drugs																
Donepezil	Ex	Ex	Ex	Md	Po	Ex	No	No	No	Md	Po	Md	Md	Po	Md	Md
AZD3293	Ex	Ex	Ex	Ex	Po	Ex	No	No	No	Ex	Po	Po	Po	Md	Po	Po
Tranylcypromine	Ex	Ex	Ex	Po	Ex	Ex	Yes	No	No	Md	Md	Po	Ex	Po	Po	Ex

ADS: Adsorption, DIS: Distribution, METAB: Metabolism, EXCR: Excretion, TOX: Toxicity, Caco-2: Caco-2 permeability, HIA: Human intestinal absorption, F20: 20% bioavailability, BBB: Blood-brain barrier, VDSS: Volume of distribution at steady state, CLplas: Plasma clearance, T0.5: Half-life, ROA: Rat oral toxicity, CC: Carcinogenicity, Neuro: Neurotoxicity, Neph: Nephrotoxicity, GEN: Genotoxicity, OPCPPE: 4-oxo-3-phenyl-4H-chromen-7-yl 3-phenylprop-2-enoate, AS7RH: Astragalin-7-rhamnoside, BABR: Benzyl alcohol beta-D-rutinoside, BN2OL: [1,1'-binaphthalen]-2-ol, V6H3M: Vitexin-6''-(3-hydroxyl-3-methylglutarate), PEPV: Phenylethyl primeveroside, 4FQA: 4-O-feruloyl-D-quinic acid. Ex: Excellent, Md: Medium, Po: Poor

5.5. Conclusion

It can be concluded that both fresh and dry lemongrass teas displayed neuroprotective properties *in vitro*, though the fresh infusion was better, possibly due to the higher abundance of some phytochemicals such as benzyl alcohol beta-D-rutinoside, kaempferitrin, neocuscutoside C. LC-MS profiling of the lemongrass teas showed the presence of 49 phytochemical compounds. Computational studies revealed that of all the phytochemical compounds tested, benzyl alcohol beta-D-rutinoside, kaempferitrin, neocuscutoside C, and aspulvinone H had the highest number of stable interactions with AChE, BChE, BACE-1, and MAO, respectively. While there are previous reports on the neuroprotective potentials of aspulvinone H and kaempferitrin, this study, for the first time, reports the potent neuroprotective properties of benzyl alcohol beta-D-rutinoside and neocuscutoside C. However, of all the compounds tested for the pharmacokinetic properties, neocuscutoside C satisfied most of the rules. Consequently, these compounds, especially neocuscutoside C, could be explored in developing new therapeutic agents for the management of neurodegenerative disorders like Alzheimer's and Parkinson's diseases. However, there is a need to validate the outcome of this study in *in vivo* studies and clinical trials.

References

Al-Khodairy, F. M., Khan, M. K. A., Kunhi, M., Pulicat, M. S., Akhtar, S., & Arif, J. M. 2013. *In Silico* prediction of mechanism of Erysolin-induced apoptosis in human breast cancer cell lines. *American Journal of Bioinformatics Research*, 3(3), 62–71.

Aribisala, J. O., Abdulsalam, R. A., Dweba, Y., Madonsela, K. and Sabiu, S. 2022. Identification of secondary metabolites from *Crescentia cujete* as promising antibacterial therapeutics targeting type 2A topoisomerases through molecular dynamics simulation. *Computers in Biology and Medicine*, 145: 105432.

Avoseh, O., Oyedeji, O., Rungqu, P., Nkeh-Chungag, B. and Oyedeji, A. 2015. Cymbopogon species; ethnopharmacology, phytochemistry and the pharmacological importance. *Molecules*, 20 (5): 7438-7453.

Balogun, F. O., Naidoo, K., Aribisala, J. O., Pillay, C. and Sabiu, S. 2022. Cheminformatics identification and validation of dipeptidyl peptidase-iv modulators from shikimate pathway-derived phenolic acids towards interventive type-2 diabetes therapy. *Metabolites*, 12 (10): 937.

Cancela, S., Canclini, L., Mourglia-Ettlin, G., Hernández, P. and Merlino, A. 2020. Neuroprotective effects of novel nitrones: *In vitro* and *in silico* studies. *European Journal of Pharmacology*, 871: 172926.

Das, D., Nanda, M., Banjare, P. and Lanjhiyana, S. 2024. Exploration of multitargeted antialzheimer's activity of safflower leaves phytoconstituents: *In silico* molecular docking approach. *European Journal of Medicinal Chemistry Reports*, 10: 100119.

Duangupama, T., Pratuangdejkul, J., Chongruchiroj, S., Pittayakhajonwut, P., Intaraudom, C., Tadtong, S., Nunthanavanit, P., Samee, W., He, Y.-W. and Tanasupawat, S. 2023. New insights into the neuroprotective and beta-secretase1 inhibitor profiles of tirandamycin B isolated from a newly found *Streptomyces composti* sp. nov. *Scientific Reports*, 13 (1): 4825.

Ekpenyong, C. E., Akpan, E. and Nyoh, A. 2015. Ethnopharmacology, phytochemistry, and biological activities of *Cymbopogon citratus* (DC.) Stapf extracts. *Chinese Journal of Natural Medicines*, 13 (5): 321-337.

Fatima, K., Ashfaq, U. A., ul Qamar, M. T., Asif, M., Haque, A., Qasim, M., Alamri, M. A., Muhseen, Z. T., Noor, F. and Sadaqat, M. 2024. Advanced network pharmacology and molecular docking-based mechanism study to explore the multi-target pharmacological mechanism of *Cymbopogon citratus* against Alzheimer's disease. *South African Journal of Botany*, 165: 466-477.

Gholami, A., Minai-Tehrani, D. and Eriksson, L. A. 2023. *In silico* and *in vitro* studies confirm Ondansetron as a novel acetylcholinesterase and butyrylcholinesterase inhibitor. *Scientific Reports*, 13 (1): 643.

Gupta, S., Parihar, D., Shah, M., Yadav, S., Managori, H., Bhowmick, S., Patil, P. C., Alissa, S. A., Wabaidur, S. M. and Islam, M. A. 2020. Computational screening of promising beta-secretase 1 inhibitors through multi-step molecular docking and molecular dynamics simulations-Pharmacoinformatics approach. *Journal of Molecular Structure*, 1205: 127660.

Gyebi, G. A., Ogunyemi, O. M., Ibrahim, I. M., Ogunro, O. B., Afolabi, S. O., Ojo, R. J., Anyanwu, G. O., El-Saber Batiha, G. and Adebayo, J. O. 2023. Identification of potential inhibitors of cholinergic and β-secretase enzymes from phytochemicals derived from *Gongronema latifolium* Benth leaf: an integrated computational analysis. *Molecular Diversity*, 28: 1305-1322.

Hacke, A. C. M., Miyoshi, E., Marques, J. A. and Pereira, R. P. 2021. *Cymbopogon citratus* (DC.) Stapf, citral and geraniol exhibit anticonvulsant and neuroprotective effects in pentylenetetrazole-induced seizures in zebrafish. *Journal of Ethnopharmacology*, 275: 114142.

Haider, M. S., Ashraf, W., Javaid, S., Rasool, M. F., Rahman, H. M. A., Saleem, H., Anjum, S. M. M., Siddique, F., Morales-Bayuelo, A. and Kaya, S. 2021. Chemical characterization and evaluation of the neuroprotective potential of *Indigofera sessiliflora* through *in-silico* studies and behavioral tests in scopolamine-induced memory compromised rats. *Saudi Journal of Biological Sciences*, 28 (8): 4384-4398.

Jalal, K., Khan, K., Haleem, D. J. and Uddin, R. 2022. *In silico* study to identify new monoamine oxidase type a (MAO-A) selective inhibitors from natural source by virtual screening and molecular dynamics simulation. *Journal of Molecular Structure*, 1254: 132244.

Kazeem, M. I. and Davies, T. C. 2016. Anti-diabetic functional foods as sources of insulin secreting, insulin sensitizing and insulin mimetic agents. *Journal of Functional Foods*, 20: 122-138.

Kim, J. H., Thao, N. P., Han, Y. K., Lee, Y. S., Luyen, B. T. T., Oanh, H. V., Kim, Y. H. and Yang, S. Y. 2018. The insight of *in vitro* and *in silico* studies on cholinesterase inhibitors from the

roots of *Cimicifuga dahurica* (Turcz.) Maxim. *Journal of Enzyme Inhibition and Medicinal Chemistry*, 33 (1): 1174-1180.

Kumar, G. and Patnaik, R. 2016. Exploring neuroprotective potential of *Withania somnifera* phytochemicals by inhibition of GluN2B-containing NMDA receptors: An *in silico* study. *Medical Hypotheses*, 92: 35-43.

Kundu, D. and Dubey, V. K. 2021. Potential alternatives to current cholinesterase inhibitors: An *in silico* drug repurposing approach. *Drug Development and Industrial Pharmacy*, 47 (6): 919-930.

Madi, Y. F., Choucry, M. A., El-Marasy, S. A., Meselhy, M. R. and El-Kashoury, E.-S. A. 2020. UPLC-Orbitrap HRMS metabolic profiling of *Cymbopogon citratus* cultivated in Egypt; neuroprotective effect against $AlCl_3$-induced neurotoxicity in rats. *Journal of Ethnopharmacology*, 259: 112930.

Masondo, N. A., Stafford, G. I., Aremu, A. O. and Makunga, N. P. 2019. Acetylcholinesterase inhibitors from southern African plants: An overview of ethnobotanical, pharmacological potential and phytochemical research including and beyond Alzheimer's disease treatment. *South African Journal of Botany*, 120: 39-64.

Mazumder, M. K. and Choudhury, S. 2019. Tea polyphenols as multi-target therapeutics for Alzheimer's disease: An *in silico* study. *Medical Hypotheses*, 125: 94-99.

Mendes, G. O., Pita, S. S. d. R., Carvalho, P. B. d., Silva, M. P. d., Taranto, A. G. and Leite, F. H. A. 2023. Molecular multi-target approach for human acetylcholinesterase, butyrylcholinesterase and β-secretase 1: Next generation for alzheimer's disease treatment. *Pharmaceuticals*, 16 (6): 880.

Moorkoth, S., Prathyusha, N. S., Manandhar, S., Xue, Y., Sankhe, R., Pai, K. and Kumar, N. 2021. Antidepressant-like effect of dehydrozingerone from *Zingiber officinale* by elevating monoamines in brain: *In silico* and *in vivo* studies. *Pharmacological Reports*, 73: 1273-1286.

Murali, M., Ahmed, F., Gowtham, H. G., Aribisala, J. O., Abdulsalam, R. A., Shati, A. A., Alfaifi, M. Y., Sayyed, R., Sabiu, S. and Amruthesh, K. N. 2023. Exploration of CviR-mediated quorum sensing inhibitors from *Cladosporium* spp. against *Chromobacterium violaceum* through computational studies. *Scientific Reports*, 13 (1): 15505.

Negrelle, R. and Gomes, E. 2007. *Cymbopogon citratus* (DC.) Stapf: Chemical composition and biological activities. *Revista Brasileira de Plantas Medicinais*, 9 (1): 80-92.

Oladeji, O. S., Adelowo, F. E., Ayodele, D. T. and Odelade, K. A. 2019. Phytochemistry and pharmacological activities of *Cymbopogon citratus*: A review. *Scientific African*, 6: e00137.

Onder, F. C., Sahin, K., Senturk, M., Durdagi, S. and Ay, M. 2022. Identifying highly effective coumarin-based novel cholinesterase inhibitors by *in silico* and *in vitro* studies. *Journal of Molecular Graphics and Modelling*, 115: 108210.

Othman, A., Sayed, A. M., Amen, Y. and Shimizu, K. 2022. Possible neuroprotective effects of amide alkaloids from *Bassia indica* and *Agathophora alopecuroides*: *In vitro* and *in silico* investigations. *RSC advances*, 12 (29): 18746-18758.

Paudel, P., Seong, S. H., Shrestha, S., Jung, H. A. and Choi, J. S. 2019. In vitro and in silico human monoamine oxidase inhibitory potential of anthraquinones, naphthopyrones, and naphthalenic lactones from *Cassia obtusifolia* Linn seeds. *ACS Omega*, 4 (14): 16139-16152.

Perry, N. S., Houghton, P. J., Sampson, J., Theobald, A. E., Hart, S., Lis-Balchin, M., Hoult, J. R. S., Evans, P., Jenner, P. and Milligan, S. 2001. *In-vitro* activity of *S. lavandulaefolia* (Spanish sage) relevant to treatment of Alzheimer's disease. *Journal of Pharmacy and Pharmacology*, 53 (10): 1347-1356.

Puksasook, T., Kimura, S., Tadtong, S., Jiaranaikulwanitch, J., Pratuangdejkul, J., Kitphati, W., Suwanborirux, K., Saito, N. and Nukoolkarn, V. 2017. Semisynthesis and biological evaluation of

prenylated resveratrol derivatives as multi-targeted agents for Alzheimer's disease. *Journal of Natural Medicines*, 71: 665-682.

Racchi, M., Mazzucchelli, M., Porrello, E., Lanni, C. and Govoni, S. 2004. Acetylcholinesterase inhibitors: novel activities of old molecules. *Pharmacological Research*, 50 (4): 441-451.

Rojek, K., Serefko, A., Poleszak, E., Szopa, A., Wróbel, A., Guz, M., Xiao, J. and Skalicka-Woźniak, K. 2022. Neurobehavioral properties of *Cymbopogon* essential oils and its components. *Phytochemistry Reviews*, 21 (2): 327-338.

Sabiu, S., Balogun, F. O. and Amoo, S. O. 2021. Phenolics profiling of *Carpobrotus edulis* (L.) NE Br. and insights into molecular dynamics of their significance in type 2 diabetes therapy and its retinopathy complication. *Molecules*, 26 (16): 4867.

Santi, M. D., Arredondo, F., Carvalho, D., Echeverry, C., Prunell, G., Peralta, M. A., Cabrera, J. L., Ortega, M. G., Savio, E. and Abin-Carriquiry, J. A. 2020. Neuroprotective effects of prenylated flavanones isolated from Dalea species, *in vitro* and *in silico* studies. *European Journal of Medicinal Chemistry*, 206: 112718.

Sheeja Malar, D., Beema Shafreen, R., Karutha Pandian, S. and Pandima Devi, K. 2017. Cholinesterase inhibitory, anti-amyloidogenic and neuroprotective effect of the medicinal plant *Grewia tiliaefolia* – An in vitro and in silico study. *Pharmaceutical Biology*, 55 (1): 381-393.

Soreq, H. and Seidman, S. 2001. Acetylcholinesterase—new roles for an old actor. *Nature Reviews Neuroscience*, 2 (4): 294-302.

Steinmetz, J. D., Seeher, K. M., Schiess, N., Nichols, E., Cao, B., Servili, C., Cavallera, V., Cousin, E., Hagins, H. and Moberg, M. E. 2024. Global, regional, and national burden of disorders affecting the nervous system, 1990–2021: A systematic analysis for the Global Burden of Disease Study 2021. *The Lancet Neurology*, 23 (4): 344-381.

Suleria, H. A., Barrow, C. J. and Dunshea, F. R. 2020. Screening and characterization of phenolic compounds and their antioxidant capacity in different fruit peels. *Foods*, 9 (9): 1206.

Umukoro, S., Adeola, A. H., Ben-Azu, B. and Ajayi, A. M. 2018. Lemon grass tea enhanced memory function and attenuated scopolamine-induced amnesia in mice via inhibition of oxidative stress and acetyl-cholinesterase activity. *Journal of Herbs, Spices & Medicinal Plants*, 24 (4): 407-420.

Wallace, W. E., Moorthy, A. S. 2023. NIST mass spectrometry data center standard reference libraries and software tools: Application to seized drug analysis. *Journal of Forensic Sciences*, 68(5): 1484-1493.

WHO. 2002. *WHO Traditional Medicine Strategy 2002 - 2005*. Geneva: World Health Organization.

Wu, Y., Su, X., Lu, J., Wu, M., Yang, S. Y., Mai, Y., Deng, W. and Xue, Y. 2022. *In vitro* and *in silico* analysis of phytochemicals from *Fallopia dentatoalata* as dual functional cholinesterase inhibitors for the treatment of Alzheimer's disease. *Frontiers in Pharmacology*, 13: 905708.

Yang, X., Wang, K., Liu, Q. and Zhang, X. 2020. Discovery of monoamine oxidase A inhibitory peptides from hairtail (*Trichiurus japonicus*) using *in vitro* simulated gastrointestinal digestion and in silico studies. *Bioorganic Chemistry*, 101: 104032.

CHAPTER 6

6. Lemongrass infusion alleviates metabolic derangement via insulin signaling in D-galactose-induced ageing in *Drosophila melanogaster*

Mutiu Idowu Kazeem, John Jason Mellem and Saheed Sabiu

Department of Biotechnology and Food Science, Faculty of Applied Sciences, Durban University of Technology, P. O. Box 1334, Durban 4000, South Africa

Preface: This manuscript studied the effect of the inclusion of fresh and dry lemongrass tea on biochemical and molecular parameters in D-galactose-induced ageing in *Drosophila melanogaster*. The manuscript is submitted to the journal, *Journal of Functional Foods*.

6.1. Abstract

This study evaluated the pro-longevity effect of dietary inclusion of lemongrass infusions in D-galactose-induced ageing in *Drosophila melanogaster*. The flies were randomized into five groups comprising a control (fed on a normal fly diet) and four other groups with a D-galactose diet. Fresh lemongrass infusion (0.8 mg/mL), dry lemongrass infusion (0.8 mg/mL), and gallic acid were included in the diets of groups 3, 4, and 5, respectively. After 14 days, the flies were homogenized, and biochemical parameters were determined. The concentration of glucose, triglyceride, malondialdehyde, and hydrogen peroxide increased significantly by 26, 38, 116, and 110% respectively, in the D-galactose-fed flies. This was followed by a decrease in the activities of all the antioxidant enzymes (superoxide dismutase, catalase, and glutathione peroxidase), reduced glutathione, and thiol in the D-galactose-treated flies. The D-galactose-fed flies also experienced a 70% and 37% increase in acetylcholinesterase and monoamine oxidase activity. However, the inclusion of dry lemongrass infusion restored all the alterations except reduced glutathione and thiol observed in the D-galactose flies. The dry lemongrass infusion also upregulated the SOD1, CAT, and dFOXO genes while downregulating the DILP2 gene. It can be concluded that, though both fresh and dry lemongrass infusions extended the lifespan of the flies, the dry lemongrass infusion sustained it by restoring all the metabolic perturbations caused by D-galactose. This may be due to the presence of bioactive phytochemical compounds in the dry lemongrass infusion.

Further studies may be conducted to isolate the bioactive compounds responsible for the anti-ageing effects of lemongrass tea.

Keywords: Ageing, Lemongrass, *Drosophila melanogaster*, Oxidative stress, Longevity

6.2. Introduction

While longevity is a common aspiration, it often comes with physical and physiological decline (Luo *et al.* 2021). This predisposes old people to many diseases such as metabolic (e.g, diabetes mellitus), cardiovascular (e.g, hypertension), and neurodegenerative disorders (e.g, Alzheimer's disease) (Kazeem, Mellem and Sabiu 2024). The prevalence of people aged 60 years and above is projected to reach 2 billion by the year 2050, as against 800 million in 2017, representing 22% of the global population (Grinin, Grinin and Korotayev 2023). This increase may be due to two reasons, namely, people now live longer than in previous years and give birth to fewer children. As the number of children per population reduces, the percentage of old people will automatically increase (Higo and Khan 2015). Since the number of old people has increased drastically and they are more susceptible to debilitating diseases, there is a need to develop therapeutic interventions to promote healthy ageing.

Throughout history, the interaction of humans with plants has been intricately connected, as they serve as a source of food, clothing, shelter, and medicine (Gurib-Fakim 2006). About 80% of the world's population depends on medicinal plants for the treatment of their diseases, and many of these plants have been validated for therapeutic purposes. Lemongrass (*Cymbopogon citratus*) originates from Southwest Asia and now grows in different parts of the globe, especially Asia, South America, and Africa (Negrelle and Gomes 2007). The tea prepared from the fresh and dry lemongrass leaves is taken for pleasure due to its characteristic aroma, as well as for medicine to treat different ailments (Ekpenyong, Akpan and Nyoh 2015). Its essential oil is also used as a flavouring agent, in cosmetics, and industrial preservative (Ekpenyong and Akpan 2017). Studies have revealed that lemongrass has numerous pharmacological properties, including antidiabetic, antimicrobial, antimalarial, anticancer, and neuroprotective activities (Ekpenyong, Akpan and Nyoh 2015; Oladeji *et al.* 2019). However, there is a scarcity of information on its anti-ageing potential *in vivo*.

Several *in vivo* models are used to test the anti-ageing properties of proposed therapeutic agents, such as yeast, *Caenorhabditis elegans*, *Drosophila melanogaster*, and rodents. *Drosophila melanogaster*, commonly known as the fruit fly, is a versatile model organism that has been used in biomedical research (Jennings 2011). It is a small fly with compound eyes and wings, with a lifespan of 40 – 120 days, depending on diet and environment (Suter 2019). Compared to the vertebrate models, *Drosophila melanogaster* is easier and cheaper to grow in the laboratory, they have shorter life cycles, produce numerous embryos, and are easy to genetically modify (Kazeem, Mellem and Sabiu 2024). Though the fruit fly may not be physically similar to man, there is a conservation of important biological mechanisms that regulate development and survival in both organisms (Jennings 2011). Previous studies have revealed *Drosophila melanogaster* as an effective model for the evaluation of the anti-ageing potential of plants (Boyd *et al.* 2011; Oyebode *et al.* 2020)

Consequently, this study evaluated the influence of supplementation of diets with fresh and dry infusions of lemongrass in D-galactose-induced ageing in *Drosophila melanogaster* with a view to determining its effects on lifespan and modulation of relevant genes.

6.3. Materials and methods

D-galactose and gallic acid were obtained from Sigma Aldrich, Saint Louis, USA. Biochemical assay kits were procured from Randox Laboratories, County Antrim, UK. All other chemicals used were of analytical grade, and water was glass-distilled.

6.3.1. Drosophila stock and culture

Wild-type Harwich strain of *D. melanogaster* was obtained from the *Drosophila* Research Laboratory, Department of Biochemistry, University of Ibadan, Ibadan, Nigeria. The flies were originally obtained from the National Species Stock Center, Bowling Green, OH, USA. The flies were acclimatized for 7 days and reared in the *Drosophila* Laboratory, Department of Biochemistry, Lagos State University, Lagos, Nigeria. Cornmeal media containing 1% w/v brewer's yeast, 1% w/v powdered milk, 1% w/v agar, and 0.08% v/w nipagin was used to culture the flies. Conditions include: Constant temperature and humidity (22-24 °C; 60-70% relative humidity) under a 12 h dark/light cycle.

6.3.2. Experimental design

Drosophila melanogaster of 1 to 3-day-old were treated with different concentrations (0, 0.1, 0.2, 0.4, and 0.8 mg/mL) of lemongrass tea (50 flies/vial; n = 5) throughout their lifespan. Flies were transferred to fresh food once every 2–3 days, and the number of dead flies was counted at each transfer. Life span data were recorded using Microsoft Excel (Microsoft, Redmond, WA, USA) and plotted as percentage survival. Based on the data obtained from these studies, 0.8 mg/mL of the fresh and dry lemongrass infusion was selected for the main experiment (Oyebode *et al.* 2020).

Consequently, a new set of 1 to 3-day-old flies was randomized into five groups (each comprising 5 vials containing 25 flies each), namely,

Group 1 (Control): Fed on normal cornmeal medium
Group 2 (Gal): Fed on a diet containing 25 mg/g D-galactose
Group 3 (Gal + FLG): Fed on a diet containing 25 mg/g D-galactose and 0.8 mg/mL fresh lemongrass infusion
Group 4 (Gal + DLG): Fed on a diet containing 25 mg/g D-galactose and 0.8 mg/mL dry lemongrass infusion
Group 5 (Gal + GA): Fed on a diet containing 25 mg/g D-galactose and 50 µM gallic acid (as positive control) (Ogunsuyi *et al*. 2020a)
The experiment lasted for 14 days, after which the flies were anaesthetized and homogenized appropriately for further studies.

6.3.3. Climbing assay

The negative geotaxis assay determined the locomotor function of flies from each group. Ten (10) flies from each of the five experimental groups were placed in a graduated vial, gently tapped down to the bottom, and allowed to climb up. The number of flies that climbed up to the 6 cm mark in 6 s was recorded. Three repetitions were made, and the data were expressed as mean + standard error of mean (SEM) of three replicates (Boyd *et al.* 2011).

6.3.4. Preparation of samples for biochemical assays

Treated flies per group were anaesthetized on ice, weighed, homogenized in 0.1 M potassium phosphate buffer, pH 7.4 (1:10 (flies/volume), and centrifuged at 4000 *g* for 10 min at 4 °C. The

supernatants were obtained and kept at -20 °C to evaluate biochemical assays (Oyebode *et al*. 2020).

6.3.5. Determination of biochemical indices

6.3.5.1. Determination of protein concentration

The total protein concentration of the flies' homogenate was determined using the Biuret reagent. 20 µL of the fly homogenate was mixed with 1000 µL of Biuret reagent. The mixture was incubated for 10 min at room temperature, and absorbance was taken at 550 nm (Lowry *et al.* 1951).

6.3.5.2. Determination of triglyceride concentration

The level of triacylglycerol in the flies' whole body was quantified using the Randox Assay kit. This reaction consisted of 10 µL of fly homogenate and 1,000 μL of triglyceride reagent. Absorbance was taken at 546 nm, and the standard was used for the calculation and expressed in mg/dL (Tietz 1995).

6.3.5.3. Determination of glucose concentration

The level of glucose in the flies' homogenate was determined using the Randox Glucose Assay kit. This reaction consisted of 10 µL of fly homogenate and 1,000 μL of glucose reagent. The mixture was mixed and incubated for 10 min at 37 °C. Absorbance was taken at 500 nm, and the standard was used for the calculation and expressed in mg/dL (Trinder 1969).

6.3.5.4. Malondialdehyde

The reaction mixture contained 50 µL of flies' tissue homogenate, 300 µL 8.1% SDS, 500 µL acetic acid, and 500 µL 0.8% thiobarbituric acid. This was boiled at 100°C for 60 min and allowed to cool. They were later centrifuged at 8,000 × *g* for 10 min, and the absorbance of the supernatants was measured at 532 nm. The malondialdehyde level was calculated and expressed as mmol/mg protein (Ohkawa 1979).

6.3.5.5. Total thiol

The assay reaction contained 150 µL sodium phosphate buffer (0.1M, pH 7.4), 40 µL tissue homogenate, and 10 µL DTNB (10 mM). This was incubated in the dark for 30 min, and absorbance was taken at 405 nm in a SpectraMax plate reader (Molecular Devices, CA, USA).

The total thiol level was subsequently calculated from the GSH standard calibration curve and expressed as mmol GSH produced/mg protein (Ellman 1959).

6.3.5.6. Reduced glutathione (GSH)

Five hundred microliters of the flies' homogenate were mixed with 500 µL of 4% (w/v) sulfosalicylic acid and centrifuged at 600 × *g* for 10 min. Three hundred microliters of the supernatant were added to 2.7 mL of a disulfide (5,5'-dithiobis-2-nitrobenzoic acid) reagent, and the absorbance was monitored at 412 nm. Total GSH content was expressed as mmol/mg protein (Ellman 1959).

6.3.5.7. Hydrogen peroxide

The hydrogen peroxide level was determined by adding 20 µL of sample to a mixture of 520 µL phosphate buffer (0.1 M, pH 7.4), 35 µL of 100 mM xylenol orange, 35 µL of 250 mM ammonium ferrous sulfate, 85 µL sorbitol (100 mM), and 8 µL of 25mM H_2SO_4. Then, the reaction mixture was incubated at room temperature for 30 min, and the absorbance was measured in a spectrophotometer at a wavelength of 560 nm. Thereafter, H_2O_2 level was calculated and expressed in µmol/mg protein (Wolff 1994).

6.3.5.8. Superoxide dismutase (SOD)

The reaction mixture consisted of 50 µL of flies' homogenate, 100 µL of sodium carbonate buffer (0.1 M, pH 10.2), and 50 µL of adrenaline. The absorbance was measured at 30 s intervals for 5 min at 480 nm in a SpectraMax plate reader (Molecular Devices, CA, USA), and the enzyme activity was calculated and expressed as mmol/min/mg protein (Marklund and Marklund 1974).

6.3.5.9. Catalase

The reaction medium contained 170 µL of 50 mM phosphate buffer (pH 7.0), 20 µL of 300 mM hydrogen peroxide, and 10 µL of sample (1:50 dilution). Subsequently, the decrease in absorbance of H_2O_2 at a wavelength of 240 nm was recorded for 2 min (10 s interval) using a SpectraMax plate reader (Molecular Devices). Thereafter, the activity of catalase was calculated and expressed in µmol of H_2O_2 consumed/min/mg of protein (Aebi 1984).

6.3.5.10. Glutathione peroxidase (GPx)

The reaction mixture contained 2.50 mL of a 0.1 mol/L Tris–HCl buffer (pH 7.2), 75 µL of 0.04 mol/L GSH (reduced form), 100 µL of 0.1 mol/L nicotinamide adenine dinucleotide phosphate

(NADPH), and 100 µL of glutathione reductase (0.24 unit). One hundred microliters (1.75–2.00 mg protein) of the flies' homogenate was added to 2.8 mL of the reaction mixture and incubated at 25 °C for 5 min. The reaction was initiated by adding 100 µL of 0.75 mmol/L H_2O_2, and the absorbance was read at 340 nm for 5 min (Paglia and Valentine 1967).

6.3.5.11Angiotensin-converting enzyme (ACE)

The reaction mixture consisted of 0.2 mL hippuryl-L-histidyl-L-leucine dissolved to 12.5 mM in potassium phosphate-sodium chloride buffer (pH 8.3) and 0.4 mL of the flies' homogenate. The mixture was incubated at 37 °C for 1 h, and 0.5. mL of 1 N HCl was added to terminate the reaction. The absorbance was measured spectrophotometrically at 288 nm. (Cushman and Cheung 1971).

6.3.5.12. Acetylcholinesterase (AChE)

Acetylcholinesterase activity was assayed according to the standard method (Ellman *et al.* 1961). The reaction mixture was made up of 195 µL of distilled water, 20 µL of 60 mM potassium phosphate buffer (pH 8.0), 20 µL of 20 mM DTNB, 5 µL of fly homogenate, and 20 µL of 20 mM acetylthiocholine (as initiator). Thereafter, the reaction was monitored for 3 min (30-s intervals) at 412 nm. The AChE activity was thereafter calculated and expressed as U/mg protein.

6.3.5.13. Monoamine oxidase (MAO)

Briefly, the reaction mixture contained 200 µL of phosphate buffer (0.1 M, pH 7.4), 50 µL of flies' tissue homogenate, 25 µL of benzylamine (10 mM), and 500 µL of distilled water. This was incubated for 30 min, and 10% of perchloric acid was finally added. This was centrifuged at 1500 x *g* for 10 min, the supernatant was decanted, and the absorbance was taken in a spectrophotometer at 280 nm. The MAO activity was calculated and expressed as U/mg protein (Holt *et al.* 1997).

6.3.6. RNA isolation and mRNA expression analysis by RT-PCR

About 2 µg of total RNA was isolated from 25 flies per group using Trizol reagent (Invitrogen). The flies were homogenized in Trizol reagent (1 mL/100 mg tissue) and incubated at room temperature for 5 min. Chloroform (200 µL/1 mL Trizol used) was added to the mixture and mixed thoroughly before centrifuging (12000 g) for 15 min at 4 °C. The topmost layer, which contains the RNA, was pipetted into a new tube, and 500 µL isopropanol (for 1 mL Trizol) was added and incubated at room temperature for 15 min. The tube was centrifuged at 12000 g for 10 min at 4

°C, the supernatant was discarded, while the RNA pellet was washed with 70% ethanol and air-dried. The primer sequences for the genes determined in this study are shown in Table 6.1. Gene-specific primer sequences were based on published sequences in GenBank Overview (http://www.ncbi.nlm.nih.gov/genbank/), designed with the Primer3 program version 0.4.0 (http://frodo.wi.mit.edu/primer3/), and custom-made by Invitrogen1 (Table 1). After quantification, total RNA was treated with DNase I (Invitrogen1). Quantitative real-time polymerase chain reaction (qRT-PCR) was performed in 20 µL of reaction mixture containing 1 µL RT product (cDNA) as a template, 1 x PCR buffer, 25 µM dNTPs, 0.2 mM of each primer, 1.5–2.5 mM $MgCl_2$, 0.1 x SYBR GreenI Molecular Probes1, and 1 U Taq DNA polymerase (Invitrogen). The thermal cycle was done in a Thermocycler StepOne Plus (Applied Biosystems), and the protocol was performed as follows: Activation of the Taq DNA polymerase at 95 °C for 5 min, followed by 40 cycles of 15 s at 95 °C, 15 s at 60 °C, and 25 s at 72 °C. SYBR fluorescence was analyzed by Step One software version 2.0 (Applied Biosystems, NY), and the CT value for each sample was calculated using the $2-\Delta\Delta CT$ method. Glycerol 3-phosphate dehydrogenase (GPDH) was used as the reference gene. Each well was analyzed in quadruplicate, and the ΔCT value was obtained by subtracting the GPDH CT value from the CT value for each of the genes of interest. The experiment was repeated three times, and qRT-PCR quantification was performed in triplicate.

6.3.7. Statistical analysis

Analyses of data for survival and longevity were carried out using the Kaplan-Meier method, and comparisons were made using percentage survival. The biochemical data are presented as the Mean ± SEM of triplicate determinations. One-way Analysis of variance (ANOVA) was used to assess the significant differences among multiple groups under various treatments, followed by the Tukey post hoc test. Statistical significance was considered at $p < 0.05$, using the GraphPad Prism 8 statistical package.

Table 6.1. Sequence of RT-qPCR primers

Gene	Position	Primer sequence
SOD1	Left	5'-GGA GTC GGT GAT GTT GAC CT-3'
	Right	5'-GTT CGG TGA CAA CAC CAA TG-3'
CAT	Left	5'-AAC TTC TTG GCC TGC TCG TA-3'
	Right	5'-ACC AGG GCA TCA AGA ATC TG-3'
Dfoxo	Left	5'-TCG AGT GCA ATG TCG AGG AG-3'
	Right	5'-TCG AGT GCA ATG TCG AGG AG-3'
DILP2	Left	5'-GAT CCT CAA GCT GGC TTT GC-3'
	Right	5'-CTG GAC AAA CTG CAG GGG AT-3'
GAPDH	Left	5'-GCT CCT CAA TGG TTT TTC CA-3'
	Right	5'-ATG GAG ATG ATT CGC TTC GT-3'

6.4. Results

Figure 6.1 shows the effect of supplementation of the diet with fresh and dry infusions of lemongrass on the lifespan of *Drosophila melanogaster*. The control and 0.1 mg/mL group of the fresh lemongrass infusion lived for 32 days while the 0.2, 0.4, and 0.8 mg/mL groups lived for 34, 38, and 39 days, respectively (Fig. 6.1A1). Therefore, the exposure of flies to 0.2, 0.4, and 0.8 mg/mL of fresh lemongrass infusion extends the lifespan of the flies by 6.25, 18.75, and 21.88%, respectively (Fig. 61A2). Compared to the control, different concentrations (0.1, 0.2, 0.4, and 0.8 mg/mL) of dry lemongrass infusion extend the lifespan of the flies by 2, 2, 5, and 8 days, respectively (Fig. 6.1B1). The percentage increase in the lifespan of the flies on exposure to 0.1, 0.2, 0.4, and 0.8 mg/mL dry lemongrass infusion is 6.06, 6.06, 15.15, and 24.24%, respectively (Fig. 6.1B2).

The effect of diet supplementation with fresh and dry infusions of lemongrass on the climbing activity, protein, glucose, and triglyceride levels of D-galactose-induced ageing in *Drosophila melanogaster* is shown in Figure 6.2. Exposure to D-galactose significantly reduced ($p < 0.05$) the climbing activity of the flies and only dry lemongrass infusion tended to restore it (Fig. 6.2a). The protein levels of the flies across all groups were not affected by the different treatments (Fig. 6.2b).

When exposed to D-galactose, there was significant elevation ($p < 0.05$) in the glucose (Fig. 6.2c) and triglyceride concentration of the flies (Fig. 6.2d). However, supplementation with both fresh and dry lemongrass infusions reduced the glucose and triglyceride concentration.

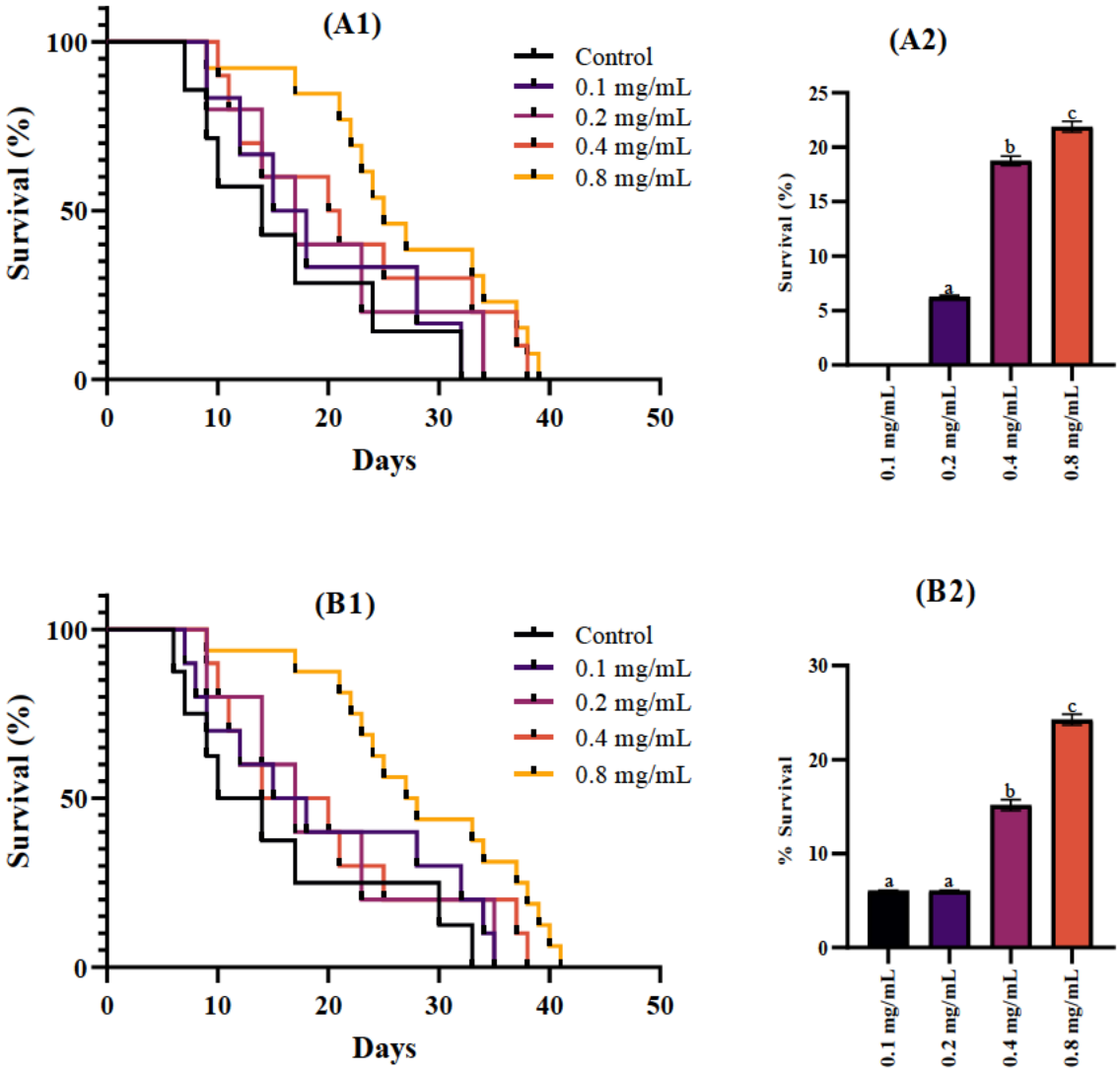

Figure 6.1. Effect of dietary inclusion of (A1) fresh and (B1) dry infusions of lemongrass on the longevity of *Drosophila melanogaster*. Percentage increase in the lifespan of *Drosophila melanogaster* after exposure to (A2) fresh and (B2) dry infusions of lemongrass. Bars with different letters are statistically different ($p < 0.05$).

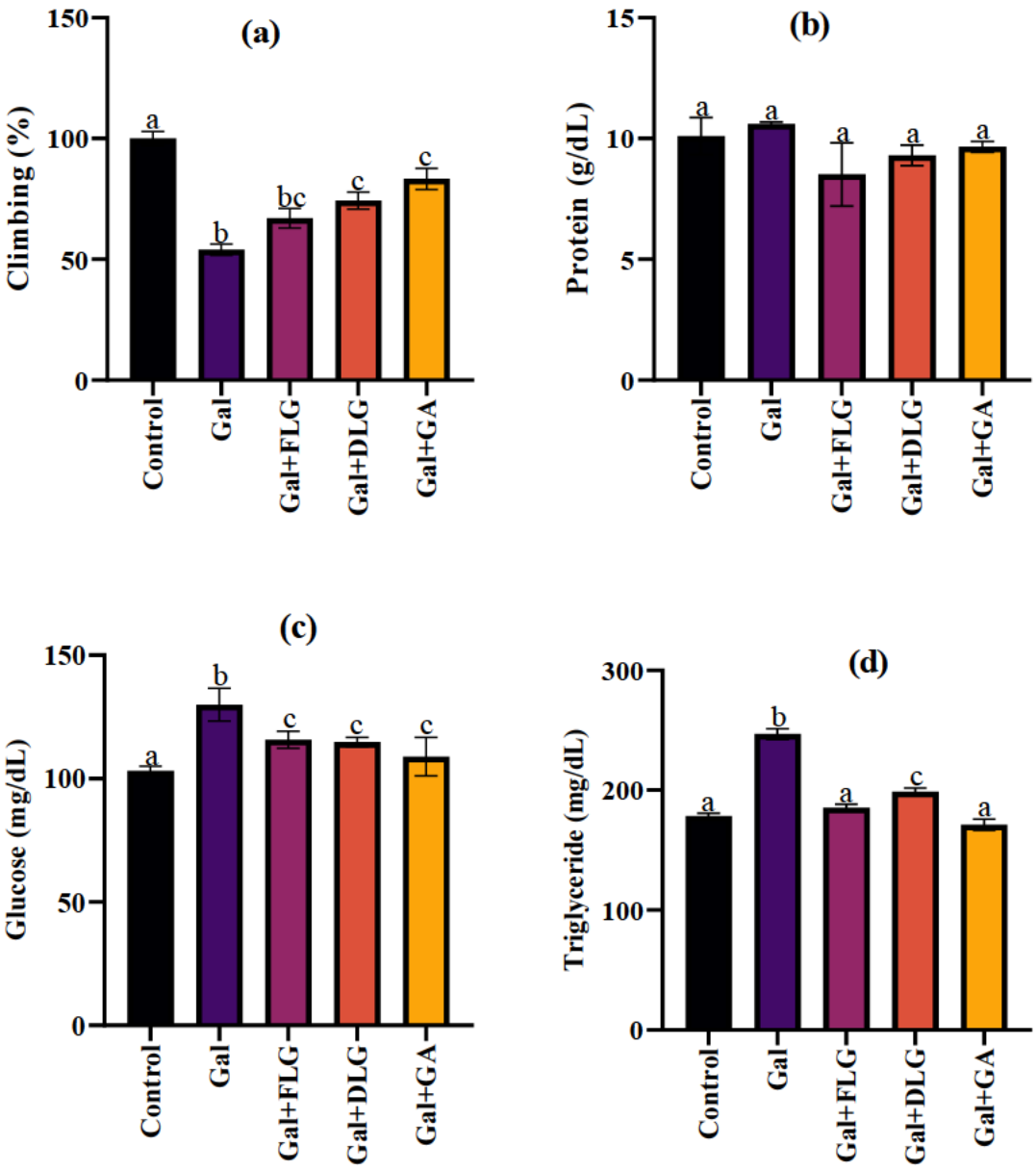

Figure 6.2. Effect of dietary inclusion of fresh and dry infusions of lemongrass on (a) climbing activity (b) protein (c) glucose and (d) triglyceride level in galactose-induced ageing in *Drosophila melanogaster*. Bars with different letters are statistically different ($p < 0.05$). Control: Normal control, Gal: Galactose-treated only, Gal+FLG: Galactose and fresh lemongrass infusion treated, Gal+DLG: Galactose and dry lemongrass infusion treated, Gal+GA: Galactose and gallic acid treated.

Figure 6.3 shows the effect of supplementation of diets with fresh and dry lemongrass infusions on the antioxidant status of D-galactose-induced ageing in *Drosophila melanogaster*. While exposure to D-galactose caused a significant increase in the malondialdehyde concentration ($p < 0.05$), fresh and dry lemongrass infusions reduced it up to the level of the control (Fig. 6.3a). The thiol (Fig. 6.3b) and reduced glutathione (Fig. 6.3c) concentrations significantly reduced ($p < 0.05$) in all categories of the flies except the positive control (group treated with D-galactose and gallic acid). Exposure of the flies to D-galactose caused a significant rise ($p < 0.05$) in the hydrogen peroxide level, and both the fresh and dry lemongrass infusions brought it down (Fig. 6.3d).

The influence of supplementation of diet with fresh and dry lemongrass infusions on the activities of antioxidant enzymes of D-galactose-induced ageing in *Drosophila melanogaster* is shown in Figure 6.4. The activity of superoxide oxidase (SOD) significantly decreased ($p < 0.05$) in the flies exposed only to D-galactose (Fig. 6.4a). However, supplementation of the diet with dry lemongrass infusion improved it, and this is comparable to the positive control (gallic acid). The reduced catalase activity in the D-galactose-exposed flies was reversed by supplementation of the diet with fresh and dry lemongrass infusions (Fig. 6.4b). Exposure of the flies to D-galactose caused a significant reduction ($p < 0.05$) in the glutathione peroxidase level, and treatment with fresh lemongrass ameliorated, and this is similar to gallic acid (Fig. 6.4c).

Figure 6.5 shows the effect of supplementation of the diet with fresh and dry lemongrass infusions on some neurologically-related enzymes of D-galactose-induced ageing in *Drosophila melanogaster*. The activity of angiotensin-converting enzyme (ACE) was not affected by the supplementation of the diet with both D-galactose and lemongrass infusions (Fig. 6.5a). Exposure of the flies to D-galactose significantly elevated ($p < 0.05$) the acetylcholinesterase (AChE) (Fig. 6.5b) and monoamine oxidase (MOA) (Fig. 6.5c) activities of the flies. While the supplementation of the diet by both fresh and dry lemongrass infusions restored the acetylcholinesterase to the level of the control, only the dry lemongrass infusion restored the monoamine oxidase activity to the level of the control flies.

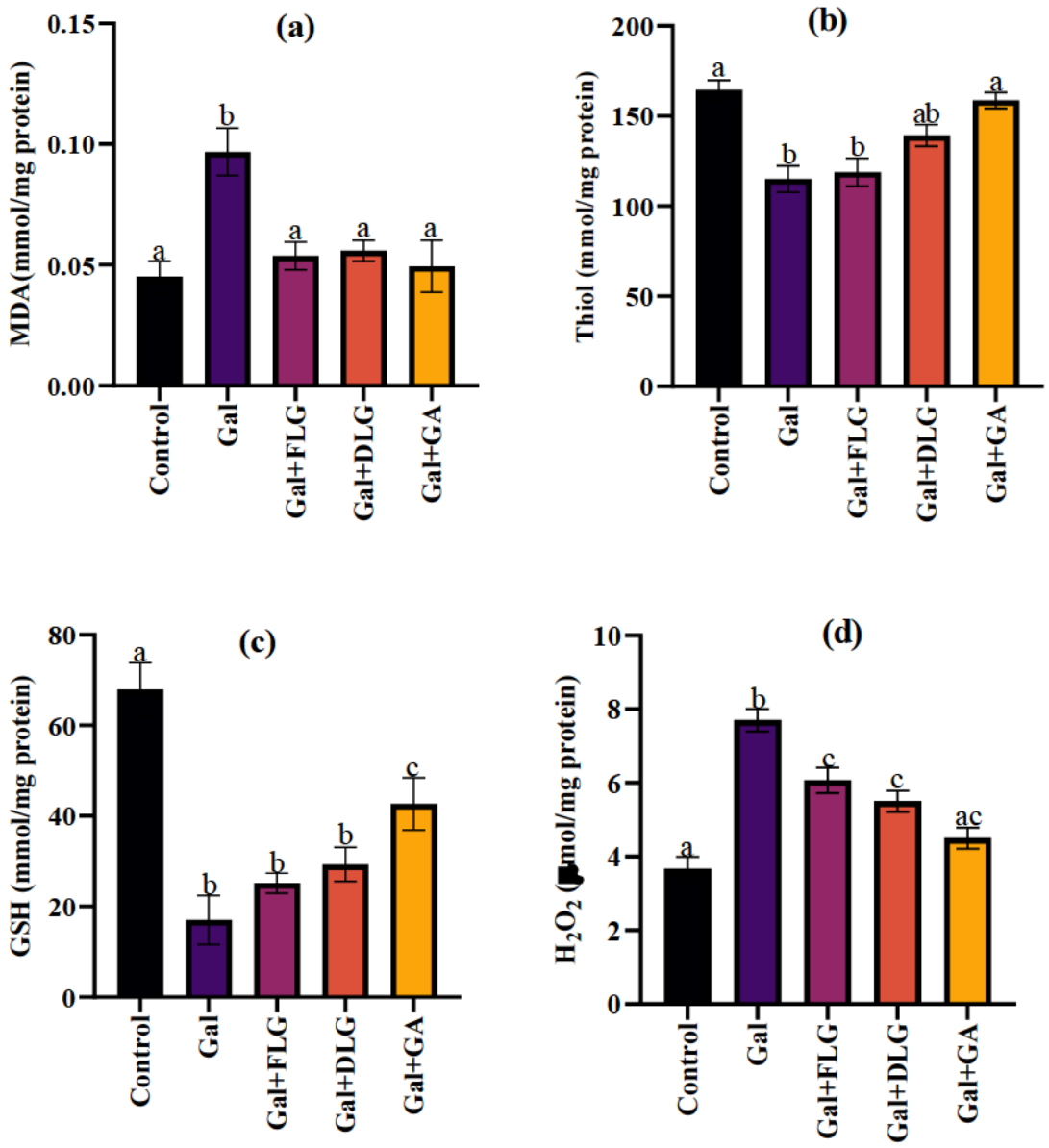

Figure 6.3. Effect of dietary inclusion of fresh and dry infusions of lemongrass on antioxidant status (a) malondialdehyde (b) thiol (c) reduced glutathione (GSH) and (d) hydrogen peroxide level in galactose-induced ageing in *Drosophila melanogaster*. Bars with different letters are statistically different ($p < 0.05$). Control: Normal control, Gal: Galactose-treated only, Gal+FLG: Galactose and fresh lemongrass infusion treated, Gal+DLG: Galactose and dry lemongrass infusion treated, Gal+GA: Galactose and gallic acid treated.

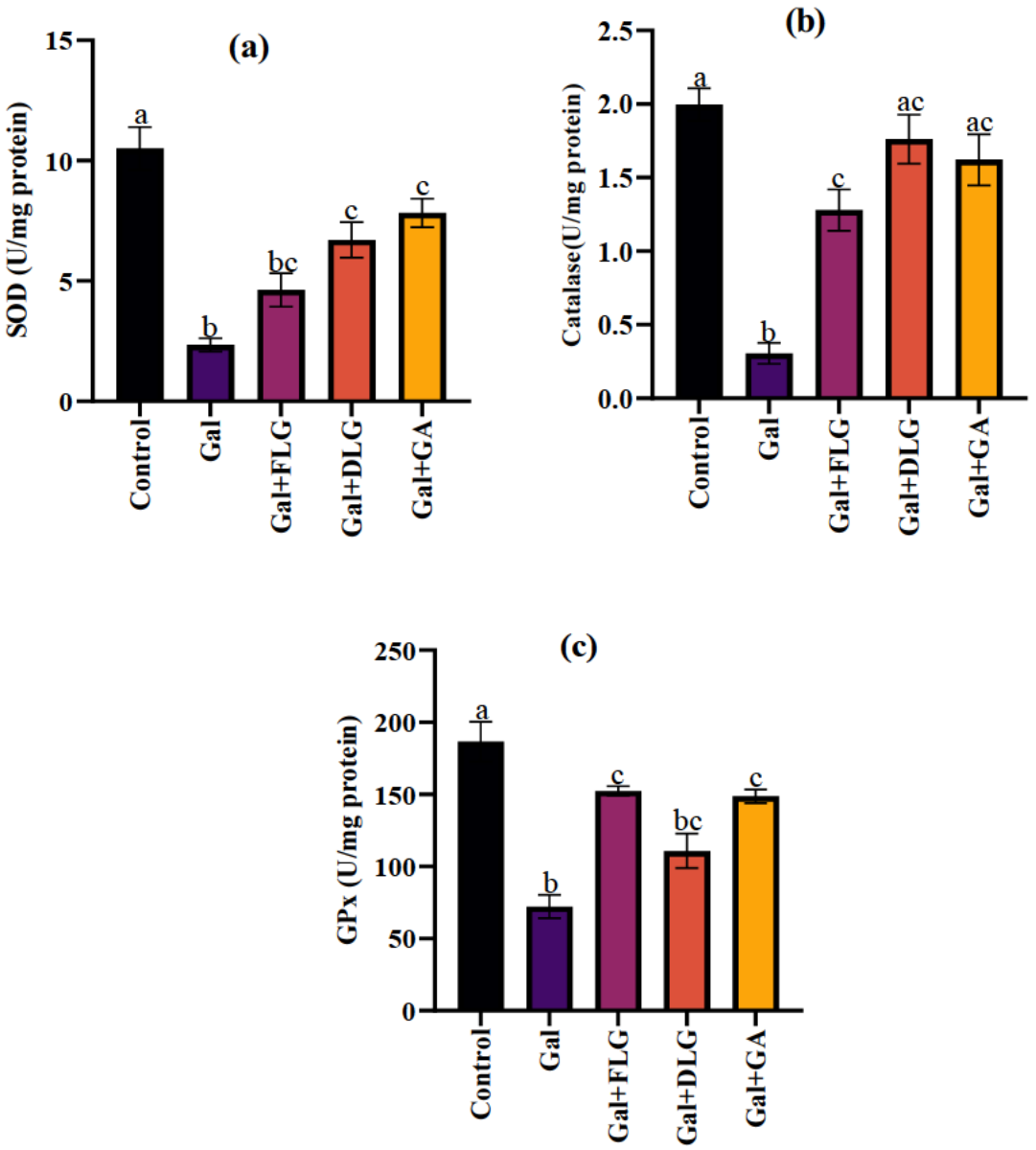

Figure 6.4. Effect of dietary inclusion of fresh and dry infusions of lemongrass on antioxidant enzymes (a) superoxide dismutase (SOD) (b) catalase and (c) glutathione peroxidase (GPx) concentration in galactose-induced ageing in *Drosophila melanogaster*. Bars with different letters are statistically different ($p < 0.05$). Control: Normal control, Gal: Galactose-treated only, Gal+FLG: Galactose and fresh lemongrass infusion treated, Gal+DLG: Galactose and dry lemongrass infusion treated, Gal+GA: Galactose and gallic acid treated.

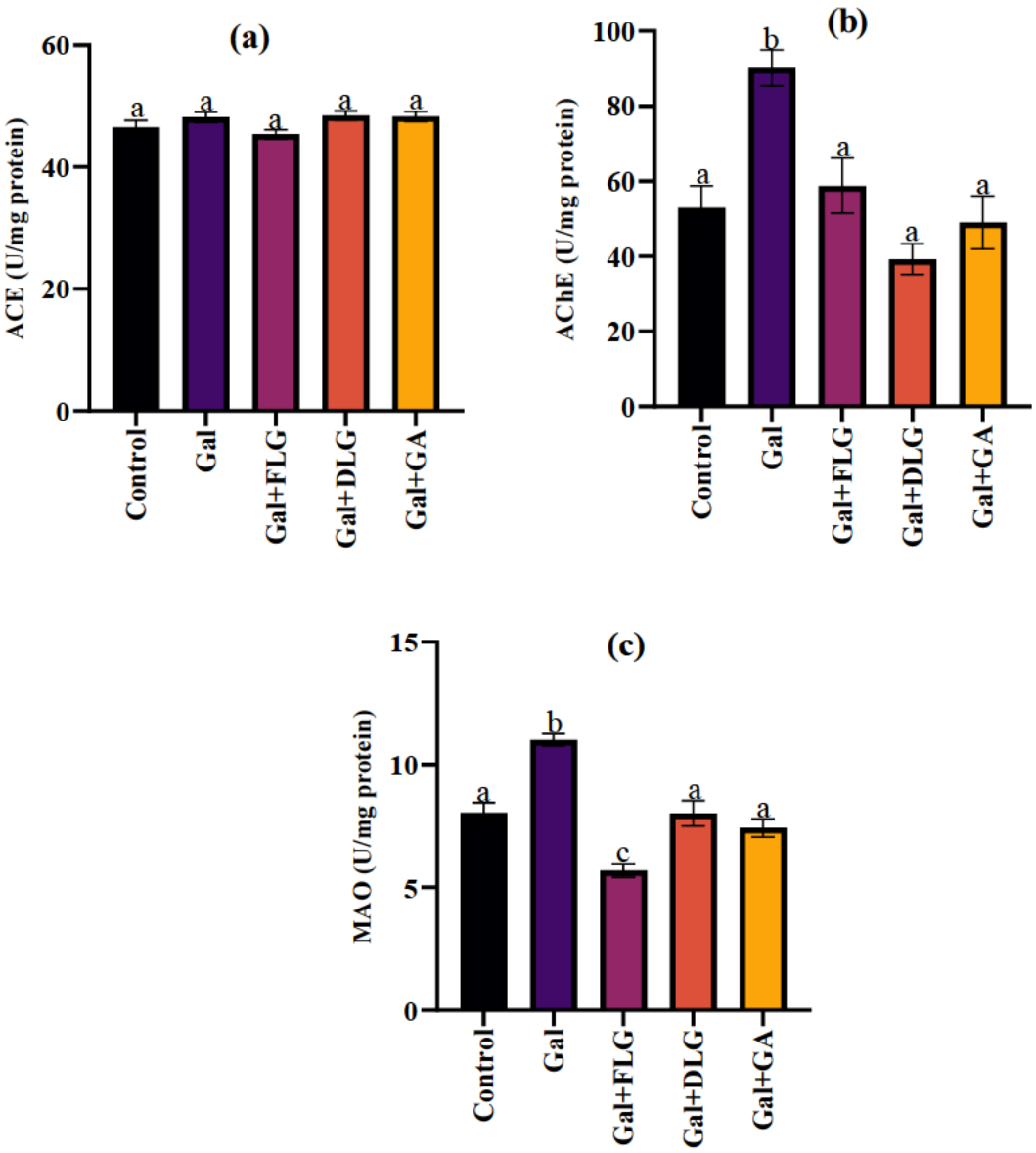

Figure 6.5. Effect of dietary inclusion of fresh and dry infusions of lemongrass on (a) angiotensin-converting enzyme (ACE) (b) acetylcholinesterase (AChE) and (c) monoamine oxidase (MAO) concentration in galactose-induced ageing in *Drosophila melanogaster*. Bars with different letters are statistically different ($p < 0.05$). Control: Normal control, Gal: Galactose-treated only, Gal+FLG: Galactose and fresh lemongrass infusion treated, Gal+DLG: Galactose and dry lemongrass infusion treated, Gal+GA: Galactose and gallic acid treated.

The effect of supplementation of diet with fresh and dry lemongrass infusions on the expression of some ageing-related genes of D-galactose-induced ageing in *Drosophila melanogaster* are shown in Figure 6.6 and Appendix 6.1. The expression of SOD1 was significantly reduced ($p < 0.05$) in the D-galactose-fed flies, and supplementation with dry lemongrass infusion reversed it similar to the control (Fig. 6.6a). The decrease ($p < 0.05$) in the expression of catalase witnessed in the D-galactose-fed flies was ameliorated by the inclusion of dry lemongrass infusion (Fig. 6.6b). The D-galactose-treated flies experienced a significant reduction ($p < 0.05$) in the expression of the dFOXO gene, and inclusion of both fresh and dry lemongrass infusions counteracted the trend (Fig. 6.6c). Treatment of flies with D-galactose significantly increased the expression of Drosophila insulin-like peptide 2 (DILP2) and inclusion of dry lemongrass infusion in their diet alleviated it (Fig. 6.6d).

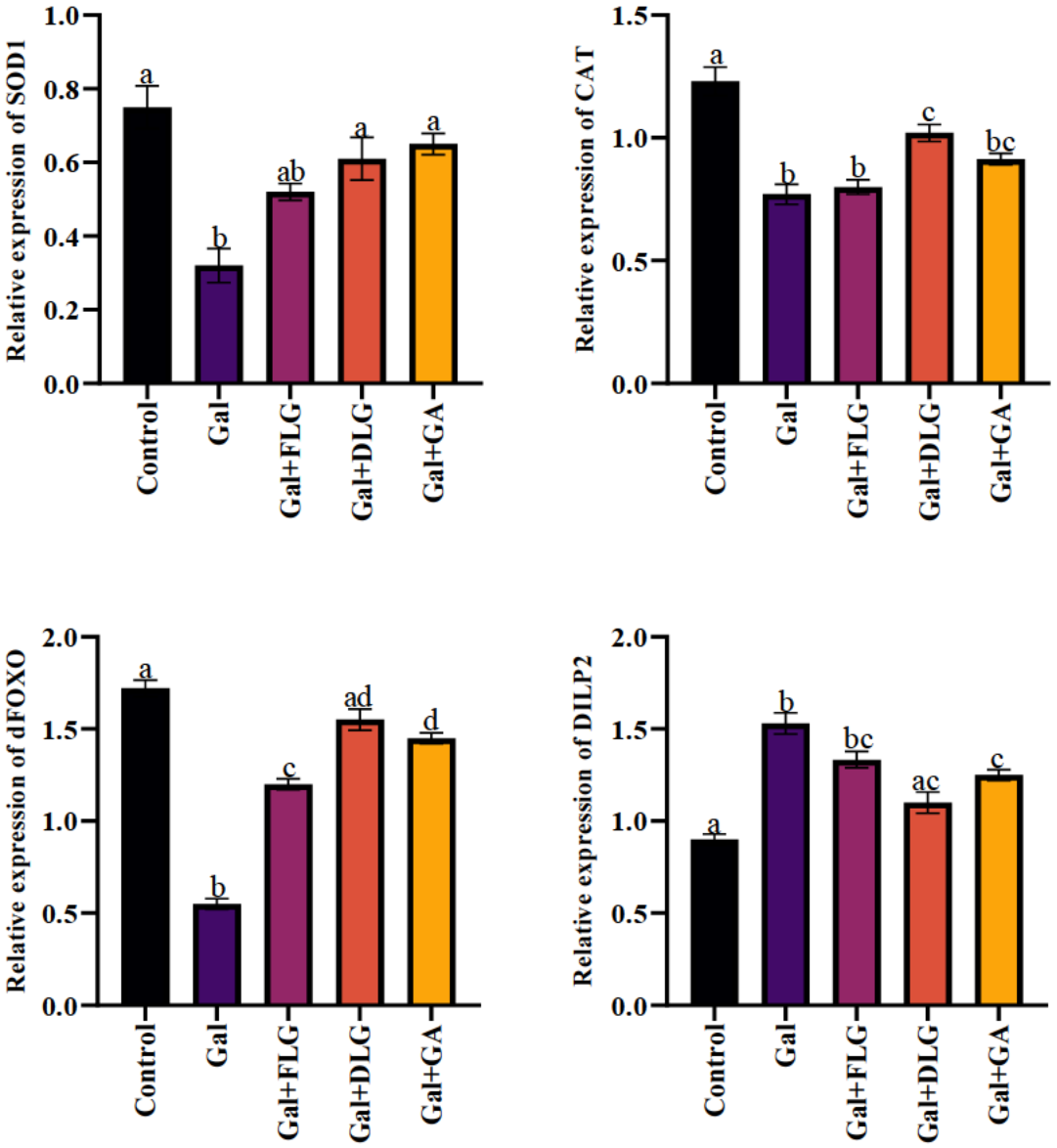

Figure 6.6. Effect of dietary inclusion of fresh and dry infusions of lemongrass on the expression of (a) superoxide dismutase 1 (SOD1) (b) catalase (CAT) (c) forkhead box O-3 (FOXO3) and (d) drosophila insulin-like peptide 2 (DILP2) gene in galactose-induced ageing in *Drosophila melanogaster*. Bars with different letters are statistically different ($p < 0.05$). Control: Normal control, Gal: Galactose-treated only, Gal+FLG: Galactose and fresh lemongrass infusion treated, Gal+DLG: Galactose and dry lemongrass infusion treated, Gal+GA: Galactose and gallic acid treated.

6.5. Discussion

This study evaluated the therapeutic effect of fresh and dry lemongrass infusions on the metabolic derangements in D-galactose-induced ageing in *Drosophila melanogaster*. The inclusion of excess D-galactose in the diet of fruit flies may produce galactitol, causing mitochondrial dysfunction (Oyebode *et al.* 2020). The excess D-galactose may also be oxidized to hydrogen peroxide, thereby decreasing superoxide dismutase (SOD) concentration and impairing redox homeostasis (Zhang *et al.* 2020). Non-enzymatic glycation can also occur from the excess D-galactose, leading to the production of Amadori products and advanced glycation end products (AGE) (Lin *et al.* 2018). The trio of mitochondrial dysfunction, impaired redox homeostasis, and formation of advanced glycation end products (AGEs) increased the level of reactive oxygen species and caused oxidative stress (Azman and Zakaria 2019). The onset of oxidative stress may cause cellular apoptosis, cognitive defects, and degenerative changes that are associated with ageing (Cui *et al.* 2004).

The observation that different concentrations of fresh and dry lemongrass extend the lifespan of the fruit flies attests to the beneficial effect of the lemongrass on ageing (Oyebode *et al.* 2020). It is also noted that the higher the concentration of the infusion, the longer the lifespan of the flies, which implies that the effect is dose-dependent. This agrees with previous studies that the lifespan of fruit flies is strongly associated with oxidative stress, and the inclusion of antioxidants can mitigate this (Wang *et al.* 2014; Lin *et al.* 2018). It therefore means that lemongrass infusions may be rich in antioxidants to extend the lifespan of the flies.

The reduced climbing activity of the D-galactose-fed flies showed that D-galactose caused metabolic derangements in them, which impaired their physical activity (Cui *et al.* 2004). This makes the flies weak and less active when compared to the control flies. This is one of the indicators of ageing in all categories of organisms. The inclusion of dry lemongrass infusion in the diet improved the climbing activity of the flies, which suggests that lemongrass may ameliorate the weakness. The increase in the glucose and triglyceride concentration of the D-galactose-treated flies compared to the control may imply that the carbohydrate and lipid metabolism were adversely affected by D-galactose (Oyeniran, Ademiluyi and Oboh 2021). However, the glucose and triglyceride content were restored in the lemongrass infusion-treated flies, which may suggest amelioration of the metabolic derangement caused by D-galactose.

The induction of ageing by D-galactose causes several pathologies that are mediated by oxidative stress. Therefore, we evaluated the antioxidant status of the flies following treatment with D-galactose and lemongrass infusions. Malondialdehyde (MDA) is a product formed when polyunsaturated fatty acids are degraded by reactive oxygen species and serves as a marker of lipid peroxidation (Mora *et al.* 2014). The increase in the MDA level of the D-galactose-fed flies indicated that there is extensive lipid peroxidation in the flies, but this was counteracted by the fresh and dry lemongrass infusions. The hydrogen peroxide level in the galactose-treated flies is markedly high, which may be responsible for the injuries to protein, lipids, and DNA (Baek, Jang and Kim 2022). The fact that the inclusion of lemongrass infusion exacerbated the H_2O_2 level indicates that the phytochemicals in it may mop it up from the system. Thiols are organic compounds that have sulfhydryl groups and play a significant role in defending the body against the onslaught of ROS (Orr, Radyuk and Sohal 2013). One of the thiol compounds is reduced glutathione (GSH), and its activity contributes to the thiol level. It is observed that the reduced level of thiol and GSH in the D-galactose-treated group were ameliorated by the lemongrass infusion, especially the dry lemongrass infusion. This implies that lemongrass infusions contributed to the antioxidant status of the flies.

An important mechanism by which organisms protect themselves from oxidative stress is through the activities of antioxidant enzymes, including superoxide dismutase (SOD), catalase, and glutathione peroxidase (GPx). SOD catalyzes the conversion of superoxide radicals to hydrogen peroxide, while catalase converts hydrogen peroxide to water and molecular oxygen (Shen *et al.* 2013). Glutathione peroxidase (GPx), on the other hand, protects organisms from oxidative damage by reducing hydroperoxides to their hydroxyl counterparts (Flohé, Toppo and Orian 2022). The level of SOD, catalase, and GPx in the D-galactose-fed flies was very low, and this may indicate that the antioxidant status of these flies has been depleted, and so susceptible to oxidative stress (Deepashree, Shivanandappa and Ramesh 2022). This is corroborated by the high level of MDA and H_2O_2, as well as the low level of GSH and thiol in this group. The supplementation of the diet with the lemongrass infusion counteracted this reduction, which suggests that the lemongrass infusion serves as an antioxidant that protects the flies from oxidative stress.

Previous studies revealed that older people are more susceptible to hypertension and neurodegenerative disorders. This is what necessitated the assessment of some enzymes that are

involved in hypertension and neurodegeneration. Angiotensin-converting enzyme (ACE) is a major component of the renin-angiotensin system and is responsible for the maintenance of normal blood pressure and electrolyte balance (Coates 2003). The fact that the ACE level was not affected by treatment with D-galactose and lemongrass infusion may imply that this model of ageing does not affect the electrolyte balance of the flies. Acetylcholinesterase (AChE) is an enzyme that hydrolyses the neurotransmitter, acetylcholine, which controls locomotion, memory, and learning (Jha and Rizvi 2009), while monoamine oxidase (MAO) is involved in the oxidative deamination of biogenic amines such as dopamine and serotonin to their corresponding aldehyde and free amines (Ogunsuyi, Ademiluyi and Oboh 2020). D-galactose adversely increased the AChE and MOA levels of the flies, which suggests the onset of neurodegeneration (Yılmaz *et al.* 2013). However, the dietary inclusion of lemongrass infusions reversed this trend by normalizing the AChE and MAO levels. This may be due to the abundance of bioactive compounds in lemongrass.

Though reactive oxygen species are crucial in several biochemical activities, their overproduction may cause oxidative damage to cellular biomolecules, including DNA, proteins, and lipids (Ogunsuyi, Ademiluyi and Oboh 2020). The fact that the SOD1 and CAT genes are down-regulated in the D-galactose-fed flies aligns with the results obtained from the SOD and catalase activities. This confirms that reactive oxygen species were generated in these flies, and they overwhelm the system, which leads to oxidative stress (Deepashree, Shivanandappa and Ramesh 2022). Though SOD and catalase are antioxidant enzymes that should physiologically mop up these ROS, their down-regulation in this study may imply that D-galactose toxicity has depleted the antioxidant capacity of the flies (Cui *et al.* 2004). However, dry lemongrass infusion-treated flies witnessed improvement in the expression of the SOD1 and CAT genes, suggesting that the antioxidant property of the plant can counteract the ROS-mediated downregulation of both genes.

Drosophila Forkhead Box O (dFOXO) is a transcription factor that plays an important role in regulating cellular processes in *Drosophila melanogaster* (Hwangbo et al. 2004). This factor regulates the metabolism of biomolecules, thereby affecting growth and energy homeostasis (Slack *et al.* 2011). It also regulates the stress response of the fly to environmental factors. It also influences cell proliferation and differentiation, thereby controlling the cell cycle. Previous studies have reported that the deregulation of dFOXO is implicated in ageing and its associated diseases like diabetes and neurodegenerative disorders (Morris *et al.* 2015; Martins, Lithgow and Link

2016). The downregulation of the dFOXO gene experienced by the D-galactose-fed flies suggests that the dFOXO protein is impaired in response to the excessive ROS presence in the flies (Ogunsuyi *et al.* 2022). However, the presence of the lemongrass infusions upregulated the dFOXO gene, suggesting its antioxidant property. This conforms with the concurrent upregulation of the SOD1 and CAT genes, thereby empowering the flies to mop up free radicals and ameliorate ageing.

Drosophila insulin-like peptides (DILPs) are hormones, like insulin present in mammals, which regulate various physiological processes in *Drosophila melanogaster* (Semaniuk et al. 2021). They play a key role in regulating the metabolism, growth, reproduction, and lifespan of the flies (Bai, Kang and Tatar 2012). Several studies have revealed the important role of DILP2 in nutrient metabolism and the lifespan of flies (Semaniuk *et al.* 2021; Qian and Niwa 2023). The observed upregulation of the DILP2 gene in the D-galactose-fed flies may imply that the metabolism and lifespan of the flies have been impaired, leading to decreased lifespan (Montaser *et al.* 2024). Previous studies have shown that lifespan is extended when the DILP2 gene is downregulated and shortened when it is upregulated (Kannan and Fridell 2013). The supplementation of diet with dry lemongrass infusion counteracted the effect of D-galactose by normalizing the expression of the DILP2 gene. This agrees with the previous report that phenolic-rich plants compromise insulin signaling by phosphorylating the insulin receptor and the insulin-receptor substrate (Montaser *et al.* 2024).

6.6. Conclusion

This study, for the first time, evaluated the ameliorative potential of fresh and dry infusion of lemongrass in D-galactose-induced ageing in *Drosophila melanogaster*. Fresh and dry lemongrass infusion caused 22% and 24% extension in the lifespan of the flies. After 14-day treatment, dry lemongrass infusion restored the antioxidant status of the flies, modulated the antioxidant enzymes' activities, and normalized the activity of acetylcholinesterase and monoamine oxidase. The dry lemongrass infusion also upregulated the expression of SOD1, CAT, and dFOXO genes while downregulating the DILP2 gene. It can be concluded that both fresh and dry lemongrass infusions prolong the lifespan of the flies. However, dry lemongrass infusion sustained this

extension via modulation of key pathways involved in ageing, including insulin signaling and antioxidant pathways. This may be due to higher quantities of phytochemicals such as lonicerin, kaempferitrin, and neocuscutoside C in the dry lemongrass infusion. Further studies are needed to isolate the bioactive compounds responsible for the anti-ageing effects of lemongrass tea.

6.7. References

Aebi, H. 1984. Catalase *in vitro*. In: *Methods in enzymology*. Elsevier, 121-126.

Azman, K. F. and Zakaria, R. 2019. D-Galactose-induced accelerated aging model: An overview. *Biogerontology*, 20 (6): 763-782.

Baek, M., Jang, W. and Kim, C. 2022. Dual oxidase, a hydrogen-peroxide-producing enzyme, regulates neuronal oxidative damage and animal lifespan in *Drosophila melanogaster*. *Cells*, 11 (13): 2059.

Bai, H., Kang, P. and Tatar, M. 2012. Drosophila insulin-like peptide-6 (dilp6) expression from fat body extends lifespan and represses secretion of Drosophila insulin-like peptide-2 from the brain. *Aging Cell*, 11 (6): 978-985.

Boyd, O., Weng, P., Sun, X., Alberico, T., Laslo, M., Obenland, D. M., Kern, B. and Zou, S. 2011. Nectarine promotes longevity in *Drosophila melanogaster*. *Free Radical Biology and Medicine*, 50 (11): 1669-1678.

Coates, D. 2003. The angiotensin-converting enzyme (ACE). *The International Journal of Biochemistry & Cell Biology*, 35 (6): 769-773.

Cui, X., Wang, L., Zuo, P., Han, Z., Fang, Z., Li, W. and Liu, J. 2004. D-galactose-caused life shortening in *Drosophila melanogaster* and *Musca domestica* is associated with oxidative stress. *Biogerontology*, 5: 317-325.

Cushman, D. W. and Cheung, H. S. 1971. Spectrophotometric assay and properties of the angiotensin-converting enzyme of rabbit lung. *Biochemical Pharmacology*, 20 (7): 1637-1648.

Deepashree, S., Shivanandappa, T. and Ramesh, S. R. 2022. Genetic repression of the antioxidant enzymes reduces the lifespan in *Drosophila melanogaster*. *Journal of Comparative Physiology B*, 192 (1): 1-13.

Ekpenyong, C. E., Akpan, E. and Nyoh, A. 2015. Ethnopharmacology, phytochemistry, and biological activities of *Cymbopogon citratus* (DC.) Stapf extracts. *Chinese Journal of Natural Medicines*, 13 (5): 321-337.

Ekpenyong, C. E. and Akpan, E. E. 2017. Use of *Cymbopogon citratus* essential oil in food preservation: Recent advances and future perspectives. *Critical Reviews in Food Science and Nutrition*, 57 (12): 2541-2559.

Ellman, G. L. 1959. Tissue sulfhydryl groups. *Archives of Biochemistry and Biophysics*, 82 (1): 70-77.

Ellman, G. L., Courtney, K. D., Andres Jr, V. and Featherstone, R. M. 1961. A new and rapid colorimetric determination of acetylcholinesterase activity. *Biochemical Pharmacology*, 7 (2): 88-95.

Flohé, L., Toppo, S. and Orian, L. 2022. The glutathione peroxidase family: Discoveries and mechanism. *Free Radical Biology and Medicine*, 187: 113-122.

Grinin, L., Grinin, A. and Korotayev, A. 2023. Global aging: An integral problem of the future. how to turn a problem into a development driver? In: *Reconsidering the limits to growth: A report to the Russian association of the club of Rome*. Springer, 117-135.

Gurib-Fakim, A. 2006. Medicinal plants: Traditions of yesterday and drugs of tomorrow. *Molecular Aspects of Medicine*, 27 (1): 1-93.

Higo, M. and Khan, H. T. 2015. Global population aging: Unequal distribution of risks in later life between developed and developing countries. *Global Social Policy*, 15 (2): 146-166.

Holt, A., Sharman, D. F., Baker, G. B. and Palcic, M. M. 1997. A continuous spectrophotometric assay for monoamine oxidase and related enzymes in tissue homogenates. *Analytical Biochemistry*, 244 (2): 384-392.

Hwangbo, D. S., Gersham, B., Tu, M.-P., Palmer, M. and Tatar, M. 2004. Drosophila dFOXO controls lifespan and regulates insulin signalling in brain and fat body. *Nature*, 429 (6991): 562-566.

Jennings, B. H. 2011. Drosophila–a versatile model in biology & medicine. *Materials Today*, 14 (5): 190-195.

Jha, R. and Rizvi, S. I. 2009. Age-dependent decline in erythrocyte acetylcholinesterase activity: correlation with oxidative stress. *Biomedical Papers of the Medical Faculty of the University of Palacky, Olomouc, Czech Republic*, 153 (3): 195-198.

Kannan, K. and Fridell, Y.-W. C. 2013. Functional implications of Drosophila insulin-like peptides in metabolism, aging, and dietary restriction. *Frontiers in Physiology*, 4: 288.

Kazeem, M. I., Mellem, J. J. and Sabiu, S. 2024. Medicinal foods and plants with antiaging properties: A review of *in vitro* and *in vivo* studies. *Food Frontiers*, 5 (1): 24-45.

Lin, L., Yang, K., Zheng, L., Zhao, M., Sun, W., Zhu, Q. and Liu, S. 2018. Anti-aging effect of sea cucumber (*Cucumaria frondosa*) hydrolysate on fruit flies and D-galactose-induced aging mice. *Journal of Functional Foods*, 47: 11-18.

Lowry, O. H., Rosebrough, N. J., Farr, A. L. and Randall, R. J. 1951. Protein measurement with the Folin phenol reagent. *Journal of Biological Chemistry*, 193 (1): 265-275.

Luo, J., Si, H., Jia, Z. and Liu, D. 2021. Dietary anti-aging polyphenols and potential mechanisms. *Antioxidants*, 10 (2): 283.

Marklund, S. and Marklund, G. 1974. Involvement of the superoxide anion radical in the autoxidation of pyrogallol and a convenient assay for superoxide dismutase. *European Journal of Biochemistry*, 47 (3): 469-474.

Martins, R., Lithgow, G. J. and Link, W. 2016. Long live FOXO: Unraveling the role of FOXO proteins in aging and longevity. *Aging Cell*, 15 (2): 196-207.

Montaser, O., El-Aasr, M., Tawfik, H. O., Meshrif, W. S. and Elbrense, H. 2024. *Drosophila melanogaster* as a model organism for diabetes II treatment by the ethyl acetate fraction of *Atriplex halimus* L. *Journal of Experimental Zoology Part A: Ecological and Integrative Physiology*, 341 (6): 702-716.

Mora, M., Bonilla, E., Medina-Leendertz, S., Bravo, Y. and Arcaya, J. L. 2014. Minocycline increases the activity of superoxide dismutase and reduces the concentration of nitric oxide, hydrogen peroxide and mitochondrial malondialdehyde in manganese-treated *Drosophila melanogaster*. *Neurochemical Research*, 39: 1270-1278.

Morris, B. J., Willcox, D. C., Donlon, T. A. and Willcox, B. J. 2015. FOXO3: A major gene for human longevity-a mini-review. *Gerontology*, 61 (6): 515-525.

Negrelle, R. and Gomes, E. 2007. *Cymbopogon citratus* (DC.) Stapf: Chemical composition and biological activities. *Revista Brasileira de Plantas Medicinais*, 9 (1): 80-92.

Ogunsuyi, O. B., Oboh, G., Oluokun, O. O., Ademiluyi, A. O., Ogunruku, O. O. 2020a. Gallic acid protects against neurochemical alterations in transgenic Drosophila model of Alzheimer's disease. *Oriental Pharmacy and Experimental Medicine*, 20: 89-98.

Ogunsuyi, O. B., Ademiluyi, A. O. and Oboh, G. 2020b. Solanum leaf extracts exhibit antioxidant properties and inhibit monoamine oxidase and acetylcholinesterase activities (*in vitro*) in *Drosophila melanogaster*. *Journal of Basic and Clinical Physiology and Pharmacology*, 31 (3).

Ogunsuyi, O. B., Olagoke, O. C., Afolabi, B. A., Oboh, G., Ijomone, O. M., Barbosa, N. V. and da Rocha, J. B. 2022. Dietary inclusions of Solanum vegetables mitigate aluminum-induced redox and inflammation-related neurotoxicity in *Drosophila melanogaster* model. *Nutritional Neuroscience*, 25 (10): 2077-2091.

Ohkawa, H. 1979. Assay for lipid peroxidation in animal tissues by thiobarbituric acid reaction. *Analytical Biochemistry*, 44: 276-278.

Oladeji, O. S., Adelowo, F. E., Ayodele, D. T. and Odelade, K. A. 2019. Phytochemistry and pharmacological activities of *Cymbopogon citratus*: A review. *Scientific African*, 6: e00137.

Orr, W. C., Radyuk, S. N. and Sohal, R. S. 2013. Involvement of redox state in the aging of *Drosophila melanogaster*. *Antioxidants & Redox Signaling*, 19 (8): 788-803.

Oyebode, O. T., Abolaji, A. O., Oluwadare, J. O., Adedara, A. O. and Olorunsogo, O. O. 2020. Apigenin ameliorates D-galactose-induced lifespan-shortening effects via antioxidative activity and inhibition of mitochondrial-dependent apoptosis in *Drosophila melanogaster*. *Journal of Functional Foods*, 69: 103957.

Oyeniran, O. H., Ademiluyi, A. O. and Oboh, G. 2021. Modulatory effects of moringa (*Moringa oleifera* L.) leaves infested with African mistletoe (*Tapinanthus bangwensis* L.) on the antioxidant, antidiabetic, and neurochemical indices in high sucrose diet-induced diabetic-like phenotype in fruit flies (*Drosophila melanogaster* M.). *Journal of Food Biochemistry*, 45 (3): e13318.

Paglia, D. E. and Valentine, W. N. 1967. Studies on the quantitative and qualitative characterization of erythrocyte glutathione peroxidase. *The Journal of Laboratory and Clinical Medicine*, 70 (1): 158-169.

Qian, Q. and Niwa, R. 2023. Endocrine regulation of aging in the fruit fly *Drosophila melanogaster*. *Zoological Science*, 41 (1): 1-10.

Semaniuk, U., Piskovatska, V., Strilbytska, O., Strutynska, T., Burdyliuk, N., Vaiserman, A., Bubalo, V., Storey, K. B. and Lushchak, O. 2021. Drosophila insulin-like peptides: From expression to functions–a review. *Entomologia Experimentalis et Applicata*, 169 (2): 195-208.

Shen, L.-R., Xiao, F., Yuan, P., Chen, Y., Gao, Q.-K., Parnell, L. D., Meydani, M., Ordovas, J. M., Li, D. and Lai, C.-Q. 2013. Curcumin-supplemented diets increase superoxide dismutase activity and mean lifespan in Drosophila. *Age*, 35 (4): 1133-1142.

Slack, C., Giannakou, M. E., Foley, A., Goss, M. and Partridge, L. 2011. dFOXO-independent effects of reduced insulin-like signaling in Drosophila. *Aging Cell*, 10 (5): 735-748.

Suter, B. 2019. Useful flies. *International Journal of Molecular Sciences*, 20: 871..

Tietz, N. W. 1995. Clinical guide to laboratory tests. In: *Clinical guide to laboratory tests*. 1096-1096.

Trinder, P. 1969. Determination of glucose in blood using glucose oxidase with an alternative oxygen acceptor. *Annals of Clinical Biochemistry*, 6 (1): 24-27.

Wang, C., Yolitz, J., Alberico, T., Laslo, M., Sun, Y., Wheeler, C. T., Sun, X. and Zou, S. 2014. Cranberry interacts with dietary macronutrients to promote healthy aging in Drosophila. *Journals of Gerontology Series A: Biomedical Sciences and Medical Sciences*, 69 (8): 945-954.

Wolff, S. P. 1994. Ferrous ion oxidation in the presence of ferric ion indicator xylenol orange for measurement of hydroperoxides. In: *Methods in Enzymology*. Elsevier, 182-189.

Yılmaz, B. S., Altun, M. L., Orhan, I. E., Ergene, B. and Citoglu, G. S. 2013. Enzyme inhibitory and antioxidant activities of *Viburnum tinus* L. relevant to its neuroprotective potential. *Food Chemistry*, 141 (1): 582-588.

Zhang, J., Liu, X., Pan, J., Zhao, Q., Li, Y., Gao, W. and Zhang, Z. 2020. Anti-aging effect of brown black wolfberry on *Drosophila melanogaster* and D-galactose-induced aging mice. *Journal of Functional Foods*, 65: 103724.

CHAPTER 7

7. GENERAL DISCUSSION, CONCLUSION, AND RECOMMENDATIONS

7.1. General Discussion

Old people occupy about 10% of the world population, and this is expected to reach 12% and 16% in 2030 and 2050, respectively (Luo *et al.* 2021). This population of old people experiences ageing, a condition that is characterized by weakness in their physiological and physical activities, leading to morbidity and mortality (Lin *et al.* 2018). Ageing is associated with many diseases such as diabetes mellitus, cancer, hypertension, cardiovascular diseases, and neurodegenerative disorders (Grinin, Grinin and Korotayev 2023). Despite the delicate nature of ageing, there is no specific medicine for the management of the condition.

The human population is blessed with a variety of plants that provide the necessities of life, including food, shelter, and clothing (Bankole *et al.* 2024). In addition to these, they also serve as medicine for the treatment and management of diseases (Gurib-Fakim 2006). These plants include *Ageratum conyzoides*, *Ocimum gratissimum*, *Morinda lucida*, and *Cymbopogon citratus*. *Cymbopogon citratus* (lemongrass) is taken as tea for recreation, as an additive in food preparation, and as medicine to treat diseases like infection, gastrointestinal disturbance, inflammation, and hypertension (Boukhatem *et al.* 2014; Oladeji *et al.* 2019; Govindaraju, Owen and McCaffrey 2022).

This thesis evaluated the anti-ageing properties of lemongrass infusions using *in vitro*, *in silico*, and *in vivo* techniques (Figure 7.1). This study started by evaluating the influence of drying on the nutritional composition, phytochemical constituents, and *in vitro* antioxidant activities of lemongrass infusions. The result revealed that fresh and dry lemongrass infusions are rich in nutrients, minerals, amino acids, and phytochemicals. While fresh tea is richer in nutritional properties, the dry tea contains more phytochemicals. The dry lemongrass tea possessed lower EC_{50} values for the DPPH, hydroxyl, and superoxide radical scavenging abilities, thereby displaying better antioxidant activity. This may be due to higher concentrations of phytochemicals present in the dry lemongrass infusions.

This was followed by the evaluation of the anti-ageing properties of lemongrass infusions via *in vitro* and computational studies. The docking study showed that lonicerin had the lowest docking

score for collagenase and hyaluronidase, while limocitrin-7-(6”-acetylglucoside) and isovitexin-2”-O-arabinoside exhibited the lowest docking scores for elastase and tyrosinase, respectively. Kaempferitrin had the highest number of stable interactions with collagenase and hyaluronidase, while limocitrin-7-(6”-acetylglucoside) and isovitexin-2”-O-arabinoside interacted more with elastase and tyrosinase, respectively. After subjecting the top-hit compounds to ADMET profiling, all the compounds exhibited good distribution, metabolism, and elimination properties. However, kaempferitrin, quercitrin, and kaempferol-3,4-dixyloside had the best absorption tendencies. All the compounds are also deemed safe except kaempferol-3,4-dixyloside (hepatotoxic) and chamaemeloside (nephrotoxic).

Thereafter, the neuroprotective properties of lemongrass infusions were assessed using *in vitro* and *in silico* techniques. This is because neurodegenerative diseases like Alzheimer’s and Parkinson’s disease are common in older people. The i*n vitro* study revealed that both fresh and dry infusions of lemongrass had neuroprotective properties. Of all the phytochemical compounds tested, benzyl alcohol beta-D-rutinoside, kaempferitrin, neocuscutoside C, and aspulvinone H had the highest number of stable interactions with AChE, BChE, BACE-1, and MAO, respectively. While there are previous reports on the neuroprotective potentials of aspulvinone H and kaempferitrin, this study, for the first time, reports the potent neuroprotective properties of benzyl alcohol beta-D-rutinoside and neocuscutoside C.

Lastly, the pro-longevity effect of lemongrass infusions in D-galactose-induced ageing in *Drosophila melanogaster* was investigated. Fresh and dry lemongrass infusion caused 22% and 24% extension in the lifespan of the flies. After 14-day treatment, dry lemongrass infusion restored the antioxidant status of the flies, modulated the antioxidant enzymes’ activities, and normalized the activity of acetylcholinesterase and monoamine oxidase. The dry lemongrass infusion also upregulated the expression of SOD1, CAT, and dFOXO genes while downregulating the DILP2 gene. This anti-ageing activity of the dry lemongrass tea may be due higher abundance of some phytochemicals (including lonicerin, kaempferitrin, and neocuscutoside C) in it than in the fresh tea.

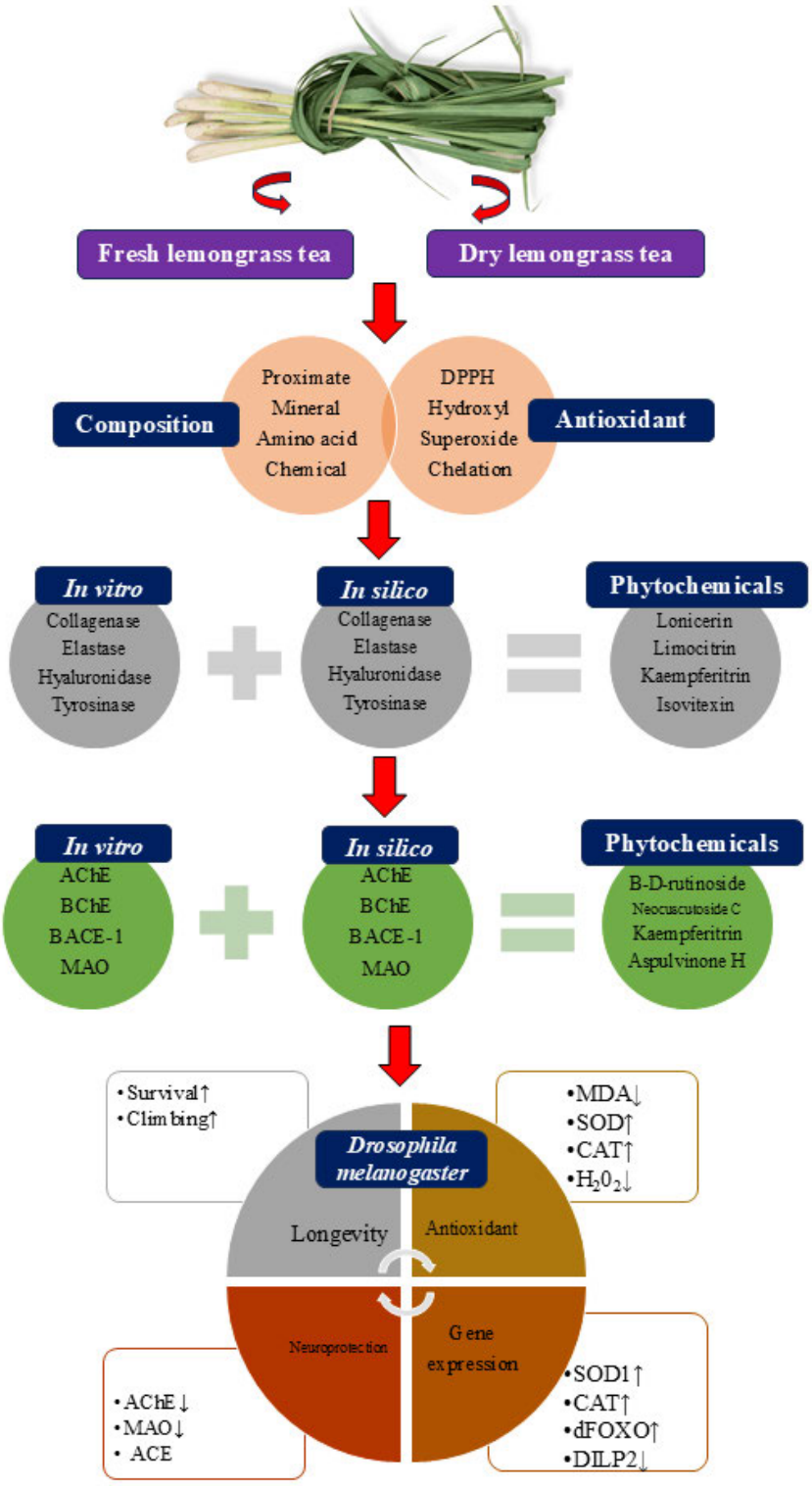

Figure 7.1. Integration of the outcome of all studies performed in this thesis

7.2. General conclusions

Overall, it can be concluded from this project that:

(i) Fresh and dry lemongrass teas are rich in both nutrients and phytochemical compounds. While the fresh infusion is richer in some nutrients, the dry infusion is richer in phytochemical compounds.

(ii) Both the fresh and dry teas possessed antioxidant activities *in vitro*. However, dry lemongrass infusion exhibited better antioxidant properties, possibly due to the richer phytochemical compounds.

(iii) Both the fresh and dry infusions of lemongrass offer neuroprotective properties in both *in vitro* and *in silico* studies. However, the fresh infusion displayed better neuroprotective activity *in vitro*.

(iv) The dry lemongrass teas exhibited a better anti-ageing property than the fresh one in the *in vitro*, *in silico*, and *in vivo* studies. This may be due to the richer content of some phytochemicals like kaempferitrin and isovitexin 2”-O-arabinoside in the dry sample.

(v) The possible mechanism of anti-ageing action of lemongrass teas is through the modulation of the genes in the oxidative stress response and insulin-signaling pathways, including CAT, SOD1, dFOXO, and DILP.

7.3. General recommendations

Arising from the outcome of this study, the following recommendations are suggested:

(i) The consumption of fresh and dry lemongrass teas is safe at 0.8 mg/mL in *Drosophila melanogaster*, and ameliorates ageing and its related complications.

(ii) There is a need to isolate the bioactive compounds responsible for the anti-ageing properties of dry lemongrass tea and test their safety and efficacy.

(iii) Pre-clinical and clinical trials should be performed on anti-ageing properties of the dry lemongrass tea and the lead compounds identified in it.

(iv) Lemongrass tea bags can be developed from dry lemongrass leaves to provide ready-to-drink beverages for consumers.

(v) The lead compounds identified and isolated from the lemongrass can be synthesized and used in the large-scale production of anti-ageing drugs.

7.4. References

Bankole, H. A., Kazeem, M. I., Fatai, A. A., Lawal, R. A., Lawanson, S. O., Ogunyemi, R. T., Ajiboye, T. O. and Olayemi, R. O. 2024. *Citrus aurantifolia* (Christm.) swingle extract ameliorates oxidative stress, dyslipidemia, and inflammation in galactose-induced aging in female rats. *South African Journal of Botany*, 168: 221-226.

Boukhatem, M. N., Ferhat, M. A., Kameli, A., Saidi, F. and Kebir, H. T. 2014. Lemongrass (*Cymbopogon citratus*) essential oil as a potent anti-inflammatory and antifungal drug. *Libyan Journal of Medicine*, 9 (1).

Govindaraju, T., Owen, A. J. and McCaffrey, T. A. 2022. Past, present and future influences of diet among older adults–A scoping review. *Ageing Research Reviews*, 77: 101600.

Grinin, L., Grinin, A. and Korotayev, A. 2023. Global Aging: An integral problem of the future. how to turn a problem into a development driver? In: *Reconsidering the limits to growth: A report to the Russian Association of the Club of Rome*. Springer, 117-135.

Gurib-Fakim, A. 2006. Medicinal plants: Traditions of yesterday and drugs of tomorrow. *Molecular Aspects of Medicine*, 27 (1): 1-93.

Lin, L., Yang, K., Zheng, L., Zhao, M., Sun, W., Zhu, Q. and Liu, S. 2018. Anti-aging effect of sea cucumber (*Cucumaria frondosa*) hydrolysate on fruit flies and D-galactose-induced aging mice. *Journal of Functional Foods*, 47: 11-18.

Luo, J., Si, H., Jia, Z. and Liu, D. 2021. Dietary anti-aging polyphenols and potential mechanisms. *Antioxidants*, 10 (2): 283.

Oladeji, O. S., Adelowo, F. E., Ayodele, D. T. and Odelade, K. A. 2019. Phytochemistry and pharmacological activities of *Cymbopogon citratus*: A review. *Scientific African*, 6: e00137.

APPENDIX

Appendix 4.1. Docking scores (kcal/mol) of phytochemical compounds from lemongrass teas against enzymes implicated in ageing

s/n	Ligands	PubChem ID	COLL	ELAS	HYA	TYR
1	Chamaemeloside	101688668	-9.0	-7.0	-6.8	-8.7
2	4-O-feruloyl-D-quinic acid	10177048	-7.9	-6.8	-6.5	-7.4
3	Benzyl alcohol beta-D-rutinoside	10549806	-8.5	-6.6	-7.5	-7.7
4	Veranisatin C	10643000	-6.0	-6.1	-6.8	-6.8
5	Ascleposide B	10740722	-6.8	-6.5	-6.8	-6.8
6	Pandangolide 1a	11687387	-6.2	-5.3	-6.4	-5.6
7	Sinensol E	11796980	-8,2	-6.8	-6.7	-7.1
8	Glochidionionoside A	11825585	-7,4	-6.0	-6.2	-6.2
9	Corchoionoside B	131751110	-10.9	-6.8	-6.3	-5.7
10	Methyl 7-epi-12-hydroxyjasmonate glucoside	131751189	-8.0	-6.0	-5.8	-7.2
11	Caffeoyl-O-methylquinic acid	131752769	-8,3	-6.3	-6.6	-7.2
12	Neocuscutoside C	131801689	-7.0	-6.6	-7.4	-8.1
13	diethyl 2-hydroxypentanedioate	13270883	-5,6	-4.7	-4.5	-5.5
14	Carboxyethylidene]-alpha-D-galactose	133960	-7,3	-5.3	-6.3	-5.8
15	Corymboside	13644660	-8.4	-6.1	-7.1	-8.3
16	Phenylethyl primeveroside	14704521	-8.3	-6.5	-7.0	-8.1
17	5-[(6-ethoxy-3,4,5-trihydroxyoxan-2-yl)methoxy]-3-hydroxy-3-methyl-5-oxopentanoic acid	156602899	-6.5	-5.6	-5.4	-5.8
18	4-oxo-3-phenyl-4H-chromen-7-yl 3-phenylprop-2-enoate	133568962	-8,3	-6.5	-7.3	-7.6
19	Phellodendric acid A	16088229	-6,2	-5.0	-4.9	-5.4
20	Dihydroferulic acid 4-O-glucuronide	NA	-7,7	-6.8	-7.2	-8.0
20	Chlorogenic acid	1794427	-8,6	-6.6	-6.9	-6.2
21	Isocarlinoside	21576182	-6.4	-5.1	-7.9	-8.6
22	Aspirin	2244	-7.9	-5.5	-5.6	-7.0
23	Eucomic acid	23757219	-8	-6.9	-7.5	-7.0
24	[1,1'-binaphthalen]-2-ol	136672961	-6,9	-6.1	-6.5	-6.4
25	8-Hydroxypinoresinol	3010930	-7,4	-6.4	-7.0	-6.7
26	10-phenyl-9,10-dihydroanthracen-9-one	NA	-7,9	-5.9	-6.3	-7.1
27	Scopolin	439514	-8,7	-6.4	-7.1	-8.2
28	Vitexin 6"-(3-hydroxy-3-methylglutarate)	44257690	-8,4	-6.3	-7.6	-7.9

30	Limocitrin 7-(6"-acetylglucoside)	44260014	-8,8	-7.4	-7.7	-7.5
31	Isovitexin 2"-O-arabinoside	44468060	-9,3	-6.1	-7.7	-9.2
32	(+)-7alpha,8alpha-Epoxyblumenol B	44559648	-4,9	-5.5	-5.8	-5.3
33	3,4-O-[(1S)-1-carboxyethylidene]-beta-D-galactose	51351726	-7,5	-5.8	-6.0	-6.4
34	Quercitrin	5280459	-9,1	-6.1	-6.9	-8.0
35	Trifolin	5282149	-7,4	-6.7	-6.8	-8.3
36	Lonicerin	5282152	-9,7	-7.3	-8.3	-9.1
37	Aspulvinone H	54675755	-8,7	-6.6	-7.8	-8.0
38	Kaempferitrin	5486199	-9,4	-6.1	-8.0	-8.6
39	Kaempferol 3,4'-dixyloside	44258938	-7.8	-7.3	-7.6	-7.9
40	Vitexin 2"-O-rhamnoside	5874704	-7.4	-6.6	-7.6	-8.4
41	Sibiricose A5	6326020	-7,3	-6.5	-7.4	-6.8
42	2-Hydroxycinnamic acid	637540	-6,6	-5.6	-5.2	-6.7
43	Caffeic acid	689043	-7,2	-5.2	-5.7	-6.7
44	3',4',5,7,8-Pentamethoxyflavanone	72703226	-6,5	-6.3	-6.5	-6.7
45	Rustoside	74977996	-8.1	-7.2	-7.1	-8.4
46	Phenylpyruvic acid	997	-7	-5.1	-5.7	-6.1
47	Herbarumin II	9992042	-6.2	-5.7	-6.5	-5.7
48	Astragalin 7-rhamnoside	57390614	-8.1	-6.1	-7.7	-8.2
49	Sinocrassoside B3	NA	-5,3	-5.6	-6.1	5.8
	Standard drugs					
1	Oleanolic acid	10494	-7.1	-7.2	-7.5	
2	Ascorbic acid	54670067				-6.3

COLL: Collagenase, ELAS: Elastase, HYA: Hyaluronidase, TYR: Tyrosinase

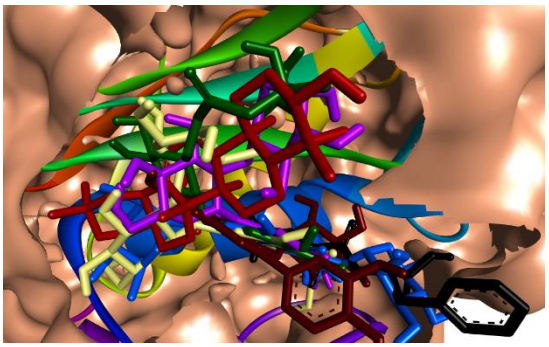

(A1)

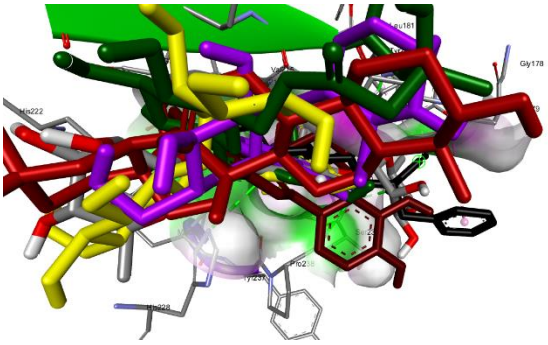

(A2)

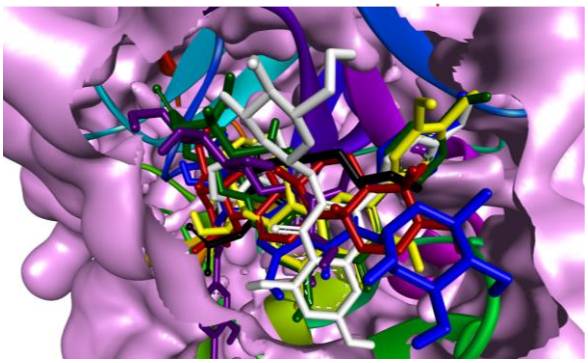

(B1)

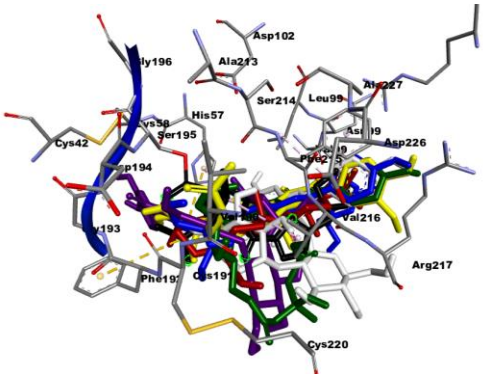

(B2)

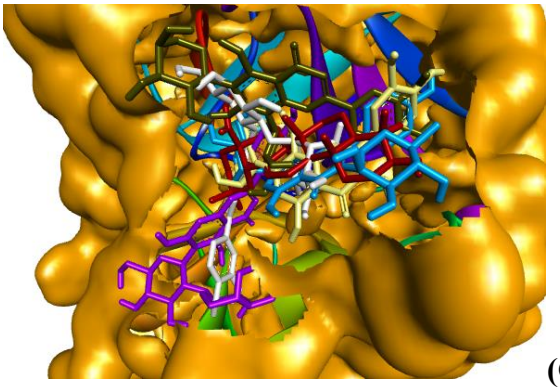

(C1)

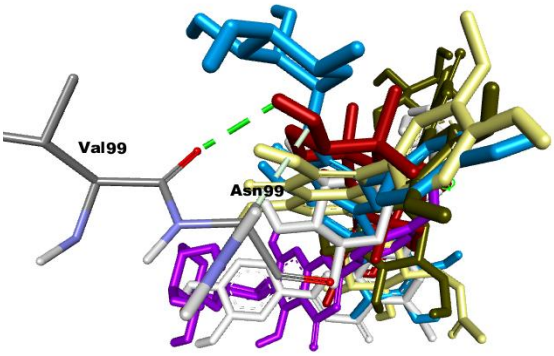

(C2)

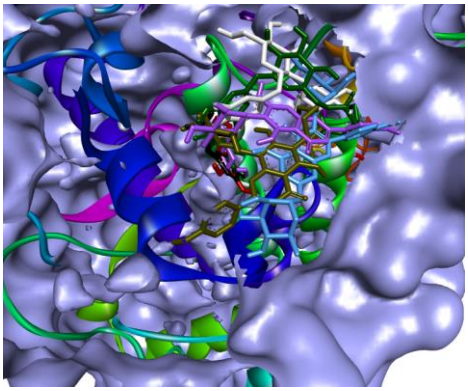

(D1)

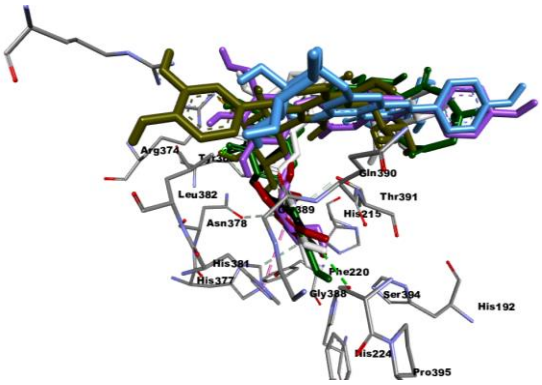

(D2)

Appendix 4.2. Validation of docking via redocking approach against the structures of (A) collagenase (B) elastase (C) hyaluronidase and (D) tyrosinase

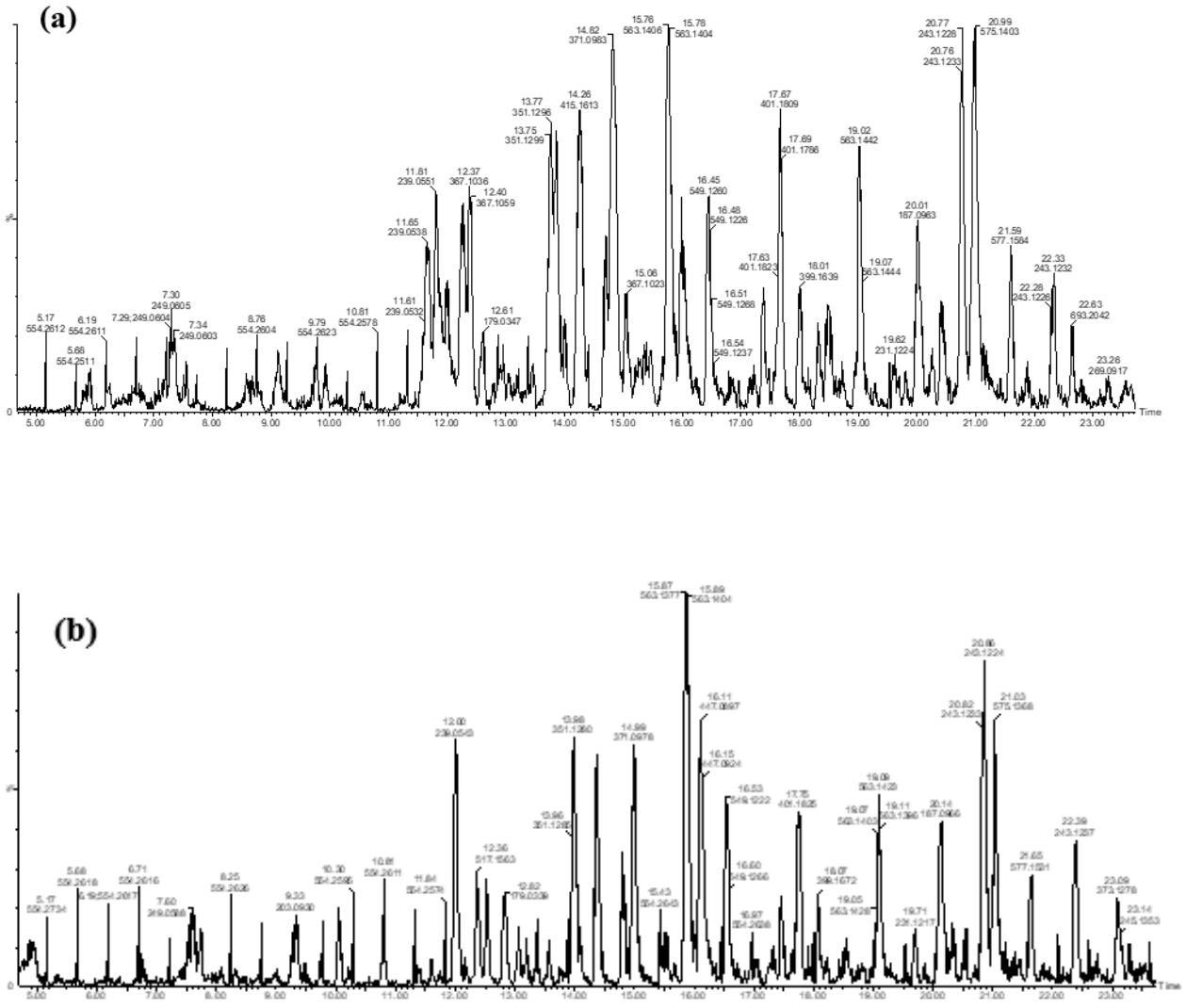

Appendix 5.1. Chromatogram of (a) fresh and (b) dry lemongrass teas.

Appendix 5.2. Docking scores (kcal/mol) of phytochemical compounds from lemongrass teas against enzymes implicated in neurodegeneration

s/n	Ligands	PubChem ID	AChE	BChE	BACE-1	MAO
1	Vitexin 6"-(3-hydroxy-3-methylglutarate)	44257690	-8.0	-10.3	-9.4	-7.0
2	Veranisatin C	10643000	-6.9	-8.3	-7.4	-6.1
3	Trifolin	5282149	-8.8	-9.4	-8.1	-6.3
4	Sinensol E	11796980	-9.3	-10.0	-9.1	-7.9
5	Sibiricose A5	6326020	-7.6	-8.3	-7.7	-8.3
6	Scopolin	439514	-8.7	-8.8	-7.4	-8.3
7	Quercitrin	5280459	-8.2	-10.0	-8.8	-6.8
8	Phenylpyruvic acid	997	-7.0	-6.5	-6.1	-7.2
9	Phellodendric acid A	16088229	-6.0	-5.5	-5.4	-6.5
10	Pandangolide 1a	11687387	-7.9	-7.7	-7.5	-7.3
11	Lonicerin	5282152	-9.2	-11	-9.5	-7.6
12	Limocitrin 7-(6"-acetylglucoside)	44260014	-9.1	-10.0	-9.0	-8.8
13	Kaempferol 3,4'-dixyloside	44258938	-8.9	-9.8	-9.0	-7.6
14	Kaempferitrin	5486199	-8.7	-10.5	-8.9	-6.9
15	Isovitexin 2"-O-arabinoside	44468060	-8.4	-9.6	-8.0	-7.9
16	Isocarlinoside	21576182	-8.8	-10.1	-9.5	-7.1
17	Herbarumin II	9992042	-7.2	-7.1	-6.4	-6.8
18	Glochidionionoside A	11825585	-7.5	-8.5	-7.2	-6.4
19	Eucomic acid	23757219	-6.9	-6.7	-6.6	-7.8
20	Dihydroferulic acid 4-O-glucuronide	NA	-8.9	-6.8	-7.6	-8.7
21	diethyl 2-hydroxypentanedioate	13270883	-6.0	-5.5	-5.1	-5.9
22	Chlorogenic acid	1794427	-9.2	-8.6	-8.3	-9.8
23	Chamaemeloside	101688668	-10.0	-10	-9.1	-7.6
24	Carboxyethylidene]-alpha-D-galactose	133960	-7.1	-6.8	-6.8	-8.1
25	Caffeoyl-O-methylquinic acid	131752769	-7.6	-8.6	-7.7	-8.1
26	Caffeic acid	689043	-7.2	-6.8	-6.3	-7.7
27	Benzyl alcohol beta-D-rutinoside	10549806	-9.9	-9.1	-8.3	-9.4
28	Astragalin 7-rhamnoside	57390614	-9.4	-9.9	-8.5	-7.4
29	Aspulvinone H	54675755	-10.6	-9.2	-9.2	-11.9

30	Aspirin	2244	-7.4	-6.3	-6.0	-7.0
31	Ascleposide B	10740722	-7.8	-9.0	-7.2	-6.8
32	8-Hydroxypinoresinol	3010930	-7.9	-8.3	-7.5	-8.9
33	4-oxo-3-phenyl-4H-chromen-7-yl 3-phenylprop-2-enoate	133568962	-10.6	-9.9	-8.7	-9.3
34	4-O-feruloyl-D-quinic acid	10177048	-9.2	-8.5	-8.3	-9.7
35	3,4-O-[(1S)-1-carboxyethylidene]-beta-D-galactose	51351726	-7.1	-6.5	-6.3	-6.9
36	3',4',5,7,8-Pentamethoxyflavanone	72703226	-8.3	-7.9	-7.3	-5.9
37	2-Hydroxycinnamic acid	637540	-7.0	-6.4	-6.2	-7.7
38	[1,1'-binaphthalen]-2-ol	136672961	-9.1	-12.0	-8.6	-9.2
39	(+)-7alpha,8alpha-Epoxyblumenol B	44559648	-6.2	-6.8	-6.2	-5.3
40	5-[(6-ethoxy-3,4,5-trihydroxyoxan-2-yl)methoxy]-3-hydroxy-3-methyl-5-oxopentanoic acid	156602899	-7.4	-7.2	-6.7	-8.2
41	Corchoionoside B	131751110	-7.1	-8.4	-8.1	-9.1
42	Corymboside	13644660	8.0	-9.1	-8.1	-7.1
43	Methyl 7-epi-12-hydroxyjasmonate glucoside	131751189	-6.8	-7.3	-8.0	-9.2
44	Neocuscutoside C	131801689	-9.3	-9.5	-10.5	-8.6
45	10-phenyl-9,10-dihydroanthracen-9-one	NA	-7.3	-10	-8.5	-8.4
46	Phenylethyl primeveroside	14704521	-8.5	-5.5	8.7	-10.1
47	Rustoside	74977996	-9.3	-9.9	-8.9	-6.6
48	Sinocrassoside B3	NA	-5.2	-7	-8.0	-6.5
49	Vitexin 2"-O-rhamnoside	5874704	-8.4	-6.7	-8.5	-7.3
	Standard drugs					
1	Donepezil	3152	-9.7	-9.5		
2	AZD3293	67979346			-8.8	
3	Tranylcypromine	19493				-6.5

NA: Not available, AChE: Acetylcholinesterase, BChE: Butyrylcholinesterase, BACE-1: β-secretase, MAO: Monoamine oxidase

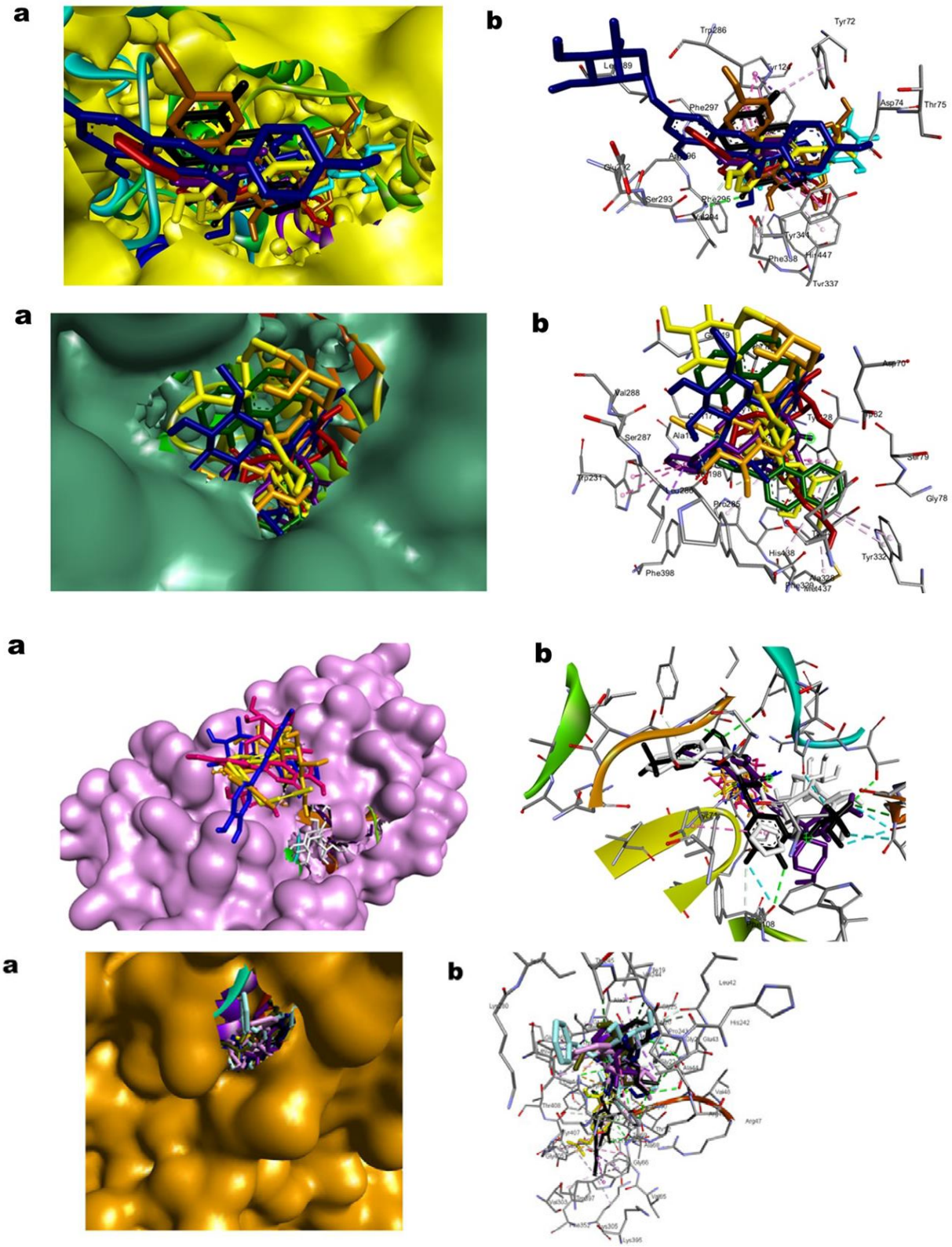

Appendix 5.3. Validation of docking via redocking approach against the structures of (1) acetylcholinesterase, (2) butyrylcholinesterase, (3) beta-secretase and (4) monoamine oxidase

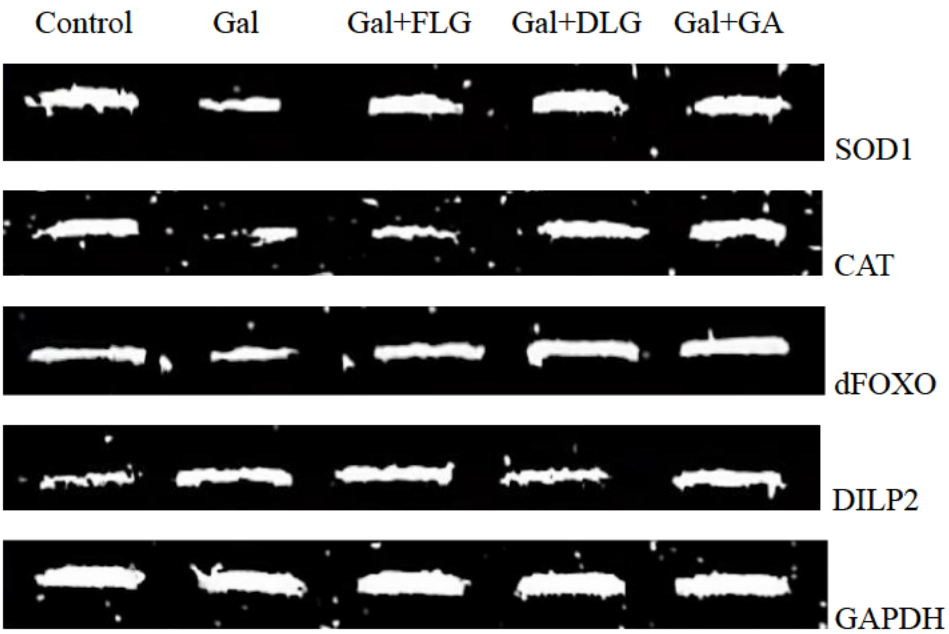

Appendix 6.1. Effect of supplementation of diet with fresh and dry lemongrass tea on the expression of relevant genes in D-galactose-induced ageing in *Drosophila melanogaster*.

Control: Normal control, Gal: D-galactose-treated flies only, Gal+FLG: D-galactose and fresh lemongrass treated flies, Gal+DLG: D-galactose and dry lemongrass treated flies, Gal+GA: D-galactose and gallic acid treated flies.

SOD1: Superoxide dismutase 1, CAT: Catalase, dFOXO: Drosophila Forkhead Box O, DILP2: Drosophila insulin-like peptide 2, GAPDH: Glyceraldehyde-3-phosphate dehydrogenase

Received: 12 June 2023 | Revised: 20 October 2023 | Accepted: 21 October 2023

DOI: 10.1002/fft2.325

FOOD FRONTIERS

REVIEW ARTICLE

Medicinal foods and plants with antiaging properties: A review of in vitro and in vivo studies

Mutiu Idowu Kazeem | John Jason Mellem | Saheed Sabiu

Department of Biotechnology and Food Science, Faculty of Applied Sciences, Durban University of Technology, Durban, South Africa

Correspondence
Saheed Sabiu, Department of Biotechnology and Food Science, Durban University of Technology, P. O. Box 1334, Durban 4000, South Africa.
Email: sabius@dut.ac.za

Funding information
National Research Foundation, Grant/Award Number: SRUG2204193723; South African Medical Research Council, Grant/Award Number: SIR; Durban University of Technology, Grant/Award Number: NA

Abstract

Aging is a natural process by which organisms experience physiological decline leading to susceptibility to morbidity and mortality. There are no known antiaging drugs but there is a myriad of medicinal foods and plants that have been used in managing the state. Several studies have also been conducted on the antiaging properties of medicinal plants and foods, but these pieces of information are scattered. This paper attempts to integrate available information on medicinal foods and plants as well as isolated chemical compounds with antiaging potential. It also provides different models (in vitro and in vivo) that are used in evaluating the potency of natural products. Current literature on the subject was obtained from different databases such as PubMed, Google Scholar, and Web of Science. A total of 119 medicinal plants and 50 isolated compounds were reported in this study. Different models were also used to evaluate the efficacy of these plants which include in vitro (enzyme inhibition, use of cell lines) and in vivo (*Caenorhabditis elegans*, yeast, fruit fly, mice, and rats) models. It can be concluded that medicinal foods and plants are reservoirs of potential therapeutic agents that can efficiently modulate metabolic processes implicated in aging and its associated disorders.

KEYWORDS
aging, bioactive compounds, functional foods, longevity, medicinal plants

1 | INTRODUCTION

One of the goals of procreation is the sustainability of the species which is a function of how long the individual lived. Conversely, the longer the number of years an individual lives the higher the tendency for him to experience a decline in physiological and physical functions, which constitutes aging (Pandey et al., 2020; Rusu et al., 2019). It is a natural and irreversible biological process marked by structural and functional changes in the cells and tissues leading to low immunity and increased susceptibility to morbidity and mortality (Klinngam et al., 2022). Aging is a primary risk factor for many chronic diseases like diabetes, hypertension, cancer, and cardiovascular and neurodegenerative disorders (Men et al., 2022). Due to the onset of the myriad of diseases at this period, aging itself can constitute a disease.

According to the World Health Organization (WHO), individuals aged 65 years and above constitute old people (World Health Organization [WHO], 2022). The prevalence of old people is increasing globally due to the increase in life expectancy rate. For instance, 258 million old people were recorded in 1980, 500 million in 2006, and 771 million in 2022 (United Nations [UN], 2022). Therefore, the number of old people now is about three times the number in 1980. However, this population is projected to increase to 994 million and 1.6 billion in 2030

and 2050, respectively (UN, 2022). Old people occupy about 10% of the world population, and this is expected to reach 12% and 16% in 2030 and 2050, respectively (Luo et al., 2021). Europe and Northern America have the largest share of aged persons with about 19% of the population, and this is expected to rise to 27% in 2050 (UN, 2022). However, 3% of the people in Sub-Saharan Africa are old which may increase to 5% in 2050.

As all organism desires to live for a long period, aging is inevitable. However, there is a paucity of information on how to attain old age without necessarily experiencing the pathological conditions associated with it. Consumption of a desirable diet is one of the veritable means of managing aging and its complications (Rusu et al., 2019). Medicinal food plants are plants that provide therapeutic benefit for the consumer in addition to their nutritional benefit (Kazeem et al., 2021). The WHO asserted that about two thirds of the global population (especially in rural areas) depend on medicinal foods and plants for the treatment of their diseases (WHO, 2002). This is mainly due to their availability, affordability, efficacy, and perceived safety. Studies have also reported the pharmacological potentials of medicinal foods and plants in the treatment and management of several diseases (Kazeem & Davies, 2016; Nafiu et al., 2013; Sabiu, 2022).

There are several reviews on the antiaging properties of medicinal foods and plants but these are not comprehensive. Although many of the studies were conducted on antiaging potentials of specific parts of the plants (Chen et al., 2020; Rusu et al., 2019), some focused on specific plant products (Bhullar & Wu, 2020; Chen et al., 2023; Dhanjal et al., 2020; Meccariello & D'Angelo, 2021), whereas others presented studies only in specific models (Okoro et al., 2021). As such, there is no comprehensive study in the literature that presents an overview of plants and foods that can be used to manage aging to date. To the best of our knowledge, this is the first paper that synthesizes information on all medicinal plants and foods with antiaging properties using different models. It also presents an in-depth review of medicinal foods and plants with antiaging properties with a view to guiding future research and development of antiaging agents.

2 | METHODOLOGY

The available information on antiaging properties of medicinal foods and plants was collected via electronic search (using PubMed, SciFinder, Google Scholar, and Web of Science) using the keywords such as "aging," "medicinal foods," "antiaging plants," and "antiaging foods". A library search for articles published in books, including review and specific ethnomedical research articles, was also used as sources of information. Reference lists of published research articles were also consulted for relevant data. A total of 268 articles covering between year 2001 and 2022 were obtained from the electronic and manual searches. After eliminating duplications and irrelevant ones, 153 articles were used for this study. Our paper excludes all in silico studies, studies on antiaging potential of polyherbal drugs, clinical trials, as well as all studies on antiaging agents of animal or microbial origin.

3 | EXPERIMENTAL MODELS OF AGING

Due to the overwhelming nature of aging and its complications, there are numerous models that have been used in the evaluation of antiaging properties of natural products. These are as follows: enzymes' inhibition, yeast, *Caenorhabditis elegans*, *Drosophila melanogaster*, cell lines, and mammalian (mouse and rat) models (Figure 1).

3.1 | Enzymatic model

Aging is a complex biological process that is mediated by many proteins and enzymes (Tlili et al., 2019). Prominent among these enzymes are collagenase, elastase, hyaluronidase, and tyrosinase. Collagenase and elastase are involved in the breaking down of collagen (which gives tensile strength) and elastin (which promotes elasticity), respectively, thereby causing wrinkles and severe atrophy on the skin (Jiratchayamaethasakul et al., 2020). Hyaluronidase destroys hyaluronic acid (which promotes skin rejuvenation), whereas tyrosinase plays a crucial role in the rate-limiting step of melanin production (Martel et al., 2019). The inhibition of one or more of these enzymes will be an effective approach to prevent or ameliorate the deleterious effect of aging.

The inhibitory properties of medicinal foods and plants on the activities of relevant antiaging enzymes are presented in Table 1. Five of the studies included in this paper tested the inhibitory properties of designated plants on all the four enzymes (collagenase, elastase, hyaluronidase, and tyrosinase). Of the five studies, two (Elgamal et al., 2021; Ersoy et al., 2019) presented their results on the basis of the half maximal inhibitory concentration (IC_{50}). Of the three plants tested in the studies, essential oil obtained from *Pluchea dioscoridis* displayed a lower IC_{50} for all the enzymes [collagenase (1.85 μg/mL), elastase (14.63 μg/mL), hyaluronidase (17.18 μg/mL), and tyrosinase (19.52 μg/mL) (Elgamal et al., 2021)], which signifies better antiaging potential than *Erigeron bonariensis* and *Hypericum* sp. (Ersoy et al., 2019). Stamen extract of *Nelumbo nucifera* displayed better inhibition of both tyrosinase and collagenase than the whole flower, whereas the results are similar for elastase and hyaluronidase (Tungmunnithum et al., 2022). *Aquilegia pubiflora* leaf extracts (Jan et al., 2021) and *Isodon rugosus* cultures (Abbasi et al., 2019) also inhibited the enzymes at varying degrees.

Three studies tested the inhibitory effect of plants on three of the enzymes (collagenase, elastase, and hyaluronidase). The aqueous extract of *Cochlospermum vitifolium* leaf displayed potent inhibition of collagenase, elastase, and hyaluronidase with IC_{50} values of 708, 5.3, and 0.04 μg/mL, respectively (German-Baez et al., 2017). Both ethanol extract of *Hypericum origanifolium* (Boran, 2018) and hexane extract of *Ocimum sanctum* (Chaiyana et al., 2019) also markedly inhibited

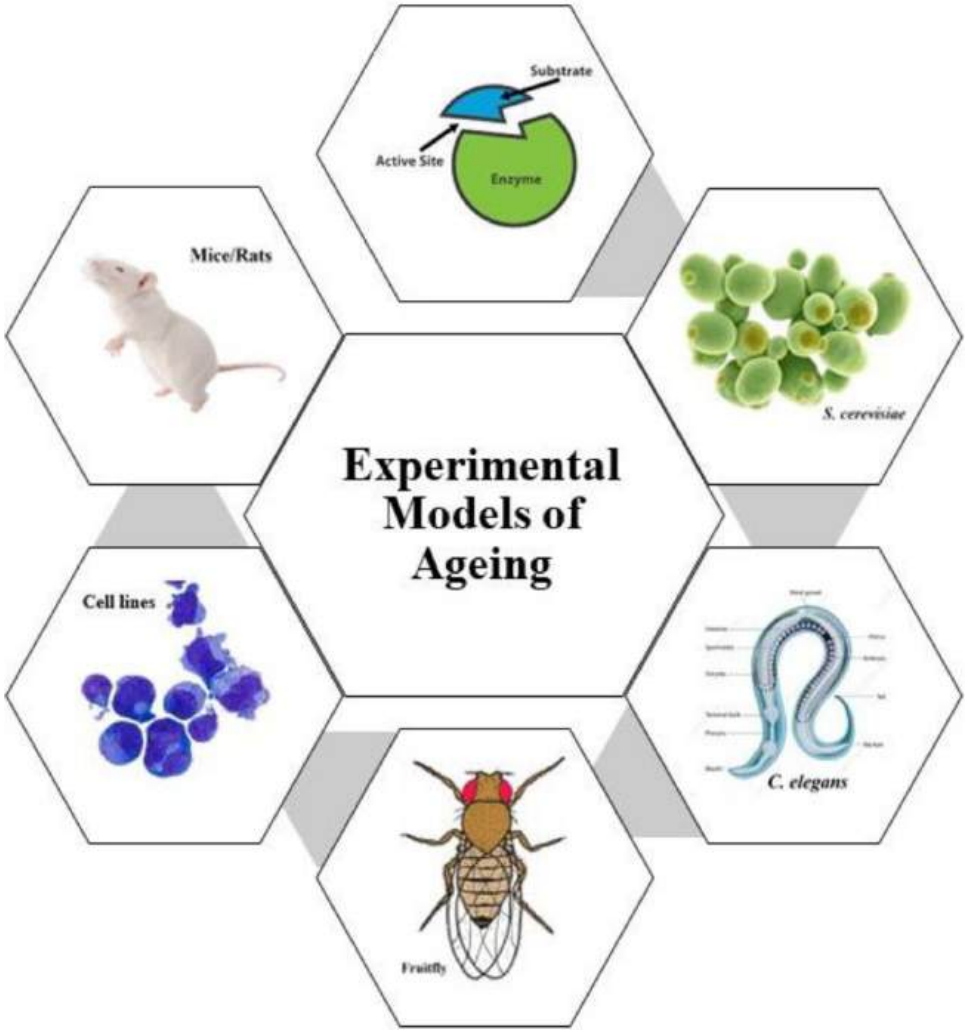

FIGURE 1 Experimental models of aging.

the three enzymes. Three studies also presented the effect of plant extracts on the activities of elastase, tyrosinase, and hyaluronidase. *Isaria tenuipes* aqueous extract exhibited better inhibition against elastase (IC_{50}: 0.006 μg/mL) and hyaluronidase (IC_{50}: 30.3 μg/mL) (Prommaban et al., 2022) compared to *Lagerstroemia speciosa* with IC_{50} values of 6.49 and 1880 μg/mL, respectively (Kolakul & Sripanidkulchai, 2017). Both plants exhibited a similar effect toward tyrosinase activity, whereas the results presented for *Thymelaea hirsuta* (Amari et al., 2021) were done qualitatively. Moreover, methanol extract of *Malaxis acuminata* displayed potent antiaging activities with IC_{50} values of 35.52, 32.24, and 175.81 μg/mL for collagenase, elastase, and tyrosinase, respectively (Bose et al., 2017), whereas the root extract of *Eutrema japonicum* exhibited better activities than the leaf and flower (Szewczyk et al., 2021).

In the test for collagenase and elastase only, ethanol extract of *Manilkara zapota* displayed most potent inhibition of both enzymes with IC_{50} 86.47 and 35.73 μg/mL, respectively (Pientaweeratch et al., 2016). Though the inhibitory effect of *Phyllanthus emblica* on collagenase is similar to *M. zapota*, it inhibited elastase in a mild manner (IC_{50}: 387.85 μg/mL). However, ethanol extract of *Garcinia picrorrhiza* displayed weak inhibition of collagenase (IC_{50}: 1169.32 μg/mL) and moderate inhibition of the elastase (IC_{50}: 152.93 μg/mL) (Utami et al., 2018). Of the three parts of *Sclerocarya birrea* extracts tested, the stem displayed higher percentage inhibition of both collagenase and elastase (Shoko et al., 2018). The extracts of both *Harungana madagascariensis* and *Psorospermun aurantiacum* had weak inhibition for tyrosinase but strongly inhibited elastase, with *P. aurantiacum* having IC_{50} of 15.40 μg/mL (Manjia et al., 2019). Ethanol extract of *Areca catechu* displayed IC_{50} 60.8 and 210 μg/mL for elastase and hyaluronidase, respectively (Lee et al., 2001), whereas *Hibiscus sabdariffa* was not active (Li et al., 2020).

Four studies reported only the anti-tyrosinase activity of some medicinal plants and foods. Of all the plants, *Cleistocalyx nervosum* methanol extract (20 μg/mL) displayed the strongest inhibition (Manosroi et al., 2015) followed by *Cassia auriculata* hydro-methanol extract (42.49 μg/mL) (Napagoda et al., 2018) and *Stenoloma chusanum* petroleum ether fraction (118.6 μg/mL) (Wu et al., 2017). Conversely, methanol extract of *Amygdalus communis* exhibited weak inhibition toward tyrosinase (Tlili et al., 2019). A study on anti-elastase property of *Alkanna tinctoria* revealed that acetone extract possessed the

TABLE 1 Inhibitory properties of medicinal foods and plants on aging-related enzymes.

Scientific name	Common name	Parts	Extract	Enzymes inhibited	Reference
Alkanna tinctoria L. Tausch	Dyer's bugloss	Root	Different solvents	Elastase	Jaradat et al. (2018)
Amygdalus communis	NA	Hull	Methanol	Tyrosinase	Tlili et al. (2019)
Aquilegia pubiflora Wall. Ex Royle	Himalayan columbine	Leaf	Water, ethyl acetate, methanol, ethanol	Collagenase, elastase, tyrosinase, hyaluronidase	Jan et al. (2021)
Areca catechu Linn.	NA	Whole plant	Ethanol	Elastase, hyaluronidase	Lee et al. (2001)
Cassia auriculata Linn.	NA	Flower	Hydro-methanol	Tyrosinase	Napagoda et al. (2018)
Cleistocalyx nervosum	Ma Kiang	Leaf	Methanol	Tyrosinase	Manosroi et al. (2015)
Cochlospermum vitifolium	Silk-cotton tree	Leaf	Water	Collagenase, elastase, hyaluronidase	German-Baez et al. (2017)
Cordyceps militaris (L.) Fr. Link	NA	Whole plant	Water	Elastase, tyrosinase, hyaluronidase	(Prommaban et al. (2022)
Eutrema japonicum Koidz	Japanese horseradish	Flower, leaf, root	Methanol-acetone-water	Collagenase, tyrosinase, hyaluronidase	Szewczyk et al. (2021)
Garcinia picrorrhiza Miq.	Sesoot	Fruit	Ethanol	Collagenase, elastase	Utami et al. (2018)
Harungana madagascariensis	NA	Stem	Methylene chloride	Elastase, tyrosinase	Manjia et al. (2019)
Hibiscus sabdariffa	NA	Calyx	Water	Collagenase, tyrosinase	Li et al. (2020)
Hypericum origanifolium Willd.	NA	Aerial part	Ethanol	Collagenase, elastase, hyaluronidase	Boran (2018)
Hypericum sp.	NA	Flower	Methanol	Collagenase, elastase, tyrosinase, hyaluronidase	Ersoy et al. (2019)
Isaria tenuipes Peck	NA	Whole plant	Water	Elastase, tyrosinase, hyaluronidase	Prommaban et al. (2022)
Isodon rugosus (Wall. Ex Benth.) Codd.	NA	Seed	Water	Collagenase, elastase, tyrosinase, hyaluronidase	Abbasi et al. (2019)
Lagerstroemia speciosa Lagerstroemia floribunda	NA	Flower	Ethanol	Elastase, tyrosinase, hyaluronidase	Kolakul and Sripanidkulchai (2017)
Malaxis acuminata D. Don	Jeevaka	Leaf, stem	Methanol	Collagenase, elastase, tyrosinase	Bose et al. (2017)
Manilkara zapota P. Royen	Sapota	Fruit	Ethanol	Collagenase, elastase	Pientaweeratch et al. (2016)
Nelumbo nucifera Gaertn	Sacred lotus	Flower	Hydro-ethanol	Collagenase, elastase, tyrosinase, hyaluronidase	Tungmunnithum et al. (2022)
Ocimum sanctum Linn.	Queen of herb	Whole plant	Hexane	Collagenase, elastase, hyaluronidase	Chaiyana et al. (2019)
Phyllanthus emblica Linn.	Amla	Fruit	Ethanol	Collagenase, elastase	Pientaweeratch et al. (2016)

(Continues)

TABLE 1 (Continued)

Scientific name	Common name	Parts	Extract	Enzymes inhibited	Reference
Pluchea dioscoridis (L.) DC *Erigeron bonariensis* Linn.	NA	Shoot	Essential oil	Collagenase, elastase, tyrosinase, hyaluronidase	Elgamal et al. (2021)
Psorospermun aurantiacum	NA	Leaf	Methylene chloride	Elastase, tyrosinase	Manjia et al. (2019)
Sclerocarya birrea Hochst	Marula	Shoot	Methanol	Collagenase, elastase	Shoko et al. (2018)
Stenoloma chusanum	NA	Whole plant	Ethanol	Tyrosinase	Wu et al. (2017)
Thymelaea hirsute (L.) Endl	Methnane	Leaf, stem, flower	Water	Elastase, tyrosinase, hyaluronidase	Amari et al. (2021)
Trigonella foenum-graecum	Fenugreek	Seed	Ethanol	Collagenase	Eaknai et al. (2022)

Abbreviation: NA: Not available.

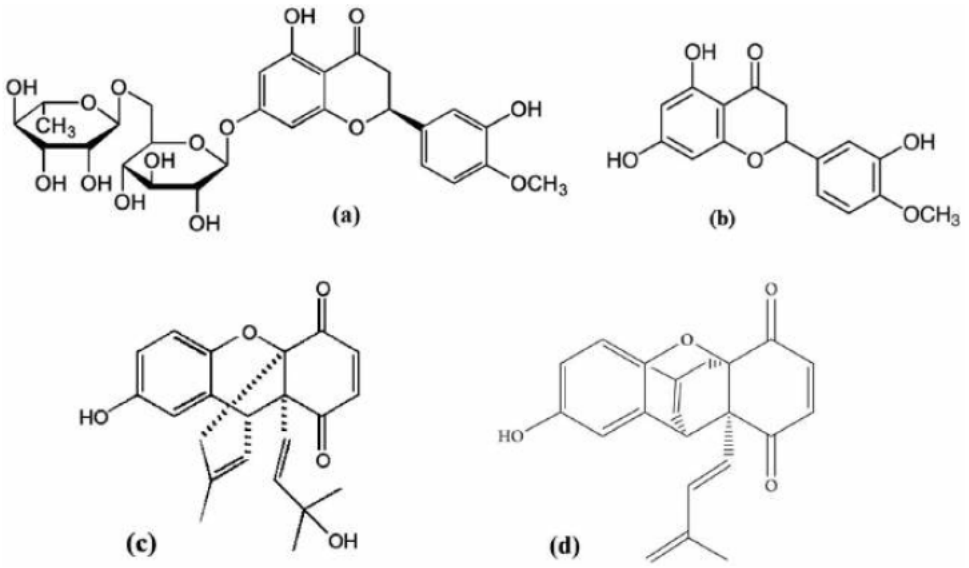

FIGURE 2 Structures of chemical compounds tested for antiaging properties in yeast model: (a) hesperidin, (b) hesperetin, (c) allomicrophyllone, and (d) ehretiquinone (Farooq et al., 2019).

TABLE 2 Anti-aging properties of medicinal foods and plants in *Saccharomyces cerevisiae*.

Scientific name	Common name	Parts	Extract/Compound	Dose	ΔLifespan%	Reference
Citrus species	Citrus	Fruit	Hesperidin	10 μM	36.93	Sun et al. (2012)
Haberlea rhodopensis	NA	Leaf	Methanol	1.0 mg/mL	29.50	Georgieva et al. (2015)
Humulus japonicus	Japanese hop	Leaf	Ethanol	20 μg/mL	22.22	Sung et al. (2015)
Onosma bracteatum Wall	NA	Whole plant	Allomicrophyllone	3.0 μM	30.53	Farooq et al. (2019)
			Ehretiquinone	3.0 μM	28.90	
			Ehretiquinone C	1.0 μM	38.67	
			Ehretiquinone D	1.0 μM	29.17	
Prunus persica	Honey peach	Fruit	Glucosides	7.5 μM	24.93	Wang et al. (2018)

Abbreviation: NA, not available.

TABLE 3 Anti-aging properties of medicinal foods and plants in *Caenorhabditis elegans*.

Scientific name	Common name	Parts	Extract/compound	Dose	ΔLongevity (%)	Reference
Acanthopanax sessiliflorus	Acanthopanax	Stem	Aqueous	500 μg/mL	17.40	Park et al. (2014)
Arctium lappa	Burdock	Seed	Lignans	100 μM	25.00	Su and Wink (2015)
Mongholicus bunge	Huangqi	Leaf	Calycosin	200 μM	21.42	Lu et al. (2017)
Betula utilis	Silver birch	Bark	Ethanol	50 μg/mL	35.99	Pandey et al. (2020)
Bletilla striata	NA	Whole plant	Polysaccharide	50 μg/mL	16.67	Zhang et al. (2015)
Calycophyllum spruceanum	Tree of youth	Stem bark	Aqueous	300 μg/mL	16.00	Peixoto et al. (2018)
Citrus medica	Finger citron	Fruit	Flavonoids	200 μg/mL	31.26	Luo et al. (2020)
Cordyceps militaris	NA	Whole plant	Polysaccharide	250 μg/mL	16.58	Liu et al. (2016)
Cuscuta chinensis	Chinese dodder	Seed	Methanol	30 μg/mL	24.35	Sayed et al. (2021)
Damnacanthus officinarum	DOH	Root	*n*-Butanol	800 μg/mL	17.24	Yang et al. (2012)
Eucommia ulmoides	Chinese rubber	Bark	Methanol	30 μg/mL	9.28	Sayed et al. (2021)
Eugenia uniflora L.	Purple pitanga	Fruit	Phenolics	500 μg/mL	16.67	Tambara et al. (2018)
Fagopyrum esculentum	Buckwheat	Seed	Trypsin inhibitor	10 μM	21.20	Li et al. (2015)
Glochidion zeylanicum	Man pu	Leaf	Methanol	100 μg/mL	10.01	Duangjan et al. (2019)
Glycine max	Soybean	Seed	Fermented	500 μg/mL	16.44	Ibe et al. (2013)
Glycyrrhizae radix	NA	Whole plant	Aqueous	0.24 mg/mL	11.76	Ruan et al. (2016)
Juniperus communis	Juniper berry	Fruit	Oil	10 ppm	18.54	Pandey et al. (2018)
Lithocarpus polystachyrus	NA	Leaf	Trilobatin	250 μM	22.10	Li, Li et al. (2021)
Malus domestica	Apple	Whole plant	Acetone	10 mg/mL	39.60	Vayndorf et al. (2013)
Olea europaea L.	Olive	Fruit	Oil	250 μM	21.13	Cañuelo et al. (2012)
Paeonia suffruticosa And.	Tree peony	Flower	Ethanol	150 mg/L	16.47	Wang, Xue et al. (2020)
Panax notoginseng	Notoginseng	Root	Polysaccharides	500 μg/mL	21.70	Feng et al. (2019)
Phyllanthus emblica	NA	Fruit	Polyphenols	0.8 mg/mL	18.53	Wu et al. (2022)
Pinus densiflora	Pinus	Leaf	Dehydroabietic acid	10 μM	15.50	Kim et al. (2015)
Platycladus orientalis L.	Chinese thuja	Seed	*n*-Butanol	500 μg/mL	24.54	Liu et al. (2013)
Polygonum multiflorum	NA	Whole plant	Aqueous	1 mg/mL	18.60	Saier et al. (2018)
Portulaca oleracea	Global panacea	Whole plant	Ethyl acetate	1 mg/mL	16.47	Zhang et al. (2020)
Ribes fasciculatum	NA	Stem	Ethyl acetate	500 μg/mL	16.30	Jeon and Cha (2016)
Rosa rugosa	NA	Flower	Tea	200 μg/mL	38.10	Zhang et al. (2019)
Scutellaria baicalensis	Baical skullcap	Leaf	Baicalein	100 μM	15.78	Havermann et al. (2016)
Sesamum indicum L.	Sesame	Seed	Peptide	12.5 μg/mL	15.60	Wang et al. (2018)
Silybum marianum	Milk thistle	Fruit	2,3-Dehydrosilybin	10 μM	16.09	Filippopoulou et al. (2017)
Sophora moorcroftiana	NA	Seed	Polysaccharides	4 mg/mL	66.90	Zhang et al. (2018)
Syzygium cumini	NA	Leaf	Beta-caryophyllene	50 μM	22.70	Pant et al. (2014)
Stereospermum suaveolens	NA	Aerial part	Verminoside	25 μM	20.79	Pant et al. (2015)

(Continues)

TABLE 3 (Continued)

Scientific name	Common name	Parts	Extract/compound	Dose	ΔLongevity (%)	Reference
Streblus asper	NA	Leaf	Ethanol	50 μg/mL	3.49	Prasansuklab et al. (2017)
Trachyspermum ammi	Carom	Seed	Oil	10 ppm	12.45	Rathor et al. (2017)
Zanthoxylum armatum	Indian thorny ash	Fruit	Tambulin	50 μM	16.80	Pandey et al. (2019)

Abbreviation: NA, not available.

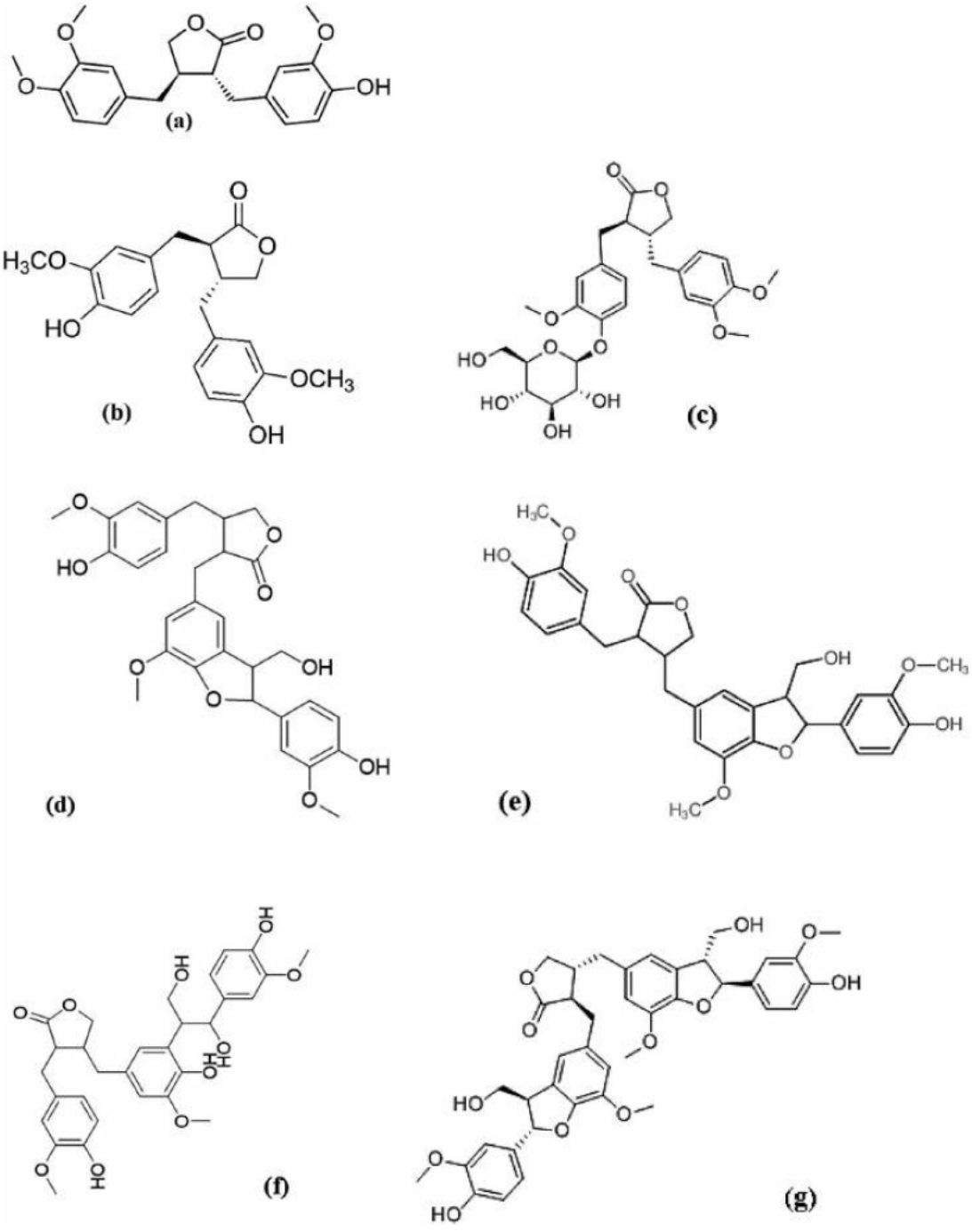

FIGURE 3 Structures of anti-aging chemical compounds isolated from *Arctium lappa* seeds: (a) arctigenin, (b) matairesinol, (c) arctiin, (d) iso-lappaol A, (e) lappaol A, (f) lappaol C, and (g) lappaol F (Su & Wink, 2015).

TABLE 4 Anti-aging properties of medicinal foods and plants in *Drosophila melanogaster*.

Scientific name	Common name	Parts	Extract/ compound	Dose	ΔLongevity (%)		Reference
					Male	Female	
Euterpe oleracea Mart	Acai palm	Fruit	Water	2.0%	22.00	ND	Sun et al. (2010)
Ganoderma sinense	NA	Fruit	Ethanol	3.0%	2.70	ND	Teseo et al. (2021)
Humulus lupulus Linn.	NA	Whole plant	Xanthohumol	0.5 mg/mL	14.89	ND	Wongchum and Dechakhamphu (2021)
Ipomoea batata Linn.	Purple sweet potato	Tuber	Water	2 mg/mL	14.50	ND	Han et al. (2021)
Lasia spinosa	NA	Stem	Ethanol	0.5 mg/mL	22.90	ND	Men et al. (2022)
Ludwigia octovalvis	NA	Whole plant	Ethanol	100 μg/mL	16.10	24.20	Lin et al. (2014)
Lycium barbarum	NA	Fruit	Polysaccharide	0.04%	16.20	19.20	Tang et al. (2019)
Panax notoginseng	Red ginseng	Root	Water	25 μg/mL	14.35	8.18	Lee et al. (2019)
Panax notoginseng	Red ginseng	Root	Ethanol	3.0%	2.70	ND	Teseo et al. (2021)
Platanus orientalis	Plane tree	Fruit	Tiliroside	0.1 μg/mL	14.71	ND	Chatzigeorgiou et al. (2017)
Zingiber officinale	Ginger	Rhizome	Ethanol	2 mg/mL	7.30	ND	Zhou et al. (2018)

Abbreviations: NA, not available; ND, not determined.

best activity with IC_{50} 10.02 μg/mL (Jaradat et al., 2018), whereas ethanol extract of *Trigonella foenum-graecum* seed exhibited moderate inhibition of collagenase activity (IC_{50}: 560 μg/mL) (Eaknai et al., 2022).

3.2 | *Saccharomyces cerevisiae* (yeast)

The antiaging properties of medicinal foods and plants in *Saccharomyces cerevisiae* are shown in Table 2. Treatment of K6001 yeast with ethanol leaf extract of *Humulus japonicus* and methanol extract of *Haberlea rhodopensis* extended the lifespan of the yeast by 22% and 30%, respectively (Georgieva et al., 2015; Sung et al., 2015). Comparative evaluation of the antiaging properties of hesperidin (Figure 2a) and hesperetin (Figure 2b) isolated from citrus fruits revealed that only hesperidin extended the lifespan of the K6001 yeast by about 37% and inhibited the generation of reactive oxygen species (ROS) (Sun et al., 2012). The study also revealed that hesperidin repressed the UTH1 gene while it activated SOD gene and Sir2 signaling pathway (Sun et al., 2012). In a related study, sesquiterpene glucosides isolated from *Prunus persica* fruits increased the lifespan of the yeast by a quarter and improved its survival under oxidative stress (Wang et al., 2018). Four benzoquinone derivatives, namely, allomicrophyllone (Figure 2c), ehretiquinone (Figure 2d), ehretiquinone C, and ehretiquinone D displayed good antiaging properties by extending the lifespan of the yeast but ehretiquinone C exhibited the strongest activity with 38% lifespan extension (Farooq et al., 2019).

3.3 | *Caenorhabditis elegans* model

C. elegans is a small (about 1 mm in length and 80 μm in diameter), eukaryotic and saprophytic nematode that feeds on bacteria such as *Escherichia coli* (Zheng & Greenway, 2012). It has a life cycle of about 3 days and can live in the laboratory for about 3 weeks at 20°C (Markaki & Tavernarakis, 2020). It is a nonpathogenic animal that exists mostly as hermaphrodites and produces more than 300 offspring within a short period (Markaki & Tavernarakis, 2010). This model is suitable for aging research due to its short life cycle, short generation time, ease, and low maintenance cost in the laboratory (Leung et al., 2008). Its transparent body and possession of many organs found in mammals as well as withstanding indefinite storage in −80°C freezer or liquid nitrogen encourages researchers in using it to study aging and related diseases (Giunti et al., 2021).

Table 3 shows the antiaging properties of medicinal foods and plants in *C. elegans*. Treatment of *C. elegans* worms with aqueous extracts of *Acanthopanax sessiliflorus*, *Calycophyllum spruceanum* (Peixoto et al., 2018), *Glycyrrhizae radix* (Ruan et al., 2016), and *Polygonum multiflorum* (Saier et al., 2018) extended the lifespan of the worms by 17.40%, 16.00%, 11.76%, and 18.60%, respectively. Ethanol extracts of *Betula utilis* bark (Pandey et al., 2020), *Paeonia suffruticosa* flower (Wang, Xue, et al., 2020), and *Streblus asper* leaves (Prasansuklab et al., 2017) prolonged the lifespan of the worms by 36%, 16.5%, and 3.5%, respectively. Methanol extracts of *Cuscuta chinensis* seeds (Sayed et al., 2021), *Eucommia ulmoides* bark (Sayed et al., 2021), and *Glochidion zeylanicum* leaf (Duangjan et al., 2019) also extended the lifespan of *C. elegans*

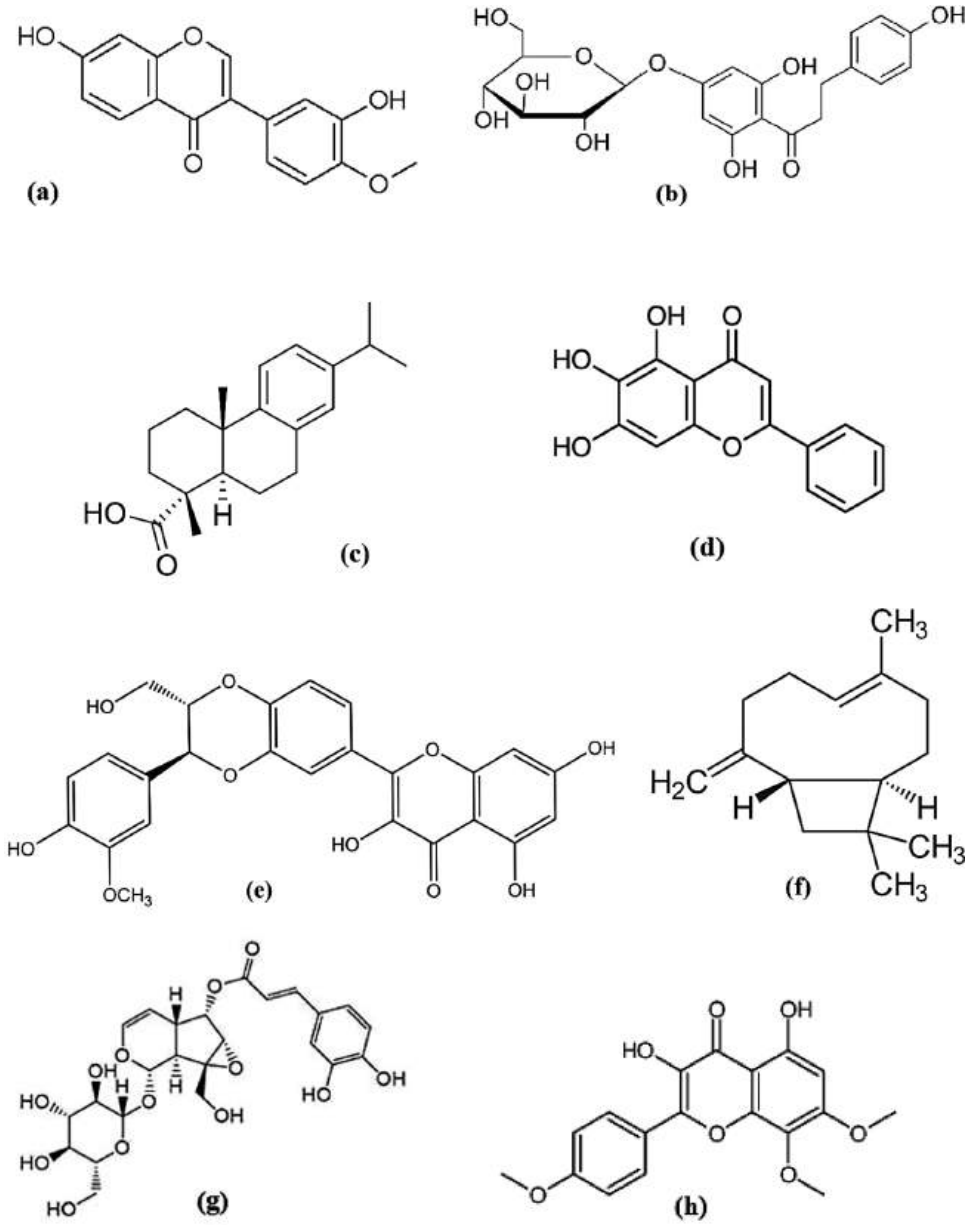

FIGURE 4 Structures of chemical compounds tested for anti-aging properties in *Caenorhabditis elegans* model: (a) calycosin, (b) trilobatin, (c) dehydroabietic acid, (d) baicalein, (e) 2, 3-dehydrosilybin, (f) beta-caryophyllene, (g) verminoside, and (h) tambulin.

by 24.35%, 9.28%, and 10%, respectively. Treatment of the worms with butanol extracts of *Damnacanthus officinarum* root (Yang et al., 2012) and *Platycladus orientalis* (Liu et al., 2013) seed increased their lifespan by 17.24% and 24.54%, respectively. However, ethyl acetate extracts of both *Portulaca oleracea* (Zhang et al., 2020) and *Ribes fasciculatum* (Jeon & Cha, 2016) produced 16% increase in the lifespan of the worms. Essential oil from *Juniperus communis* (Pandey et al., 2018), *Olea europaea* (Cañuelo et al., 2012) and *Trachyspermum ammi* (Rathor et al., 2017) prolonged the lifespan of the worms by 19%, 21%, and 12%, respectively. Polysaccharides from *Bletilla striata* (Zhang et al., 2015), *Cordyceps militaris* (Liu et al., 2016), *Panax notoginseng* (Feng et al., 2019), and *Sophora moorcroftiana* (Zhang et al., 2018) make the worms live longer by 16.67%, 16.58%, 21.70%, and 67%, respectively.

Evaluation of the antiaging properties of lignans (Figure 3) isolated from *Arctium lappa* seeds revealed that the six isolated compounds have varying antiaging effects (Su & Wink, 2015). Although the lifespan enhancing effect of arctigenin, arctiin, iso-lappaol A, lappaol C, and lappaol F ranges from 11.2% to 15.2% and is not significantly different from one another, matairesinol elicited 25% increase in the lifespan of *C. elegans*. Further study also showed that these lignans upregulated the expression of both DAF-16 and JNK-1, thereby promoting stress resistance and longevity (Su & Wink, 2015). Calycosin (isolated from *Mongholicus bunge*) (Lu et al., 2017) (Figure 4a), trilobatin (isolated from *Lithocarpus polystachyrus*) (Li, Li, et al., 2021) (Figure 4b), beta-caryophyllene (isolated from *Syzygium cumini*) (Pant et al., 2014) (Figure 4f) and verminoside (isolated from

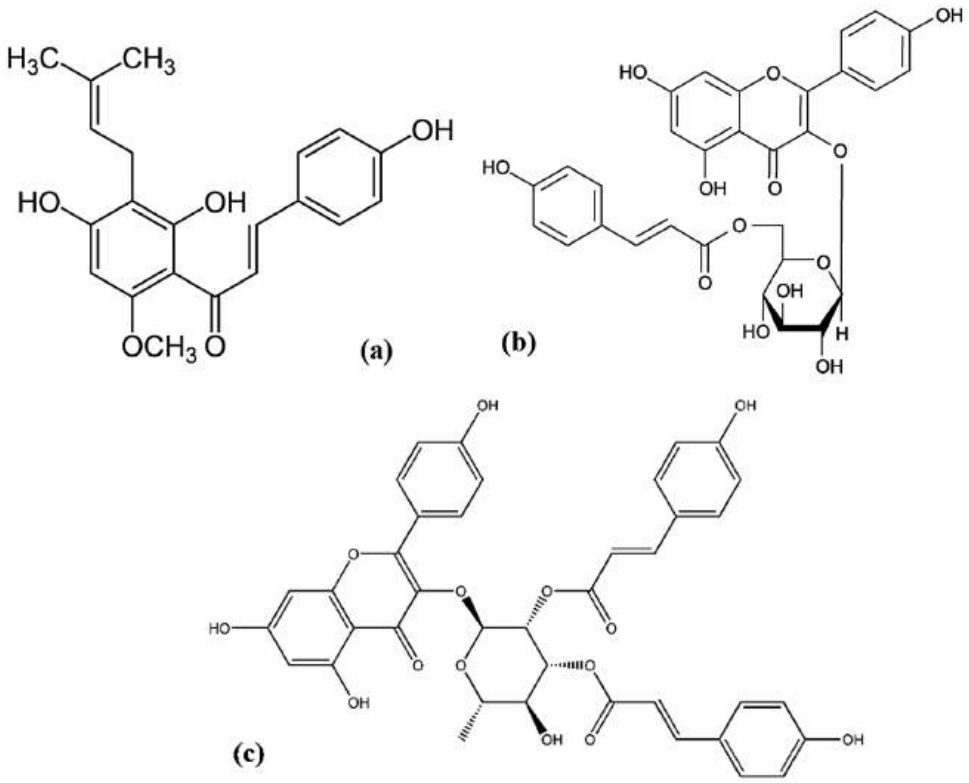

FIGURE 5 Structures of chemical compounds tested for antiaging properties in *Drosophila melanogaster*: (a) xanthohumol, (b) tiliroside, and (c) platanoside (Chartzigeorgiou et al., 2017).

Stereospermum suaveolens) (Pant et al., 2015) (Figure 4g) caused similar extension (about 22%) in the lifespan of the worm via modulation of DAF-16 pathway. A decreased effect (about 16%) in the lifespan change of the worms resulted from the influence of dehydroabietic acid (Figure 4c) (Kim et al., 2015), baicalein (Figure 4d) (Havermann et al., 2016), 2,3-dehydrosilybin (Figure 4e) (Filippopoulou et al., 2017) and tambulin (Figure 4h) (Pandey et al., 2019) by affecting the SIRT1, SKN-1, and DAF-16, respectively. Phenolic extracts from *Eugenia uniflora* (Tambara et al., 2018) and *P. emblica* (Wu et al., 2022) elicited 16.67% and 18.53% extension in the lifespan of the worm, respectively, whereas that of *Citrus medica* (Luo et al., 2020) prolonged their lifespan by 31.26%.

It is worth noting that of all the samples tested for their antiaging properties, polysaccharides extracted from the seeds of *S. moorcroftiana* elicited the highest increase (67%) in the lifespan of the worms. This is then followed by the duo of acetone extract of *Malus domestica* (40%) (Vayndorf et al., 2013) and tea made from the flowers of *Rosa rugosa* (38%) (Zhang et al., 2019), respectively. The antiaging activities of these plants were attributed to many mechanisms, including antioxidant effect (Ibe et al., 2013; Luo et al., 2020), heat shock resistance (Park et al., 2014; Wu et al., 2022), hormesis (Cañuelo et al., 2012; Sayed et al., 2021), neuroprotection (Yang et al., 2012), and the upregulation of the insulin-like signaling pathway (Li et al., 2015; Ruan et al., 2016).

3.4 | *Drosophila melanogaster* (fruit fly) model

D. melanogaster, commonly known as fruit fly, is a small fly characterized with compound eyes and wings (Jennings, 2011). It has a lifespan of approximately 40–120 days depending on its diet and environment, whereas it has a generation time of about 10–12 days (Abolaji et al., 2013). Though humans and fruit fly are not similar, important biological mechanisms that regulate development and survival are conserved between the species (Jennings, 2011). Similarly, about 65% of human disease-associated genes have a homolog in drosophila, making it easy to study genetic pathways in humans (Bilder & Irvine, 2017). *D. melanogaster* is a veritable model for the study of aging with ease of use and manipulation, simple genome, short generation time at room temperature, cheap, and easy to maintain as a result of the small body size and lifespan (Abolaji et al., 2013).

Table 4 reveals the antiaging properties of medicinal foods and plants in *D. melanogaster*. Inclusion of aqueous extract of *Ipomoea batata* (Han et al., 2021) and *P. notoginseng* (Han et al., 2021) in the diet of *D. melanogaster* increased their longevity by more than 14%. Similarly, 3% ethanol extract of *Ganoderma sinense* fruits and *P. notoginseng* caused a minute (2.7%) rise in the longevity of the flies (Teseo et al., 2021). Supplementation of the fruit fly diet with *Lycium barbarum* polysaccharide (Tang et al., 2019) and *Ludwigia octovalvis* ethanol extract (Lin et al., 2014) extended their lifespan by about 16%. Further analysis

TABLE 5 Anti-aging properties of medicinal foods and plants in cell line models.

Scientific name	Common name	Parts	Extract/compound	Cell type	Effects	Reference
Andrographis paniculata	King of bitters	Whole plant	Ethanol	EpSC	↑Proliferation; ↑Integrin β1	You et al. (2015)
Antrodia salmonea	NA	Whole plant	Antcins	Fibroblast	↑Proliferation; ↓ROS	Senthil et al. (2016)
Camellia japonica	Yabu-tsubaki	Leaf	Water	Keratinocyte	↓ROS; ↓cell damage	Mizutani and Masaki (2014)
Citrus bergamia	Bergamot	Fruit	Juice	Cardiomyocyt	↓Cellular Senescence	Da Pozzo et al. (2018)
Cornus sanguinea	Common dogwood	Drupe	Rutin	Fibroblasts	↓ROS; ↓cellular senescence	Iannuzzi et al. (2021)
		Drupe	Halleridone	Fibroblasts	↓Cellular senescence; ↓IL6	
		Drupe	Hydroxytyrosol	Fibroblasts	↓Cellular senescence	
Dalbergia odorifera	Chinese rosewood	Heartwood	Isoparvifuran	Fibroblast	↓Senescence; ↑proliferation	Yin et al. (2020)
Haberlea rhodopensis	Resurrection plant	Whole plant	Water	Fibroblast	↑Collagen; ↑elastin	Dell'Acqua and Schweikert (2012)
Kaempferia parviflora	Thai black ginger	Rhizome	Polymethoxyflavones	Fibroblast	↓Senescence; ↓ROS	Klinngam et al. (2022)
Sambucus nigra	Elderberry	Fruit	Ethanol	Keratinocyte	↓MMP-1; ↓inflammation	Lin et al. (2019)
Tagetes erecta	Marigold	Whole plant	Methanol	Fibroblast	↑Collagen; ↓MMP-2	Kang et al. (2018)
Terminalia chebula	NA	Gall	Water	Fibroblast	↑Proliferation; ↓MMP-2	Manosroi et al. (2010)
Thamnolia vermicularis	NA	Whole plant	β-Sitosterol	Fibroblast	↑Hyaluronic acid synthase	Haiyuan et al. (2019)
Thamnolia vermicularis	NA	Whole plant	Vermicularin	Fibroblast	↓ROS; ↓MMP-1	

Note: "↑": Increase, "↓": decrease.
Abbreviations: EpSC, epidermal skin cell; IL-6, interleukin-6; MMP-1, matrix metalloproteinase-1, MMP-2, matrix metalloproteinase-2, NA, not available; ROS, reactive oxygen species.

revealed that both samples displayed their antiaging potential through their antioxidant capacities. Ethanol extracts of *Lasia spinosa* stem (Men et al., 2022) and *Zingiber officinale* rhizome (Zhou et al., 2018) when included in the diet of the fruit fly also increased the longevity of the flies by 23% and 7%, respectively.

Supplementation of the fruit fly diet with 0.5 mg/mL of xanthohumol (isolated from *Humulus lupulus* Linn.) (Figure 5a) increased the lifespan of the flies by 15% (Wongchum & Dechakhamphu, 2021). It also increased the survival of the flies after exposure to toxicants (hydrogen peroxide and paraquat). Bioassay-guided isolation of the of antiaging bioactive compounds from *Platanus orientalis* (Chatzigeorgiou et al., 2017) yielded two compounds, namely, tiliroside (Figure 5b) and platanoside (Figure 5c). Enrichment of the fruit fly diet with both compounds decreased oxidative stress, whereas tiliroside increased their longevity by about 15% and mitigated the age-related reduction in locomotive activity. Further study revealed that tiliroside upregulated genes involved UPS, chaperone, and antioxidant responses (Chatzigeorgiou et al., 2017).

3.5 | In vitro cell culture model

The antiaging effects of medicinal foods and plants using cell culture are depicted in Table 5. Aqueous extracts of *H. rhodopensis* (Dell'Acqua & Schweikert, 2012) and *Terminalia chebula* (Manosroi et al., 2010) as well as methanol extract of *Tagetes erecta* (Kang et al., 2018) displayed antiaging property in a fibroblast by increasing the collagen content and reducing matrix metalloproteinase-2 activity. Aqueous extract of *Camellia japonica* (Mizutani & Masaki, 2014) and ethanol extract of *Sambucus nigra* (Lin et al., 2019) also reduced aging in the keratinocyte by decreasing ROS and matrix metalloproteinase-1 activity, respectively. In addition, *Citrus bergamia* juice reduced cellular senescence in the cardiomyocyte (Da Pozzo et al., 2018), whereas ethanol extracts of *Andrographis paniculata* increased the level of proliferation of the human epidermal skin stem cells (You et al., 2015).

Six compounds (antcin A, antcin B, antcin C, antcin H, antcin K, and antcin M), isolated from *Antrodia salmonea* (Figure 6a–f), were subjected to antiaging assays (Senthil et al., 2016). Preliminary toxicity

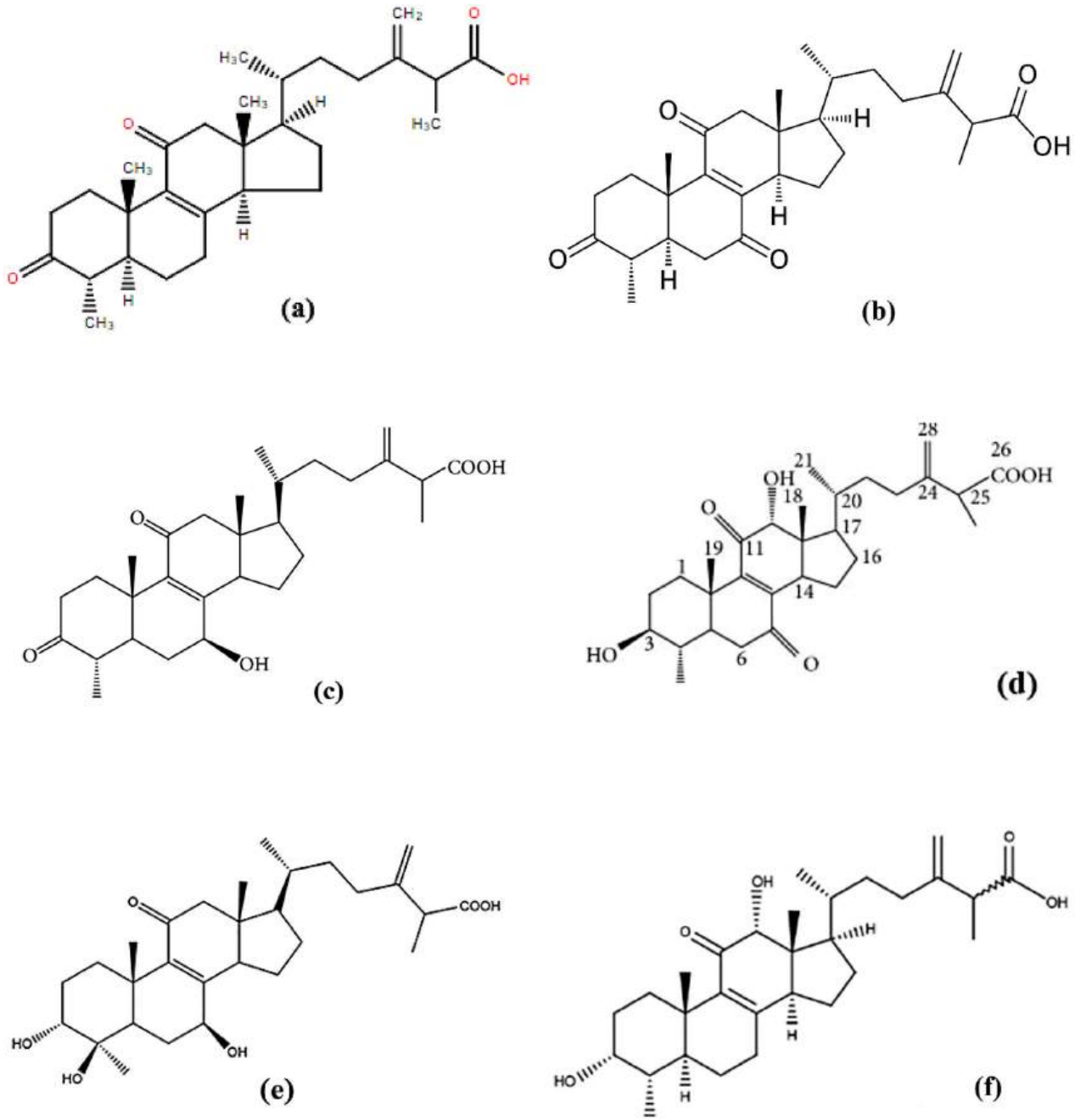

FIGURE 6 Structures of anti-aging chemical compounds isolated from *Antrodia cinnamomea*: (a) antcin A, (b) antcin B, (c) antcin C, (d) antcin H, (e) antcin K, and (f) antcin M (Senthil et al., 2016).

screening revealed that antcin A, antcin C, and antcin M showed no significant cytotoxicity toward the human normal dermal fibroblast (HNDF). However, treatment of antcin A, antcin C, and antcin M in high-glucose induced cellular senescence in the HNDF revealed that only antcin M (Figure 6f) displayed significant protection, whereas others showed moderate inhibition. The study also showed that the mechanism of antiaging action of antcin M is the activation of Nrf-2 and Sirt-1 pathways (Senthil et al., 2016). Similarly, rutin (Figure 7a), halleridone (Figure 7b), and hydroxytyrosol (Figure 7c) isolated from *Cornus sanguinea* counteracted hydrogen peroxide-induced cellular senescence in both human dermal and gingival fibroblasts (Iannuzzi et al., 2021). However, only halleridone reduced the gene expression of pro-inflammatory cytokine, IL-6 in the cells.

Three polymethoxyflavones [5,7-dimethoxyflavone (Figure 7e), 5,7,4′-trimethoxyflavone (Figure 7f), and 3,5,7,3′,4′-pentamethoxyflavone (Figure 7g)] isolated from *Kaempferia parviflora* rhizome suppressed cellular senescence and ROS in primary human dermal fibroblast by upregulating the expression of lamin B1 (Klinngam et al., 2022). Isoparvifuran (Figure 7d) purified from *Dalbergia odorifera* also mitigated cellular senescence while encouraging cell proliferation in the fibroblast by activating SIRT1 and inhibiting Akt/mTOR signaling pathway (Yin et al., 2020). In another study, β-sitosterol (Figure 7h) and

TABLE 6 Anti-aging properties of medicinal foods and plants in galactose-induced aging in mice.

Scientific name	Common name	Parts	Extract/compound	Dose	Effects	Reference
Alchemilla mollis	Lady's mantle	Leaf	Ethanol	1.0%	↓Erythema index; ↓wrinkle	Hwang, Ngo et al. (2018)
Aloe sp.	NA	Leaf	Aloin	30 mg/kg	↑Memory; ↓MDA; ↓TNF-α	Zhong, Wang, Wang et al. (2019)
Anoectochilus roxburghii	King of medicines	Whole plant	Ethanol	490 mg/kg	↑Memory; ↑GSH-Px; ↑SOD	Wang, Chen et al. (2020)
Aronia melanocarpa	Chokeberry	Fruit	Diet	1.0%	↓AGE; ↓MDA; ↑Nrf2; ↑Nf-κB	Jeong et al. (2017)
Brassica oleracea	Red cabbage	Leaf	CY3D5G	150 mg/kg	↓MDA; ↑T-AOC; ↑GSH-Px	Zhang et al. (2021)
Caulerpa racemosa	Seagrape	Fruit	Water	300 mg/kg	↓Glucose; ↑PGC-1α	Permatasari et al. (2021)
Coeloglossum viride	Zang wangla	Tuber	Water	5 mg/kg	↑Memory; ↑BDNF; ↓TNF-α	Zhong, Wang, Wu et al. (2019)
Dioscorea alata Linn	Yam	Tuber	Dioscorin	80 mg/kg	↓AGE; ↓Latency; ↓MDA	Han et al. (2014)
Hibiscus syriacus Linn.	Rose of Sharon	Root	Water	1.0%	↑Erythema index; ↑melanin	Yang et al. (2019)
Larrea tridentata	Creosote bush	Leaf	NDGA	3.5 mg/kg	↑Lifespan; ↑tumorigenesis	Spindler et al. (2015)
Morus alba Linn.	Mulberry	Fruit	Ethanol	500 mg/kg	↑Memory; ↑neuronal function	Kim and Oh (2013)
Nephelium lappaceum	Rambutan	Peel	Phenolics	200 mg/kg	↓MDA; ↑T-AOC; ↑GSH-Px	Zhuang et al. (2017)
Olea europaea	Olive	Fruit	Phenolics	6 mg/kg	↑Memory; ↑neuronal function	Luceri et al. (2017)
Polygonatum multiflorum	NA	Whole plant	TSG	20 μM	↑Memory; ↑lifespan; ↓Klotho	Zhou et al. (2015)
Prunus domestica Linn.	Plum	Fruit	Diet	10%	↓AGE; ↓MDA; ↑Nrf2; ↑Nf-κB	Jeong et al. (2017)
Syzygium aromaticum	Clove	Fruit	Ethanol	1.0%	↓Wrinkle; ↑TGF-β1; ↑elastin	Hwang, Lin et al. (2018)
Triticum aestivum	Wheat	Seed	Fermented wheat	20 mg/kg	↑Memory; ↓TG; ↓TC; ↓MDA	Zhao et al. (2021)

Note: "↑": Increase, "↓": decrease.

Abbreviations: AGE, advanced glycation end product; BDNF, brain-derived neurotrophic factor; CY3D5G, cyanidin-3-diglucoside-5-glucoside; GPx, glutathione peroxidase; GSH-Px, reduced glutathione; MDA, malondialdehyde; NA, not available; NDGA, nordihydroguaiaretic acid; Nf-κB, nuclear factor kappa B; Nrf2, nuclear factor erythroid-2-related factor-2; PGC-1α, peroxisome proliferator-activated receptor-gamma coactivator-1 alpha; SOD, superoxide dismutase; T-AOC, total antioxidant capacity; TC, total cholesterol; TG, triglyceride; TGF-β1, transforming growth factor beta-1; TNF-α, tumor necrosis factor alpha; TSG, tetrahydroxystilbene glucoside.

vermicularin (Figure 7i) isolated from *Thamnolia vermicularis* displayed antiaging property (Haiyuan et al., 2019). Although β-sitosterol promoted the biosynthesis of hyaluronic acid by increasing the expression of hyaluronic acid synthase, vermicularin reduced the ROS and matrix metalloproteinase-1 activity.

3.6 | Mouse model

The therapeutic potentials of medicinal foods and plants in galactose-induced aging in mice are depicted in Table 6. Administration of 1.0% aqueous extract of *Hibiscus syriacus* (Yang et al., 2019) and ethanol extract of *Alchemilla mollis* (Hwang, Ngo et al., 2018) to UVB-induced photoaging in hairless mice improved the erythema index and melanin content while reducing the level of wrinkleness, respectively. Supplementation of diets with *Prunus domestica* and *Aronia melanocarpa* fruits for 8 weeks reduced the levels of both advanced glycation end products (AGE) and malondialdehyde (MDA), whereas they increased the expression of nuclear factor erythroid-2-related factor-2 (Nrf2) and nuclear factor kappa B (Nf-κB) in D-galactose-induced aged mice (Jeong et al., 2017). Administration of *Anoectochilus roxburghii* ethanol extract (490 mg/kg) also improved memory and antioxidant

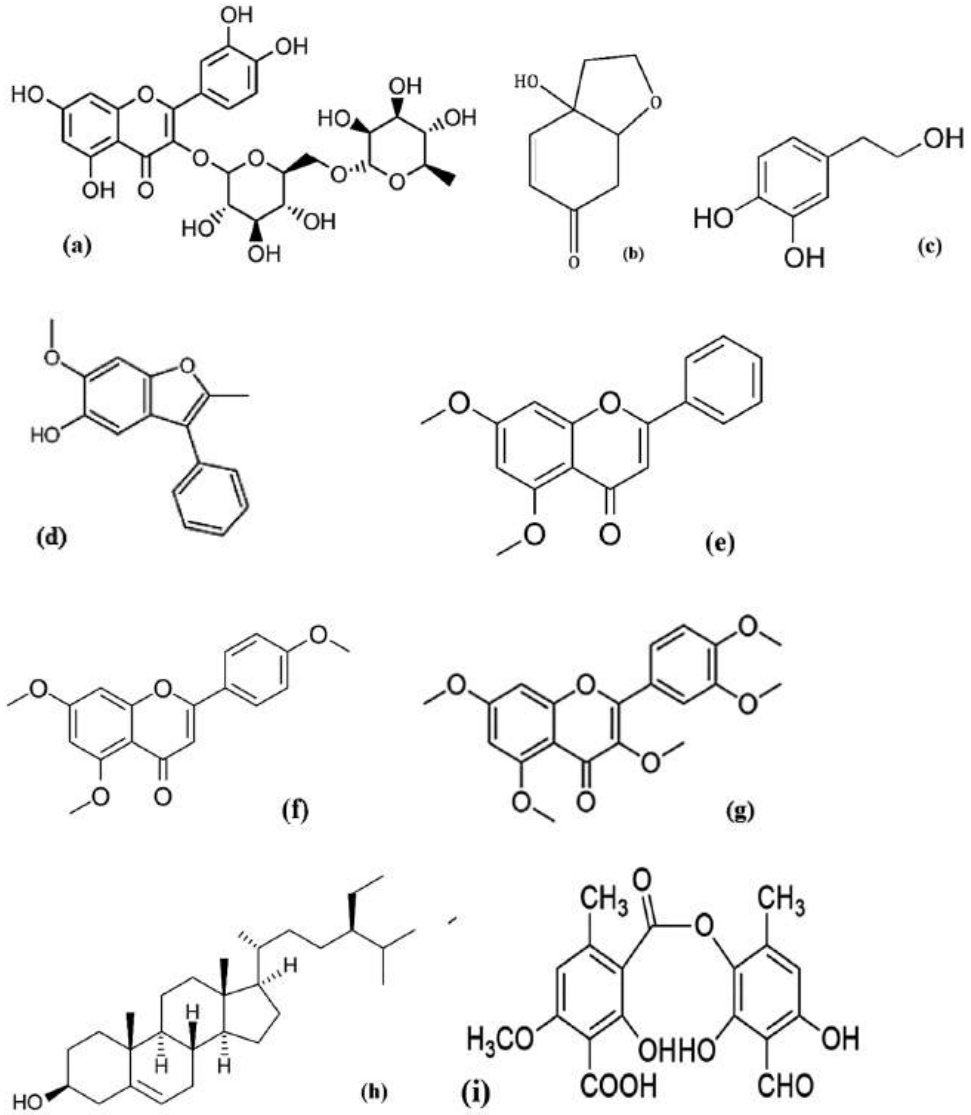

FIGURE 7 Structures of chemical compounds tested for anti-aging properties in cell line models: (a) rutin, (b) halleridone, (c) hydroxytyrosol, (d) isoparvifuran (e), 5,7-dimethoxyflavone, (f) 5,7,4'-trimethoxyflavone, (g) 3,4,5,7,4'-pentamethoxyflavone, (h) β-sitosterol, and (i) vermicularin.

enzymes (superoxide dismutase and glutathione peroxidase) levels in D-galactose-induced aged mice (Wang, Chen, et al., 2020).

Phenolic extract (200 mg/kg) of *Nephelium lappaceum* peels boosted the antioxidant status of the D-galactose-induced aged mice (Zhuang et al., 2017), whereas aqueous extract (300 mg/kg) of *Caulerpa racemosa* increased peroxisome proliferator-activated receptor-gamma coactivator-1 alpha (PGC-1α) of the animals (Permatasari et al., 2021). Increased serum PGC-1α is correlated with improved antioxidant capacity and antiaging capacity. Administration of both *Coeloglossum viride* aqueous extract and fermented wheat to chemically induced aged rats improved the memory of the animals (Zhao et al., 2021; Zhong, Wang, Wu, et al., 2019). Long-term administration of both phenolic extract of *O. europaea* fruit and *Morus alba* ethanol extract improved the memory and neuronal function in the treated mice (Kim & Oh, 2013; Luceri et al., 2017). Expectedly, *Syzygium aromaticum* ethanol extract reduced the wrinkleness of the hairless mice skin and improved skin parameters such as elastin (Hwang, Lin, et al., 2018).

Besides extracts and plant formulations, secondary metabolites such as dioscorin (Figure 8a) isolated from *Dioscorea alata* was tested for antiaging property in D-galactose-induced aging in mice (Han et al., 2014). Five-week administration of dioscorin (80 mg/kg) reduced the latency of the animals as well as the concentration of AGE and MDA (Han et al., 2014). Thirty-day oral administration of 20 μM tetrahydroxystilbene glucoside (TSG) (Figure 8b) isolated from *Polygonatum multiflorum* improved the memory and lifespan of SAMP8 mice and reduced the level of insulin receptors (Zhou et al., 2015). Molecular analysis revealed that the antiaging activity of TSG is due to the modulation of the neural insulin and insulin-like growth factor-1 signaling. Oral administration of aloin (Figure 8c) improved the memory of D-galactose-induced aged mice as well as attenuated the levels of

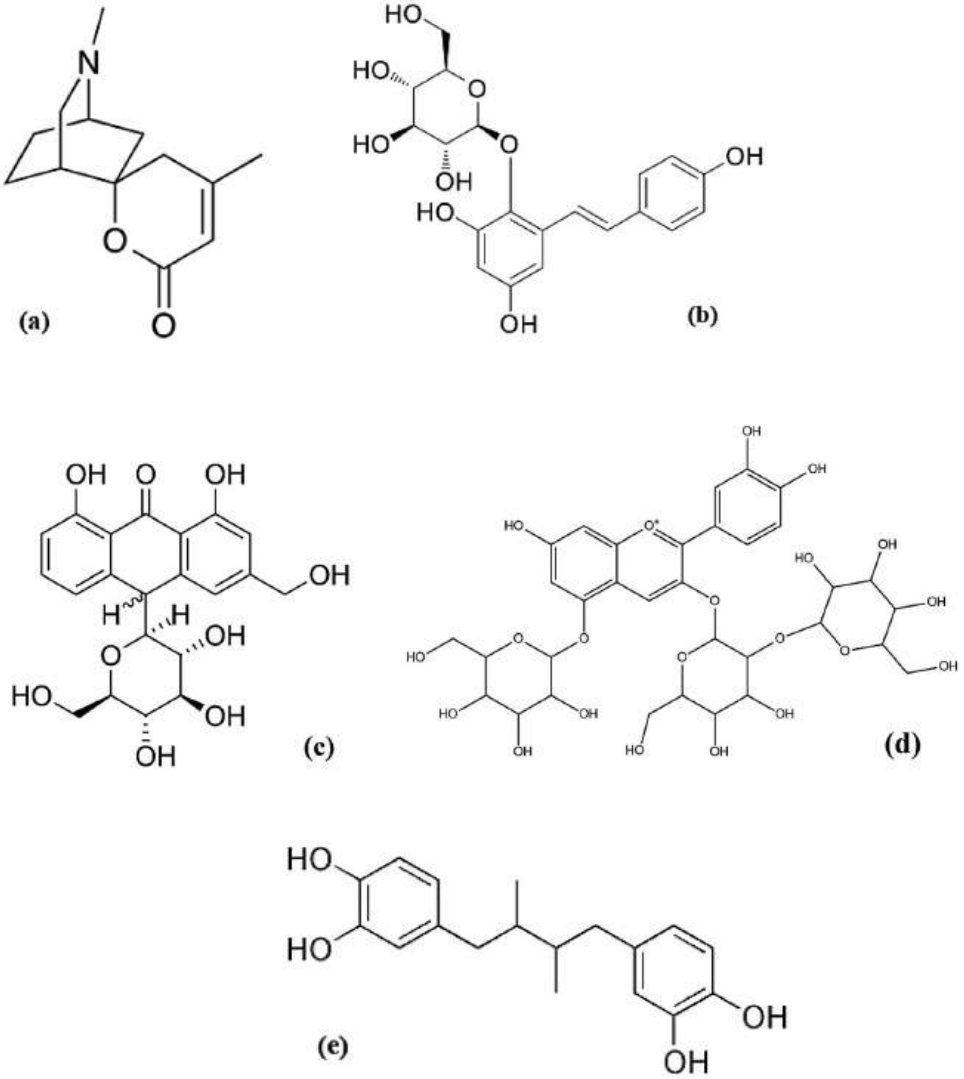

FIGURE 8 Structures of chemical compounds tested for anti-aging properties in mice: (a) dioscorin, (b) tetrahydroxystilbene glucoside, (c) aloin, (d) cyanidin-3-diglucoside-5-glucoside, and (e) nordihydroguaiaretic acid.

oxidative stress and inflammation caused by the aging (Zhong, Wang, Wang, et al., 2019). This is mediated by the downregulation of the ERK, p38, and NF-κB signaling pathway. Dietary supplementation of cyanidin-3-diglucoside-5-glucoside (Figure 8d) obtained from *Brassica oleracea* leaf improved the antioxidant status of D-galactose-induced aged mice after 6 weeks of treatment (Zhang et al., 2021) by elevating the expression of proteins in glycolysis, citric acid cycle, and actin cytoskeleton. Nordihydroguaiaretic acid (Figure 8e) supplemented in the diet of aged mice extended the lifespan of the animals, reduced tumor growth rate, whereas it increased tumor formation (Spindler et al., 2015).

3.7 | Rat model

Table 7 shows the ameliorative properties of medicinal foods and plants in galactose-induced aged rats. Administration of the aqueous extract of *Alpinia oxyphylla* fruit to D-galactose-induced aged male Wistar rats improved the longevity and survival of the animals, while decreasing the senescence-related features (Chang et al., 2021). Protocatechuic acid (Figure 9a) isolated from the *A. oxyphylla* fruit also restored the endogenous antioxidant status and normalizes aging-related alteration in aged rats after treatment for 7 days (Zhang et al., 2011). Guilingji, a traditional Chinese medicine made from *Panax ginseng*, when administered to aged rats for 28 days, improved the memory and cholinergic system of the animals while reducing their oxidative stress status (Zhao et al., 2020). Supplementation of aged rats' diet with *Bactris setosa* fruits for 12 weeks elevated the antioxidant enzyme activity and upregulated the expression of hepatic SIRT1 and Nrf2, thereby ameliorating oxidative stress associated with aging (Da Cunha & Arruda, 2017).

Oral administration of total saponin from *Aralia taibaiensis* root to D-galactose-induced aged rats improved the memory of the animals and increased the total antioxidant capacity, whereas it decreased the product of lipid peroxidation, malondialdehyde (MDA) (Li, Zhai, et al.,

TABLE 7 Antiaging properties of medicinal foods and plants in galactose-induced ageing in rats.

Scientific name	Common name	Parts	Extract/compound	Dose	Effects	Reference
Alpinia oxyphylla Miq.	NA	Fruit	Protocatechuic acid	10 mg/kg	↓MDA; ↑GPx; ↑catalase	Zhang et al. (2011)
Alpinia oxyphylla Miq.	NA	Fruit	Water	100 mg/kg	↑Longevity; ↓senescence	Chang et al. (2021)
Aralia taibaiensis	NA	Root	Saponin	200 mg/kg	↑Memory; ↓MDA; ↑T-AOC	Li, Zhai et al. (2021)
Bacopa monnieri Linn.	NA	Whole plant	Bacoside	200 mg/kg	↓IL-1β, ↓TNF-α; ↓iNOS	Rastogi et al. (2012)
Bactris setosa Mart.	Tucum-do-cerrado	Fruit	Feed supplement	15%	↑SOD; ↑SIRT1; ↑Nrf2	Da Cunha and Arruda (2017)
Panax notoginseng	Ginseng	Rhizome	Water	150 mg/kg	↑Memory; ↓MDA; ↓AChE	Zhao et al. (2020)
Trillium tschonoskii Max.	NA	Rhizome	Diosgenin glucoside	100 mg/kg	↑Memory; ↓autophagy	Wang et al. (2018)

Note: "↑": Increase, "↓": decrease.

Abbreviations: AChE, acetylcholinesterase; IL-1β, interleukin-1 beta; IL-6, interleukin-6; iNOS, inducible nitric oxide synthase.; MDA, malondialdehyde; MDA, malondialdehyde; NA, not available; Nrf2, nuclear factor erythroid-2-related factor-2; SOD, superoxide dismutase; T-AOC, total antioxidant capacity; TNF-α, tumor necrosis factor alpha.

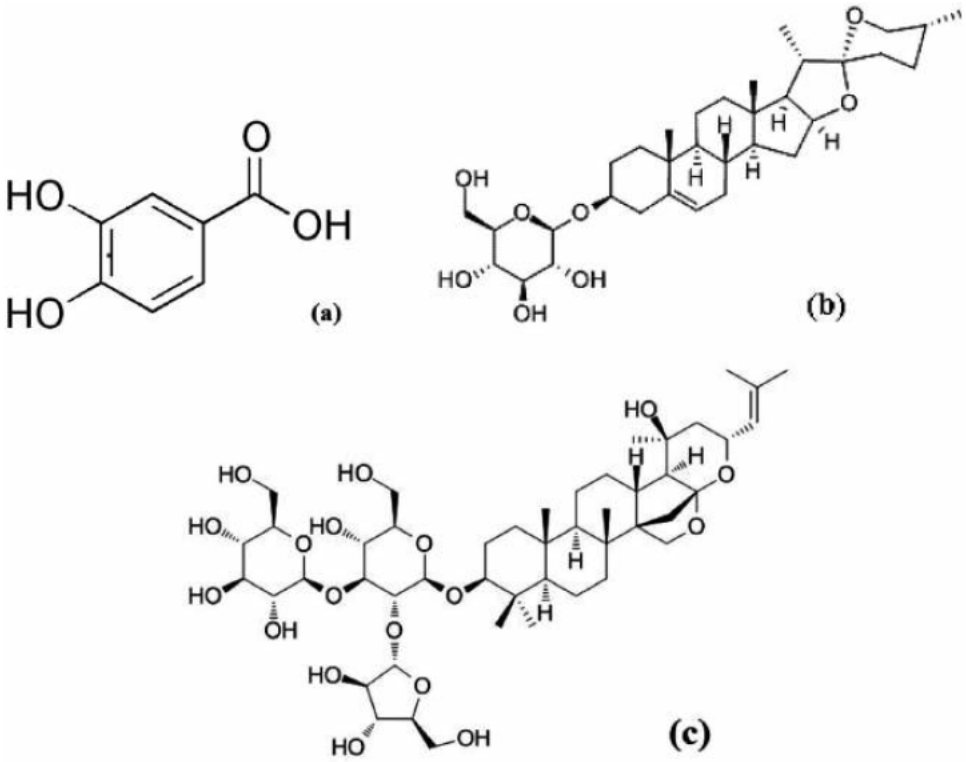

FIGURE 9 Structures of chemical compounds tested for anti-aging properties in rats: (a) protocatechuic acid, (b) diosgenin glucoside, and (c) bacoside.

2021). Similarly, saponin isolated from *Trillium tschonoskii*, otherwise called diosgenin glucoside (Figure 9b), enhanced learning as well as memory of galactose-induced aged rats and reduced dysfunctional autophagy associated with aging by modulating Rheb-mTOR signaling (Wang et al., 2018). Bacoside (Figure 9c) isolated from the crude saponin extract of *Bacopa monnieri* ameliorated neuroinflammation associated with aging by attenuating inflammatory cytokines (TNF-α and IL-1β) and iNOS after 3 months of treatment in galactose-induced aging in rats (Rastogi et al., 2012).

4 | CONCLUSION

Aging is a natural and inevitable process that occurs in all living organisms. This phenomenon is associated with the incidence of chronic diseases like diabetes, hypertension, and neurological disorders. Due to its importance, many studies have been conducted on the antiaging properties of medicinal plants and foods using different models. This study summarizes the use of different models (enzymes inhibition, yeast, cell lines, invertebrate, and vertebrate) for testing the efficacy of medicinal plants and foods in ameliorating aging and its associated disorders. A total of 119 medicinal plants and 50 isolated compounds were reported in this study. Most of the studies reported in this paper were performed in *C. elegans* and this is followed by the inhibition of aging-related enzymes. Although only two of the models are in vitro (enzyme inhibition and cell lines), five others (*C. elegans*, *D. melanogaster*, mice, rats, and yeast) are in vivo studies. Of these in vivo studies, *C. elegans* and *D. melanogaster* are more proficient than others due to the extensive generation of relevant data and are devoid of any ethical or regulatory concerns. Our study also revealed that results of antiaging properties of medicinal foods and plants using different models are complementary and corroboratory.

Though most of the reports originated from Asia especially China, these studies revealed that most medicinal plants and foods tested have antiaging properties. Some of the studies also reported the molecular mechanisms underlying the antiaging potentials of some medicinal plants and isolated phytochemicals. However, there is the need to perform mechanistic and in silico studies on the other plants evaluated. The ultimate aim of any study is to improve the lives of man and enable him to live healthy in old-age. Therefore, clinical trials should be conducted on some of these plants and phytochemicals that displayed strong antiaging effects in animal models. Although further research is advocated on these antiaging medicinal plants, more attention should be focused on the consumption of the edible ones among them.

AUTHOR CONTRIBUTIONS

Mutiu Idowu Kazeem was involved in conceptualization, literature search, writing draft, and revision of manuscript. John Jason Mellem co-supervised the study, while Saheed Sabiu was involved in conceptualization, revision of manuscript, funds mobilization and supervision of the study.

ACKNOWLEDGMENTS

The authors hereby gracefully acknowledge the assistance of the Directorate of Research and Postgraduate Support, Durban University of Technology toward the implementation of this study. We also acknowedge the financial assistance of the South African Medical Research Council under a Self-Initiated Research Grant and the National Research Foundation's Competitive Programme for Rated Researchers Suppport (SRUG2204193723) to Saheed Sabiu.

CONFLICT OF INTEREST STATEMENT

The authors confirm that there are no conflicts of interest.

ORCID

Mutiu Idowu Kazeem https://orcid.org/0000-0002-8058-1938

REFERENCES

Abbasi, B. H., Siddiquah, A., Tungmunnithum, D., Bose, S., Younas, M., Garros, L., Drouet, S., Giglioli-Guivarc'h, N., & Hano, C. (2019). *Isodon rugosus* (Wall. ex Benth.) codd in vitro cultures: Establishment, phytochemical characterization and in vitro antioxidant and anti-aging activities. *International Journal of Molecular Sciences*, *20*(2), 452. https://doi.org/10.3390/ijms20020452

Abolaji, A., Kamdem, J., Farombi, E., & Rocha, J. (2013). *Drosophila melanogaster* as a promising model organism in toxicological studies. *Archives of Basic and Applied Medicine*, *1*(1), 33–38.

Amari, N. O., Razafimandimby, B., Auberon, F., Azoulay, S., Fernandez, X., Berkani, A., Bouchara, J.-P., & Landreau, A. (2021). Antifungal and antiaging evaluation of aerial part extracts of *Thymelaea hirsuta* (L.) Endl. *Natural Product Communications*, *16*(2), 1–10. https://doi.org/10.1177/1934578X20987932

Bhullar, K. S., & Wu, J. (2020). Dietary peptides in aging: Evidence and prospects. *Food Science and Human Wellness*, *9*(1), 1–7. https://doi.org/10.1016/j.fshw.2020.01.001

Bilder, D., & Irvine, K. D. (2017). Taking stock of the *Drosophila* research ecosystem. *Genetics*, *206*(3), 1227–1236. https://doi.org/10.1534/genetics.117.202390

Boran, R. (2018). Investigations of anti-aging potential of *Hypericum origanifolium* Willd. for skincare formulations. *Industrial Crops and Products*, *118*, 290–295. https://doi.org/10.1016/j.indcrop.2018.03.058

Bose, B., Choudhury, H., Tandon, P., & Kumaria, S. (2017). Studies on secondary metabolite profiling, anti-inflammatory potential, in vitro photoprotective and skin-aging related enzyme inhibitory activities of *Malaxis acuminata*, a threatened orchid of nutraceutical importance. *Journal of Photochemistry and Photobiology B: Biology*, *173*, 686–695. https://doi.org/10.1016/j.jphotobiol.2017.07.010

Cañuelo, A., Gilbert-López, B., Pacheco-Liñán, P., Martínez-Lara, E., Siles, E., & Miranda-Vizuete, A. (2012). Tyrosol, a main phenol present in extra virgin olive oil, increases lifespan and stress resistance in *Caenorhabditis elegans*. *Mechanisms of Ageing and Development*, *133*(8), 563–574. https://doi.org/10.1016/j.mad.2012.07.004

Chaiyana, W., Anuchapreeda, S., Punyoyai, C., Neimkhum, W., Lee, K.-H., Lin, W.-C., Lue, S.-C., Viernstein, H., & Mueller, M. (2019). *Ocimum sanctum* Linn. as a natural source of skin anti-ageing compounds. *Industrial Crops and Products*, *127*, 217–224. https://doi.org/10.1016/j.indcrop.2018.10.081

Chang, Y.-M., Shibu, M. A., Chen, C.-S., Tamilselvi, S., Tsai, C.-T., Tsai, C.-C., Kumar, K. A., Lin, H.-J., Mahalakshmi, B., & Kuo, W.-W. (2021). Adipose derived mesenchymal stem cells along with *Alpinia oxyphylla* extract alleviate mitochondria-mediated cardiac apoptosis in aging models and cardiac function in aging rats. *Journal of Ethnopharmacology*, *264*, 113297. https://doi.org/10.1016/j.jep.2020.113297

Chatzigeorgiou, S., Thai, Q. D., Tchoumtchoua, J., Tallas, K., Tsakiri, E. N., Papassideri, I., Halabalaki, M., Skaltsounis, A.-L., & Trougakos, I. P. (2017). Isolation of natural products with anti-ageing activity from the fruits of *Platanus orientalis*. *Phytomedicine*, *33*, 53–61. https://doi.org/10.1016/j.phymed.2017.07.009

Chen, J.-C., Wang, R., & Wei, C.-C. (2023). Anti-aging effects of dietary phytochemicals: From *Caenorhabditis elegans*, *Drosophila melanogaster*, rodents to clinical studies. *Critical Reviews in Food Science and Nutrition*, 1–26. https://doi.org/10.1080/10408398.2022.2160961

Chen, Q., Xu, B., Huang, W., Amrouche, A. T., Maurizio, B., Simal-Gandara, J., Tundis, R., Xiao, J., Zou, L., & Lu, B. (2020). Edible flowers as functional raw materials: A review on anti-aging properties. *Trends in Food Science & Technology*, *106*, 30–47.

Da Cunha, M. D. S. B., & Arruda, S. F. (2017). Tucum-do-Cerrado (*Bactris setosa Mart.*) may promote anti-aging effect by upregulating SIRT1-Nrf2 pathway and attenuating oxidative stress and inflammation. *Nutrients*, *9*(11), 1243. https://doi.org/10.3390/nu9111243

Da Pozzo, E., De Leo, M., Faraone, I., Milella, L., Cavallini, C., Piragine, E., Testai, L., Calderone, V., Pistelli, L., & Braca, A. (2018). Antioxidant and antisenescence effects of bergamot juice. *Oxidative Medicine and Cellular Longevity*, *2018*(3), 1–14. https://doi.org/10.1155/2018/9395804

Dell'Acqua, G., & Schweikert, K. (2012). Skin benefits of a myconoside-rich extract from resurrection plant *Haberlea rhodopensis*. *International Journal of Cosmetic Science*, *34*(2), 132–139. https://doi.org/10.1111/j.1468-2494.2011.00692.x

Dhanjal, D. S., Bhardwaj, S., Sharma, R., Bhardwaj, K., Kumar, D., Chopra, C., Nepovimova, E., Singh, R., & Kuca, K. (2020). Plant fortification of the diet for anti-ageing effects: A review. *Nutrients*, *12*(10), 3008. https://doi.org/10.3390/nu12103008

Duangjan, C., Rangsinth, P., Gu, X., Zhang, S., Wink, M., & Tencomnao, T. (2019). Glochidion zeylanicum leaf extracts exhibit lifespan extending and oxidative stress resistance properties in Caenorhabditis elegans via DAF-16/FoxO and SKN-1/Nrf-2 signaling pathways. *Phytomedicine*, *64*. https://doi.org/10.1016/j.phymed.2019.1530611

Eaknai, W., Bunwatcharaphansakun, P., Phungbun, C., Jantimaporn, A., Chaisri, S., Boonrungsiman, S., Nimmannit, U., & Khongkow, M. (2022). Ethanolic fenugreek extract: Its molecular mechanisms against skin aging and the enhanced functions by nanoencapsulation. *Pharmaceuticals*, *15*(2), 254. https://doi.org/10.3390/ph15020254

Elgamal, A. M., Ahmed, R. F., Abd-ElGawad, A. M., El Gendy, A. E.-N. G., Elshamy, A. I., & Nassar, M. I. (2021). Chemical profiles, anticancer, and anti-aging activities of essential oils of *Pluchea dioscoridis* (L.) DC. and *Erigeron bonariensis* L. *Plants*, *10*(4), 667. https://doi.org/10.3390/plants10040667

Ersoy, E., Ozkan, E. E., Boga, M., Yilmaz, M. A., & Mat, A. (2019). Anti-aging potential and anti-tyrosinase activity of three *Hypericum species* with focus on phytochemical composition by LC–MS/MS. *Industrial Crops and Products*, *141*, 111735. https://doi.org/10.1016/j.indcrop.2019.111735

Farooq, U., Pan, Y., Disasa, D., & Qi, J. (2019). Novel anti-aging benzoquinone derivatives from *Onosma bracteatum* Wall. *Molecules*, *24*(7), 1428. https://doi.org/10.3390/molecules24071428

Feng, S., Cheng, H., Xu, Z., Feng, S., Yuan, M., Huang, Y., Liao, J., & Ding, C. (2019). Antioxidant and anti-aging activities and structural elucidation of polysaccharides from *Panax notoginseng* root. *Process Biochemistry*, *78*, 189–199. https://doi.org/10.1016/j.procbio.2019.01.007

Filippopoulou, K., Papaevgeniou, N., Lefaki, M., Paraskevopoulou, A., Biedermann, D., Křen, V., & Chondrogianni, N. (2017). 2, 3-Dehydrosilybin A/B as a pro-longevity and anti-aggregation compound. *Free Radical Biology and Medicine*, *103*, 256–267. https://doi.org/10.1016/j.freeradbiomed.2016.12.042

Georgieva, M., Moyankova, D., Djilianov, D., Uzunova, K., & Miloshev, G. (2015). Methanol extracts from the resurrection plant *Haberlea rhodopensis* ameliorate cellular vitality in chronologically ageing *Saccharomyces cerevisiae* cells. *Biogerontology*, *16*(4), 461–472. https://doi.org/10.1007/s10522-015-9566-z

German-Baez, L., Valdez-Flores, M., Figueroa-Perez, M., Garduno-Felix, K., Valdez-Ortiz, R., Meza-Ayala, K., & Valdez-Ortiz, A. (2017). Anti-aging and nutraceutical characterization of plant infusions used in traditional medicine. *Pakistan Journal of Nutrition*, *16*(4), 285–292. https://doi.org/10.3923/pjn.2017.285.292

Giunti, S., Andersen, N., Rayes, D., & De Rosa, M. J. (2021). Drug discovery: Insights from the invertebrate *Caenorhabditis elegans*. *Pharmacology Research & Perspectives*, *9*(2), e00721.

Haiyuan, Y., Shen, X., Liu, D., Hong, M., & Lu, Y. (2019). The protective effects of β-sitosterol and vermicularin from *Thamnolia vermicularis* (Sw.) Ach. against skin aging in vitro. *Anais da Academia Brasileira de Ciências*, *91*(4), e20181088.

Han, C.-H., Lin, Y.-F., Lin, Y.-S., Lee, T.-L., Huang, W.-J., Lin, S.-Y., & Hou, W.-C. (2014). Effects of yam tuber protein, dioscorin, on attenuating oxidative status and learning dysfunction in D-galactose-induced BALB/c mice. *Food and Chemical Toxicology*, *65*, 356–363. https://doi.org/10.1016/j.fct.2014.01.012

Han, Y., Guo, Y., Cui, S. W., Li, H., Shan, Y., & Wang, H. (2021). Purple sweet potato extract extends lifespan by activating autophagy pathway in male *Drosophila melanogaster*. *Experimental Gerontology*, *144*, 111190. https://doi.org/10.1016/j.exger.2020.111190

Havermann, S., Humpf, H.-U., & Wätjen, W. (2016). Baicalein modulates stress-resistance and life span in *C. elegans* via SKN-1 but not DAF-16. *Fitoterapia*, *113*, 123–127. https://doi.org/10.1016/j.fitote.2016.06.018

Hwang, E., Lin, P., Ngo, H. T., & Yi, T.-H. (2018). Clove attenuates UVB-induced photodamage and repairs skin barrier function in hairless mice. *Food & Function*, *9*(9), 4936–4947.

Hwang, E., Ngo, H. T., Seo, S. A., Park, B., Zhang, M., & Yi, T.-H. (2018). Protective effect of dietary *Alchemilla mollis* on UVB-irradiated premature skin aging through regulation of transcription factor NFATc1 and Nrf2/ARE pathways. *Phytomedicine*, *39*, 125–136. https://doi.org/10.1016/j.phymed.2017.12.025

Iannuzzi, A. M., Giacomelli, C., De Leo, M., Russo, L., Camangi, F., De Tommasi, N., Braca, A., Martini, C., & Trincavelli, M. L. (2021). *Cornus sanguinea* fruits: A source of antioxidant and antisenescence compounds acting on aged human dermal and gingival fibroblasts. *Planta Medica*, *87*(10–11), 879–891. https://doi.org/10.1055/a-1471-6666

Ibe, S., Kumada, K., Yoshida, K., & Otobe, K. (2013). Natto (fermented soybean) extract extends the adult lifespan of *Caenorhabditis elegans*. *Bioscience, Biotechnology, and Biochemistry*, *77*(2), 392–394. https://doi.org/10.1271/bbb.120726

Jan, H., Usman, H., Shah, M., Zaman, G., Mushtaq, S., Drouet, S., Hano, C., & Abbasi, B. H. (2021). Phytochemical analysis and versatile in vitro evaluation of antimicrobial, cytotoxic and enzyme inhibition potential of different extracts of traditionally used *Aquilegia pubiflora* Wall. Ex Royle. *BMC Complementary Medicine and Therapies*, *21*(1), 1–19. https://doi.org/10.1186/s12906-021-03333-y

Jaradat, N. A., Zaid, A. N., Hussen, F., Issa, L., Altamimi, M., Fuqaha, B., Nawahda, A., & Assadi, M. (2018). Phytoconstituents, antioxidant, sun protection and skin anti-wrinkle effects using four solvents fractions of the root bark of the traditional plant *Alkanna tinctoria* (L.). *European Journal of Integrative Medicine*, *21*, 88–93. https://doi.org/10.1016/j.eujim.2018.07.003

Jennings, B. H. (2011). *Drosophila*—A versatile model in biology & medicine. *Materials Today*, *14*(5), 190–195.

Jeon, H., & Cha, D. S. (2016). Anti-aging properties of *Ribes fasciculatum* in *Caenorhabditis elegans*. *Chinese Journal of Natural Medicines*, *14*(5), 335–342.

Jeong, H., Liu, Y., & Kim, H. (2017). Dried plum and chokeberry ameliorate D-galactose-induced aging in mice by regulation of Pl3k/Akt-mediated Nrf2 and Nf-kB pathways. *Experimental Gerontology*, *95*, 16–25. https://doi.org/10.1016/j.exger.2017.05.004

Jiratchayamaethasakul, C., Ding, Y., Hwang, O., Im, S.-T., Jang, Y., Myung, S.-W., Lee, J. M., Kim, H.-S., Ko, S.-C., & Lee, S.-H. (2020). In vitro screening of elastase, collagenase, hyaluronidase, and tyrosinase inhibitory and

antioxidant activities of 22 halophyte plant extracts for novel cosmeceuticals. *Fisheries and Aquatic Sciences*, *23*(1), 1–9. https://doi.org/10.1186/s41240-020-00149-8

Kang, C. H., Rhie, S. J., & Kim, Y. C. (2018). Antioxidant and skin anti-aging effects of marigold methanol extract. *Toxicological Research*, *34*(1), 31–39. https://doi.org/10.5487/TR.2018.34.1.031

Kazeem, M., Bankole, H., Ogunrinola, O., Wusu, A., & Kappo, A. (2021). Functional foods with dipeptidyl peptidase-4 inhibitory potential and management of type 2 diabetes: A review. *Food Frontiers*, *2*(2), 153–162. https://doi.org/10.1002/fft2.71

Kazeem, M. I., & Davies, T. C. (2016). Anti-diabetic functional foods as sources of insulin secreting, insulin sensitizing and insulin mimetic agents. *Journal of Functional Foods*, *20*, 122–138. https://doi.org/10.1016/j.jff.2015.10.013

Kim, H. G., & Oh, M. S. (2013). Memory-enhancing effect of *Mori Fructus* via induction of nerve growth factor. *British Journal of Nutrition*, *110*(1), 86–94. https://doi.org/10.1017/S0007114512004710

Kim, J., Kang, Y.-G., Lee, J.-y., Choi, D.-h., Cho, Y.-u., Shin, J.-M., Park, J. S., Lee, J. H., Kim, W. G., & Seo, D. B. (2015). The natural phytochemical dehydroabietic acid is an anti-aging reagent that mediates the direct activation of SIRT1. *Molecular and Cellular Endocrinology*, *412*, 216–225. https://doi.org/10.1016/j.mce.2015.05.006

Klinngam, W., Rungkamoltip, P., Thongin, S., Joothamongkhon, J., Khumkhrong, P., Khongkow, M., Namdee, K., Tepaamorndech, S., Chaikul, P., & Kanlayavattanakul, M. (2022). Polymethoxyflavones from *Kaempferia parviflora* ameliorate skin aging in primary human dermal fibroblasts and ex vivo human skin. *Biomedicine & Pharmacotherapy*, *145*, 112461.

Kolakul, P., & Sripanidkulchai, B. (2017). Phytochemicals and anti-aging potentials of the extracts from *Lagerstroemia speciosa* and *Lagerstroemia floribunda*. *Industrial Crops and Products*, *109*, 707–716. https://doi.org/10.1016/j.indcrop.2017.09.026

Lee, K. K., Cho, J. J., Park, E. J., & Choi, J. D. (2001). Anti-elastase and anti-hyaluronidase of phenolic substance from *Areca catechu* as a new anti-ageing agent. *International Journal of Cosmetic Science*, *23*(6), 341–346. https://doi.org/10.1046/j.0412-5463.2001.00102.x

Lee, S-H., Lee, H-Y., Yu, M., Yeom, E., Lee, J-H., Yoon, A., Lee, K-S., & Min, K-J. (2019). Extension of Drosophila lifespan by Korean red ginseng through a mechanism dependent on dSir2 and insulin/IGF-1 signaling. *Aging*, *11*, 9369–9387. https://doi.org/10.18632/aging.102387

Leung, M. C., Williams, P. L., Benedetto, A., Au, C., Helmcke, K. J., Aschner, M., & Meyer, J. N. (2008). *Caenorhabditis elegans*: An emerging model in biomedical and environmental toxicology. *Toxicological Sciences*, *106*(1), 5–28. https://doi.org/10.1093/toxsci/kfn121

Li, H., Zhai, B., Sun, J., Fan, Y., Zou, J., Cheng, J., Zhang, X., Shi, Y., & Guo, D. (2021). Antioxidant, anti-aging and organ protective effects of total saponins from *Aralia taibaiensis*. *Drug Design, Development and Therapy*, *15*, 4025. https://doi.org/10.2147/DDDT.S330222

Li, J., Cui, X., Wang, Z., & Li, Y. (2015). rBTI extends *Caenorhabditis elegans* lifespan by mimicking calorie restriction. *Experimental Gerontology*, *67*, 62–71. https://doi.org/10.1016/j.exger.2015.05.001

Li, J., Lu, Y. R., Lin, I. F., Kang, W., Chen, H. B., Lu, H. F., & Wang, H. M. D. (2020). Reversing UVB-induced photoaging with *Hibiscus sabdariffa* calyx aqueous extract. *Journal of the Science of Food and Agriculture*, *100*(2), 672–681. https://doi.org/10.1002/jsfa.10063

Li, N., Li, X., Shi, Y.-L., Gao, J.-M., He, Y.-Q., Li, F., Shi, J.-S., & Gong, Q.-H. (2021). Trilobatin, a component from *Lithocarpus polystachyrus* Rehd., increases longevity in *C. elegans* through activating SKN1/SIRT3/DAF16 signaling pathway. *Frontiers in Pharmacology*, *12*, 655045. https://doi.org/10.3389/fphar.2021.655045

Lin, P., Hwang, E., Ngo, H. T., Seo, S. A., & Yi, T.-H. (2019). *Sambucus nigra* L. ameliorates UVB-induced photoaging and inflammatory response in human skin keratinocytes. *Cytotechnology*, *71*(5), 1003–1017. https://doi.org/10.1007/s10616-019-00342-1

Lin, W.-S., Chen, J.-Y., Wang, J.-C., Chen, L.-Y., Lin, C.-H., Hsieh, T.-R., Wang, M.-F., Fu, T.-F., & Wang, P.-Y. (2014). The anti-aging effects of *Ludwigia octovalvis* on *Drosophila melanogaster* and SAMP8 mice. *Age*, *36*(2), 689–703. https://doi.org/10.1007/s11357-013-9606-z

Liu, H., Liang, F., Su, W., Wang, N., Lv, M., Li, P., Pei, Z., Zhang, Y., Xie, X.-Q., & Wang, L. (2013). Lifespan extension by n-butanol extract from seed of *Platycladus orientalis* in *Caenorhabditis elegans*. *Journal of Ethnopharmacology*, *147*(2), 366–372. https://doi.org/10.1016/j.jep.2013.03.019

Liu, X., Huang, Y., Chen, Y., & Cao, Y. (2016). Partial structural characterization, as well as immunomodulatory and anti-aging activities of CP2-c2-s2 polysaccharide from *Cordyceps militaris*. *RSC Advances*, *6*(106), 104094–104103. https://doi.org/10.1039/C6RA23612J

Lu, L., Zhao, X., Zhang, J., Li, M., Qi, Y., & Zhou, L. (2017). Calycosin promotes lifespan in *Caenorhabditis elegans* through insulin signaling pathway via daf-16, age-1 and daf-2. *Journal of Bioscience and Bioengineering*, *124*(1), 1–7. https://doi.org/10.1016/j.jbiosc.2017.02.021

Luceri, C., Bigagli, E., Pitozzi, V., & Giovannelli, L. (2017). A nutrigenomics approach for the study of anti-aging interventions: Olive oil phenols and the modulation of gene and microRNA expression profiles in mouse brain. *European Journal of Nutrition*, *56*(2), 865–877. https://doi.org/10.1007/s00394-015-1134-4

Luo, J., Si, H., Jia, Z., & Liu, D. (2021). Dietary anti-aging polyphenols and potential mechanisms. *Antioxidants*, *10*(2), 283. https://doi.org/10.3390/antiox10020283

Luo, X., Wang, J., Chen, H., Zhou, A., Song, M., Zhong, Q., Chen, H., & Cao, Y. (2020). Identification of flavonoids from finger citron and evaluation on their antioxidative and antiaging activities. *Frontiers in Nutrition*, *7*, 584900. https://doi.org/10.3389/fnut.2020.584900

Manjia, J. N., Njayou, F., Joshi, A., Upadhyay, K., Shirsath, K., Devkar, R., & Moundipa, P. (2019). The anti-aging potential of medicinal plants in Cameroon-*Harungana madagascariensis* Lam. and *Psorospermum aurantiacum* Engl. prevent in vitro ultraviolet B light-induced skin damage. *European Journal of Integrative Medicine*, *29*, 100925. https://doi.org/10.1016/j.eujim.2019.05.011

Manosroi, A., Jantrawut, P., Akihisa, T., Manosroi, W., & Manosroi, J. (2010). In vitro anti-aging activities of *Terminalia chebula* gall extract. *Pharmaceutical Biology*, *48*(4), 469–481. https://doi.org/10.3109/13880200903586286

Manosroi, J., Chankhampan, C., Kumguan, K., Manosroi, W., & Manosroi, A. (2015). In vitro anti-aging activities of extracts from leaves of Ma Kiang (*Cleistocalyx nervosum* var. paniala). *Pharmaceutical Biology*, *53*(6), 862–869. https://doi.org/10.3109/13880209.2014.946058

Markaki, M., & Tavernarakis, N. (2010). Modeling human diseases in *Caenorhabditis elegans*. *Biotechnology Journal*, *5*(12), 1261–1276. https://doi.org/10.1002/biot.201000183

Markaki, M., & Tavernarakis, N. (2020). *Caenorhabditis elegans* as a model system for human diseases. *Current Opinion in Biotechnology*, *63*, 118–125. https://doi.org/10.1016/j.copbio.2019.12.011

Martel, J., Ojcius, D. M., Ko, Y. F., Chang, C. J., & Young, J. D. (2019). Antiaging effects of bioactive molecules isolated from plants and fungi. *Medicinal Research Reviews*, *39*(5), 1515–1552. https://doi.org/10.1002/med.21559

Meccariello, R., & D'Angelo, S. (2021). Impact of polyphenolic-food on longevity: An elixir of life. An overview. *Antioxidants*, *10*(4), 507. https://doi.org/10.3390/antiox10040507

Men, T. T., Khang, D. T., Tuan, N. T., & Trang, D. T. X. (2022). Anti-aging effects of *Lasia spinosa* L. stem extract on *Drosophila melanogaster*. *Food Science and Technology*, *42*(11–12), 1–7. https://doi.org/10.1590/fst.38721

Mizutani, T., & Masaki, H. (2014). Anti-photoaging capability of antioxidant extract from *C amellia* japonica leaf. *Experimental Dermatology*, *23*, 23–26. https://doi.org/10.1111/exd.12395

Nafiu, M. O., Salawu, M. O., & Kazeem, M. I. (2013). Antioxidant activity of African medicinal plants. In *Medicinal plant research in Africa* (pp. 787–803). Elsevier.

Napagoda, M. T., Kumari, M., Qader, M. M., De Soyza, S. G., & Jayasinghe, L. (2018). Evaluation of tyrosinase inhibitory potential in flowers of *Cassia auriculata* L. for the development of natural skin whitening formulation. *European Journal of Integrative Medicine*, *21*, 39–42. https://doi.org/10.1016/j.eujim.2018.06.005

Okoro, N. O., Odiba, A. S., Osadebe, P. O., Omeje, E. O., Liao, G., Fang, W., Jin, C., & Wang, B. (2021). Bioactive phytochemicals with anti-aging and lifespan extending potentials in *Caenorhabditis elegans*. *Molecules*, *26*(23), 7323. https://doi.org/10.3390/molecules26237323

Pandey, S., Phulara, S. C., Mishra, S. K., Bajpai, R., Kumar, A., Niranjan, A., Lehri, A., Upreti, D. K., & Chauhan, P. S. (2020). *Betula utilis* extract prolongs life expectancy, protects against amyloid-β toxicity and reduces Alpha Synuclien in *Caenorhabditis elegans* via DAF-16 and SKN-1. *Comparative Biochemistry and Physiology Part C: Toxicology & Pharmacology*, *228*, 108647.

Pandey, S., Tiwari, S., Kumar, A., Niranjan, A., Chand, J., Lehri, A., & Chauhan, P. S. (2018). Antioxidant and anti-aging potential of Juniper berry (*Juniperus communis* L.) essential oil in *Caenorhabditis elegans* model system. *Industrial Crops and Products*, *120*, 113–122. https://doi.org/10.1016/j.indcrop.2018.04.066

Pandey, T., Sammi, S. R., Nooreen, Z., Mishra, A., Ahmad, A., Bhatta, R. S., & Pandey, R. (2019). Anti-ageing and anti-Parkinsonian effects of natural flavonol, tambulin from *Zanthoxyllum aramatum* promotes longevity in *Caenorhabditis elegans*. *Experimental Gerontology*, *120*, 50–61. https://doi.org/10.1016/j.exger.2019.02.016

Pant, A., Asthana, J., Yadav, A., Rathor, L., Srivastava, S., Gupta, M., & Pandey, R. (2015). Verminoside mediates life span extension and alleviates stress in *Caenorhabditis elegans*. *Free Radical Research*, *49*(11), 1384–1392. https://doi.org/10.3109/10715762.2015.1075017

Pant, A., Saikia, S. K., Shukla, V., Asthana, J., Akhoon, B. A., & Pandey, R. (2014). Beta-caryophyllene modulates expression of stress response genes and mediates longevity in *Caenorhabditis elegans*. *Experimental Gerontology*, *57*, 81–95. https://doi.org/10.1016/j.exger.2014.05.007

Park, J.-K., Kim, C.-K., Gong, S.-K., Yu, A.-R., Lee, M.-Y., & Park, S.-K. (2014). *Acanthopanax sessiliflorus* stem confers increased resistance to environmental stresses and lifespan extension in *Caenorhabditis elegans*. *Nutrition Research and Practice*, *8*(5), 526–532. https://doi.org/10.4162/nrp.2014.8.5.526

Peixoto, H., Roxo, M., Koolen, H., Da Silva, F., Silva, E., Braun, M. S., Wang, X., & Wink, M. (2018). *Calycophyllum spruceanum* (Benth.), the amazonian "tree of youth" prolongs longevity and enhances stress resistance in *Caenorhabditis elegans*. *Molecules*, *23*(3), 534. https://doi.org/10.3390/molecules23030534

Permatasari, H. K., Nurkolis, F., Augusta, P. S., Mayulu, N., Kuswari, M., Taslim, N. A., Wewengkang, D. S., Batubara, S. C., & Gunawan, W. B. (2021). Kombucha tea from seagrapes (*Caulerpa racemosa*) potential as a functional anti-ageing food: In vitro and in vivo study. *Heliyon*, *7*(9), e07944. https://doi.org/10.1016/j.heliyon.2021.e07944

Pientaweeratch, S., Panapisal, V., & Tansirikongkol, A. (2016). Antioxidant, anti-collagenase and anti-elastase activities of *Phyllanthus emblica*, *Manilkara zapota* and silymarin: An in vitro comparative study for anti-aging applications. *Pharmaceutical Biology*, *54*(9), 1865–1872. https://doi.org/10.3109/13880209.2015.1133658

Prasansuklab, A., Meemon, K., Sobhon, P., & Tencomnao, T. (2017). Ethanolic extract of *Streblus asper* leaves protects against glutamate-induced toxicity in HT22 hippocampal neuronal cells and extends lifespan of *Caenorhabditis elegans*. *BMC Complementary and Alternative Medicine*, *17*(1), 1–14. https://doi.org/10.1186/s12906-017-2050-3

Prommaban, A., Sriyab, S., Marsup, P., Neimkhum, W., Sirithunyalug, J., Anuchapreeda, S., To-Anun, C., & Chaiyana, W. (2022). Comparison of chemical profiles, antioxidation, inhibition of skin extracellular matrix degradation, and anti-tyrosinase activity between mycelium and fruiting body of *Cordyceps militaris* and *Isaria tenuipes*. *Pharmaceutical Biology*, *60*(1), 225–234. https://doi.org/10.1080/13880209.2021.2025255

Rastogi, M., Ojha, R. P., Devi, B. P., Aggarwal, A., Agrawal, A., & Dubey, G. (2012). Amelioration of age associated neuroinflammation on long term bacosides treatment. *Neurochemical Research*, *37*(4), 869–874. https://doi.org/10.1007/s11064-011-0681-1

Rathor, L., Pant, A., Nagar, A., Tandon, S., Trivedi, S., & Pandey, R. (2017). *Trachyspermum ammi* L.(Carom) oil induces alterations in SOD-3, GST-4 expression and prolongs lifespan in *Caenorhabditis elegans*. *Proceedings of the National Academy of Sciences, India Section B: Biological Sciences*, *87*(4), 1355–1362. https://doi.org/10.1007/s40011-016-0710-6

Ruan, Q., Qiao, Y., Zhao, Y., Xu, Y., Wang, M., Duan, J., & Wang, D. (2016). Beneficial effects of *Glycyrrhizae* radix extract in preventing oxidative damage and extending the lifespan of *Caenorhabditis elegans*. *Journal of Ethnopharmacology*, *177*, 101–110. https://doi.org/10.1016/j.jep.2015.10.008

Rusu, M. E., Simedrea, R., Gheldiu, A.-M., Mocan, A., Vlase, L., Popa, D.-S., & Ferreira, I. C. (2019). Benefits of tree nut consumption on aging and age-related diseases: Mechanisms of actions. *Trends in Food Science & Technology*, *88*, 104–120.

Sabiu, S. 2022. *Therapeutic use of plant secondary metabolites*. Bentham Science Publishers.

Saier, C., Büchter, C., Koch, K., & Wätjen, W. (2018). *Polygonum multiflorum* extract exerts antioxidative effects and increases life span and stress resistance in the model organism *Caenorhabditis elegans* via DAF-16 and SIR-2.1. *Plants*, *7*(3), 60. https://doi.org/10.3390/plants7030060

Sayed, S. M., Siems, K., Schmitz-Linneweber, C., Luyten, W., & Saul, N. (2021). Enhanced healthspan in *Caenorhabditis elegans* treated with extracts from the traditional Chinese medicine plants *Cuscuta chinensis* Lam. and *Eucommia ulmoides* Oliv. *Frontiers in Pharmacology*, *12*, 604435. https://doi.org/10.3389/fphar.2021.604435

Senthil, K. K., Gokila, V. M., Mau, J.-L., Lin, C.-C., Chu, F.-H., Wei, C.-C., Liao, V. H.-C., & Wang, S.-Y. (2016). A steroid like phytochemical Antcin M is an anti-aging reagent that eliminates hyperglycemia-accelerated premature senescence in dermal fibroblasts by direct activation of Nrf2 and SIRT-1. *Oncotarget*, *7*(39), 62836. https://doi.org/10.18632/oncotarget.11229

Shoko, T., Maharaj, V. J., Naidoo, D., Tselanyane, M., Nthambeleni, R., Khorombi, E., & Apostolides, Z. (2018). Anti-aging potential of extracts from *Sclerocarya birrea* (A. Rich.) Hochst and its chemical profiling by UPLC-Q-TOF-MS. *BMC Complementary and Alternative Medicine*, *18*(1), 1–14. https://doi.org/10.1186/s12906-018-2112-1

Spindler, S. R., Mote, P. L., Lublin, A. L., Flegal, J. M., Dhahbi, J. M., & Li, R. (2015). Nordihydroguaiaretic acid extends the lifespan of *Drosophila* and mice, increases mortality-related tumors and hemorrhagic diathesis, and alters energy homeostasis in mice. *Journals of Gerontology Series A: Biomedical Sciences and Medical Sciences*, *70*(12), 1479–1489. https://doi.org/10.1093/gerona/glu190

Su, S., & Wink, M. (2015). Natural lignans from *Arctium lappa* as antiaging agents in *Caenorhabditis elegans*. *Phytochemistry*, *117*, 340–350. https://doi.org/10.1016/j.phytochem.2015.06.021

Sun, X., Seeberger, J., Alberico, T., Wang, C., Wheeler, C. T., Schauss, A. G., & Zou, S. (2010). Açai palm fruit (Euterpe oleracea Mart.) pulp improves survival of flies on a high fat diet. *Experimental Gerontology*, *45*, 243–251. https://doi.org/10.1016/j.exger.2010.01.008

Sun, K., Xiang, L., Ishihara, S., Matsuura, A., Sakagami, Y., & Qi, J. (2012). Anti-aging effects of hesperidin on *Saccharomyces cerevisiae* via inhibition of reactive oxygen species and UTH1 gene expression. *Bioscience, Biotechnology, and Biochemistry*, *76*(4), 640–645. https://doi.org/10.1271/bbb.110535

Sung, B., Chung, J. W., Bae, H. R., Choi, J. S., Kim, C. M., & Kim, N. D. (2015). *Humulus japonicus* extract exhibits antioxidative and anti-aging effects via modulation of the AMPK-SIRT1 pathway. *Experimental and Therapeutic Medicine*, *9*(5), 1819–1826. https://doi.org/10.3892/etm.2015.2302

Szewczyk, K., Pietrzak, W., Klimek, K., Miazga-Karska, M., Firlej, A., Flisiński, M., & Grzywa-Celińska, A. (2021). Flavonoid and phenolic acids

content and in vitro study of the potential anti-aging properties of *Eutrema japonicum* (Miq.) Koidz cultivated in Wasabi Farm Poland. *International Journal of Molecular Sciences*, *22*(12), 6219. https://doi.org/10.3390/ijms22126219

Tambara, A. L., de Los Santos Moraes, L., Dal Forno, A. H., Boldori, J. R., Soares, A. T. G., de Freitas Rodrigues, C., Mariutti, L. R. B., Mercadante, A. Z., de Ávila, D. S., & Denardin, C. C. (2018). Purple pitanga fruit (*Eugenia uniflora* L.) protects against oxidative stress and increase the lifespan in *Caenorhabditis elegans* via the DAF-16/FOXO pathway. *Food and Chemical Toxicology*, *120*, 639–650. https://doi.org/10.1016/j.fct.2018.07.057

Tang, R., Chen, X., Dang, T., Deng, Y., Zou, Z., Liu, Q., Gong, G., Song, S., Ma, F., & Huang, L. (2019). *Lycium barbarum* polysaccharides extend the mean lifespan of *Drosophila melanogaster*. *Food & Function*, *10*(7), 4231–4241.

Teseo, S., Houot, B., Yang, K., Monnier, V., Liu, G., & Tricoire, H. (2021). *G. sinense* and *P. notoginseng* extracts improve healthspan of aging flies and provide protection in a huntington disease model. *Aging and Disease*, *12*(2), 425. https://doi.org/10.14336/AD.2020.0714-1

Tlili, N., Kirkan, B., & Sarikurkcu, C. (2019). LC–ESI–MS/MS characterization, antioxidant power and inhibitory effects on α-amylase and tyrosinase of bioactive compounds from hulls of *Amygdalus communis*: The influence of the extracting solvents. *Industrial Crops and Products*, *128*, 147–152. https://doi.org/10.1016/j.indcrop.2018.11.014

Tungmunnithum, D., Drouet, S., & Hano, C. (2022). Validation of a high-performance liquid chromatography with photodiode array detection method for the separation and quantification of antioxidant and skin anti-aging flavonoids from *Nelumbo nucifera* Gaertn. stamen extract. *Molecules*, *27*(3), 1102. https://doi.org/10.3390/molecules27031102

United Nations (UN). (2022). *World population prospects 2022: Summary of results*. United Nations.

Utami, S., Sachrowardi, Q. R., Damayanti, N. A., Wardhana, A., Syarif, I., Nafik, S., Arrahman, B. C., Kusuma, H. S. W., & Widowati, W. (2018). Antioxidants, anticollagenase and antielastase potentials of ethanolic extract of ripe sesoot (*Garcinia picrorrhiza* Miq.) fruit as antiaging. *Journal of Herbmed Pharmacology*, *7*(2), 88–93. https://doi.org/10.15171/jhp.2018.15

Vayndorf, E. M., Lee, S. S., & Liu, R. H. (2013). Whole apple extracts increase lifespan, healthspan and resistance to stress in Caenorhabditis elegans. *Journal of Functional Foods*, *5*, 1235–1243. https://doi.org/10.1016/j.jff.2013.04.0062

Wang, L., Chen, Q., Zhuang, S., Wen, Y., Cheng, W., Zeng, Z., Jiang, T., & Tang, C. (2020). Effect of *Anoectochilus roxburghii* flavonoids extract on H_2O_2-Induced oxidative stress in LO2 cells and D-gal induced aging mice model. *Journal of Ethnopharmacology*, *254*, 112670. https://doi.org/10.1016/j.jep.2020.112670

Wang, L., Du, J., Zhao, F., Chen, Z., Chang, J., Qin, F., Wang, Z., Wang, F., Chen, X., & Chen, N. (2018). Trillium tschonoskii maxim saponin mitigates D-galactose-induced brain aging of rats through rescuing dysfunctional autophagy mediated by Rheb-mTOR signal pathway. *Biomedicine & Pharmacotherapy*, *98*, 516–522.

Wang, S., Xue, J., Zhang, S., Zheng, S., Xue, Y., Xu, D., & Zhang, X. (2020). Composition of peony petal fatty acids and flavonoids and their effect on *Caenorhabditis elegans* lifespan. *Plant Physiology and Biochemistry*, *155*, 1–12. https://doi.org/10.1016/j.plaphy.2020.06.029

World Health Organization (WHO). 2002. *WHO Traditional Medicine Strategy 2002—2005*. World Health Organization.

World Health Organization (WHO). 2022. *World health statistics 2022: Monitoring health for the SDGs, sustainable development goals*. World Health Organization.

Wongchum, N., & Dechakhamphu, A. (2021). Xanthohumol prolongs lifespan and decreases stress-induced mortality in *Drosophila melanogaster*. *Comparative Biochemistry and Physiology Part C: Toxicology & Pharmacology*, *244*, 108994.

Wu, M., Cai, J., Fang, Z., Li, S., Huang, Z., Tang, Z., Luo, Q., & Chen, H. (2022). The composition and anti-aging activities of polyphenol extract from *Phyllanthus emblica* L. fruit. *Nutrients*, *14*(4), 857. https://doi.org/10.3390/nu14040857

Wu, S., Li, J., Wang, Q., Cao, J., Yu, H., Cao, H., & Xiao, J. (2017). Chemical composition, antioxidant and anti-tyrosinase activities of fractions from *Stenoloma chusanum*. *Industrial Crops and Products*, *107*, 539–545. https://doi.org/10.1016/j.indcrop.2017.04.033

Yang, J.-E., Ngo, H. T., Hwang, E., Seo, S. A., Park, S. W., & Yi, T.-H. (2019). Dietary enzyme-treated *Hibiscus syriacus* L. protects skin against chronic UVB-induced photoaging via enhancement of skin hydration and collagen synthesis. *Archives of Biochemistry and Biophysics*, *662*, 190–200. https://doi.org/10.1016/j.abb.2018.12.020

Yang, X., Zhang, P., Wu, J., Xiong, S., Jin, N., & Huang, Z. (2012). The neuroprotective and lifespan-extension activities of *Damnacanthus officinarum* extracts in *Caenorhabditis elegans*. *Journal of Ethnopharmacology*, *141*(1), 41–47. https://doi.org/10.1016/j.jep.2012.01.025

Yin, Z., Park, R., & Choi, B.-M. (2020). Isoparvifuran isolated from *Dalbergia odorifera* attenuates H_2O_2-induced senescence of BJ cells through SIRT1 activation and AKT/mTOR pathway inhibition. *Biochemical and Biophysical Research Communications*, *533*(4), 925–931. https://doi.org/10.1016/j.bbrc.2020.09.096

You, J., Roh, K.-B., Li, Z., Liu, G., Tang, J., Shin, S., Park, D., & Jung, E. (2015). The antiaging properties of *Andrographis paniculata* by activation epidermal cell stemness. *Molecules*, *20*(9), 17557–17569. https://doi.org/10.3390/molecules200917557

Zhang, J., Xiao, Y., Guan, Y., Rui, X., Zhang, Y., Dong, M., & Ma, W. (2019). An aqueous polyphenol extract from Rosa rugosa tea has antiaging effects on Caenorhabditis elegans. *Journal of Food Biochemistry*, *43*, e12796. https://doi.org/10.1111/jfbc.127963

Zhang, N., Zhang, Z., Xu, W., & Jing, P. (2021). TMT-based quantitative proteomic analysis of hepatic tissue reveals the effects of dietary cyanidin-3-diglucoside-5-glucoside-rich extract on alleviating D-galactose-induced aging in mice. *Journal of Proteomics*, *232*, 104042. https://doi.org/10.1016/j.jprot.2020.104042

Zhang, W., Zheng, B., Deng, N., Wang, H., Li, T., & Liu, R. H. (2020). Effects of ethyl acetate fractional extract from *Portulaca oleracea* L.(PO-EA) on lifespan and healthspan in *Caenorhabditis elegans*. *Journal of Food Science*, *85*(12), 4367–4376. https://doi.org/10.1111/1750-3841.15507

Zhang, X., Shi, G. F., Liu, X. Z., An, L. J., & Guan, S. (2011). Anti-ageing effects of protocatechuic acid from *Alpinia* on spleen and liver antioxidative system of senescent mice. *Cell Biochemistry and Function*, *29*(4), 342–347. https://doi.org/10.1002/cbf.1757

Zhang, Y., Dan-Yang, M., Jin, W., Yan-Ping, L., Xu, Y., Shi, D., Xing-Ming, M., & Kai-Zhong, D. (2018). Constituent and effects of polysaccharides isolated from *Sophora moorcroftiana* seeds on lifespan, reproduction, stress resistance, and antimicrobial capacity in *Caenorhabditis elegans*. *Chinese Journal of Natural Medicines*, *16*(4), 252–260. https://doi.org/10.1016/S1875-5364(18)30055-4

Zhang, Y., Lv, T., Li, M., Xue, T., Liu, H., Zhang, W., Ding, X., & Zhuang, Z. (2015). Anti-aging effect of polysaccharide from *Bletilla striata* on nematode *Caenorhabditis elegans*. *Pharmacognosy Magazine*, *11*(43), 449.

Zhao, S.-J., Liu, X.-J., Tian, J.-S., Gao, X.-X., Liu, H.-L., Du, G.-H., & Qin, X.-M. (2020). Effects of guilingji on aging rats and its underlying mechanisms. *Rejuvenation Research*, *23*(2), 138–149. https://doi.org/10.1089/rej.2018.2118

Zhao, Y., Liao, A.-M., Liu, N., Huang, J.-H., Lv, X., Yang, C.-R., Chen, W.-J., Hou, Y.-C., Ma, L.-J., & Hui, M. (2021). Potential anti-aging effects of fermented wheat germ in aging mice. *Food Bioscience*, *42*, 101182. https://doi.org/10.1016/j.fbio.2021.101182

Zheng, J., & Greenway, F. (2012). *Caenorhabditis elegans* as a model for obesity research. *International Journal of Obesity*, *36*(2), 186–194. https://doi.org/10.1038/ijo.2011.93

Zhong, J., Wang, F., Wang, Z., Shen, C., Zheng, Y., Ma, F., Zhu, T., Chen, L., Tang, Q., & Zhu, J. (2019). Aloin attenuates cognitive impairment and inflammation induced by d-galactose via down-regulating ERK, p38 and

NF-κB signaling pathway. *International Immunopharmacology*, *72*, 48–54. https://doi.org/10.1016/j.intimp.2019.03.050

Zhong, S.-J., Wang, L., Wu, H.-T., Lan, R., & Qin, X.-Y. (2019). *Coelogloss-sum viride* var. *bracteatum* extract improves learning and memory of chemically-induced aging mice through upregulating neurotrophins BDNF and FGF2 and sequestering neuroinflammation. *Journal of Functional Foods*, *57*, 40–47. https://doi.org/10.1016/j.jff.2019.03.045

Zhou, X., Yang, Q., Xie, Y., Sun, J., Hu, J., Qiu, P., Cao, W., & Wang, S. (2015). Tetrahydroxystilbene glucoside extends mouse life span via upregulating neural klotho and downregulating neural insulin or insulin-like growth factor 1. *Neurobiology of Aging*, *36*(3), 1462–1470. https://doi.org/10.1016/j.neurobiolaging.2014.11.002

Zhou, Y.-Z., Xue, L.-Y., Gao, L., Qin, X.-M., & Du, G.-H. (2018). Ginger extract extends the lifespan of *Drosophila melanogaster* through antioxidation and ameliorating metabolic dysfunction. *Journal of Functional Foods*, *49*, 295–305. https://doi.org/10.1016/j.jff.2018.08.040

Zhuang, Y., Ma, Q., Guo, Y., & Sun, L. (2017). Protective effects of rambutan (*Nephelium lappaceum*) peel phenolics on H_2O_2-induced oxidative damages in HepG2 cells and D-galactose-induced aging mice. *Food and Chemical Toxicology*, *108*, 554–562. https://doi.org/10.1016/j.fct.2017.01.022

How to cite this article: Kazeem, M. I., Mellem, J. J., & Sabiu, S. (2024). Medicinal foods and plants with antiaging properties: A review of in vitro and in vivo studies. *Food Frontiers*, *5*, 24–45. https://doi.org/10.1002/fft2.325

Food Bioscience 68 (2025) 106355

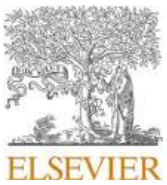

Contents lists available at ScienceDirect

Food Bioscience

journal homepage: www.elsevier.com/locate/fbio

Lemongrass (*Cymbopogon citratus*) infusions exhibit neuroprotective properties: Evidence from *in vitro* and *in silico* studies

Mutiu Idowu Kazeem, Rukayat Abiola Abdulsalam, John Jason Mellem, Saheed Sabiu *

Department of Biotechnology and Food Science, Faculty of Applied Sciences, Durban University of Technology, P. O. Box 1334, Durban, 4000, South Africa

ARTICLE INFO

Keywords:
Lemongrass
Alzheimer's disease
Molecular dynamics simulation
Acetylcholinesterase
Monoamine oxidase
Tea

ABSTRACT

The prevalence of neurological disorders is high, especially in the elderly, and current therapies only provide temporary relief and elicit serious adverse effects. This study evaluated the neuroprotective effect of *Cymbopogon citratus* (lemongrass) teas using *in vitro* and *in silico* techniques. The inhibitory effect of the infusions from fresh and dry lemongrass was tested against four enzymes implicated in neurological diseases viz; acetylcholinesterase (AChE), butyrylcholinesterase (BChE), β-secretase (BACE-1), and monoamine oxidase (MAO). This was followed by molecular docking and molecular dynamic simulation studies to assess the interactions of the metabolites present in lemongrass on the selected enzymes. The fresh lemongrass tea displayed a better inhibitory effect on the activities of BACE-1 (IC_{50}: 38.24 μg/mL) and MAO (IC_{50}: 78.62 μg/mL), and is comparable to the standard drugs. Molecular docking revealed that resulting complexes from 4-oxo-3-phenyl-4H-chromen-7-yl 3-phenyl-prop-2-enoate (OPCPPE) as well as aspulvinone H (−10.6 kcal/mol), [1,1′-binaphthalen]-2-ol (−12.1 kcal/mol), neocuscutoside C (−10.5 kcal/mol) and aspulvinone H (−11.9 kcal/mol) had the lowest scores for AChE, BChE, BACE-1, and MAO, respectively. A further probe through a 120-ns molecular dynamics simulation on the top-performing metabolites showed that the resulting complexes formed with chamaemeloside (−66.59 kcal/mol), isocarlinoside (−65.79 kcal/mol), neocuscutoside C (−41.09 kcal/mol), and aspulvinone H (−72.28 kcal/mol) against AChE, BChE, BACE-1 and MAO, respectively, had the lowest binding free energy values compared to the respective standards. In conclusion, the fresh lemongrass tea elicited better neuroprotective properties *in vitro* and its phenolic constituents (especially aspulvinone H and neocuscutoside C) are potent inhibitors of neurological targets *in silico*. There is a need for further studies on the *in vivo* neuroprotective potentials of these compounds.

1. Introduction

Neurological disorders (NDs) are ailments that affect the nervous system characterized by behavioral changes and cognitive deficits (Haider et al., 2021). These pathologies cause continuous alterations in the neuronal structure and function leading to cellular death (Paudel et al., 2019). Globally, more than 3 billion people are living with neurological disorders and over 80 % of neurological deaths and ill health occur in low and middle-income countries (Steinmetz et al., 2024). They are the leading cause of ill health and disability and cause severe hardship to individuals, families, and society at large (Gyebi et al., 2023). These pathologies (which include dementia, Alzheimer's, Parkinson's, and Huntington's disease) may differ in their etiology but share neural cell death, neuroinflammation, and brain damage (Paudel et al., 2019). The onset of these ailments may affect the mobility, memory, and speech of the patients thereby causing life-long disabilities and a socio-economic burden on the society.

Approved therapies for the management of neurological disorders only achieve symptomatic relief and do not cure these diseases while they also cause serious adverse effects (Santi et al., 2020). Consequently, there is an urgent need to search for neuroprotective agents from alternative sources like plants. About 80 % of the global population relies on medicinal foods and plants for the treatment of diseases due to their accessibility, affordability, efficacy, and perceived safety (WHO, 2002). Several medicinal plants have been validated for their various therapeutic properties including antioxidant, antidiabetic, anticancer, hepatoprotective, cardioprotective, and neuroprotective agents (Cancela et al., 2020; Kazeem & Davies, 2016). These therapeutic effects

This article is part of a special issue entitled: Bioproducts and functional food published in Food Bioscience.

* Corresponding author.
E-mail address: sabius@dut.ac.za (S. Sabiu).

https://doi.org/10.1016/j.fbio.2025.106355
Received 18 September 2024; Received in revised form 11 January 2025; Accepted 12 March 2025
Available online 15 March 2025

are attributed to the presence of phytochemical compounds including polyphenols, flavonoids, saponins, terpenes, and glycosides.

Cymbopogon citratus (Poaceae), commonly referred to as lemongrass, is a perennial grass that is native to Asia but widely distributed in all regions of the globe (Oladeji et al., 2019). Infusions prepared from the leaves are consumed for nutritional and/or therapeutic purposes similar to other herbal teas like green or rooibos tea (Ekpenyong et al., 2015). Due to its aromatic nature, the leaf's essential oil is used in the food, soap, cosmetic, and pharmaceutical industries (Avoseh et al., 2015). It is used in traditional medicine for the treatment of cold, pain, fever, indigestion, and gastrointestinal disturbances (Ekpenyong et al., 2015). Several studies have reported the pharmacological properties of the plant including antioxidant, antimicrobial, anti-inflammatory, antidiabetic, and antimalarial properties (Negrelle & Gomes, 2007; Oladeji et al., 2019). Though there are some studies on the neuroprotective potentials of lemongrass leaves in the literature (Fatima et al., 2024; Hacke et al., 2021; Madi et al., 2020; Rojek et al., 2022; Umukoro et al., 2018), there is a need to provide detailed information on the mechanism of neuroprotective activity of the lemongrass teas.

Previous studies have revealed that many enzymes serve as therapeutic targets for neurological disorders. These include [acetylcholinesterase (AChE), butyrylcholinesterase (BChE), β-secretase (BACE-1), and monoamine oxidase (MOA)]. AChE and BChE hydrolyze and inactivate acetylcholine, thereby controlling the concentration of the neurotransmitter at the synapse (Masondo et al., 2019). However, excessive inactivation of acetylcholine is implicated in the pathogenesis of Alzheimer's disease. Beta-site Amyloid Precursor Protein Cleaving Enzyme 1 (BACE-1), otherwise called β-secretase, catalyzes the initial cleavage of the amyloid precursor protein (APP) leading to the generation of amyloid-β (Aβ) peptides (Gyebi et al., 2023). Accumulation of amyloid-β in the brain causes Alzheimer's disease and BACE-1 is a potential therapeutic target of the disease (Mazumder & Choudhury, 2019; Mendes et al., 2023). Monoamine oxidase (MOA) is an enzyme that catalyzes the oxidative deamination of monoaminergic neurotransmitters such as serotonin, dopamine, epinephrine and norepinephrine (Moorkoth et al., 2021). It is implicated in the pathogenesis of depression, Alzheimer's and Parkinson's disease (Jalal et al., 2022).

Therefore, this study investigated the inhibitory properties of lemongrass infusions on neurological targets [acetylcholinesterase (AChE), butyrylcholinesterase (BChE), β-secretase (BACE-1), and monoamine oxidase (MOA)] *in vitro* and complemented the findings with computational studies through establishment of intermolecular interactions between its metabolites and the target enzymes as a way of lending credence to its mechanism of neuroprotective action. This is hoped to contribute towards discovering novel therapeutic agents for managing neurological disorders.

2. Materials and methods

2.1. Materials

All the enzymes and their substrates namely acetylcholinesterase (AChE) type V from electric eel, butyrylcholinesterase (BChE) from equine serum, acetylthiocholine iodide, butyrylcholine iodide, kynuramine as well as β-secretase and monoamine oxidase from humans are obtained from Sigma Aldrich, Missouri, USA. The reference drugs donepezil, AZD3293, and tranylcypromine were products of Pfizer Inc., New York, USA. All other chemicals are of analytical grade and the water used is glass-distilled. All materials used in this study are properly stored and used within 3 months.

2.2. Preparation of lemongrass teas

Leaves of lemongrass were harvested from farmland in the Iba area of Lagos in October 2021. It was identified and authenticated at the Department of Botany, Lagos State University, Nigeria, and was assigned the voucher number: LSH/21/1055. The leaves were gently rinsed in tap water to remove soil and dirt. A portion was cut into pieces using a stainless-steel kitchen knife spread on foil paper and dried to constant weight on the laboratory table at ambient temperature while the second portion was used fresh. After drying, the sample was milled using an electric grinder (Silver Crest, Germany). One litre of boiled distilled water was poured on a 100 g milled sample, shaken, and left to steep for 24 h to produce an infusion. Another 1.0 L of boiled distilled was poured on the second portion (100 g) of the fresh lemongrass and left to steep for 24 h. Both infusions were filtered and concentrated in a lyophilizer (Virtis BenchTop, SP Scientific Series, USA). The lyophilized infusions were used for subsequent analysis by dissolving in distilled water to give stock solutions of 1.0 mg/mL and different concentrations (3.13, 6.25, 12.5, 25, 50, and 100 μg/mL). All infusions were stored at 4 °C before analysis.

2.3. Metabolite profiling using liquid chromatography-mass spectrometry (LC-MS)

The phytochemical composition of the teas obtained from fresh and dry lemongrass leaves was assessed using a previous method (Suleria et al., 2020). Agilent 6520 Accurate-Mass QTOF was applied in a positive and negative mode. Synergi Hydro-RP (4 μm particle size, 4.6 mm internal diameter, and 250 mm length with 80 Å pore size were used to separate phenolic compounds, and the flow rate was set at 800 μL/min. An aliquot of 10 μL from each sample was injected while gradient was 0–5 min (0–10 %), 5–25 min (10–25 % B), 25–35 min (25–35 % B), 35–45 min (40–60 % B) 45–75 min (40–55 % B), 75–80 min (55–88 % B) (80–82 min (80–90 % B), 82–85 min (90–100 % B), 85–90 min (0 % B). Mobile phase A was 0.1 % formic acid in water and mobile phase B was 95 % acetonitrile with 0.1 % formic acid. A full scan mode was achieved in the range of 100–1000 amu with the following conditions; capillary voltage (3500 V), nozzle voltage (500 V), nitrogen gas flow rate (9 L/min) at 325 °C and nebulization was set as 45 psi while 10, 20 and 30 eV collision energies were used. Acquisition of data was performed through employment of MassLynx4.1 software, while detection and confirmation of metabolites were processed using the MS-DIAL software and MS-FINDER (RIKEN Centre for Sustainable Resource Science: Metabolome Informatics Research Team, Kanagawa, Japan). For further confirmation, identification of the profiled metabolites was also performed by comparing the respective mass spectra obtained against the National Institute of Standards and Technology (NIST) library (Wallace & Moorthy, 2023).

2.4. In vitro inhibitory studies

2.4.1. Cholinesterase inhibition assay

The acetylcholinesterase (AChE) inhibitory activity of the lemongrass infusions was evaluated (Perry et al., 2001). Forty microliters of (0.28 U/ml) acetylcholinesterase, 140 μL of 3.3 mM of 5,5-dithiobis-(2--nitrobenzoic) acid (prepared in 0.1 M phosphate-buffered solution, pH 7.0, containing 6 mM $NaHCO_3$), lemongrass infusions (3.13–100 μg/mL), and 80 μl of phosphate buffer (pH 8.0) were added to each well of microplate. The solution was incubated for 20 min at 25 °C. Acetylthiocholine iodide (0.05 mM, 40 μl) was added to each well and the absorbance was determined in a microtiter plate reader (Synergy MX Biotech) at 412 nm for 3 min immediately after the addition of the substrate. The same experiment was used to determine the butyrylcholinesterase (BChE) activity of the extracts using butyrylcholine iodide. The enzyme inhibitory activities were expressed as percentage inhibition.

2.4.2. Beta-secretase inhibition assay

The β-secretase inhibitory property of the lemongrass infusions was performed using standard method (Puksasook et al., 2017). Briefly, 20 μL of 0.1 U/mL β-secretase and 20 μL of lemongrass infusions dissolved

in 100 mM sodium acetate buffer pH 4.5 were added to the 96-well and incubated at 37 °C for 10 min. Then 50 μL of 750 mM β-secretase substrate in 100 mM sodium acetate buffer pH 4.5 was added and incubated at 37 °C for 20 min. After that, 10 μL of stop buffer (2.5 M sodium acetate buffer pH 4.5) was added to the 96-well plate. Then, the fluorescence was measured at 380 nm (excitation wavelength) and 510 nm (emission wavelength) using a microplate reader (Spectramax, USA). AZD3293 was used as the positive control.

2.4.3. Monoamine oxidase inhibitory assay

The monoamine oxidase inhibitory property of the samples was evaluated (Yang et al., 2020). Briefly, 50 μL of potassium phosphate buffer (0.1 M, pH 7.4) and 50 μL of monoamine oxidase solution (final protein concentration was 0.0006 mg/mL) were mixed with 50 μL of lemongrass infusions (prepared in potassium phosphate buffer), followed by incubation at 37 °C for 30 min. Thereafter, 50 μL kynuramine (40 μM) was added to the mixture to initiate the reaction, followed by incubation at 37 °C for 20 min and the reaction was terminated by the addition of 75 μL of 2 M NaOH. The fluorescence was subsequently measured at excitation and emission wavelengths of 310 and 380 nm, respectively. Tranylcypromine was used as a positive control.

2.5. In silico studies

2.5.1. Collection and preparation of the identified metabolites

The 3D structures of the 49 identified/annotated metabolites from *Cymbopogon citratus* using MS-DIAL software and MS-FINDER coupled with further confirmation by comparing the respective mass spectra obtained against NIST library and those of the reference drugs [donepezil with ID 3152 (standard for acetylcholinesterase and butyrylcholinesterase)], [AZD3293 with ID 67979346 (standard for β-secretase)], and [tranylcypromine with ID 19493 (standard for monoamine oxidase)], were obtained from PubChem (https://pubchem.ncbi.nlm.nih.gov/) and then optimized via the additions of nonpolar hydrogen atoms and charges using the Avogadro software (Aribisala et al., 2022). The optimized ligands were saved in Mol2 format for subsequent molecular docking.

2.5.1.1. Collection and preparation of therapeutic targets. The X-ray crystal structures of AChE (ID: 4PQE), BChE (ID: 1P0I), BACE (ID: 11SGZ), and MAO-A (ID: 2BXS) were acquired from the Protein Data Bank (https://www.rcsb.orgs/) and prepared through the removal of non-standard amino acids and water molecules using UCSF chimera software v 1.14 (Gyebi et al., 2023). The cleaned structures were then saved in PDB format for molecular docking.

2.5.2. Molecular docking and validation of C. citratus metabolites

The docking procedure entailed the selection of amino residues at the active site of the protein whose grid box coordinates coincide with the established x-y-z coordinates; AChE [centre (X: 32.03; Y: 7.10; Z: 14.59) radius (22.20)], BChE [centre (X: 23.13; Y: 47.61; Z: 33.33), radius (5.0)], BACE-1 [centre (X: 32.67; Y: 6.14; Z: 12.66), radius (12.20)], and MOA [centre (X: 4.85; Y: 35.25; Z: 17.94), radius (25.20)].

Subsequent docking at the active site of the proteins was ensured by dragging the grid box to fit the established, well-defined x-y-z coordinates. Thereafter, the optimized 3D structures of the ligands (*C. citratus* metabolites and reference drugs) and cleaned proteins (AChE, BChE, BACE, and MAO-A) were subjected to molecular docking using the Autodock vina package on Python Prescription v 0.9.5 (PyRx), which allows for multiple docking of ligands (Onder et al., 2022). Finally, the ligands were ranked based on their binding affinity, and the top five docked complexes with the best pose were saved in PDB format and subjected to MD simulations.

To validate the docking conformation, the superimposition and redocking techniques were employed, where the appropriate root-mean-square deviation (RMSD) of a docked compound from its reference point (position of native inhibitors) in each target was calculated (Al-Khodairy et al., 2013). The best conformational clusters from this dock were ranked based on the RMSD between their docked position and the ligand's experimentally determined position (Al-Khodairy et al., 2013).

2.5.3. Molecular dynamics simulation

The MD simulation was performed as previously described (Sabiu et al., 2021). Succinctly, the simulations were performed over a 120 ns period using the AMBER 14 package of the Centre for High-Performance Computing (CHPC), South Africa. The FF18SB variant of the AMBER force field was adopted to describe the operating systems. The ANTECHAMBER was employed to create the ligands' atomic partial charges by exploiting the general amber force field (GAFF) procedures and restrained electrostatic potential (RESP). The hydrogen atoms, Na^{+}, and Cl counter ions of the Leap module were used to neutralize the systems. In each case of the simulation, the numbering of the amino acid residues was done accordingly, and the systems were suspended inside an orthorhombic box of TIP3P water molecules in a manner that all atoms were within 8 Å of any box edge. The bonds of hydrogen atoms in each case of the simulation were constrained using the SHAKE algorithm. Each simulation had a 2 fs step size, which corresponded to the isobaric–isothermal ensemble (NPT) with randomized seeding, a temperature of 300 K, constant pressure of 1 bar, and a Langevin thermostat with a 1.0 ps collision frequency and a pressure-coupling constant of 2 ps. Following that, the results of the 120 ns MD simulation were examined and regarded as post-dynamic data.

2.5.4. Post-MD simulation

The post-MD simulation was carried out as earlier described (Jalal et al., 2022). Briefly, after the simulation, the systems' coordinates were combined and analyzed using the AMBER 14 PTRAJ module of CHPC. After this, the root mean square fluctuation (RMSF), the radius of gyration (RoG), root mean square deviation (RMSD), and solvent accessibility surface area (SASA) were analyzed using the CPPTRAJ module of the same package, and their raw data generated using Origin V6. Similarly, using the Molecular Mechanics/GB Surface Area approach, the free binding energy (ΔG) in each case of the simulation was calculated using the expression ΔG bind = Gcomplex – (G Receptor + G ligand) by averaging among 100,000 snapshots taken from a 120 ns MD simulation trajectory. The complexes' interactions in each simulation case were visualized and analyzed post-MD simulation using Discovery Studio version 21.1.0.

2.5.5. Determination of ADMET properties

The ADMETlab 3.0 web (https://admetlab3.scbdd.com/) was used to forecast the adsorption, distribution, metabolism, excretion, and toxicological properties of the compounds with the top docking score.

2.6. Statistical analysis

The *in vitro* enzyme inhibitory studies were performed in triplicates and data were expressed as mean ± standard error of the mean (SEM). IC_{50} values were obtained from percentage inhibitions using Microsoft Excel software (Microsoft, 2010). Analysis of variance (ANOVA) was used to assess differences in the percentage inhibitory activities and mean values of the samples using the GraphPad Prism statistical package (GraphPad Software, USA). Statistical significance was considered at $p < 0.05$. Except otherwise stated, the raw data plots for the *in silico* evaluations were generated using the Origin data analysis software V18 (OriginLab, Northampton, MA, USA).

3. Results and discussion

3.1. Phytochemical composition

Table 1 and Figs. S1a–b show the results of the LC-MS profile of the infusions from fresh and dry lemongrass leaves. The chromatogram revealed the presence of 49 phytochemical compounds in all the samples tested. Corymboside, veranisatin C, chamaemeloside, neocuscutoside C, and herbarumin II had the highest peaks in the chromatogram, which suggests that they have the highest relative abundances.

3.2. In vitro study

One of the neurological disorders associated with aging is Alzheimer's disease, caused by a continuous deficiency in cholinergic neurotransmission and affects about 10 % of old people (Racchi et al., 2004). Hydrolysis of synaptic acetylcholine is important in cholinergic neurotransmission and is mediated by two enzymes – acetylcholinesterase (AChE) and butyrylcholinesterase (BChE) (Soreq & Seidman, 2001). Fig. 1 shows the percentage inhibition of neurological-related enzymes by fresh and dry infusions of lemongrass. Both fresh and dry infusions of lemongrass similarly inhibited acetylcholinesterase except at low concentration (6.25 μg/mL) where the dry infusion is higher (Fig. 1a). Butyrylcholinesterase was also inhibited in the same manner by the fresh and dry teas of lemongrass except at the concentration of 3.13 and 6.25 μg/mL (Fig. 1b). Table 2 shows that both fresh and dry teas have similar IC_{50} values for both acetylcholinesterase and butyrylcholinesterase, though the standard donepezil has higher values for butyrylcholinesterase. The effective inhibition of both AChE and BChE activities as depicted by the low IC_{50} values by both fresh and dry teas of lemongrass leaf indicated that the infusions can diminish the undesirable inactivation of acetylcholine experienced in Alzheimer's disease (Sheeja Malar et al., 2017). This will, in turn, enhance the brain acetylcholine level thereby improving the memory and cognitive deficit of the patients.

Many studies have reported the accumulation of amyloid-β in the brain as the main cause of Alzheimer's disease and BACE-1 is a potential therapeutic target of the disease (Mazumder & Choudhury, 2019; Mendes et al., 2023). MOA, on the other hand, serves as a therapeutic target for the management of depression, as well as Alzheimer's and Parkinson's disease (Jalal et al., 2022). At all concentrations tested, the fresh lemongrass tea significantly ($p < 0.05$) inhibited β-secretase compared to the dry sample except at the lowest concentration (Fig. 1c). Both the fresh and dry lemongrass teas inhibited monoamine oxidase similarly at concentrations of 6.25 and 50 μg/mL but inhibition by the fresh tea was significantly higher than the dry one at other concentrations (Fig. 1d). The IC_{50} values for the inhibition of neurologically-related enzymes by the fresh and dry infusions of lemongrass is shown in Table 2. The fresh lemongrass tea has significantly lower IC_{50} values ($p < 0.05$) for the inhibition of β-secretase and monoamine oxidase than the dry infusion. While the standard β-secretase inhibitor (AZD3293) has a similar IC_{50} value as the dry infusion, the standard monoamine oxidase inhibitor (tranylcypromine) has a lower IC_{50} value than both infusions. The significant inhibition of both β-secretase and monoamine oxidase by fresh lemongrass infusion may be due to the conservation of phytochemicals and nutrients, which might have been lost in the dry lemongrass due to drying (Duangupama et al., 2023). Previous studies revealed that drying may contribute to the loss of phytochemicals and nutrients in plants (Devi, Bains, & Kaur, 2021; Oliveira-Alves et al., 2021).

3.3. Molecular docking

To determine the probable interactions between the phenolic compounds found in lemongrass and target enzymes evaluated in the *in vitro* study, computational analysis was performed using molecular docking

Table 1
LC-MS profiling of phytochemical compounds from fresh and dry lemongrass infusions.

s/n	RT	*m/z*	Phytochemical compounds	PubChem D
1	7.302	249.06046	carboxyethylidene]-alpha-D-galactose	133960
2	7.302	249.06046	3,4-O-[(1S)-1-carboxyethylidene]-beta-D-galactose	51351726
3	9.125	203.09221	Phellodendric acid A	16088229
4	9.125	203.09221	diethyl 2-hydroxypentanedioate	13270883
5	12.012	239.05424	Eucomic acid	23757219
6	12.170	353.08673	Chlorogenic acid	1794427
7	12.170	353.08673	Scopolin	439514
8	12.271	367.09875	4-oxo-3-phenyl-4H-chromen-7-yl 3-phenylprop-2-enoate	133568962
9	12.365	517.15710	Sibiricose A5	6326020
10	12.532/15.188	367.10294	Caffeoyl-O-methylquinic acid	131752769
11	12.532/15.188	367.10294	4-O-feruloyl-D-quinic acid	10177048
12	12.828	179.03342	Caffeic acid	689043
13	12.828	179.03342	Aspirin	2244
14	13.058	417.17783	Ascleposide B	10740722
15	13.555	431.18668	Aspulvinone H	54675755
16	13.555	431.18668	Sinensol E	11796980
17	13.989	351.12982	5-[(6-ethoxy-3,4,5-trihydroxyoxan-2-yl) methoxy]-3-hydroxy-3-methyl-5-oxopentanoic acid	156602899
18	14.363	415.15979	Phenylethyl primeveroside	14704521
19	14.363	415.15979	Benzyl alcohol beta-D-rutinoside	10549806
20	14.801/15.480	579.13489	Rustoside	74977996
21	14.801/15.480	579.13489	Isocarlinoside	21576182
22	14.995	371.09760	Veranisatin C	10643000
23	14.995	371.09760	Dihydroferulic acid 4-O-glucuronide	190069
24	15.675	163.03993	2-Hydroxycinnamic acid	637540
25	15.675	163.03993	Phenylpyruvic acid	997
26	15.859/19.078	563.13928	Corymboside	13644660
27	15.859/19.078	563.13928	Isovitexin 2″-O-arabinoside	44468060
28	16.048	593.14948	Astragalin 7-rhamnoside	57390614
29	16.048	593.14948	Lonicerin	5282152
30	16.520	549.12396	Kaempferol 3,4′-dixyloside	44258938
31	16.520	549.12396	Limocitrin 7-(6″-acetylglucoside)	44260014
32	17.728	401.18091	Methyl 7-epi-12-hydroxyjasmonate glucoside	131751189
33	17.728	401.18091	Glochidionionoside A	11825585
34	18.062	399.16385	Corchoionoside B	131751110
35	18.421	447.09097	Quercitrin	5280459
36	18.421	447.09097	Trifolin	5282149
37	20.107	239.13066	(+)-7alpha,8alpha-Epoxyblumenol B	44559648
38	20.830/22.375	243.12306	Pandangolide 1a	11687387
39	20.830/22.375	243.12306	Herbarumin II	9992042
40	21.017	575.14044	Chamaemeloside	101688668
41	21.017	575.14044	Vitexin 6′′-(3-hydroxy-3-methylglutarate)	44257690
42	21.630	577.15460	Kaempferitrin	5486199
43	21.630	577.15460	Vitexin 2″-O-rhamnoside	5874704
44	22.659	693.20367	Neocuscutoside C	131801689
45	22.659	693.20367	Sinocrassoside B3	NA
46	23.088	373.13046	8-Hydroxypinoresinol	3010930
47	23.088	373.13046	3′,4′,5,7,8-Pentamethoxyflavanone	72703226
48	23.287	269.09729	[1,1′-binaphthalen]-2-ol	136672961
49	23.287	269.09729	10-phenyl-9,10-dihydroanthracen-9-one	NA

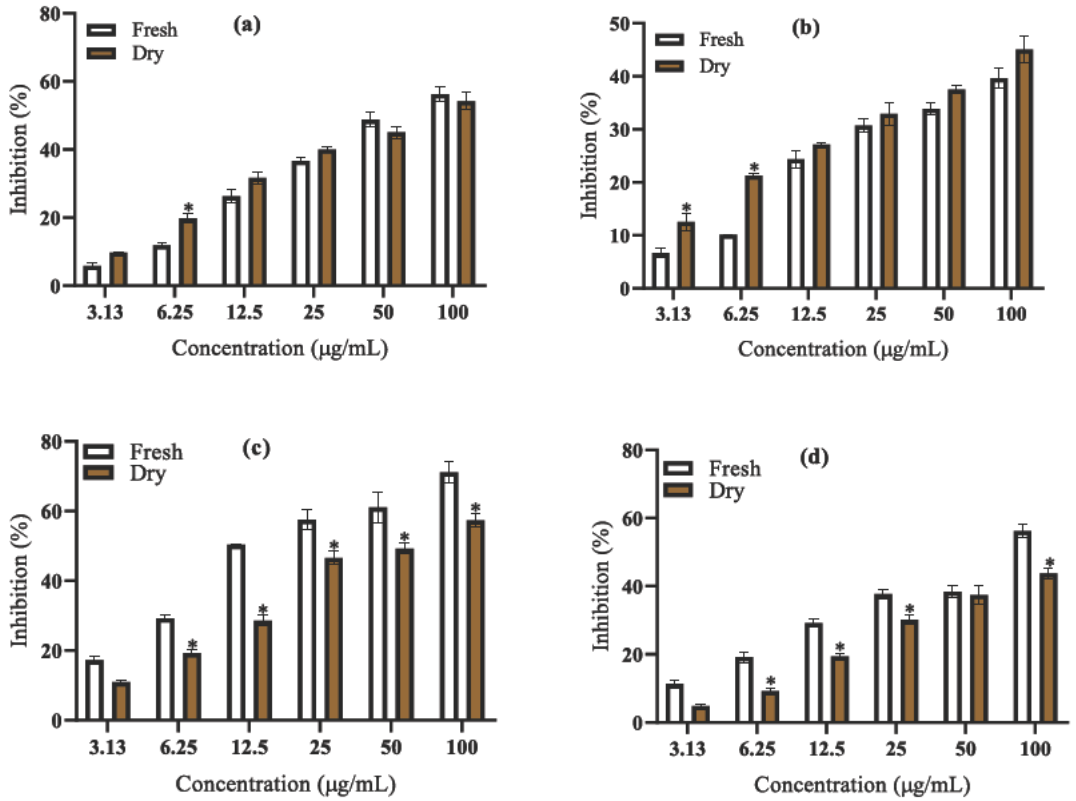

Fig. 1. Inhibitory properties of lemongrass infusions on the activities of neurological-related enzymes (a) acetylcholinesterase and (b) butyrylcholinesterase (c) β-secretase and (d) monoamine oxidase. Values are expressed as mean ± SEM of triplicate determinations. *Values are significantly different at ($p < 0.05$).

Table 2
IC_{50} values for the inhibitory activities of neurological-related enzymes by fresh and dry lemongrass teas.

Samples	IC_{50} values (μg/mL)			
	AChE	BChE	β-secretase	MAO
Fresh infusion	72.62 ± 3.53[a]	119.70 ± 4.42[a]	38.24 ± 4.21[a]	78.62 ± 2.33[a]
Dry infusion	76.27 ± 5.47[a]	107.20 ± 7.14[a]	67.50 ± 2.76[b]	102.50 ± 6.74[b]
Donepezil	71.66 ± 2.18[a]	76.51 ± 2.05[b]		
AZD3293			56.47 ± 0.94[b]	
Tranylcypromine				65.55 ± 2.64[c]

The values are expressed as means ± SEM of triplicate determinations. Means down vertical columns not sharing a common letter are significantly different ($P < 0.05$) from each other.
AChE: Acetylcholinesterase, BChE: Butyrylcholinesterase, MAO: Monoamine oxidase.

and molecular dynamic simulation. Table S1 contains the docking scores of all 49 compounds and standards against acetylcholinesterase, butyrylcholinesterase, β-secretase and monoamine oxidase, as revealed by the LC-MS. The docking scores of the top five compounds of lemongrass tea and standard drugs against selected targets of neurodegeneration are presented in Table 3. While both aspulvinone H and 4-oxo-3-phenyl-4H-chromen-7-yl 3-phenylprop-2-enoate (OPCPPE) had the lowest docking scores of 10.6 kcal/mol for AChE, [1,1′-binaphthalen]-2-ol has the lowest docking score of 12.1 kcal/mol for BChE. Neocuscutoside C and aspulvinone H exhibited the lowest docking scores of 10.5 and 11.9 kcal/mol for β-secretase and monoamine oxidase, respectively. All the standard drugs tested had higher docking scores than the profiled compounds. Molecular docking is a tool that predicts the mode of interaction of chemical compounds with the active sites of the enzymes (Wu et al., 2022). The lowest docking scores of OPCPPE (and aspulvinone H), [1,1′-binaphthalen]-2-ol, neocuscutoside C and chlorogenic acid for AChE, BChE, BACE-1 and MAO respectively, indicated that they have better affinities for these enzymes than other compounds and standards (Jalal et al., 2022; Kim et al., 2018). This is because the lower the docking score of a compound, the better the pose and affinity towards the enzyme. The outcome of the docking validation exercise is presented in Fig. S2, and the superimposition demonstrated that the top-hit compounds, the reference standards, and the docked native inhibitors in each case had relative binding orientation at the receptor binding domains of each target with RMSD values of 0.5 Å. These findings supported the validity of the docking scores obtained in the study.

3.4. Molecular dynamics simulation

Since docking indicates the preliminary interaction of a ligand to the active site of a receptor, the behaviours of the compounds were subjected to binding energy calculations using molecular dynamics (MD) simulation. Table 4 shows the results of the thermodynamic profiles of the top compounds of lemongrass tea against each of the target enzymes. As for BACE-1 and MOA, the top five compounds had lower free binding energies (72.28 to 31.42 kcal/mol) than the reference standards, AZD3293 (23.56 kcal/mol) and tranylcypromine (20.19 kcal/mol).

Table 3
Docking scores of the top five compounds of lemongrass infusions and standards against enzymes implicated in neurodegeneration.

Targets	Compound/Standard	PubChem ID	Docking score (kcal/mol)
Acetylcholinesterase	4-oxo-3-phenyl-4H-chromen-7-yl 3-phenylprop-2-enoate	133568962	**−10.6**
	Aspulvinone H	54675755	**−10.6**
	Astragalin 7-rhamnoside	57390614	9.4
	Benzyl alcohol beta-D-rutinoside	10549806	9.9
	Chamaemeloside	101688668	10.0
	Donepezil[a]	3152	9.7
Butyrylcholinesterase	[1,1′-binaphthalen]-2-ol	136672961	**−12.1**
	Isocarlinoside	21576182	10.1
	Kaempferitrin	5486199	10.5
	Lonicerin	5282152	11.0
	Vitexin 6''-(3-hydroxy-3-methylglutarate)	44257690	10.3
	Donepezil[a]	3152	9.5
Beta-secretase	Neocuscutoside C	131801689	**−10.5**
	Lonicerin	5282152	9.5
	Aspulvinone H	54675755	9.2
	Isocarlinoside	21576182	9.5
	Vitexin 6''-(3-hydroxy-3-methylglutarate)	44257690	9.4
	AZD3293[a]	67979346	8.8
Monoamine oxidase	Chlorogenic acid	1794427	9.8
	Benzyl alcohol beta-D-rutinoside	10549806	9.4
	Aspulvinone H	54675755	**−11.9**
	Phenylethyl primeveroside	14704521	10.1
	4-O-feruloyl-D-quinic acid	10177048	9.7
	Tranylcypromine[a]	19493	6.5

[a] Reference standards.

This conforms with the docking scores obtained which implies that these compounds have stronger affinities for these enzymes and form more stable complexes (Balogun et al., 2022; Moorkoth et al., 2021). While four of the selected compounds displayed lower free binding energies (46.10 to 66.59 kcal/mol) for acetylcholinesterase than the standard, donepezil (40.17 kcal/mol), 4-oxo-3-phenyl-4H-chromen-7-yl 3-phenylprop-2-enoate (OPCPPE) had a higher free binding energy of 37.29 kcal/mol. Of the top five compounds, the duo of [1,1′-binaphthalen]-2-ol and Vitexin-6''-(3-hydroxyl-3-methylglutarate) possessed higher binding free energies of 29.85 and 40.89 kcal/mol, respectively, for BChE than the reference standard, donepezil (45.82 kcal/mol). However, benzyl alcohol beta-D-rutinoside, isocarlinoside, neocuscutoside C, and aspulvinone H have the lowest binding energies for AChE, BChE, BACE-1 and MAO, respectively. This suggests that these compounds have the best affinity for the enzymes and are the best inhibitors of the targets (Haider et al., 2021; Sheeja Malar et al., 2017).

3.5. Post-molecular dynamics simulation

Enzyme-ligand complex is prone to conformational changes caused by the binding ligand, and this may modify the biological activity of the enzyme. This necessitated further evaluation of the stability, flexibility, and compactness of the resulting complex through post-MD simulation analysis. The results of the post-MD simulation of the interaction of the top five compounds with selected enzymes are shown in Table 5 and Figs. 2–5.

3.5.1. Root mean square deviation (RMSD)

In the AChE complex, there was an initial convergence in the RMSD up to 20 ns after which they diverged throughout the simulation period (Fig. 2a). The unbound AChE has a higher average RMSD value (1.65 Å) than the complexes except for aspulvinone H and donepezil. The system converged up to around 30 ns and 45 ns after which the unbound BChE,

Table 4
Energy component profiles (kcal/mol) of the top five compounds of lemongrass teas and standards against enzymes implicated in neurodegeneration.

Complex	ΔEvdW	ΔEelec	ΔGgas	ΔGsolv	ΔEsur	ΔGbind
Acetylcholinesterase						
OPCPPE[a]	51.36 ± 3.02	4.68 ± 3.45	56.05 ± 4.21	18.75 ± 2.35	6.39 ± 0.36	37.29 ± 3.35
Aspulvinone H	53.5 ± 4.68	26.15 ± 9.91	79.67 ± 11.62	33.56 ± 5.39	6.79 ± 0.35	46.10 ± 7.70
Astragalin-7-rhamnoside	57.94 ± 5.33	44.86 ± 15.74	102.79 ± 14.07	54.79 ± 9.56	7.05 ± 0.36	47.99 ± 6.34
Benzyl alcohol beta-D-rutinoside	49.85 ± 5.49	58.18 ± 12.51	108.03 ± 12.16	55.29 ± 5.68	7.08 ± 0.43	52.75 ± 8.79
Chamaemeloside	65.64 ± 4.95	64.69 ± 11.89	130.33 ± 9.64	63.74 ± 6.17	8.81 ± 0.31	66.59 ± 5.33
Donepezil	51.10 ± 3.24	249.54 ± 10.21	300.66 ± 11.08	260.51 ± 10.72	6.21 ± 0.30	40.15 ± 3.63
Butyrylcholinesterase						
[1,1′-binaphthalen]-2-ol	52.57 ± 4.40	271.06 ± 17.79	323.63 ± 19.72	293.78 ± 17.80	6.53 ± 0.42	29.85 ± 3.89
Isocarlinoside	45.75 ± 7.19	80.46 ± 20.01	126.21 ± 16.71	60.42 ± 10.37	6.50 ± 0.49	65.79 ± 8.36
Kaempferitrin	53.59 ± 5.23	78.06 ± 11.76	131.65 ± 10.79	68.16 ± 7.83	7.69 ± 0.35	63.49 ± 6.70
Lonicerin	56.47 ± 4.94	44.79 ± 10.49	101.26 ± 9.42	47.45 ± 5.43	7.36 ± 0.35	53.80 ± 6.44
Vitexin-6''-(3-hydroxyl-3-methylglutarate)	52.31 ± 5.79	43.45 ± 15.36	95.76 ± 16.82	54.87 ± 11.97	6.58 ± 0.61	40.89 ± 8.06
Donepezil	51.98 ± 3.89	131.1 ± 8.82	183.10 ± 10.58	137.28 ± 8.55	6.37 ± 0.36	45.82 ± 5.64
Beta-secretase						
Neocuscutoside C	56.40 ± 5.68	42.65 ± 9.08	99.05 ± 11.43	57.96 ± 7.13	7.11 ± 0.64	41.09 ± 6.36
Lonicerin	46.15 ± 7.91	33.01 ± 23.65	79.16 ± 29.63	47.74 ± 16.12	6.05 ± 1.08	31.42 ± 14.75
Aspulvinone H	44.12 ± 3.80	38.44 ± 5.21	82.56 ± 6.76	43.86 ± 3.96	5.84 ± 0.47	38.69 ± 4.37
Isocarlinoside	46.54 ± 7.35	54.88 ± 13.13	101.42 ± 14.36	66.78 ± 7.50	6.27 ± 1.12	34.65 ± 9.56
Vitexin 6''-(3-hydroxy-3-methylglutarate)	47.07 ± 4.66	49.75 ± 16.82	96.82 ± 17.60	57.64 ± 10.22	6.77 ± 0.56	39.18 ± 9.74
AZD3293	34.16 ± 7.29	173.71 ± 22.58	207.85 ± 26.21	184.28 ± 20.97	4.43 ± 0.86	23.56 ± 7.36
Monoamine oxidase						
Chlorogenic acid	55.10 ± 3.15	38.49 ± 12.69	93.60 ± 11.92	47.36 ± 6.72	6.78 ± 0.13	46.24 ± 7.26
Benzyl alcohol beta-D-rutinoside	58.10 ± 3.85	75.26 ± 13.08	133.36 ± 12.90	62.80 ± 6.84	7.67 ± 0.21	70.56 ± 8.23
Aspulvinone H	71.87 ± 3.39	42.70 ± 5.75	114.58 ± 5.30	42.29 ± 3.56	8.59 ± 0.17	72.28 ± 4.11
Phenylethyl primeveroside	47.29 ± 3.18	29.29 ± 8.76	76.58 ± 10.06	32.26 ± 6.92	6.18 ± 0.31	44.32 ± 4.53
4-O-feruloyl-D-quinic acid	57.14 ± 3.68	45.72 ± 9.13	102.85 ± 8.24	50.99 ± 5.09	7.24 ± 0.18	51.86 ± 5.73
Tranylcypromine	19.33 ± 2.31	73.51 ± 10.84	92.84 ± 10.78	72.64 ± 9.68	3.14 ± 0.11	20.19 ± 2.86

[a] 4-oxo-3-phenyl-4H-chromen-7-yl 3-phenylprop-2-enoate.

Table 5
Post-molecular dynamics simulation of the interaction of top five compounds of lemongrass teas with enzymes implicated in neurodegeneration.

	RMSD (Å)	RMSF(Å)	ROG (Å)	SASA (Å)	No of H-bonds	Distance of H bonds (Å)	Angle (°) of H-bonds
Acetylcholinesterase							
Unbound	1.65 ± 0.25	1.03 ± 0.58	22.92 ± 0.07	21663.24 ± 369.16	250.72 ± 10.85	2.86 ± 0.06	151.66 ± 7.53
OPCPPE[a]	1.24 ± 0.26	0.95 ± 0.48	22.86 ± 0.05	21217.75 ± 334.07	253.07 ± 10.59	2.86 ± 0.06	151.44 ± 7.62
Aspulvinone H	1.84 ± 0.20	1.08 ± 0.60	22.94 ± 0.07	21539.44 ± 462.15	252.83 ± 10.38	2.86 ± 0.06	151.67 ± 7.62
Astragalin-7-rhamnoside	1.44 ± 0.14	0.98 ± 0.49	22.99 ± 0.06	21560.89 ± 413.64	251.99 ± 10.56	2.86 ± 0.06	151.49 ± 7.71
Benzyl alcohol beta-D-rutinoside	1.49 ± 0.13	1.02 ± 0.56	22.88 ± 0.07	21226.43 ± 391.75	251.86 ± 10.23	2.86 ± 0.06	151.47 ± 7.62
Chamaemeloside	1.32 ± 0.18	1.02 ± 0.58	22.85 ± 0.06	21033.03 ± 342.62	256.47 ± 10.22	2.86 ± 0.06	151.57 ± 7.65
Donepezil	1.84 ± 0.10	0.99 ± 0.54	22.89 ± 0.06	21385.68 ± 354.78	255.04 ± 10.10	2.86 ± 0.06	151.49 ± 7.69
Butyrylcholinesterase							
Unbound	2.40 ± 0.49	1.33 ± 1.05	23.31 ± 0.12	21271.65 ± 502.71	249.38 ± 10.85	2.86 ± 0.06	152.14 ± 7.56
[1,1′-binaphthalen]-2-ol	1.59 ± 0.23	1.13 ± 0.68	23.11 ± 0.08	20315.76 ± 475.35	252.98 ± 11.15	2.86 ± 0.06	151.87 ± 7.61
Isocarlinoside	1.68 ± 017	1.12 ± 0.61	23.17 ± 0.07	20489.09 ± 415.42	265.27 ± 11.16	2.86 ± 0.06	151.88 ± 7.68
Kaempferitrin	1.45 ± 0.12	1.04 ± 0.55	23.02 ± 0.06	19912.06 ± 336.48	263.86 ± 10.47	2.86 ± 0.06	151.69 ± 7.69
Lonicerin	1.99 ± 0.30	1.12 ± 0.82	23.15 ± 0.07	20297.06 ± 415.39	258.73 ± 10.26	2.86 ± 0.06	151.92 ± 7.66
Vitexin-6′′-(3-hydroxyl-3-methylglutarate)	2.14 ± 0.43	1.28 ± 0.76	23.23 ± 0.12	20852.46 ± 523.60	259.96 ± 10.46	2.86 ± 0.06	152.13 ± 7.59
Donepezil	1.59 ± 0.12	1.07 ± 0.57	23.16 ± 0.07	20514.45 ± 426.25	254.16 ± 10.33	2.86 ± 0.06	151.87 ± 7.57
Beta-secretase							
Unbound	1.49 ± 0.17	1.15 ± 0.64	21.17 ± 0.09	16437.93 ± 341.26	184.46 ± 8.67	2.85 ± 0.06	151.89 ± 7.71
Neocuscutoside C	2.00 ± 0.29	1.21 ± 0.58	21.44 ± 0.14	16503.24 ± 295.76	185.18 ± 8.76	2.85 ± 0.06	151.89 ± 7.58
Lonicerin	1.83 ± 0.28	1.23 ± 0.65	21.50 ± 0.13	16940.72 ± 402.13	186.16 ± 8.80	2.85 ± 0.06	152.02 ± 7.66
Aspulvinone H	2.49 ± 0.41	1.15 ± 0.65	21.44 ± 0.09	16677.27 ± 295.09	189.25 ± 9.13	2.85 ± 0.06	152.12 ± 7.58
Isocarlinoside	1.79 ± 0.29	1.16 ± 0.57	20.99 ± 0.12	16036.45 ± 329.44	193.06 ± 8.97	2.85 ± 0.06	151.92 ± 7.61
Vitexin 6′′-(3-hydroxy-3-methylglutarate)	1.86 ± 0.29	1.43 ± 0.65	21.27 ± 0.31	16539.11 ± 425.75	189.17 ± 8.94	2.85 ± 0.06	152.17 ± 7.68
AZD3293	1.99 ± 0.21	1.16 ± 0.62	21.12 ± 0.14	16300.84 ± 313.36	192.07 ± 8.59	2.85 ± 0.06	151.92 ± 7.60
Monoamine oxidase							
Unbound	3.89 ± 1.42	1.89 ± 2.09	24.69 ± 0.51	21648.36 ± 516.29	254.63 ± 10.55	2.85 ± 0.06	152.03 ± 7.17
Chlorogenic acid	3.96 ± 0.65	1.56 ± 1.41	24.44 ± 0.27	21167.02 ± 445.95	254.36 ± 10.49	2.85 ± 0.06	152.01 ± 7.17
Benzyl alcohol beta-D-rutinoside	3.83 ± 0.74	1.45 ± 1.40	24.69 ± 0.21	21584.19 ± 454.64	253.02 ± 10.62	2.85 ± 0.06	151.82 ± 7.39
Aspulvinone H	4.29 ± 0.94	1.46 ± 1.46	24.22 ± 0.34	20647.14 ± 413.91	257.59 ± 10.77	2.86 ± 0.06	151.89 ± 7.30
Phenylethyl primeveroside	4.67 ± 1.06	1.82 ± 2.05	25.02 ± 0.40	21518.15 ± 470.35	252.45 ± 10.66	2.86 ± 0.06	151.89 ± 7.29
4-O-feruloyl-D-quinic acid	3.23 ± 0.70	1.51 ± 1.34	24.94 ± 0.28	21275.25 ± 391.14	252.09 ± 11.45	2.85 ± 0.06	151.89 ± 7.32
Tranylcypromine	4.98 ± 1.85	2.21 ± 2.68	24.48 ± 0.56	21602.32 ± 531.63	251.79 ± 11.81	2.86 ± 0.06	152.03 ± 7.15

[a] 4-oxo-3-phenyl-4H-chromen-7-yl 3-phenylprop-2-enoate.

donepezil, and [1,1′-binaphthalen]-2-ol complexes diverged (Fig. 2b). The mean RMSD value of the unbound BChE (2.40 Å) is higher than all the complexes while [1,1′-binaphthalen]-2-ol has the same RMSD value (1.59 Å) as donepezil. As for the BACE-1, convergence was achieved up to around 20 ns and 40 ns after which the aspulvinone H complex diverged throughout the simulation period (Fig. 2c). The unbound BACE-1 has a lower RMSD value (1.49 Å) than all the complexes. The MOA system witnessed continuous divergence among all the complexes throughout the simulation period (Fig. 2d). While all other complexes have higher RMSD values than the unbound MOA (3.89 Å), benzyl alcohol beta-D-rutinoside and 4-O-feruloyl-D-quinic acid had a lower RMSD value of 3.83 and 3.23 Å, respectively. The RMSD value depicts the stability of the protein-ligand complex and a low RMSD value signifies higher stability of the complex (Mendes et al., 2023). The fact that all the resulting complexes from BChE and AChE (except aspulvinone and donepezil) had lower RMSD indicated that the ligand complexes are more stable than the free enzymes (Murali et al., 2023). Conversely, the unbound β-secretase is more stable than all the ligand-complexes because it has the lowest RMSD value compared to the complexes (Jalal et al., 2022). However, the OPCPPE, kaempferitrin, and 4-O-feruloyl-D-quinic acid possessed the lowest RMSD values for acetylcholinesterase, butyrylcholinesterase and monoamine oxidase-bound complexes respectively, it implies they formed the most stable complexes with their respective enzymes (Gholami et al., 2023; Othman et al., 2022).

3.5.2. Root mean square fluctuation (RMSF)

The root mean square fluctuation (RMSF) measures the effect of a binding compound on the active site of an enzyme, thereby providing information on the flexibility of the protein-ligand complex (Cancela et al., 2020), and is determined by the extent of fluctuations in the system. There were fluctuations in the AChE system especially at the 75, 250, 375 and 500 amino acid residues (Fig. 3a). The RMSF value of the unbound AChE (1.03 Å) is higher than all the complexes except aspulvinone H (1.08 Å). The fluctuations among the BChE system followed a similar pattern and occurred mostly at 75, 275, and 375 amino acid residues (Fig. 3b). The unbound BChE displayed the highest RMSF value (1.33 Å) than other complexes suggesting that the complexes are more flexible and have better stability (Gupta et al., 2020). Both donepezil-acetylcholinesterase and donepezil-butyrylcholinesterase complexes had lower RMSF values compared to unbound enzymes, which indicates lower fluctuation and better flexibility of the complexes (Gyebi et al., 2023). Consistent fluctuations were observed throughout the β-secretase systems and are prominent at 60, 90, 270, and 300 amino acid residues (Fig. 3c). Neocuscutoside C, lonicerin, and vitexin 6′′-(3-hydroxy-3-methylglutarate) displayed higher RMSF values than the unbound β-secretase and AZD3293-β-secretase complex (1.15 Å), implying that AZD3293 may be more flexible and stable than some tested metabolites (Othman et al., 2022). The MOA system witnessed fewer fluctuations in the amino acid residues which occurred around 250 and 475 residues (Fig. 3d). The unbound MOA has a higher RMSF value (3.89 Å) than other complexes, except tranylcypromine, which suggests that all the metabolite-monoamine oxidase complexes displayed lesser fluctuations and improved stability of the complexes (Cancela et al., 2020).

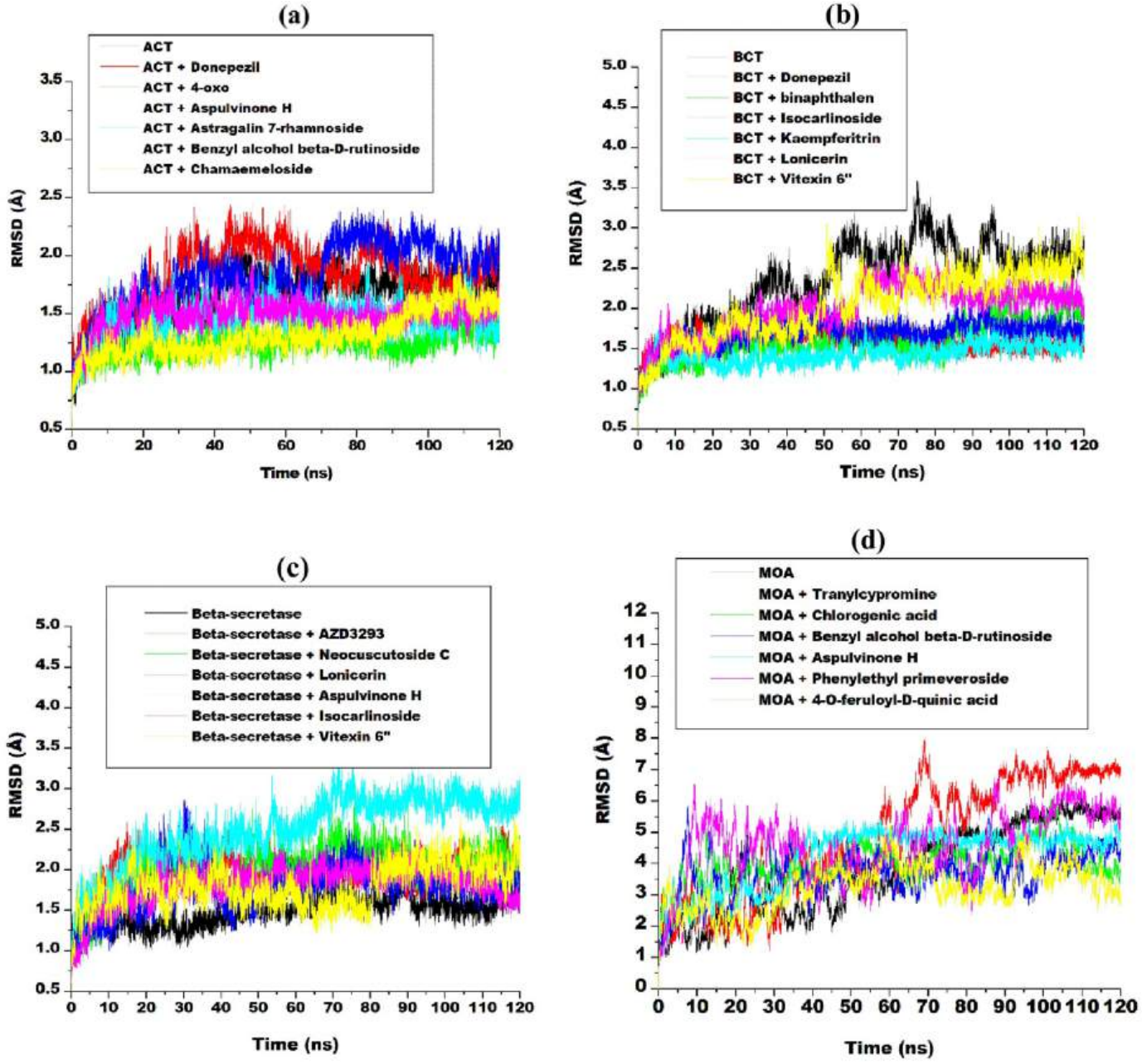

Fig. 2. Comparative plots of alpha-carbon of (a) acetylcholinesterase (b) butyrylcholinesterase (c) beta-secretase and (d) monoamine oxidase and top five compounds in lemongrass teas presented as root mean square deviation (RMSD) over 120 ns molecular dynamic simulation.

3.5.3. Radius of gyration (ROG)

The radius of gyration (ROG) measures the compactness of the resulting complex from the interaction of the ligand and enzymes, the lower the ROG value the better the compactness of the complex (Aribisala et al., 2022). Fig. 4a revealed that there is a convergence of all the complexes in the AChE system throughout the simulation period. The unbound AChE as well as aspulvinone H and astragalin-7-rhamnoside complexes possessed higher radius of gyration (ROG) values than other complexes, which signifies that they are less compact and stable than other complexes (Kundu & Dubey, 2021). Though there is a convergence in the ROG plot among the complexes up to 50 ns, they diverged afterwards to the end of the simulation period (Fig. 4b). The ROG value of the unbound butyrylcholinesterase (1.33 Å) is higher than all the complexes, which may imply that binding of the metabolites to the enzymes improved the compactness of the resulting complex. There is a similar pattern in the convergence in the ROG plot of the β-secretase and its complexes (Fig. 4c). The unbound β-secretase has a lower ROG value (21.17 Å) than other complexes except for isocarlinoside (20.99 Å) and AZD3293 (21.12 Å), which suggests that isocarlinoside- β-secretase complex is the most compact and is better than the standard drug, AZD3293 (Gyebi et al., 2023). Throughout the simulation period, there is a consistent divergence in the ROG plot of the MOA and its complexes (Fig. 4d). The ROG value of the unbound monoamine oxidase (24.69 Å) is the same as that of benzyl alcohol beta-D-rutinoside, and is higher than other complexes except phenylethyl primeveroside (25.02 Å) and 4-O-feruloyl-D-quinic acid (24.94 Å). This shows that the binding of benzyl alcohol beta-D-rutinoside to the monoamine oxidase does not affect the compactness of the unbound enzyme (Balogun et al., 2022). However, the binding of aspulvinone H to the MAO caused the best reduction in the ROG values compared to other complexes thereby eliciting more compactness and stability of the complex.

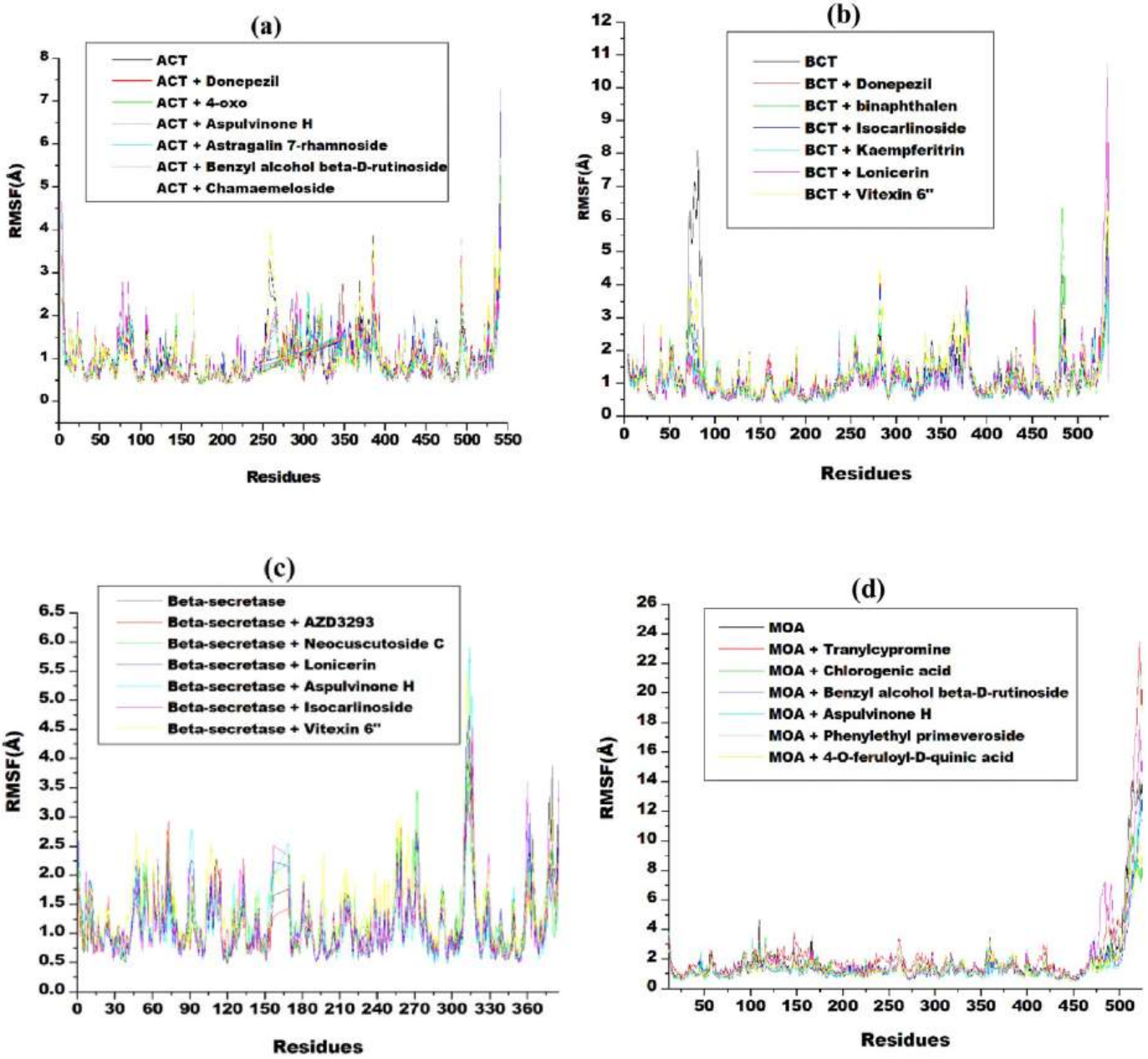

Fig. 3. Comparative plots of alpha-carbon of (a) acetylcholinesterase (b) butyrylcholinesterase (c) beta-secretase and (d) monoamine oxidase and top five compounds in lemongrass teas presented as root mean square fluctuations (RMSF) over 120 ns molecular dynamic simulation.

3.5.4. Solvent accessibility surface area (SASA)

The solvent accessibility surface area (SASA) value assesses the behaviour of the amino acid residues of the enzymes when exposed to solvents (Gyebi et al., 2023). When the SASA value is low, it indicates low surface area and better stability. There are consistent fluctuations in the SASA plot of all the investigated enzymes (Fig. 5a–d). The SASA values for the unbound acetylcholinesterase (21663.24 Å), butyrylcholinesterase (21271.65 Å), and monoamine oxidase (21648.36 Å) are higher than all other complexes. This suggests that all the resulting complexes from these interactions are more stable than the unbound enzymes (Gholami et al., 2023). As for β-secretase, the SASA value of the unbound form (16437.93 Å) is only higher than that of isocarlinoside complex (16036.45 Å) and the standard drug, AZD3293 (16300.84 Å), while other complexes have higher SASA values. This indicated that isocarlinoside has the lowest surface area and is more stable than all other complexes (Sabiu et al., 2021). Chamamaeloside (21033.03 Å), kaempferitrin (19912.06 Å), isocarlinoside (16036.45 Å), and aspulvinone H (20647.14 Å) exhibited lowest SASA values for acetylcholinesterase, butyrylcholinesterase, β-secretase, and monoamine oxidase respectively. This signifies that these complexes are the most stable and are more stable than the complexes resulting from all the standard drugs.

3.6. Forms and nature of interactions

The form and number of interactions between the enzymes and the ligands provide information on their compatibility and affect the binding energy of the resulting complex (Kundu & Dubey, 2021). Fig. 6 shows the interaction plots of the topmost lemongrass metabolite (benzyl alcohol beta-D-rutinoside) and standard drug (donepezil) with acetylcholinesterase before and after 120 ns molecular dynamics simulation. Out of the top five compounds that formed complexes with

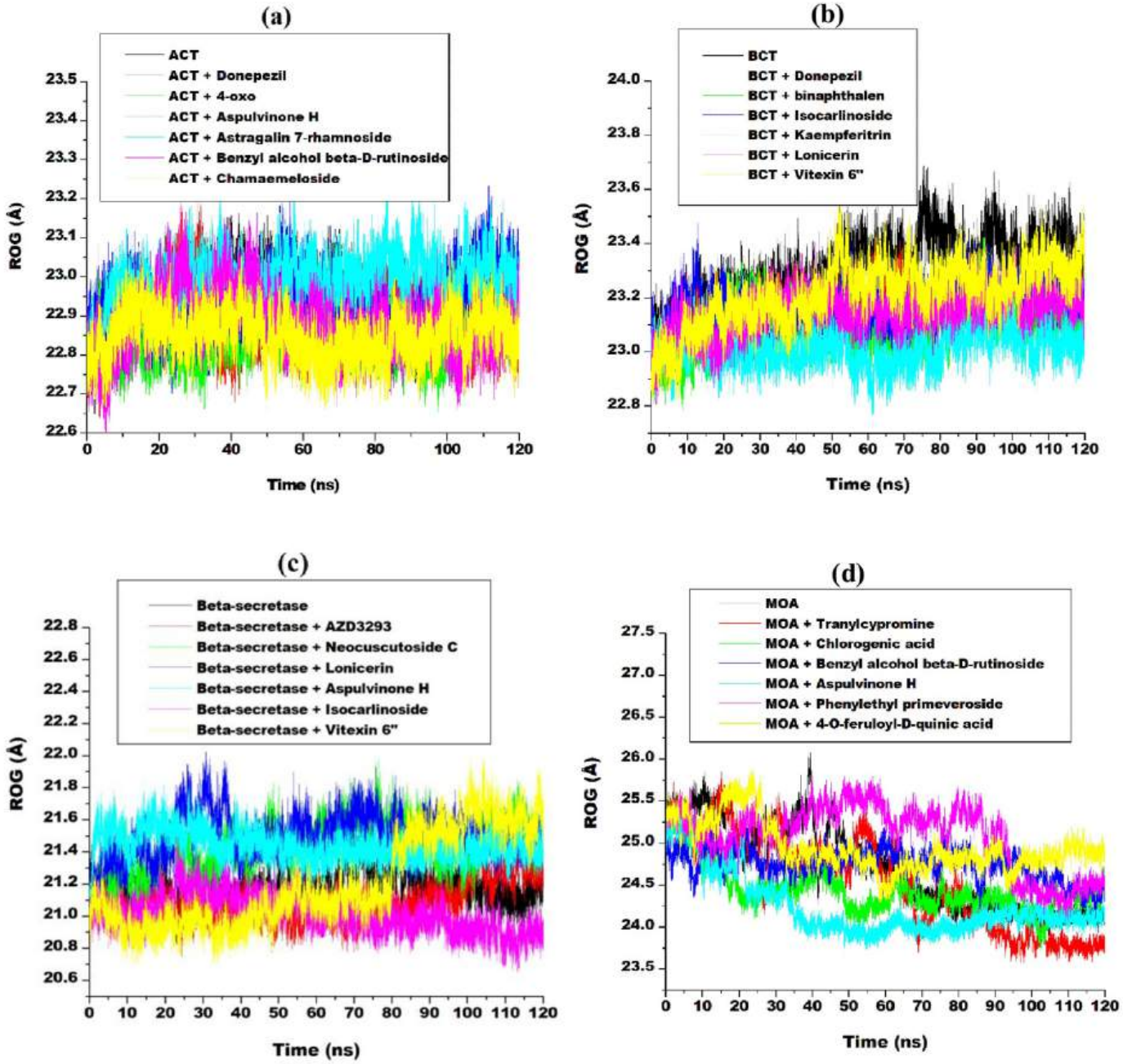

Fig. 4. Comparative plots of alpha-carbon of (a) acetylcholinesterase (b) butyrylcholinesterase (c) beta-secretase and (d) monoamine oxidase and top five compounds in lemongrass teas presented as radius of gyration (ROG) over 120 ns molecular dynamic simulation.

acetylcholinesterase, benzyl alcohol beta-D-rutinoside has the highest number of interactions comprising six hydrogen bonds (Trp83, Gly119, Ser122, Glu199, Ser200 and Tyr329), fifteen van der Waals forces and four other interactions (Val70, Pro85, Arg288 and Tyr333). Ten of these interactions were consistent before and after the simulation (Fig. 6A1 and 6A2). This is better than observation with the donepezil which has 20 interactions comprising two hydrogen bonds (Ser122 and Tyr333), fourteen van der Waals forces and four other interactions (Val70, Asp71, Hie276 and Trp278), out of which only five were consistent (Fig. 6B1 and 6B2). This may be due to the low binding energy of the complex and higher number of hydrogen bonds, which implies that benzyl alcohol beta-D-rutinoside has a better affinity for acetylcholinesterase than donepezil, and the resulting complex is also more stable.

All the top five compounds that interacted with butyrylcholinesterase had a higher number of interactions (19–26 bonds) than the standard drug, donepezil with 18 interactions. Fig. 7 shows the interaction plots of the topmost compound (kaempferitrin) with butyrylcholinesterase before and after molecular dynamic simulation. Kaempferitrin has twenty-six interactions with butyrylcholinesterase compared to eighteen interactions donepezil (standard) had with the protein. Kaempferitrin has five hydrogen bonds (Gly114, Glu194, Ala196, Glu273 and Hie435), seventeen van der Waals's forces and four others (Trp79, Val277, Pro282 and Tyr437) while donepezil has four hydrogen bonds (Gly113, Thr117, Ala325 and Hie435), ten van der Waals's forces and four other interactions (Phe326, Tyr329, Trp427 and Met431). Thirteen of the interactions of the kaempferitrin-butyrylcholinesterase complex were stable throughout the simulation period (Fig. 7A1 and 7A2). Since the number of hydrogen bonds in a complex contributes to its stability and conformation, this study revealed kaempferitrin-butyrylcholinesterase complex is more stable than the donepezil-

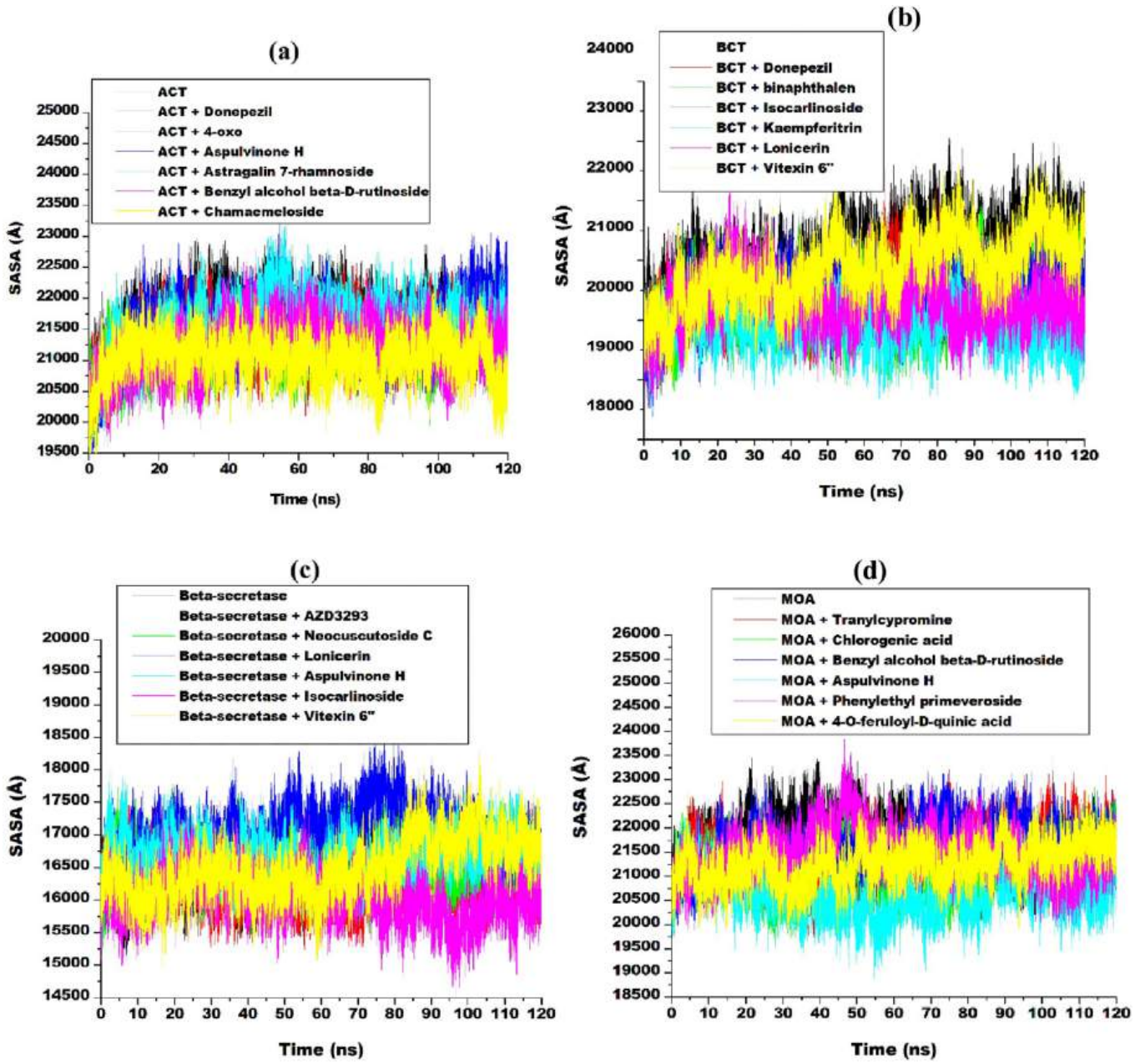

Fig. 5. Comparative plots of alpha-carbon of (a) acetylcholinesterase (b) butyrylcholinesterase (c) beta-secretase and (d) monoamine oxidase and top five compounds in lemongrass teas presented as solvent accessibility surface area (SASA) over 120 ns molecular dynamic simulation.

butyrylcholinesterase complex (Gyebi et al., 2023). This also conforms with the lower binding energy of the kaempferitrin complex.

The interaction of the topmost compound (neocuscutoside C) with β-secretase before and after 120 ns molecular dynamic simulation is shown in Fig. 8. Though all the compounds have a higher number of interactions with the protein than the standard drug (AZD3293), neocuscutoside has the highest number of interactions. Neocuscutoside C has twenty interactions with β-secretase comprising six hydrogen bonds (Gln15, Thr75, Gln76, Trp118, Asp220 and Arg227), ten van der Waals's forces and four other interactions (Leu33, Tyr74, Phe111 and Ile121), out of which seven are consistent throughout the simulation period (Fig. 8A1 and 8A2). This is in contrast to the ten interactions of AZD3293 consisting of three hydrogen bonds (Ser13, Asn114 and Glu302), five van der Waals's forces and two other interactions (Asp303 and Val404), out of which only one was stable (Fig. 8B1 and 8B2). The fact that the number of interactions between the β-secretase and neocuscutoside C doubles that of β-secretase and AZD3293 signifies the formation of a more stable complex (Santi et al., 2020). The higher number of interactions and hydrogen bonds may imply neocuscutoside C has a better affinity for the enzyme and may result in better efficacy (Kumar & Patnaik, 2016). This may be due to the lower docking score and binding energy of the neocuscutoside C compared to the AZD3293.

Fig. 9 shows the interaction plots of aspulvinone H and standard (tranylcypromine) with monoamine oxidase before and after molecular dynamics simulation. This is because of all the top five compounds, aspulvinone H possessed the highest number of interactions. All the top five compounds also have a higher number of interactions with the protein than tranylcypromine. Aspulvinone has thirty-five interactions with monoamine oxidase comprising five hydrogen bonds (Arg40, Tyr58, Ala261, Tyr396 and Met434), twenty-four van der Waals's forces and six other interactions (Ser13, Ile196, Ile262, Pro263, Tyr433 and Ala436), seventeen of which were conserved throughout the simulation

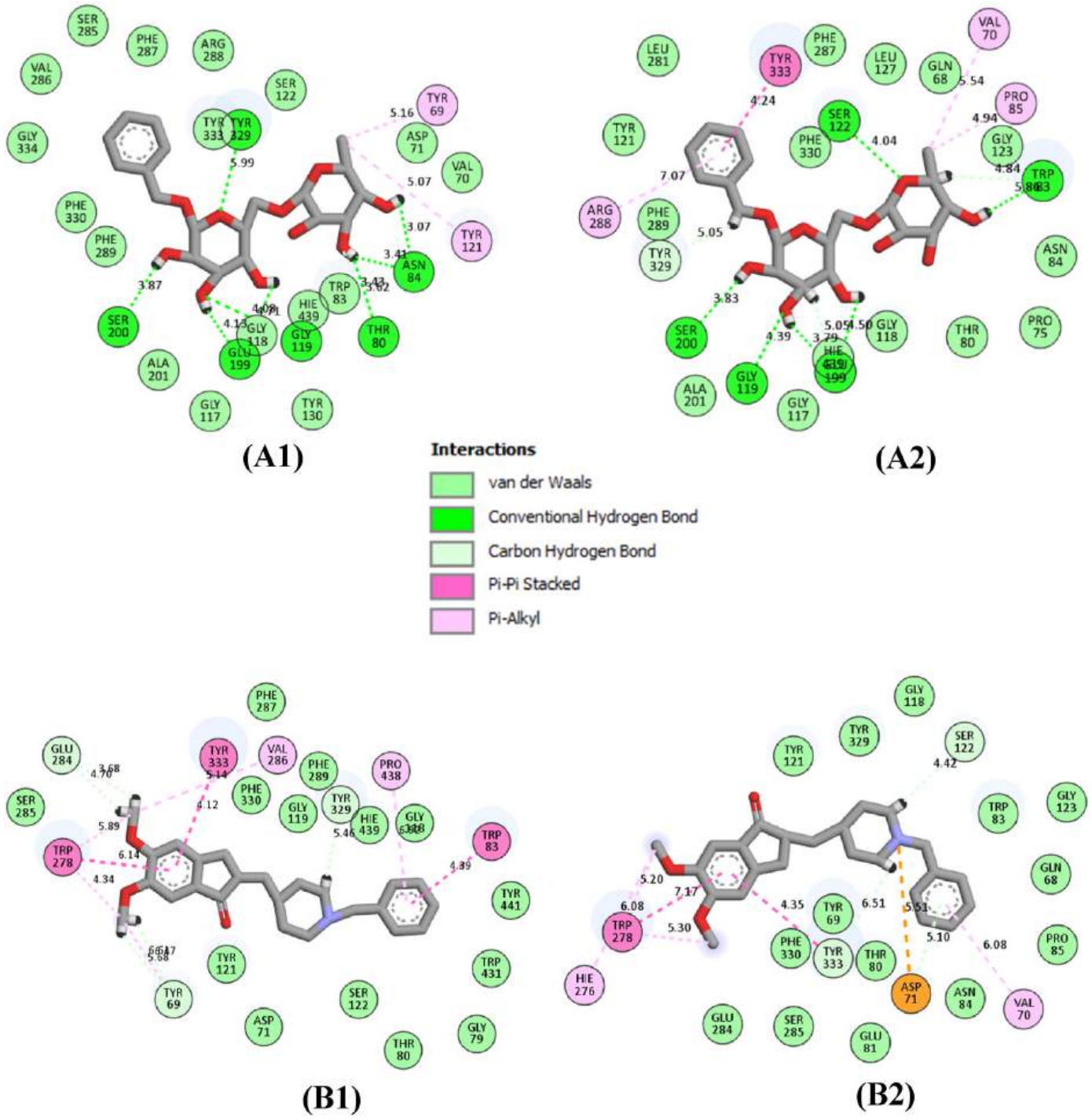

Fig. 6. 2D interaction plots of (A) benzyl alcohol beta-D-rutinoside and (B) donepezil against acetylcholinesterase before (A1, B1) and after (A2, B2) 120 ns molecular dynamics simulation.

period (Fig. 9A1 and 9A2). Conversely, tranylcypromine has fifteen interactions consisting of eleven van der Waals's forces and four other interactions (Gly10, Glu32, Ala33 and Ile262). The possession of a higher number of interactions (35) and hydrogen bonds (5) by aspulvinone H-monoamine oxidase complex than the tranylcypromine-monoamine oxidase complex may imply it has a better affinity for the enzyme (Das et al., 2024), which makes the complex more stable. This may be connected with the lower docking score (11.9 kCal/mol) and binding energy (72.28) of the complex compared to tranylcypromine.

3.7. ADMET properties prediction

The process involved in drug development is a long and cumbersome one but may not yield the desired results at the end. To reduce this burden, *in silico* determination of the desirable properties of would-be drugs can be determined. These include adsorption, distribution, metabolism, excretion and toxicity, jointly referred to as ADMET properties. This will provide information on drug-likeness, bioavailability and safety of the compounds. Before an oral drug reaches the systemic circulation, it must pass through intestinal cell membranes and this is called adsorption. Table 6 shows the results obtained for the ADMET

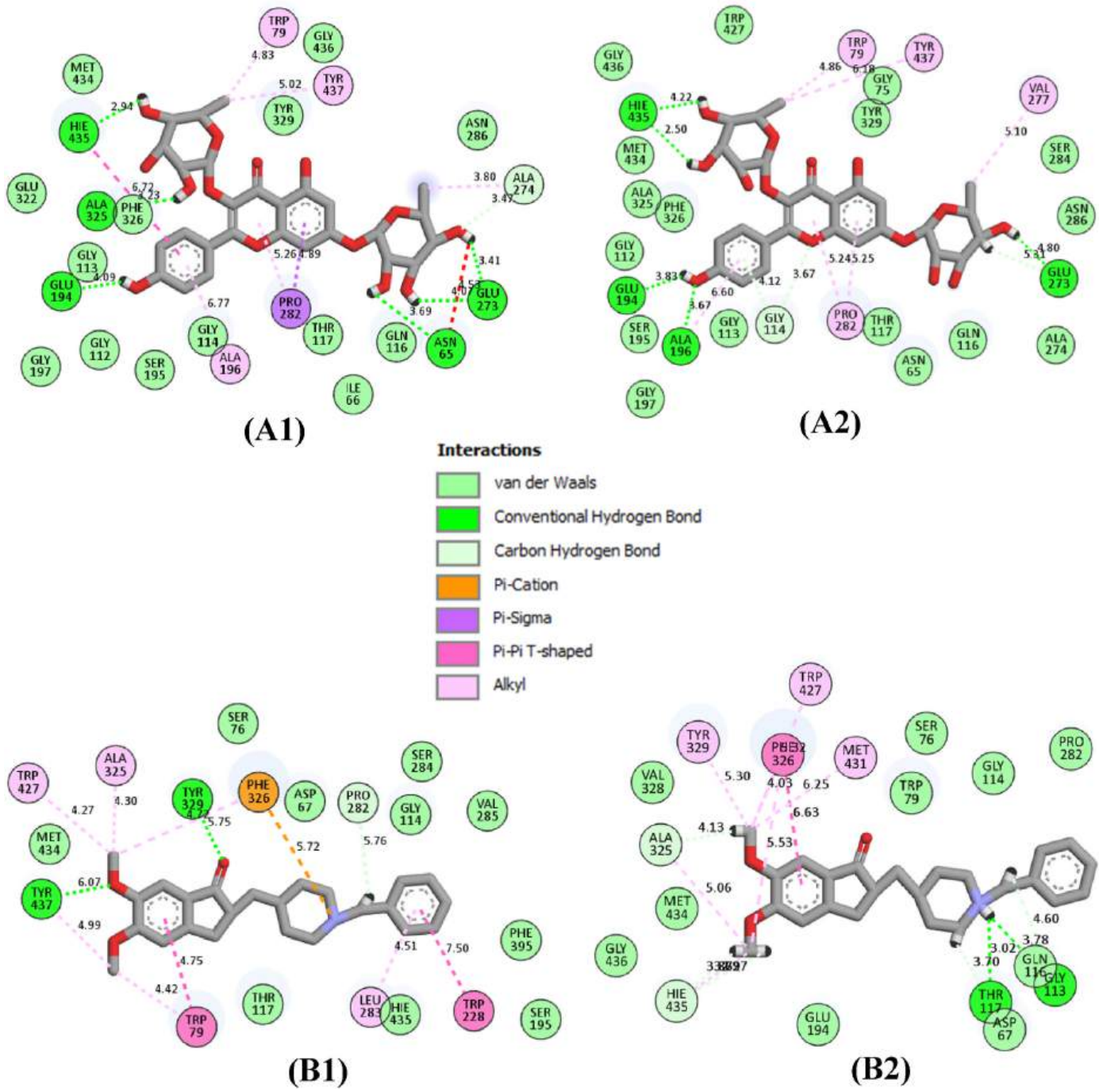

Fig. 7. 2D interaction plots of (A) kaempferitrin and (B) donepezil against butyrylcholinesterase before (A1, B1) and after (A2, B2) 120 ns molecular dynamics simulation.

profiling of the top-hit compounds from lemongrass. All the compounds tested except astragalin 7-rhamnoside, isocarlinoside and phenylethyl primeveroside are easily adsorbed by the cell membranes, as determined by the Caco-2 permeability, human intestinal absorption (HIA) and F20 value. This suggests these compounds are safely delivered into the system and are available for distribution consequently (Lanrewaju, Enitan-Folami, Nyaga, Sabiu, & Swalaha, 2024).

All the compounds tested displayed good activity in blood-brain barrier (BBB) penetration and volume of distribution at steady state (VDS). This implies that these compounds can cross the blood-brain barrier to reach their targets and the compounds are distributed effectively in the body (Jongwachirachai et al., 2024). Drug toxicity, diminished pharmacological impact, and adverse drug effects can all result from drug interactions and metabolism. A significant determinant of such reactions is the use of the cytochrome P450 system (Verma et al., 2022). Except for 4-oxo-3-phenyl-4H-chromen-7-yl 3-phenyl-prop-2-enoate (OPCPPE), aspulvinone H and [1,1′-binaphthalen]-2-ol, none of the compounds inhibited the activities of cytochrome P450 enzymes (CYP1A2, CYP2C19 and CYP3A4), indicating their inability to initiate drug-drug interaction when used alongside other drugs. Plasma clearance (CL plasma) is the overall capacity of the body to eliminate a drug while half-life (T0.5) is the time it takes for the concentration of the drug to reduce by half (Shode et al., 2022). All the compounds evaluated possessed good CLplasma and T0.5 except OPCPPE and [1,

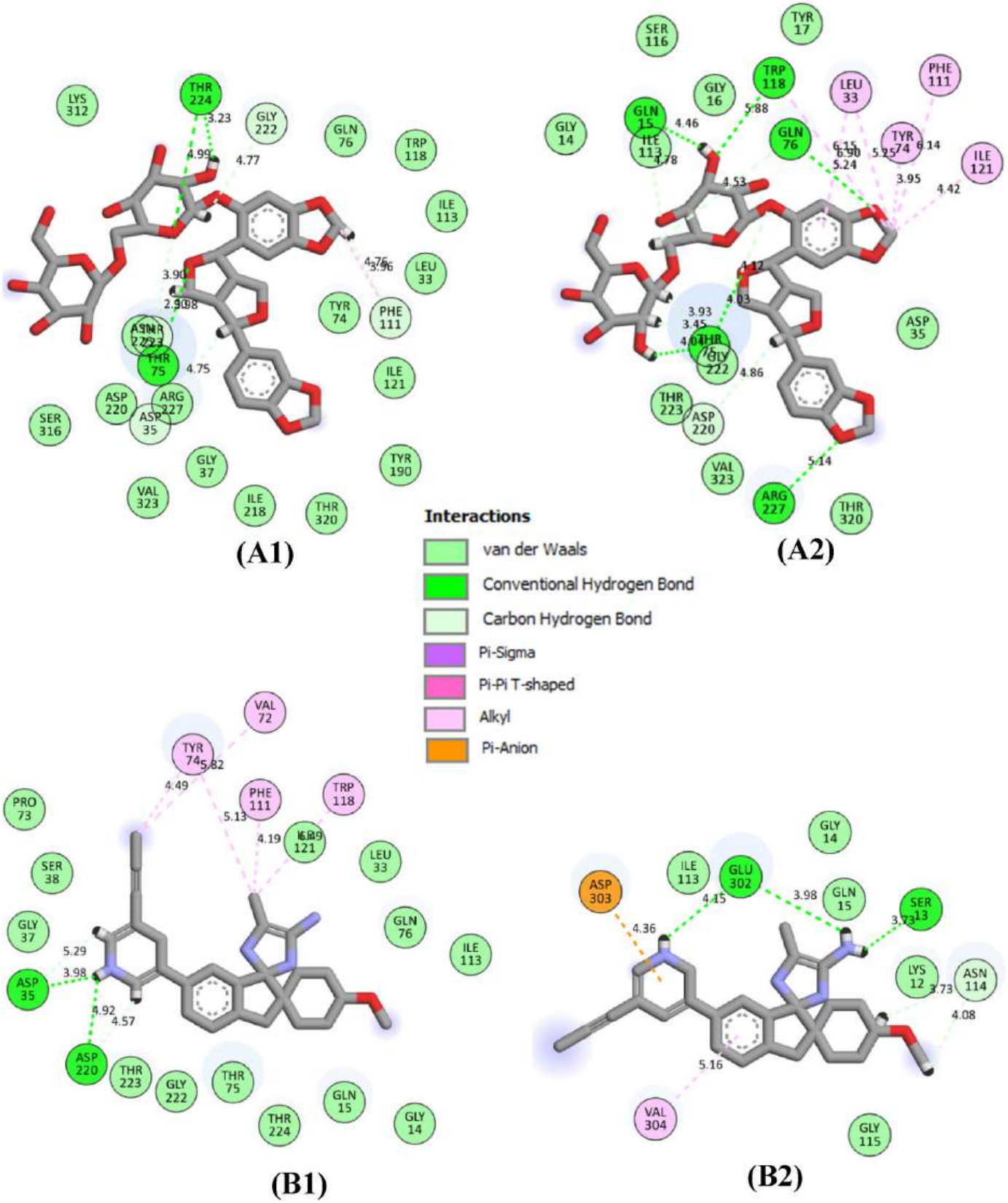

Fig. 8. 2D interaction plots of (A) neocuscutoside C and (B) AZD3293 against beta-secretase before (A1, B1) and after (A2, B2) 120 ns molecular dynamics simulation.

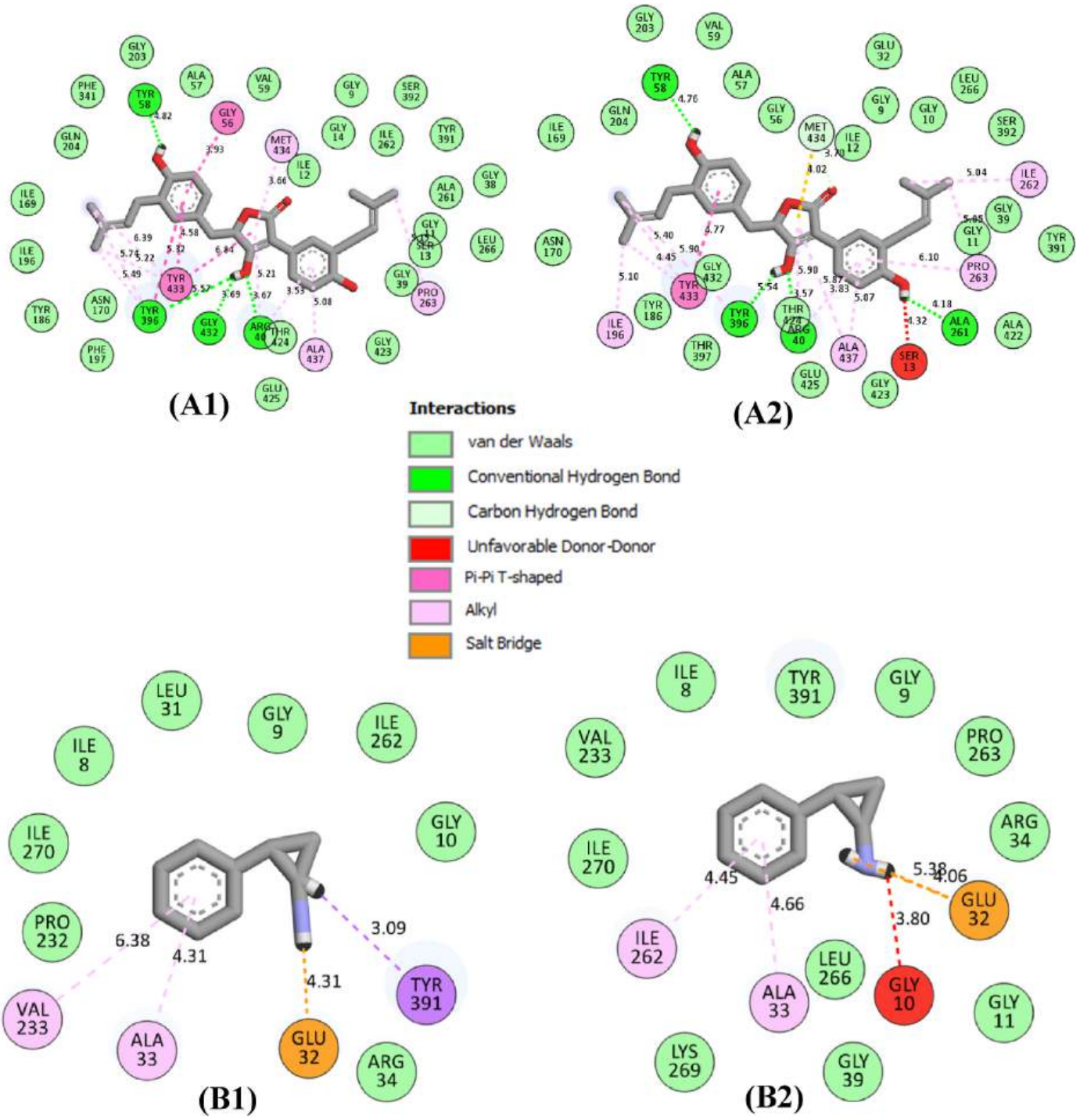

Fig. 9. 2D interaction plots of (A) aspulvinone H and (B) tranylcypromine against monoamine oxidase before (A1, B1) and after (A2, B2) 120 ns molecular dynamics simulation.

1′-binaphthalen]-2-ol, which suggest that when ingested they are excreted from the body at the appropriate time (Verma et al., 2022). While all the compounds are not toxic orally in rat oral acute toxicity (ROA) and are not carcinogenic (CC), both OPCPPE and [1,1′-binaphthalen]-2-ol performed poorly in the neurotoxicity (Neuro) prediction. Of all the compounds, aspulvinone H, astragalin, chamaemeloside, and [1,1′-binaphthalen]-2-ol displayed poor values in terms of nephrotoxicity (Neph) and genotoxicity (GEN), which implies that the compounds are relatively safe.

4. Conclusion

It can be concluded that both fresh and dry lemongrass teas displayed neuroprotective properties *in vitro*, though the fresh infusion was better. LC-MS profiling of the lemongrass teas showed the presence of 49 phytochemical compounds. Computational studies revealed that of all the phytochemical compounds tested, benzyl alcohol beta-D-rutinoside, kaempferitrin, neocuscutoside C, and aspulvinone H had the highest number of stable interactions with AChE, BChE, BACE-1, and MAO, respectively. While there are previous reports on the neuroprotective potentials of aspulvinone H and kaempferitrin, this study for the first

Table 6
ADMET properties of all the top compounds of lemongrass docked against neurological-related enzymes.

Compounds	ADS			DIS			METAB			EXCR		TOX				
	Caco2	HIA	F20	BBB	PPB	VDSS	CYP1A2	CYP2C19	CYP3A4	CLplas	T0.5	ROA	CC	Neuro	Neph	GEN
OPCPPE	Ex	Ex	Ex	Ex	Po	Ex	Yes	Yes	No	Md	Po	Ex	Md	Po	Md	Ex
Aspulvinone H	Ex	Po	Po	Ex	Po	Ex	No	Yes	No	Ex	Md	Md	Ex	Md	Po	Po
AS7RH	Po	Po	Po	Ex	Ex	Ex	No	No	No	Ex	Md	Ex	Ex	Ex	Po	Po
BABR	Po	Po	Md	Ex	Ex	Ex	No	No	No	Ex	Md	Ex	Ex	Ex	Po	Ex
Chamaemeloside	Po	Md	Po	Ex	Ex	Ex	No	No	No	Ex	Md	Ex	Ex	Ex	Po	Po
BN2OL	Ex	Ex	Ex	Md	Po	Ex	Yes	Yes	No	Ex	Po	Ex	Md	Po	Po	Po
Isocarlinoside	Po	Po	Po	Ex	Ex	Ex	No	No	No	Ex	Ex	Ex	Ex	Ex	Md	Po
Kaempferitrin	Po	Md	Po	Ex	Ex	Ex	No	No	No	Ex	Md	Ex	Ex	Ex	Md	Po
Lonicerin	Po	Po	Ex	Ex	Ex	Ex	No	No	No	Ex	Md	Ex	Ex	Ex	Md	Po
V6H3M	Po	Ex	Po	Ex	Ex	Ex	No	No	No	Ex	Md	Md	Ex	Ex	Md	Po
Neocuscutoside C	Po	Ex	Ex	Md	Ex	Ex	No	No	No	Ex	Md	Md	Md	Md	Ex	Po
Chlorogenic acid	Po	Ex	Po	Ex	Ex	Ex	No	No	No	Ex	Md	Ex	Ex	Ex	Md	Ex
PEPV	Po	Po	Po	Ex	Ex	Ex	No	No	No	Ex	Md	Ex	Ex	Md	Ex	Ex
4FQA	Po	Ex	Po	Ex	Ex	Ex	No	No	No	Ex	Md	Ex	Md	Md	Po	Ex
Standard drugs																
Donepezil	Ex	Ex	Ex	Md	Po	Ex	No	No	No	Md	Po	Md	Md	Po	Md	Md
AZD3293	Ex	Ex	Ex	Ex	Po	Ex	No	No	No	Ex	Po	Po	Po	Md	Po	Po
Tranylcypromine	Ex	Ex	Ex	Po	Ex	Ex	Yes	No	No	Md	Md	Po	Ex	Po	Po	Ex

ADS: Adsorption, DIS: Distribution, METAB: Metabolism, EXCR: Excretion, TOX: Toxicity, Caco-2: Caco-2 permeability, HIA: Human intestinal absorption, F20: 20% bioavailability, BBB: Blood-brain barrier, VDSS: Volume of distribution at steady state, CLplas: Plasma clearance, T0.5: Half-life, ROA: Rat oral toxicity, CC: Carcinogenicity, Neuro: Neurotoxicity, Neph: Nephrotoxicity, GEN: Genotoxicity, OPCPPE: 4-oxo-3-phenyl-4H-chromen-7-yl 3-phenylprop-2-enoate, AS7RH: Astragalin-7-rhamnoside, BABR: Benzyl alcohol beta-D-rutinoside, BN2OL: [1,1′-binaphthalen]-2-ol, V6H3M: Vitexin-6’’-(3-hydroxyl-3-methylglutarate), PEPV: Phenylethyl primeveroside, 4FQA: 4-O-feruloyl-D-quinic acid. Ex: Excellent, Md: Medium, Po: Poor.

time, reports the potent neuroprotective properties of benzyl alcohol beta-D-rutinoside and neocuscutoside C. Consequently, these compounds could be explored in developing new therapeutic agents for the management of neurodegenerative disorders like Alzheimer’s and Parkinson’s diseases.

CRediT authorship contribution statement

Mutiu Idowu Kazeem: Writing – review & editing, Writing – original draft, Methodology, Investigation, Data curation, Conceptualization. **Rukayat Abiola Abdulsalam:** Software, Methodology, Formal analysis, Data curation. **John Jason Mellem:** Writing – review & editing, Supervision, Resources, Project administration, Funding acquisition, Conceptualization. **Saheed Sabiu:** Writing – review & editing, Validation, Supervision, Resources, Project administration, Funding acquisition, Conceptualization.

Declaration of competing interest

The authors declare that they have no known competing financial interests or personal relationships that could influence the work reported in this paper.

Acknowledgements

The authors appreciate the support of the Directorate of Research and Postgraduate Support, Durban University of Technology, South Africa, towards the conduct of this work. We also acknowledge the financial support of the South African Medical Research Council under a Self-Initiated Research Grant and the National Research Foundation’s Competitive Programme for Rated Researchers Support (SRUG2204193723) to Saheed Sabiu.

Appendix A. Supplementary data

Supplementary data to this article can be found online at https://doi.org/10.1016/j.fbio.2025.106355.

Data availability

Data will be made available on request.

References

Al-Khodairy, F. M., Khan, M. K. A., Kunhi, M., Pulicat, M. S., Akhtar, S., & Arif, J. M. (2013). In Silico prediction of mechanism of Erysolin-induced apoptosis in human breast cancer cell lines. *American Journal of Bioinformatics Research, 3*(3), 62–71.

Aribisala, J. O., Abdulsalam, R. A., Dweba, Y., Madonsela, K., & Sabiu, S. (2022). Identification of secondary metabolites from *Crescentia cujete* as promising antibacterial therapeutics targeting type 2A topoisomerases through molecular dynamics simulation. *Computers in Biology and Medicine, 145*, Article 105432.

Avoseh, O., Oyedeji, O., Rungqu, P., Nkeh-Chungag, B., & Oyedeji, A. (2015). Cymbopogon species; ethnopharmacology, phytochemistry and the pharmacological importance. *Molecules, 20*(5), 7438–7453.

Balogun, F. O., Naidoo, K., Aribisala, J. O., Pillay, C., & Sabiu, S. (2022). Cheminformatics Identification and validation of dipeptidyl peptidase-iv modulators from shikimate pathway-derived phenolic acids towards interventive type-2 diabetes therapy. *Metabolites, 12*(10), 937.

Cancela, S., Canclini, L., Mourglia-Ettlin, G., Hernández, P., & Merlino, A. (2020). Neuroprotective effects of novel nitrones: In vitro and in silico studies. *European Journal of Pharmacology, 871*, Article 172926.

Das, D., Nanda, M., Banjare, P., & Lanjhiyana, S. (2024). Exploration of multitargeted antialzheimer’s activity of safflower leaves phytoconstituents: In silico molecular docking approach. *European Journal of Medicinal Chemistry Reports, 10*, Article 100119.

Devi, C. B., Bains, K., & Kaur, H. (2021). Effect of drying processes on nutritional composition, bioactive compounds and antoxidant activity of wheatgrass (*Triticum aestivum* L.). *Journal of Food Science and Technology, 56*(1), 491–496.

Duangupama, T., Pratuangdejkul, J., Chongruchiroj, S., Pittayakhajonwut, P., Intaraudom, C., Tadtong, S., Nunthanavanit, P., Samee, W., He, Y.-W., & Tanasupawat, S. (2023). New insights into the neuroprotective and beta-secretase1 inhibitor profiles of tirandamycin B isolated from a newly found Streptomyces composti sp. nov. *Scientific Reports, 13*(1), 4825.

Ekpenyong, C. E., Akpan, E., & Nyoh, A. (2015). Ethnopharmacology, phytochemistry, and biological activities of *Cymbopogon citratus* (DC.) Stapf extracts. *Chinese Journal of Natural Medicines, 13*(5), 321–337.

Fatima, K., Ashfaq, U. A., ul Qamar, M. T., Asif, M., Haque, A., Qasim, M., Alamri, M. A., Muhseen, Z. T., Noor, F., & Sadaqat, M. (2024). Advanced network pharmacology and molecular docking-based mechanism study to explore the multi-target pharmacological mechanism of *Cymbopogon citratus* against Alzheimer’s disease. *South African Journal of Botany, 165*, 466–477.

Gholami, A., Minai-Tehrani, D., & Eriksson, L. A. (2023). In silico and in vitro studies confirm Ondansetron as a novel acetylcholinesterase and butyrylcholinesterase inhibitor. *Scientific Reports, 13*(1), 643.

Gupta, S., Parihar, D., Shah, M., Yadav, S., Managori, H., Bhowmick, S., Patil, P. C., Alissa, S. A., Wabaidur, S. M., & Islam, M. A. (2020). Computational screening of promising beta-secretase 1 inhibitors through multi-step molecular docking and

molecular dynamics simulations-Pharmacoinformatics approach. *Journal of Molecular Structure, 1205*, Article 127660.
Gyebi, G. A., Ogunyemi, O. M., Ibrahim, I. M., Ogunro, O. B., Afolabi, S. O., Ojo, R. J., Anyanwu, G. O., El-Saber Batiha, G., & Adebayo, J. O. (2023). Identification of potential inhibitors of cholinergic and β-secretase enzymes from phytochemicals derived from gongronema latifolium benth leaf: An integrated computational analysis. *Molecular Diversity*, 1–18.
Hacke, A. C. M., Miyoshi, E., Marques, J. A., & Pereira, R. P. (2021). *Cymbopogon citratus* (DC.) Stapf, citral and geraniol exhibit anticonvulsant and neuroprotective effects in pentylenetetrazole-induced seizures in zebrafish. *Journal of Ethnopharmacology, 275*, Article 114142.
Haider, M. S., Ashraf, W., Javaid, S., Rasool, M. F., Rahman, H. M. A., Saleem, H., Anjum, S. M. M., Siddique, F., Morales-Bayuelo, A., & Kaya, S. (2021). Chemical characterization and evaluation of the neuroprotective potential of *Indigofera sessiliflora* through in-silico studies and behavioral tests in scopolamine-induced memory compromised rats. *Saudi Journal of Biological Sciences, 28*(8), 4384–4398.
Jalal, K., Khan, K., Haleem, D. J., & Uddin, R. (2022). In silico study to identify new monoamine oxidase type a (MAO-A) selective inhibitors from natural source by virtual screening and molecular dynamics simulation. *Journal of Molecular Structure, 1254*, Article 132244.
Jongwachirachai, P., Ruankham, W., Apiraksattayakul, S., Intharakham, S., Prachayasittikul, V., Suwanjang, W., Prachayasittikul, V., Prachayasittikul, S., & Phopin, K. (2024). Neuroprotective properties of coriander-derived compounds on neuronal cell damage under oxidative stress-induced SH-SY5Y neuroblastoma and in silico ADMET analysis. *Neurochemical Research, 49*, 3308–3325.
Kazeem, M. I., & Davies, T. C. (2016). Anti-diabetic functional foods as sources of insulin secreting, insulin sensitizing and insulin mimetic agents. *Journal of Functional Foods, 20*, 122–138.
Kim, J. H., Thao, N. P., Han, Y. K., Lee, Y. S., Luyen, B. T. T., Oanh, H. V., Kim, Y. H., & Yang, S. Y. (2018). The insight of in vitro and in silico studies on cholinesterase inhibitors from the roots of *Cimicifuga dahurica* (Turcz.) Maxim. *Journal of Enzyme Inhibition and Medicinal Chemistry, 33*(1), 1174–1180.
Kumar, G., & Patnaik, R. (2016). Exploring neuroprotective potential of withania somnifera phytochemicals by inhibition of GluN2B-containing NMDA receptors: An in silico study. *Medical Hypotheses, 92*, 35–43.
Kundu, D., & Dubey, V. K. (2021). Potential alternatives to current cholinesterase inhibitors: An in silico drug repurposing approach. *Drug Development and Industrial Pharmacy, 47*(6), 919–930.
Lanrewaju, A. A., Enitan-Folami, A. M., Nyaga, M. M., Sabiu, S., & Swalaha, F. M. (2024). Metabolites profiling and cheminformatics bioprospection of selected medicinal plants against the main protease and RNA-dependent RNA polymerase of SARS-CoV-2. *Journal of Biomolecular Structure and Dynamics, 42*(13), 6740–6760.
Madi, Y. F., Choucry, M. A., El-Marasy, S. A., Meselhy, M. R., & El-Kashoury, E.-S. A. (2020). UPLC-Orbitrap HRMS metabolic profiling of *Cymbopogon citratus* cultivated in Egypt; neuroprotective effect against AlCl3-induced neurotoxicity in rats. *Journal of Ethnopharmacology, 259*, Article 112930.
Masondo, N. A., Stafford, G. I., Aremu, A. O., & Makunga, N. P. (2019). Acetylcholinesterase inhibitors from southern African plants: An overview of ethnobotanical, pharmacological potential and phytochemical research including and beyond Alzheimer's disease treatment. *South African Journal of Botany, 120*, 39–64.
Mazumder, M. K., & Choudhury, S. (2019). Tea polyphenols as multi-target therapeutics for Alzheimer's disease: An in silico study. *Medical Hypotheses, 125*, 94–99.
Mendes, G. O., Pita, S. S.d. R., Carvalho, P. B.d., Silva, M. P.d., Taranto, A. G., & Leite, F. H. A. (2023). Molecular multi-target approach for human acetylcholinesterase, butyrylcholinesterase and β-secretase 1: Next generation for Alzheimer's disease treatment. *Pharmaceuticals, 16*(6), 880.
Moorkoth, S., Prathyusha, N. S., Manandhar, S., Xue, Y., Sankhe, R., Pai, K., & Kumar, N. (2021). Antidepressant-like effect of dehydrozingerone from zingiber officinale by elevating monoamines in brain: In silico and in vivo studies. *Pharmacological Reports, 73*, 1273–1286.
Murali, M., Ahmed, F., Gowtham, H. G., Aribisala, J. O., Abdulsalam, R. A., Shati, A. A., Alfaifi, M. Y., Sayyed, R., Sabiu, S., & Amruthesh, K. N. (2023). Exploration of CviR-mediated quorum sensing inhibitors from *Cladosporium* spp. against *Chromobacterium violaceum* through computational studies. *Scientific Reports, 13*(1), Article 15505.
Negrelle, R., & Gomes, E. (2007). *Cymbopogon citratus* (DC.) stapf: Chemical composition and biological activities. *Revista Brasileira de Plantas Medicinais, 9*(1), 80–92.
Oladeji, O. S., Adelowo, F. E., Ayodele, D. T., & Odelade, K. A. (2019). Phytochemistry and pharmacological activities of *Cymbopogon citratus*: A review. *Scientific African, 6*, Article e00137.
Oliveira-Alves, S. C., Andrade, F., Prazeres, I., Silva, A. B., Capelo, J., Duarte, B., Caçador, I., Coelho, J., Serra, A. T., & Bronze, M. R. (2021). Impact of drying processes on the nutritional composition,volatile profile, phytochemical content and bioactivity of *Salicornia ramosissima* J.Woods. *Antioxidants, 10*, 1312.
Onder, F. C., Sahin, K., Senturk, M., Durdagi, S., & Ay, M. (2022). Identifying highly effective coumarin-based novel cholinesterase inhibitors by in silico and in vitro studies. *Journal of Molecular Graphics and Modelling, 115*, Article 108210.
Othman, A., Sayed, A. M., Amen, Y., & Shimizu, K. (2022). Possible neuroprotective effects of amide alkaloids from bassia indica and agathophora alopecuroides: In vitro and in silico investigations. *RSC Advances, 12*(29), 18746–18758.
Paudel, P., Seong, S. H., Shrestha, S., Jung, H. A., & Choi, J. S. (2019). In vitro and in silico human monoamine oxidase inhibitory potential of anthraquinones, naphthopyrones, and naphthalenic lactones from *Cassia obtusifolia* Linn seeds. *ACS Omega, 4*(14), 16139–16152.
Perry, N. S., Houghton, P. J., Sampson, J., Theobald, A. E., Hart, S., Lis-Balchin, M., Hoult, J. R. S., Evans, P., Jenner, P., & Milligan, S. (2001). In-vitro activity of *S. lavandulaefolia* (Spanish sage) relevant to treatment of Alzheimer's disease. *Journal of Pharmacy and Pharmacology, 53*(10), 1347–1356.
Puksasook, T., Kimura, S., Tadtong, S., Jiaranaikulwanitch, J., Pratuangdejkul, J., Kitphati, W., Suwanborirux, K., Saito, N., & Nukoolkarn, V. (2017). Semisynthesis and biological evaluation of prenylated resveratrol derivatives as multi-targeted agents for Alzheimer's disease. *Journal of Natural Medicines, 71*, 665–682.
Racchi, M., Mazzucchelli, M., Porrello, E., Lanni, C., & Govoni, S. (2004). Acetylcholinesterase inhibitors: Novel activities of old molecules. *Pharmacological Research, 50*(4), 441–451.
Rojek, K., Serefko, A., Poleszak, E., Szopa, A., Wróbel, A., Guz, M., Xiao, J., & Skalicka-Woźniak, K. (2022). Neurobehavioral properties of *Cymbopogon* essential oils and its components. *Phytochemistry Reviews, 21*(2), 327–338.
Sabiu, S., Balogun, F. O., & Amoo, S. O. (2021). Phenolics profiling of *Carpobrotus edulis* (L.) NE Br. and insights into molecular dynamics of their significance in type 2 diabetes therapy and its retinopathy complication. *Molecules, 26*(16), 4867.
Santi, M. D., Arredondo, F., Carvalho, D., Echeverry, C., Prunell, G., Peralta, M. A., Cabrera, J. L., Ortega, M. G., Savio, E., & Abin-Carriquiry, J. A. (2020). Neuroprotective effects of prenylated flavanones isolated from Dalea species, in vitro and in silico studies. *European Journal of Medicinal Chemistry, 206*, Article 112718.
Sheeja Malar, D., Beema Shafreen, R., Karutha Pandian, S., & Pandima Devi, K. (2017). Cholinesterase inhibitory, anti-amyloidogenic and neuroprotective effect of the medicinal plant Grewia tiliaefolia–An in vitro and in silico study. *Pharmaceutical Biology, 55*(1), 381–393.
Shode, F., Idowu, A., Uhomoibhi, O., & Sabiu, S. (2022). Repurposing drugs and identification of inhibitors of integral proteins (spike protein and main protease) of SARS-CoV-2. *Journal of Biomolecular Structure & Dynamics, 40*(14), 6587–6602.
Soreq, H., & Seidman, S. (2001). Acetylcholinesterase—new roles for an old actor. *Nature Reviews Neuroscience, 2*(4), 294–302.
Steinmetz, J. D., Seeher, K. M., Schiess, N., Nichols, E., Cao, B., Servili, C., Cavallera, V., Cousin, E., Hagins, H., & Moberg, M. E. (2024). Global, regional, and national burden of disorders affecting the nervous system, 1990–2021: A systematic analysis for the global burden of disease study 2021. *The Lancet Neurology, 23*(4), 344–381.
Suleria, H. A., Barrow, C. J., & Dunshea, F. R. (2020). Screening and characterization of phenolic compounds and their antioxidant capacity in different fruit peels. *Foods, 9*(9), 1206.
Umukoro, S., Adeola, A. H., Ben-Azu, B., & Ajayi, A. M. (2018). Lemon grass tea enhanced memory function and attenuated scopolamine-induced amnesia in mice via inhibition of oxidative stress and acetyl-cholinesterase activity. *Journal of Herbs, Spices, & Medicinal Plants, 24*(4), 407–420.
Verma, A. K., Ahmed, S. F., Hossain, M. S., Bhojiya, A. A., Mathur, A., Upadhyay, S. K., Srivastava, A. K., Vishvakarma, N. K., Barik, M., Rahaman, M. M., & Bahadur, N. M. (2022). Molecular docking and simulation studies of flavonoid compounds against PBP-2a of methicillin- resistant Staphylococcus aureus. *Journal of Biomolecular Structure & Dynamics, 40*(21), 10561–10577.
Wallace, W. E., & Moorthy, A. S. (2023). NIST mass spectrometry data center reference libraries and software tools: Application to seized drug analysis. *Journal of Forensic Sciences*. https://doi.org/10.1111/1556-4029.15284
WHO. (2002). *WHO traditional medicine strategy 2002 - 2005*. Geneva: World Health Organization.
Wu, Y., Su, X., Lu, J., Wu, M., Yang, S. Y., Mai, Y., Deng, W., & Xue, Y. (2022). In Vitro and in silico analysis of phytochemicals from *Fallopia dentatoalata* as dual functional cholinesterase inhibitors for the treatment of Alzheimer's disease. *Frontiers in Pharmacology, 13*, Article 905708.
Yang, X., Wang, K., Liu, Q., & Zhang, X. (2020). Discovery of monoamine oxidase A inhibitory peptides from hairtail (*Trichiurus japonicus*) using in vitro simulated gastrointestinal digestion and in silico studies. *Bioorganic Chemistry, 101*, Article 104032.